Development of anisotropic clay soil beds for geotechnical centrifuge testing

by

Eric Paul Ritchie

A dissertation submitted for the Degree of Doctor of Philosophy

City, University of London

School of Science and Technology

Geotechnical Engineering

December 2023

Contents

List of Tables

List of Figures

Acknowledgements

I am privileged to have been able to undertake doctoral studies within the Geotechnical Engineering Research Group at City, University of London where I spent four fantastic years with wonderful colleagues.

Firstly, I would like to thank my supervisor Dr Sam Divall, I will be forever grateful for the opportunities and the continuous support provided throughout my studies. His humour and guidance have made this experience so enjoyable and without which my experience of conducting a Ph.D. would have not been the same. I would also like to thank my second supervisor Professor Sarah Stallebrass for her caring and supportive nature, always providing key insights into the research and limiting my overthinking.

I would also like to thank the entire research group, Professor Neil Taylor for being so generous with his time, sharing his vast Geotechnical Engineering and Centrifuge Modelling knowledge. 'I would not do it like that' is something that will stay with me forever, my confidence and critical thinking ability would not have developed the same without those discussions. Dr Andrew McNamara for his centrifuge modelling insights, brilliant sense of humour and sharing my passion for pies. Mr Ciaran Kennedy for continually pushing me and having the ability to make my laugh even when I could not interpret laboratory results. Dr Leonardo Lalicata, Dr Richard Goodey, Dr Brett Mckinley, Dr Tanghetti and Mr Hashmi Sohawon for making the research group at City, University of London so special.

The Apparatus used for this research would not have been produced without the skill and guidance from the technical staff at City, University of London. My sincere gratitude goes Melvyn Hayes, Richard Leach, Jim Ford and Keith Pamment.

A special thanks is due to the George Daniels trust for sponsoring this research and providing additional funding due to the COVID 19 Pandemic, I am forever grateful for the opportunities that George Daniels trust has provided me.

To my friends and family, a massive thank you for the constant support and always providing the perfect distraction during the most challenging parts of this research. Last, but by no means least, I would like to thank my wife Saima for her continual support, love, and patience tolerating me being consistently late home for dinner and having to listen to hours of talk about pore pressure transducers and laboratory testing, without which this thesis would not been possible.

Declaration

I grant powers of discretion to the University Librarian to allow this dissertation to be copied in whole or in part without further reference to me. This permission covers only single copies made for study purposes, subject to normal conditions of acknowledgement.

Abstract

This research concerns the development of a technique to create sedimented anisotropic clay soil bed suitable for modelling construction events using a geotechnical centrifuge. Geotechnical centrifuge testing has been used to investigate complex geotechnical events; however, natural soil is fundamentally different to a 'typical' homogenous clay soil bed. Natural soil contains structure (Mitchel, 1976) which, in part, governs soil behaviour (Leroueil & Vaughan, 1990). Changing key soil parameters, such as strength, and creating anisotropy where soil properties such as permeability vary in the vertical and horizontal directions. Modelling the soil permeability is also essential for modelling long-term soil behaviour (Wongsaroj et al., 2007). Currently no method for creating a sedimented soil bed suitable for centrifuge modelling exists. At the element testing scale sedimenting a dilute soil slurry has been effectively used to recreate a sedimented structure comparable to a naturally occurring sedimented sample (Stallebrass et al., 2007). This research sought to develop a framework to create centrifuge soil beds which include permeability anisotropy and to conduct a small series of centrifuge tunnel tests to assess the influence of different soil beds on the resultant soil behaviour.

A series of 15 centrifuge sedimentation tests (60 sedimentation columns) were completed at 100*g* to develop a framework where the resultant soil structure and permeability of different sample preparations could be determined. The key findings of the results were as follows:

1. It was possible to sediment a sample on the centrifuge such that it contains a sedimented structure and permeability anisotropy.
2. Anisotropy was dependent on the initial water content and the constituent parts of the slurry.
3. The water content required to develop a sedimented structure can be significantly reduced using a dispersion agent.

Following the development of a framework and the selection of a suitable sample preparation technique the procure was transferred into a centrifuge soil container to create a sedimented soil bed. The soil bed consisted of four sedimented clay layers with a permeability anisotropy of approximately four. A tunnel construction event was then modelled on the centrifuge using both a reconstitutes soil beds and a sedimented soil bed at 100*g*. The key findings of the results were as follows:

I. The sedimentation procedure was applied to create a soil bed in a centrifuge strongbox.
II. Following tunnel construction, the sedimented soil bed had a higher undrained shear strength yet experienced a larger volume loss than an equivalent homogenous sample.
III. The homogenous soil bed experienced the largest change in pore pressure above the tunnel shoulder whereas in the sedimented soil bed the largest change occurred above the crown coinciding with a more permeable layer.

List of Symbols

a	Radial acceleration
Cc	Coefficient of consolidation
C_s	Coefficient of swelling
C_v	Coefficient of consolidation
e	Voids ratio
e_l	Voids ratio at liquid limit
e_0	Voids ratio at 1kPa vertical effective stress
g	Acceleration due to gravity ($9.81 m/s^2$)
I_v	Voids index
k	Coefficient of permeability
K_0	Coefficient of earth pressure at rest
M	Critical state friction coefficient
N	Gravity scaling factor
p’	Mean effective stress
p_e^*	Mean effective stress on either the K_0 or the isotropic reconstituted normal compression line at the same specific volume as the natural clay
q	Deviator stress
r	Radius from the centre of rotation
S_t	Sensitivity (soil strength)
T_v	Time Factor (consolidation)
u	Pore-water pressure
v	Specific volume
W_l	Liquid limit

σ'_v Vertical effective stress

σ'_{vc} Maximum vertical effective stress

κ Gradient of swelling line in v-lnp' space

λ Gradient of compression line in v-lnp' space

Subscripts

h Horizontal

v Vertical

m model

p prototype

List of Abbreviation

ICL Intrinsic compression line

LVDT Linear variable displacement transformer

PPT Pore pressure transducer

PSD Particle size distribution

SBS State boundary surface

SCL Sedimentation compression line

YSR Yield stress ratio

1. Introduction

As urban areas expand, so does the need for infrastructure. Fundamental to urban development is maximising the use of available space by relocating transportation and other services underground utilising tunnels and shafts. Underground construction changes the state of soil which results in ground movements. These movements can be both in the short-term, defined as the movements experienced during the construction event, and/or, the long-term, defined as movements that occur after construction has been completed. Depending on ground conditions long-term movements, can continue to develop over many years after completion of the project and can, in some cases, account for 50% of the total movements experienced (ultimate settlement). Ground movements have the potential to damage existing infrastructure, if large or uncontrolled (Mair et al., 1996). Guidance for movements associated with the construction of underground structures tends to focus on the short-term behaviour. Therefore, it is crucial to understand long-term ground movements following a construction event. Geotechnical researchers use three primary ways of investigating ground behaviour.

1. Field monitoring,
2. Numerical analysis, and
3. Reduced scale modelling

These methods are not to be viewed in isolation, but as tools that are used collectively to understand soil behaviour and produce guidance for practicing engineers. Field monitoring has demonstrated that long-term movements can be significant (e.g., Richards et al., 2006; Hill & Staerk, 2016) and subsequently there has been numerical models created to simulate this behaviour (e.g., Wongsaroj et al., 2007; Soga., et al., 2017). However, due to the often complex ground conditions and restricted monitoring points available, there is typically a limited amount of reliable long-term monitoring data available. Consequently, validating numerical models with just field monitoring data can be challenging. Another method of observing long-term ground movements would be advantageous to enhancing our understanding and predictive capabilities regarding long-term movements.

Reduced scale models can be conducted under an increased gravitational field in a geotechnical centrifuge. This allows the soil model to have a stress history profile representative of field studies. Centrifuge tests benefit from well-controlled, well defined boundary conditions where the soil models' properties are often well documented (Taylor, 1995). Centrifuge tests have the added advantage that a year's worth of seepage/consolidation events can be modelled in under

an hour at 100 times Earth's gravitational acceleration due to scaling laws. Centrifuge modelling has proven successful in investigating complex construction events and their subsequent short-term responses.

However, these construction events are simulated in a reconstituted soil bed, and there is a fundamental difference between this and many natural soil deposits. Natural sedimented soil has inherent anisotropy due to the layering developed during the soil formation process creating a unique structure. Soil structure is defined by the soil's particle arrangement (fabric) and the interparticle bonding (Mitchel, 1976). Soil structure in part, governs soil behaviour (Leroueil & Vaughan, 1990). Layering and soil structure can increase soil strength and the horizontal permeability by an order of magnitude. Correctly modelling the permeability of soil and geotechnical structure is essential for achieving representative long-term soil behaviour (Wongsaroj et al., 2007). Currently, there is no method for creating a soil bed with anisotropic permeabilities suitable for the investigation of ground movements within a centrifuge. However, at a smaller element testing scale sedimentation has proven to be a viable technique for creating samples that have layering and anisotropy similar to a natural deposit. If a soil bed could be sedimented within a centrifuge container, it would allow for a geotechnical event to be modelled in layered anisotropic soil on the centrifuge.

1.2 Objectives

The primary aim of this research project is to develop a technique for creating sedimented clay soil beds with distinct layers for use in centrifuge modelling.

The following are identified as the main objectives:

- Develop a new sedimentation column apparatus to create clay element testing samples with a sedimented structure on the centrifuge.
- Develop a horizontal permeability apparatus to investigate the ratio of vertical and horizontal permeability in sedimented clays.
- Determine how different sample preparation techniques, predominately of Speswhite kaolin clay slurries influences the anisotropy (in terms of permeability).
- Determine if different sample preparation techniques influence one-dimensional compression lines in an oedometer.
- Sediment a soil bed in a centrifuge strongbox with predetermined permeabilities and layer thicknesses.

- Compare the response of homogenous and sedimented soil beds following a tunnel construction event on the centrifuge.

2. Background

This background chapter provides an overview of soil layering, soil structure, their inter-relationship and their effect on soil properties. The effect of different soil properties on a tunnel construction event is also summarised within this chapter. Additionally, this chapter presents the research methodology adopted for this dissertation.

2.1 Significance of soil structure on engineering parameters

All soil has a structure, irrespective of its origin i.e., a soil will always have an arrangement of particles and a degree of particle bonding. Figure 2.1 illustrates an idealised sedimented soil sample which has been subjected to one dimensional consolidation. During the sedimentation process soil particles have been sorted by particle size, creating a layered soil sample. Figure 2.2 depicts the same soil sample after it has been reconstituted and consolidated one dimensionally to the same vertical effective stress. A reconstituted sample is where any soil sample has been broken down into a slurry and consolidated to create a new soil sample. Typically, samples are reconstituted to remove variability in soil structure for consistency in geotechnical modelling and testing. The reconstituted soil sample has a random particle arrangement with no particle size sorting, where the larger particles distributed throughout the soil matrix.

At a clay particle scale, there is also a difference between the sedimented and reconstituted soil samples, as illustrated in Figure 2.1-2.2. Within the reconstituted soil sample, clay platelets are orientated perpendicular to the direction of load, whereas in the sedimented sample, the platelets have a more open fabric with less particle orientation explaining the greater voids ratio achievable for the same effective stress (after Leroueil & Vaughan, 1990). Both the reconstituted and sedimented sample will have anisotropic permeability, with permeability in the horizontal direction larger than the vertical. When considering the entire soil element, as illustrated in Figure 2.1-2.2 the degree of anisotropy is significantly larger in the sedimented sample. This anisotropy is primarily influenced by the layering of particle sizes rather than the difference in clay platelet orientation. Therefore, when investigating a smaller element as magnified in Figure 2.1-2.2, the degree of permeability would be significantly reduced.

Little et al. (1992) and others have conducted permeability testing on sedimented clay soils and found the horizontal permeability can be an order of magnitude larger than the vertical

permeability. Increased anisotropy is primarily due to the layering present in a sedimented sample.

The layering and more open structure also influences mechanical behaviour. Strength and stiffness of sedimented clays have been investigated by various authors (e.g., Leroueil & Vaughan, 1990; Burland, 1990; Stallebrass et al., 2007) in which the behaviour of sedimented samples are compared with reconstituted samples. Leroueil & Vaughan (1990) conducted a series of tests on natural samples with different soil structures and concluded that soil structure, in part, governs soil behaviour. Tests conducted by Leroueil & Vaughan (1990), Burland (1990) and Stallebrass et al. (2007) note that a structured soil can exist in a state that is not achievable once the soil has been reconstituted. This can be practically explained by the different fabrics illustrated in Figures 2.1-2.2. Cotecchia & Chandler (2000) developed a framework to account for the presence of soil structure.

For this dissertation, a sedimented structures refers to a sample containing the features in Figure 2.1. Further details of the work completed on sedimented and reconstituted clay are presented in Chapter 3.

2.2 Influence of soil structure on the ground response to tunnelling

Hill & Staerk (2016) monitored excavations at Whitechapel's Crossrail sites and presented ground settlement data from two and half years. This report detailed the significant difference between two tunnelling locations, one tunnel situated within 2m of a more permeable sand seam, and the other 6m away from this permeable sand seam. The rate of soil settlement of the excavation site located further away from the sand seam took twice as long to decay to less than 2mm per year. Hill & Staerk (2016) reported that the long-term movements had increased the volume loss by 110%, and settlement at the centre of the tunnel trough had increased by 25%.

Similar observations were reported in Cooper et al. (2002) whilst monitoring the construction of Piccadilly line trial tunnel. Long-term ground movements increased the total settlement by between 16-47% , with significant variation attributed to different ground conditions.

Numerical analysis completed by Wongsaroj et al. (2007) concluded that modelling soil layers and representative soil and tunnel permeability were necessary to simulate the response observed at St James Park following the Jubilee line extension. Wongsaroj et al. (2013) extended this work by conducting a parametric study in which the permeability anisotropy of

the soil and the tunnel lining permeability were varied. Wongsaroj et al. (2013) found that as the permeability anisotropy increases, the magnitude of displacement, changes in pore pressure, and the extent of pore pressure change also increased. Studies conducted by Gonzalez et al. (2012), Avgerinos et al. (2016) and Laver at al. (2016) have all incorporated soil structure into numerical models and have similar conclusions. Soil and tunnel lining parameters need to be selected carefully to incorporate soil structure and anisotropy. These studies also acknowledge the need for more long-term monitoring data. Due to the practical challenges of recording field data, (e.g., time constraints and a limited number of observation points) utilising centrifuge modelling could, therefore, be advantageous.

Typically, centrifuge tests have focused on the short-term response to a construction event in clay due to the complexities of recreating representative soil and geotechnical structure permeabilities. These centrifuge tests have contributed to the understanding of subsurface movements and changes in pore water pressures by using image analysis and buried pore pressure transducers. These tests have also improved the empirical predictions (e.g., Mair, 1979; Taylor, 1984; Divall, 2013). Currently there are limited methods of creating a soil bed with a sedimented structure for use in centrifuge modelling. At an element testing scale, a sedimented soil structure has been created within a laboratory by mixing a soil and water slurry and allowing the particles to sediment under self-weight.

Although, modelling representative soil and tunnel permeability is essential for correctly modelling the long-term response to a construction event (Wongsaroj et al., 2007; 2013), modelling the permeability of a geotechnical structure falls outside the scope of this research project. The focus was to develop a method and framework of creating a soil bed with a sedimented structure for use in a centrifuge model. However, it is understood that to be able to observe representative long-term ground movements the geotechnical structures permeability would also need to be correctly modelled.

2.3 Research methodology

This research project utilises element testing and centrifuge modelling. The centrifuge tests were completed using the Geotechnical Centrifuge Facility at City, University of London. The centrifuge served as a tool for accelerating the sedimentation process, to create element sized sedimented samples for testing. These tests investigated how different sample preparation techniques affected the resultant soil structure and soil properties. Once a suitable slurry

preparation technique was determined the centrifuge was used to create a larger sedimented centrifuge soil bed where a tunnel construction event was modelled.

2.3.1 Element tests

Sedimentation columns were developed such that multiple samples could be sedimented on the centrifuge swing simultaneously. After the completion of the sedimentation process, the columns acted as a permeameter to measure the vertical permeability. Additionally, a horizontal permeameter was designed such that, after the vertical permeability was determined, the samples could be extruded, and the horizontal permeability measured. The ratio of horizontal to vertical permeability (permeability anisotropy) was used as a method of determining whether a sedimented structure had developed.

Select samples were also tested in an oedometer. To minimise sample disturbance a custom oedometer ring and guide were developed with the same diameter as the sedimentation columns. These tests were compared to reconstituted samples, similar to Stallebrass et al. (2007) to determine if a sedimented structure was developed. Additionally this also enabled the centrifuge sample to be designed to include specific layer thicknesses and permeability anisotropies.

2.3.2 Geotechnical centrifuge testing

The centrifuge served as a tool to create sedimented soil samples, utilising the increased radial acceleration field generated to reduce the time taken to sediment samples. Once a framework was developed through element tests, the centrifuge was used to sediment a soil bed suitable for use in a centrifuge strongbox and to model a tunnel construction event.

Geotechnical centrifuge testing is an effective way of reproducing a soil with a known stress history and repeatable boundary conditions (Taylor, 1995) and is frequently used to model complex geotechnical construction events. In this dissertation, a series of centrifuge tests modelled a tunnel construction event in both reconstituted and sedimented soil samples. These tests used established methods of simulating a tunnel collapse developed during previous research projects at City, University of London (Grant, 1998).

3.Previous work on structured clays

The aim of this research project is to create a bed of soil suitable for testing in a centrifuge model with a sedimented structure consistent with Figure 2.1. To achieve this, various samples preparation techniques were explored and the resultant sample were categorised. To categorise samples and determine if a sedimented structure had been developed, the influence of soil structure on soil properties needed to be understood. Typically, standard element tests are used to quantify the effect of soil structure by comparison to reconstituted samples. The same approach was used to assess if a sedimented structure was created within the laboratory (Stallebrass et al., 2007). This chapter provides an overview of the standard laboratory element tests used and the influence of a sedimented structure on soil behaviour.

3.1 Standard element tests

3.1.1 Falling head permeameter

Falling head permeameters are used to determine the vertical permeability of a fine-grained soil. A typical set up is shown in Figure 3.1. The soil sample is placed in a containing tube between two porous filters. When testing a sample extracted from a borehole (or similar) it can be difficult to achieve a good seal between the soil sample and the containing tube, resulting in preferential drainage paths around the sample and ultimately underestimates of permeability.

The soil sample has a cross sectional area of, A_1, and a height, L. It is subjected to an applied head from a small-bore tube at the top of the sample, which is ideally graduated, with a cross sectional area, A_2 that is significantly smaller than A_1. During the test, water flows through the tube, the sample itself and out the outlet at the base of the sample. The outlet is maintained at a constant elevation and the outlet tube is submerged to prevent the sample drying. Once, the sample is placed into the permeameter it is fully saturated and any air removed from the system, the sample is then ready for testing (Powrie, 2014).

At the start of the test, time is equal to 0 and the height between the outlet level and the water in the small-bore tube is measured and denoted as, h_1 which is the head of water across the sample. When the outlet is opened, a stopwatch is started, and after a period of time, T, the new height of the applied potential is measured as, h_2. This is repeated, measuring multiple heights and times to calculate the permeability of the soil sample.

From Darcy's law flow in a soil sample is given by;

$$q = A_1 ki \tag{3.1}$$

Where;

q is the flow rate of water through the sample,

k is the permeability of the soil sample, and

i is hydraulic gradient across the sample

The hydraulic gradient of the sample is defined by the applied head, h, divided by the height of the sample, L, therefore Equation 3.1 can be written as;

$$q = A_1 k \frac{h}{L} \tag{3.2}$$

From continuity, flow of water in the small-bore tube is equal to flow of water in the soil sample given by;

$$q = A_2 v \tag{3.3}$$

Where v is velocity of the fluid within the tube.

As velocity is a function of time (the applied head reduces with time) $v = \frac{-dh}{dt}$ and Equation 3.3 can be written as;

$$q = -A_2 \frac{dh}{dt} \tag{3.4}$$

From continuity, Equation 3.2 and Equation 3.4 can be equated and, therefore;

$$\frac{dh}{dt} = -\frac{A_1 k}{A_2 L} h \tag{3.5}$$

Integrating between the limits $h = h_1 \; at \; t = 0 \; and \; h = h_2 \; at \; t = T$;

$$\int_{h_1}^{h_2} \frac{dh}{h} = \int_0^T -\frac{A_1 k}{A_2 L} \tag{3.6}$$

Gives;

$$\mathrm{k} = \frac{A_2 L}{A_1 T} \ln\left(\frac{h_1}{h_2}\right) \tag{3.7}$$

A graph can be plotted of $ln\frac{h_1}{h_2}$ against T, having a slope of $\frac{kA_1}{LA_2}$. If the graph shows a decreasing slope, it indicates the soil is experiencing compression and hence the permeability is decreasing. Conversely, if the graph shows an increasing slope the sample is swelling.

A Falling head permeameter is a relatively simple method of determining vertical permeability. However, as the sample is free to swell and consolidate, it is not possible to determine the permeability of the soil samples at a known applied stress or voids ratio.

3.1.2 Measuring Permeability in an oedometer

Al-Tabbaa & Wood (1987) modified an oedometer with an 88mm internal diameter to measure both the vertical and horizontal permeability at known applied stresses (equipment shown in Figure 3.2). A clay sample was placed inside the oedometer and subjected to an applied stress. Porous filters were placed at the base and top of the sample allowing for two-way drainage. A typical test was completed in stages, where the sample was loaded and allowed to consolidate. At the end of each consolidation stage, a 5mm diameter burette was connected to the base of the sample and a head difference applied across the depth of the clay. A falling head test was then conducted measuring the variation in potential over time, and the vertical permeability was calculated using Equation 3.7.

To measure horizontal permeability, a new sample was placed into the oedometer, and the permeable top and bottom filters above were replaced with impermeable platens. An 18mm diameter permeable ceramic core was installed in the centre of the sample and a porous paper filter was placed around the soil sample, establishing hydraulic contact with porous discs above the impermeable platen. The apparatus allowed consolidation while the ceramic core was in place, such that the permeability of the sample at a variety of applied stresses could be determined.

During the consolidation stages, the porous column was connected to a base drain, this allowed radial drainage in two directions. During the falling head tests, a head difference was applied across the radius of the sample, with the higher head applied at the central porous column. This induced radial outwards flow from the sample. Figure 3.3 shows the drainage conditions during both the consolidation and falling head test phases.

Al Tabbaa and Wood (1987) calculated the permeability in the horizontal direction as follows.

From Darcy's law the flow out of the soil sample is given by:

$$v = \frac{q}{a} = \frac{q}{2\pi r L} \tag{3.8}$$

$$v = -k\frac{dp}{dr} \tag{3.9}$$

Where:

r is the external radius of the sample in mm

$-\frac{dp}{dr}$ is the change in potential with radius (note the negative as there is a loss of potential in the direction of flow)

Therefore,

$$\frac{q}{2\pi r L} = -k\frac{dp}{dr} \tag{3.10}$$

$$\frac{1}{r}dr = -dp\frac{2\pi L k}{q} \tag{3.11}$$

Integrating between the limits of a potential of p_R at a radius R and potential of p_{r_0} at a radius r_0, where r_0 is the radius to the central porous column in mm.

$$\int_{r_0}^{R}\frac{dr}{r} = \int_{p_{r_0}}^{p_R} -dp\frac{2\pi L k}{q} \tag{3.12}$$

$$ln\frac{R}{r_0} = \frac{2\pi L}{q}(Pr_0 - P_R)k \tag{3.13}$$

The flow in the manometer is given by $q = -A\frac{dh}{dt}$ from continuity. Substitution into Equation 3.13 and rearranging gives:

$$k = \frac{-A\frac{dh}{dt}\ ln\frac{R}{r_0}}{2\pi L(Pr_0 - P_R)} \tag{3.14}$$

The term $(Pr_0 - P_R)$ at any given time is the applied potential difference, H, substituting and rearranging gives:

$$\frac{2\pi Lk}{ln\frac{R}{r_0}A}dt = -\frac{dh}{H} \tag{3.15}$$

Integrating between the limits at time = 0, initial applied head = h_0 and at time T, head = h giving:

$$\int_0^T \frac{2\pi Lk}{ln\frac{R}{r_0}A}dt = \int_{h_0}^{h} -\frac{dh}{H} \tag{3.16}$$

$$\frac{2\pi Lk}{ln\frac{R}{r_0}A}T = ln\frac{h_0}{h} \tag{3.17}$$

Therefore:

$$k = ln\frac{h_0}{h}ln\frac{R}{r_0}\frac{A}{2\pi LT} \tag{3.18}$$

Equation 3.18 is used to calculate horizontal permeability. During the test the variation in potential over time is recorded in the same way as for the vertical permeability test.

3.1.3 Oedometer testing

An oedometer test is used to investigate the stress-strain behaviour in one dimensional compression and swelling of a low permeability soil. During this test, a soil sample is contained in a steel ring and submerged in a water bath. A vertical stress is applied to the sample and assumed to be acting uniformly over the sample. Drainage is allowed by porous stones placed at the top and bottom of the sample.

In a clay sample the response after the application of vertical load is not instant. An increase in load needs to be accompanied by expulsion of pore fluid. Initially, the increase in vertical load is taken by the pore-water pressure. As water is gradually expelled from the sample this is transferred as an increase in vertical effective stress. The rate of expulsion of pore fluid is dependent in part on the permeability of the sample.

Oedometer tests are typically completed in stages, where the vertical load is incrementally increased and decreased once either consolidation or swelling has stopped. Standard samples are typically 75mm in diameter and 20mm deep, however other sizes are available. The results from oedometer tests allow the stress-strain behaviour during one dimensional compression to be observed. Soil compression, swelling and bulk stiffness properties can be calculated during the loading or swelling stages.

3.2 Influence of soil structure on mechanical behaviour

This section covers existing studies on the influence of soil structure, as defined by Mitchell (1976), on the mechanical behaviour of soils. Cotecchia & Chandler (2000) aimed to develop the framework for structured clays proposed by Burland (1990) and Leroueil & Vaughan (1990).

Cotecchia & Chandler (2000) categorised the vast varieties of structures possible into two simple groups. The first being a ‘Sedimentation structure’, where the structure is formed during deposition and followed by one-dimensional compression. The term sedimented structure in Cotecchia & Chandler (2000) encompasses a range of different fabrics and varying degrees of particle bonding.

The second category is called ‘post-sedimentation structure’ encompassing all soils where other geological processes have acted after normal consolidation to alter the sedimentation structure. Geological processes can be said to include unloading, creep, thixotropy or post-depositional bonding. Processes such as cementation at deposition, weathering and tectonic

shearing were not included within the analyses presented. However, there are examples of clays where this framework could also be applicable.

Cotecchia & Chandler (2000) state that natural soils with a sedimentation structure follow a sedimentation curve (SC). In a voids ratio: effective stress space, the existence of a sedimentation curve was first observed by Terzaghi (1941) during compression tests. Figure 3.4 schematically illustrates the difference in one-dimensional compression behaviour between a structured and reconstituted sample. The structured sample can exist at a state that the reconstituted sample cannot, due to the structure developed during soil formation highlighted in Figure 2.1-2.2. Cotecchia & Chandler (2000) stated that it was useful to distinguish post-sedimentation structures that have undergone an unloading event from soil that has been subjected to other geological processes. If an unloading event had occurred, a clay should be referred to as an overconsolidated clay. If a clay's post-sedimentation structure was purely due to overconsolidation, it would return to its compression curve when loaded beyond its previous maximum effective stress.

The rate of loading due to geological events happens over a geological time scale. In contrast the loading rates of an engineering test are relatively fast. This typically results in the compression curve falling below the sedimentation curve shown as Z_1 in Figure 3.4. However, if the clay has a low sensitivity (i.e., between 1 and 1.5) or if the loading rates are comparable to geotechnical time frames, the measured compression curve tends to follow the sedimentation curve (Cotecchia & Chandler, 2000) shown as Z_2. The sensitivity of a soil can be defined as the ratio of the intact compressive strength to the remoulded material's compressive strength.

In Cotecchia & Chandler (2000) the term 'gross yield' is used to refer to a state that is outside what they define as the elastic stress domain in effective stress space. At this point, soil stiffness decreases significantly and strain increments become substantially larger due to soil structure degradation (Hight et al., 1992). Reconstituted clay may experience some additional bonding due to soil aging. Therefore, according to Cotecchia & Chandler (2000) the post sedimentation structure of a reconstituted material is only a result of unloading or creep. Natural clays, however, will have some diagenesis present in the post sedimentation structure. This means that once they are reloaded in an oedometer, they retain some of these elements. This can cause the compression curve to move beyond the sedimentation curve before what Cotecchia & Chandler defined as gross yield occurs. After this point the curve follows a much steeper path than the sedimentation curves. This potential loading path is represented as O-Y-Z_3 on Figure

3.5. The distance O-Y and the steepness of Y-Z_3 depends on the type of structure present (Cotecchia & Chandler, 2000).

Clays with a sedimentation structure at yield will have a yield stress ratio (YSR defined by Burland, 1990) equal to overconsolidation ratio (OCR). YSR is defined as the ratio between the yield stress and the effective overburden pressure. If post sedimentation structure is still present within the soil, the YSR is higher than the OCR. In general, it is the YSR that controls the compression and strength behaviour. Cotecchia & Chandler (2000) summarises that it is possible to find clays that have a variety of features:

1. Normally consolidated stiff and soft clays with sedimentation structure and a YSR of 1,
2. Overconsolidated stiff and soft clays that after testing have a gross yield very close or on the sedimentation curve (i.e., the YSR and OCR are the same or very similar), and
3. Soft and stiff clays which retain a substantial post-sedimentation structure post yield, leading to YSR significantly higher than the OCR ratio. (Such clays experience behaviour represented in Figure 3.5).

Cotecchia & Chandler (2000) reviewed compression curves of a variety of natural clays with known sensitivities. It was found that the lower the sensitivity the closer it sits to the intrinsic compression curve (ICL) from Burland (1990). Burland (1990) proposed the idea of one sedimentation compression line (SCL) for all natural clays. However, Cotecchia & Chandler (2000) proposed this should be seen as the average sensitivity for the data analysed and not as an inherent property of structured clays.

The sensitivity framework proposed by Cotecchia & Chandler (2000) is shown in Figure 3.6 for a natural clay with a sedimented structure and the same clay after reconstitution. Clays sheared from a YSR of 1 will typically exhibit peak undrained strength at the apex of the state boundary surface as shown in Figure 3.7. From this, the definition of sensitivity can be redefined as the ratio of the vertical size of the state boundary surface (SBS) for natural clay and the corresponding reconstituted clay (for the same specific volume).

The friction ratio at Critical State is regarded as a normalising factor for strength across different soil compositions (Coop et al., 1995). Cotecchia & Chandler (2000) followed this assumption, stating that after normalisation, the state boundary surface should be the same for clays with equal sensitivity, even if the type of structure and composition differ. Figure 3.8 illustrates the general behaviour of different natural clays of the same sensitivity. Clays A and

B are overconsolidated clays of different compositions consolidated to different *in situ* voids ratios, but their structures at gross yield have similar strength sensitivities. Therefore, their gross yield points in isotropic compression are located on the same isotropic gross yield surface. This also applies to clays with a post-sedimentation structure, indicating that clays with the same sensitivity but different post-sedimentation structures will also share the same SBS. Cotecchia & Chandler (2000) state that highly sensitive clays are unlikely to exist at higher stresses due to convergence towards the ICL.

To test the validity of the proposed framework, it was applied to variety of naturally occurring soils. One example is Sibari clay, which is a thinly layered clay with bands of silt and fine sand. The results of oedometer and zero lateral strain triaxial tests from Coop & Cotecchia (1995) are shown in Figure 3.9. This demonstrates that gross yield extends beyond the ICL and then converges to a narrow band with an average sensitivity of 3. This behaviour is a common feature of layered soil samples (Coop & Cotecchia, 1995).

The stress paths of reconstituted Pappadai Clay and the gross yield states of natural Pappadai Clay specimens from a single depth, consolidated to a range of mean stresses prior to gross yield, are shown in Figure 3.10 (Cotecchia & Chandler, 1997). Figure 3.10 has been normalised by equivalent pressure, p_e^*, to account for the effect of volume on clay strength. The samples were consolidated to 200kPa, then consolidated isotopically or under K_o conditions prior to shearing. Note that the asterisk is representative of the intrinsic behaviour as introduced by Burland (1990). The yield locus for the natural sample has the same geometric shape, with the main difference being the size of the SBS. Also shown in Figure 3.10 is the stress path of a sample tested after it had been compressed post gross yield. Cotecchia & Chandler (1997) state that this sample shows a lower strength sensitivity due to the weakening of bonds and structural changes within the sample and hence this plot is within the SBS.

The plots can be further normalised such that the SBS are normalised by composition, structure and volume. Both the natural and the reconstituted samples can be seen to follow the same SBS. When plotted against the normalised SBS for Bothkennar clay, it demonstrates the general applicability of the idea that there may be one SBS surface for all clays after normalisation (Figure 4.11).

Cotecchia & Chandler (2000) and other research (i.e. Burland, 1990 and Leroueil & Vaughan, 1990) have highlighted the difference in behaviour between structured and reconstituted samples. Specifically, that it is possible for a structured clay to exist at a state not achievable

by a reconstituted sample. However, there is still a geometric similarity between the behaviour of a structured clay and a reconstituted clay as highlighted in the sensitivity framework proposed by Cotecchia & Chandler (2000).

3.3 Influence of soil structure on permeability

As well as affecting the mechanical behaviour of a soil, differences in soil structure also affect the flow of water through a soil sample. In a sample with a sedimented structure similar to Figure 2.1 the vertical permeability will be governed by the fine grained material and the horizontal permeability will be governed by the coarser grained material. This anisotropy is primarily governed by the layering within the sedimented sample rather than differences in soil particle arrangement.

There is limited availability of data on anisotropy of permeability. On-site testing typically consists of borehole pumping tests. Within a laboratory, permeability is commonly determined from a falling head permeameter or inferred from consolidation tests such oedometer or triaxial tests. These methods provide a single value of permeability, not independent measurements of vertical and horizontal permeability. From the studies available, which are discussed below, it is evident that a layered sedimented soil enhances permeability anisotropy.

Al-Tabbaa & Wood (1987) investigated how the ratio of vertical to horizontal permeability varies with voids ratio for reconstituted kaolin clay. The tests conducted by Al-Tabbaa & Wood (1987) provided an indication of baseline permeabilities and anisotropy of reconstituted clay soils typically used in centrifuge soil beds. The equipment developed by Al-Tabbaa & Wood (1987), as described in Section 3.1.2, was used to directly measure the vertical and horizontal permeability of reconstituted Speswhite kaolin clay. Speswhite kaolin clay is extensively used for centrifuge modelling, the source of kaolin has changed over time and the properties are not necessarily the same as today. Al-Tabbaa & Wood (1987) reports that the kaolin tested had a liquid limit of 0.69, a plastic limit of 0.38 and 80% of particles were smaller than 2μm. To prepare samples for testing, kaolin clay was mixed to form a slurry of 120% initial water content and placed into the oedometer, resulting in a height of sample of approximately 20mm at the start of falling head tests. Throughout the falling head tests, the change in head was recorded over a period of 24 hours, with a consistent initial applied head of 400mm.

The permeability was calculated from the procedure outlined in Section 3.1.2. The results of the falling head radial flow tests are shown in Figure 3.12. The relationship between time and the logarithmic head are linear and the only notable deviations observed from this linearity

occurred during the first 15 minutes (Al-Tabbaa & Wood, 1987). Values of horizontal and vertical permeabilities obtained from these tests are plotted against voids ratio in Figure 3.13.

Al Tabbaa & Wood (1987) comment that at the start of the test, when the clay was a slurry the voids ratio was approximately 3.1, and the clay particles exhibited a random distribution with no preferred particle orientation. Therefore, in this initial state, the permeability is essentially homogenous. As the clay slurry was consolidated there was orientation of clay particles, with the platelets rotating perpendicular to the direction of applied load. Therefore, the horizontal permeability became larger than the vertical. The change in permeability versus voids ratio was also smaller in the horizontal direction. These results demonstrate how all samples have a structure and inherent anisotropy, a sedimented sample with layering as depicted in Figure 2.1 increases the magnitude of this anisotropy.

The same investigation was conducted for an overconsolidated specimen. The vertical and horizontal permeability tests were undertaken during the unloading and reloading cycles. Figure 3.14 shows the results from these tests, along with those from the normally consolidated samples, represented by the lines labelled Equations (4) and (5). This shows a reasonable correlation between the data of the overconsolidated and normally consolidated clays. Therefore, the permeability of a clay appears to be primarily dependent on the voids ratio and independent of the overconsolidation ratio. A sedimented structure allows a soil to exist at a voids ratio not possible for a reconstituted sample, therefore permeability would be larger than a comparative reconstituted sample under the same effective stress.

It has been established that one-dimensional vertical consolidation with radial drainage can lead to non-uniformities in effective stresses and deformations. This is because the clays drained faster near the boundaries causing stresses and stiffness to build up more rapidly in these areas (Gibson et al., 1963). Atkinson et al. (1985) suggested that these non-uniformities are negligible if the loading rate is sufficiently low. During the oedometer tests the load was increased every two days, and at the end of each experiment the variation of water content within the sample was measured. Al Tabbaa & Wood (1987) noted that the variation of water content was less than the accuracy of the measurements.

Al-Tabbaa & Wood (1987) identified that other potential errors in this test arise due the application of a head of water, which leads to reductions in effective stresses. This effect is greatest near the drainage boundaries, causing swelling and consequently a change in voids ratio and permeability. Secondly, some of the incoming water is consumed in saturating the

sample during swelling and, therefore, does not pass through the entire sample. The initial fall in head is therefore due to the permeability of the clay and the swelling induced by the applied head. As the applied head decreases, the clay begins to recompress, and the rate at which the water flows out of the sample exceeds that at which it enters. To mitigate this the sample could be clamped, however this would create complex stress conditions and would not prevent local swelling near the drainage boundaries. Instead, the sample was allowed to swell during the tests and the applied head was kept low to minimise this effect. The overall swelling was measured during each test and there was an insignificant change in voids ratio of around 0.001.

The initial permeability deduced from laboratory tests can be considerably higher than those determined using other apparatus such as flow pumps (Pane et al., 1983). Flow pumps allow for very low flow rates to be induced with very low head differences, which can be measured accurately. The values of permeability at the later stages of falling head tests are much closer to the values obtained by pump tests. Pane et al. (1983) suggested the discrepancy was related to the applied hydraulic gradient, however, Al-Tabbaa & Wood (1987) suggests that the discrepancy was due to the applied head. When conducting laboratory permeability tests, the increased permeability measured during the early stages of the test needs to be considered when analysing results.

There have also been studies of the permeability of naturally occurring soil samples. Burland & Hancock (1977) conducted a feasibility study for the construction of an underground car park near the Palace of Westminster. As part of this study, 14 boreholes were drilled and the ground profiles obtained coincided with the later work by King (1981) on the layers of London Clay. A summary of the borehole logs is shown in Figure 3.15. Additionally, a series of standpipes were installed to measure the ground water profile and these were later used to conduct *in situ* permeability tests. The measured permeabilities are shown in Figure 3.16 and they align with the material descriptions at different horizons. The permeability decreases from $3x10^{-7}cms^{-1}$ near the top of the layer containing sand partings to $3x10^{-9}cms^{-1}$ at the intact clay horizon. The permeability then increases again to $10^{-7}cms^{-1}$ where there was predominately a silty clay.

Hight et al. (2003) conducted a similar series of experiments in which the horizontal permeability was measured in London Clay through an *in situ* constant flow permeability test. The results are consistent with those presented by Burland & Hancock (1977) (Figure 3.17). The highest permeability was within the region where there were sandy layers. Figure 3.17

from Hight et al. (2003) shows that the permeability decreases with depth. The cause of this can be attributed to the positions of the sand and silt beds and a decreasing voids ratio with depth, but it is impossible to split the effects. There is a common feature of increasing silt sized fractions at the top of the of each London clay unit, and consequently, the horizontal permeability is higher at these locations (Hight et al., 2003).

Chandler et al. (1990) also measured the permeability of London Clay. Figure 3.18 shows a schematic of the ground conditions at the test site. The permeability was measured both *in situ* and in the laboratory, using an oedometer and triaxial cell. To measure both the vertical and horizontal permeabilities in the laboratory, block samples were removed and transported in casing tubes. Chandler et al. (1990) stated that they did not show any signs of visual disturbance after transportation. For vertical permeability measurements, samples were trimmed vertically from the block sample and for horizontal permeability measurements, samples were trimmed from the horizontal plane. Table 3.1 provides a summary of the *in situ* permeability measurements and Table 3.2 summarises the laboratory measurements . Both sets of results are plotted in Figure 3.19 . It can be determined that the ratio of horizontal to vertical permeabilities is approximately 2.

Larsson (1981) reported permeability and permeability anisotropy data of very soft marine clays, which exhibited a modest anisotropy of 1.1. The structure of soft marine clays are very similar to the slurry stage of the kaolin tests conducted by Al-Tabbaa & Wood (1987). The soil structures were essentially random with very little particle orientation and hence very modest anisotropy lower than Chandler et al. (1990) and consistent with the measurements taken at a slurry state from Al-Tabbaa & Wood (1987).

Chandler et al. (1990) investigated the relationship between voids ratio and permeability in both the vertical and horizontal direction of London clay, by consolidating horizontal and vertically trimmed sample in an oedometer cell. The results are presented in Figure 3.20, as voids ratio decreases the value of permeability anisotropy also decreases. This was not consistent with Larsson (1981) or Al-Tabbaa & Wood (1987). The authors did not address this, but the graph plotted appears to be from limited tests results and because the samples were extracted and trimmed the effect of sample disturbance was unknown. These samples due to their nature may have included other features such as fissures potentially increasing permeability. Both the above could have contributed to the difference of behaviour.

Little et al. (1992) completed a series of laboratory tests measuring the permeability of Bothkennar clay samples with different soil structures. Bothkennar clay can be divided into four distinct sections as in Paul et al. (1992). The top layer constitutes a weathered zone, with the remainder split into three layers where each has a distinct fabric. The three fabrics were: bedded, mottled, and laminated and they reflect their depositional environments. Due to the different fabrics, the permeability and permeability anisotropy of each of the layer should differ. The laminated sections show the highest degree of anisotropy due to the silt layer significantly aiding horizontal drainage. The mottled facies have a more modest anisotropy due to the disruption caused by bioturbation of the original horizontal layers.

The permeability of samples collected at three different depths were tested using a modified oedometer (similar to that described in Al-Tabbaa & Wood, 1987). The results of the tests can be seen in Figure 3.21. In the first data set presented there were some irregularities which were discounted by the author. Excluding 1A -V the permeability data was homogenous at this depth aligning with the mottled or bedded structure (Little et al, 1992).

At a depth of 8m, there was a much higher degree of anisotropy if 15A-H is disregarded as recommended Little et al. (1992). This depth corresponds with the laminated beds explaining the higher anisotropy ratio of approximately 8. The samples taken from the final depth showed modest anisotropy, there was visibly less horizontal layering within these samples. This highlights the influence of layering within a sedimented structure, causing the horizontal permeability to be approximately an order of magnitude larger than the vertical permeability.

Mahasneh & Shawabkeh (2004) were investigating the use of sand-cement-clay mixtures for the encapsulation of heavy metals. Part of the study involved a series of tests in which varying proportions of sand and clay were reconstituted to investigate the effect on permeability. The results were obtained using a falling head permeameter and plotted in Figure 3.22. The test series demonstrated that when a relatively low proportion of clay was introduced to a sand sample, the permeability reduced drastically. When clay content was between 20-30% the sand-clay mix showed the same permeability behaviour as a 100% clay sample.

Shaker & Elkady (2015) conducted a similar investigation, in which varying portions of sand and Al-Qatif clay were reconstituted. These mixtures were then compacted and subjected to a series of vertical constant head permeability tests. The samples were prepared at both optimum and wet of optimum water contents. Scanning electron microscopes were used to explain the effect of fabric on permeability. For clay contents of 20% sand grain-to-grain contacts

remained established with skeletal pores clearly visible. The clay particles either sit within the pores or coat the sand particles (Figure 3.23). Therefore, the permeability is governed by these pores, with the permeability being within one order of magnitude of clean sand.

When the clay content was increased to 30% there were still grain-to-grain contacts visible however, clay was filling most of the pores. Clay flocs begin to emerge, and this starts to force sand grains apart (as seen in Figure 3.24). Increasing the clay content beyond 30% the coating around the sand particles increased and there was full separation between the sand grains. At this point the clay forms a continuous matrix and the pores between the sand grains are almost completely infilled with clay particles. The permeability behaviour was therefore governed by the clay.

Shaker & Elkady (2005) reported a similar pattern of results to that in Mahasneh & Shawabkeh (2004). Even with a relatively low clay content (<30%) the vertical permeability was governed by the clay. In the case of a sample with a sedimented structure and considering the entire soil element i.e. Figure 2.1, the vertical permeability is governed by the finer material and the horizontal governed by the coarse material layer. Consistent with tests on laminated soils conducted by Little et al, (1992).

3.4 Summary

Sedimented clay behaviour has been observed and compared to reconstituted samples. When evaluating soil beds with a sedimented structure suitable for centrifuge modelling the same approach was adopted to verify the formation of a sedimented structure. The key indicators being that the sedimented sample should have a sensitivity, determinable through difference in normal compression lines, undrained shear strengths and the size of state boundary surfaces. Secondly, a sedimented clay should have an anisotropic permeability, because larger particles settle before smaller particles creating a layered soil. Additionally, it is typically possible to see identifiable layers. A combination of these indicators was used to assess the success of the different preparation techniques within this dissertation.

4. Centrifuge modelling

Element tests have measured the influence of structure on engineering properties. Field monitoring and numerical analyses have highlighted the impact of soil structure and anisotropic permeabilities on the resulting movements. Wongsaroj et al. (2007, 2013) and others have explained the need for more long-term monitoring, soil permeability and tunnel permeability data to validate numerical models.

Geotechnical centrifuge modelling is an established technique for investigating the ground response to complex geotechnical construction events and could be used to provide this currently missing data. Typically, centrifuge models are created from reconstituted soil. If a method for creating centrifuge samples with a sedimented structure and representative permeabilities could be established, it would enable construction events in a variety of different soil beds, including long-term movements, to be investigated.

This chapter provides an introduction to the principles of centrifuge modelling and the typical methods used to create a clay bed for use in a centrifuge model test.

4.1 Principles of centrifuge modelling

It is well known that soil behaviour is a function of stress level and stress history. *In situ* stresses change with depth and thus, geotechnical physical modelling generally requires the replication of a representative *in situ* stress profile (Mair, 1979). Achieving a similar stress history is typically achieved by applying a surcharge and allowing for consolidation. However, achieving a representative stress profile is not as simple and for this reason it is difficult to model scaled geotechnical construction events at 1g hence why centrifuge modelling is such a powerful tool for geotechnical engineers. In centrifuge modelling, a scaled soil model is subjected to a radial acceleration field many times that of Earth's gravity (Taylor, 1995). A stress similarity of the model and prototype can be achieved such that the stress at depth, h_p, in the prototype will be identical to the stresses in the reduced scale model at a depth, h_m.

$$h_m \mathrm{N} = h_p \tag{4.1}$$

Where N is equal to a radial acceleration N times greater than Earth's gravitational field, this forms the basis of the principal scaling law in geotechnical centrifuge modelling.

A soil model is created within a strongbox and placed on the arm of the geotechnical centrifuge. As the model is spun it is subjected to a radial acceleration field. Newton's second law of motion states that pulling a mass out of a straight path into a radial path will impose a radial acceleration towards the centre of rotation. This acceleration is given by;

$$a = \omega^2 r \tag{4.2}$$

Where;

a is the radial acceleration (m/s^2),

ω is the angular velocity (rad/s),

r is the radius from the centre of rotation (m), and

N is then defined as the gravity scaling factor as and can be given by the following equation;

$$N = \frac{a}{g} \tag{4.3}$$

Using the relationship from Equation 4.1, a model can be scaled at 1: N of the prototype scale. Ensuring the geometric conditions are the same in the model and prototype during the experiment when it is subjected to an acceleration field of N*g*.

4.2 Scaling laws

A stress similarity between the prototype and model forms the primary scaling law. The vertical stress in the ground at a prototype scale is given by:

$$\sigma_{vp} = \rho g h_p \tag{4.4}$$

Then the scaled model subjected to a radial acceleration field is given by:

$$\sigma_{vm} = \rho N g h_m \tag{4.5}$$

Where;

p denotes prototype,

m denotes model, and

ρ is density of soil

For stress similarity:

$$\rho g h_p = \rho N g h_m \tag{4.6}$$

Hence:

$$\frac{h_p}{h_m} = \mathrm{N} \tag{4.7}$$

A scale factor of 1: N can therefore be applied for all linear dimensions, including geometric components of the model and the resulting displacements.

Another scaling law applying to a centrifuge test pertains to consolidation. Darcy's law can be applied to a centrifuge model by considering the hydraulic gradient as a pressure gradient in both the model and the prototype. While the pore pressures remain constant in the model and prototype, the distance in the model is reduced such that:

$$i_m = N i_p \tag{4.8}$$

If the soil and permeability is the same in both the model and prototype then:

$$v_m = i_m k_m = N i_P k_P = N v_p \tag{4.9}$$

Meaning that seepage velocity has a scale factor of 1: N, (i.e., the flow paths through which the pore fluid flows also have a scale factor of 1: N). The time for seepage flow is given by:

$$t_m = \frac{L_m}{v_m} \tag{4.10}$$

$$t_m = \frac{L_p}{N} \frac{1}{N v_p} \tag{4.11}$$

$$t_m N^2 = t_p \tag{4.12}$$

Therefore, the scaling factor for seepage is 1: N^2.

Consider the dimensionless time factor, T_v, defined as:

$$T_v = \frac{c_v t}{H^2} \tag{4.13}$$

Where;

c_v is the coefficient of consolidation,

t is the time,

H is the drainage path length, and

If the time factor is the same for both the model and the prototype:

$$\frac{c_{vm} t_m}{H_m^2} = \frac{c_{vp} t_p}{H_p^2} \tag{4.14}$$

Using Equation (4.7);

$$t_m = t_p \frac{1}{N^2} \frac{c_{vp}}{c_{vm}} \tag{4.15}$$

If the soil is the same in both the model and prototype, then there is the same scaling factor for seepage flow of 1: N^2. Therefore, the seepage flow or a consolidation event over 400 days can be modelled in under 1 hour at $100g$. Centrifuge modelling scaling factors are not limited to those presented above; however, they are most relevant for this study. Marshall (2009) provides details of further scaling laws for wider geotechnical centrifuge applications.

4.3 Errors in centrifuge modelling

4.3.1 Variation in vertical acceleration field

The vertical stress in the model is dependent on the weight of soil above (as in the prototype). At prototype scale the Earth's gravity is typically considered constant over the distances relative to geotechnical engineers. However, this is not the case in centrifuge modelling. From Equation 4.2 the acceleration experienced by the model varies with radius i.e., within the model there is a linearly increasing acceleration. Therefore, the stress profile is not the same as the prototype.

Taylor (1995) compared the distribution of vertical stresses in the model and the prototype and proposed that the effective radius is set to one-third of the depth of the model. This minimises the under and over stresses within the model and ensures that at two-thirds of the model depth,

the model and prototype experience same vertical stresses. Taylor (1995) calculated that the majority of centrifuge models are less than 20% of the effective radius, resulting in a maximum error in the stress profile generally less than 3%.

4.3.2 Rotational acceleration field

Creating an inertial acceleration which is directed towards the centre of rotation also results in a lateral component of acceleration within the model. This effect is most pronounced at the models boundaries, to minimise this effect any activity should be modelled on the centreline of the model. It is considered good practice to place the centrifuge model such that its smallest plan dimension is in the radial plane (Taylor, 1995).

4.3.3 Particle size effects

Another concern for centrifuge modelling is whether scaling laws affect the soil particles themselves. If that was the case, a clay particle of 2-micron diameter at 100g would have a diameter of 2mm, similar to a fine sand. Taylor (1995) explained how this argument is fundamentally flawed as clay and sand exhibit very different stress-strain characteristics. Taylor (1995) also provided practical steps to avoid particle size effects in specific scenarios (i.e., soil continuum behaviour). Taylor (1995) did acknowledge however that there are some circumstances where particle size effects could be significant and there needs to be appropriate investigation to assess the potential impact.

4.4 Creating clay samples for centrifuge modelling

Centrifuge models can be performed on natural samples, but due to inherent variations in structure, inclusions and fissures, obtaining repeatable samples becomes difficult. Therefore, to represent more general conditions, reconstituted models are used with well-defined soil properties. This also allows for numerical models to be evaluated.

Remoulded fine-grained samples are reconstituted from a slurry, by mixing the soil with water to form slurry at a water content to approximately twice the liquid limit. This creates a smooth and easy to pour mixture. Distilled water is commonly used to create the slurry to minimise any chemical effects and avoid bacterial growth. The mixing procedure can be completed under a vacuum to de-air the sample. Subsequently, the slurry is carefully placed into the soil container, ensuring no air pockets are trapped in the sample.

There are two common options to consolidate the slurry: either under self-weight on the centrifuge or using a consolidation press. When consolidating a sample on a centrifuge,

precautions must be taken to avoid the generation of high pore pressures within the sample, leading to piping and preferential drainage. This is done by allowing the sample to consolidate in stages at incrementally increasing g levels. Consolidation of deep clay samples in a centrifuge is therefore a lengthy process (Taylor, 1995).

Alternatively, a consolidation press can be utilised for the consolidation process. Initially, small increments of stress should be applied to avoid clay slurry extrusion from the sample. To monitor consolidation the vertical settlement and/or expelled pore water are measured. After the initial consolidation phase has finished the applied stress can be doubled until the required stress is achieved. The samples can be allowed to swell under a lower applied stress to create an overconsolidated sample. This process creates a uniform consolidation pressure throughout the entire model. When removing the model from the consolidation press the drainage taps should be closed prior to unloading the sample to avoid re-entry of water. The model must establish full equilibrium of effective stress conditions before testing. For deep samples this can be lengthy process. Taylor (1995) details several techniques that could be implemented to reduce the consolidation time required.

Kaolin clay is frequently used in centrifuge modelling, due to its relatively high permeability which reduces consolidation time and ultimately the model making and testing procedure. Other source materials and combinations of clay, silt and sand can be used to achieve a wider range of soil responses (Taylor, 1995). Upon completion of a centrifuge test at the geotechnical centrifuge centre at City, University of London, the kaolin clay forming the soil test bed is recycled. This is achieved by trimming contaminated sections of the model and remixing with distilled water to form a new slurry, which following the addition of new kaolin powder and the same consolidation procedure creates another centrifuge sample.

Centrifuge modelling has been successfully used to investigate the short-term response to complex geotechnical construction and loading events. Nevertheless, a fundamental disparity exists between the reconstituted soil models created and naturally occurring soil deposits with a sedimented structure. As highlighted in previous sections, soil structure and layering changes permeability and mechanical behaviour. The use of reconstituted centrifuge models has constrained studies investigating a construction event. If a method were developed to create geotechnical centrifuge soil samples with layering and a sedimented structure it would enable the investigation of geotechnical construction events, in various ground conditions, both in the short and long-term.

5. Previous methods of creating structured/anisotropic soil beds

There have been previous attempts to recreate soil beds with a sedimented structure in the laboratory. Sedimentation column tests have studied the soil formation process and how various factors influence the resulting soil fabric. Sedimentation columns have also been used to create samples suitable for use in standard element tests to investigate whether laboratory sedimented samples fit the same framework as naturally occurring structured soil deposits.

At a geotechnical modelling scale, similar efforts have been made to include structure and layers into soil beds suitable for centrifuge modelling. This chapter presents the findings from these studies, describing the slurries and slurry conditions that facilitate the development of a sedimented structure. It also outlines current methods of creating layered soil beds for centrifuge modelling and sedimentation on the centrifuge. Finally, the chapter summarises previous studies and how these inform the basis of a method of sedimenting a soil bed for use in centrifuge modelling.

5.1 Sedimentation column tests

Sedimentation column tests are typically performed in Perspex or glass columns, where solutions of water and soil (and sometimes salt/chemical additives) are mixed (Been & Sills, 1981 and Imai 1980). These mixtures are placed into the column and allowed to settle to form a soil layer which consolidates as a result of self-weight. By monitoring the soil sedimentation process and testing the resultant soil sample, it is possible to characterise different soil samples.

After observing different sedimentation column experiments, Imai (1980) proposed four types of soil settlement where each have distinctive features. When the initial slurry concentration (soil weight per unit volume of slurry) is very low, the particles are free to settle without interaction between the soil particles. In this case, settlement is governed by Stokes law and this is referred as ‘dispersed free settling’. The second type of settlement proposed is ‘flocculated free settling’. As the initial slurry concertation increases, larger particles fall through the soil slurry and are interrupted by smaller particles, combining to form flocs. The initial slurry concentration remains low enough to allow these flocs to be sorted by their respective sizes.

As the initial concentration increases further, flocs continue to form however, due to the floc concentration and the resulting interaction between flocs, they are no longer able to be sorted by size. Instead flocs settle at a uniform rate, with a visible sharp interface between the soil and

the clear dispersion fluid above. This settlement type is referred to as ‘zone settling’. If the initial slurry concentration increases further, no visible flocs are formed, and the mixture settles at a uniform rate solely due to self-weight consolidation. This is known a ‘consolidation settlement’. Table 5.1 summarises the different settlement types with their key features.

Imai (1980) notes that when studying the sedimentation of different clay minerals, several questions were raised; what types of settling can occur in clays, what factors influence the resulting sedimentation type and how these factors affect settling characteristics?

It was broadly understood that settling behaviour is dictated by a combination of four factors;

1. Type of solid materials, especially for clays,
2. Type of dissolved electrolytes,
3. Concentration of solid material, and
4. Concentration of salt within the dispersion water.

Imai (1980) focused on varying factors 1,3 and 4 while not attempting to change the physico-chemical nature. The soils sedimented included three types of bay muds from three different bays in Japan, as well as commercially available kaolin powder and bentonite powder. Table 5.2a & 5.2b list the properties of all the materials tested, and Figure 5.1 shows their corresponding grading curves.

To prepare the samples, a predetermined amount of water, soil and salt were thoroughly mixed to create a slurry. Water content accounted for salt content using the corrected water content as per Imai et al. (1979). Once fully mixed, the slurries were transferred to the sedimentation columns. These columns were 250mm high with a 50mm internal diameter, fabricated from transparent acrylic tube. Multiple tubes could be stacked and sealed allowing for larger sample heights to be created.

Imai (1980) classified the types of settling based on photographs taken during the sedimentation process. Photographs were captured using a camera (specific details not provided) with five additional lenses to achieve required levels of magnification to see floc formation.

In the first test series, slurries of Ohsaka Bay mud at a variety of different initial water contents ranging from 700-6000% water content were allowed to sediment. The resulting sedimentation curves are presented in Figure 5.2. Imai (1980) identified three distinct stages within the sedimentation process. By observing the sedimentation curve of only the 2000% initial water

content sample (shown in Figure 5.3) the different stages can be clearly identified. During the initial stages there was no movement of the slurry water interface, but flocculation could be observed in the photographs taken during the experiment. This was referred to as the 'flocculation stage' and the time taken for this to occur was called 'flocculation time'.

The second stage was the settling stage, categorised by a sharp interface formed between the dispersing flocs and the clear water above. For the Ohsaka Bay mud, this represented a constant rate of settlement, as illustrated by the linear section of Figure 5.3. The final stage was the consolidation stage, during which movement of the interfaces reduces significantly. Analysis of the photographs taken during this period demonstrated that the flocs have settled and are in contact with each other. Any further reduction in the interface height was due to the increased load imposed, as a result of self-weight consolidation.

Imai (1980) stated that the resultant sedimentation type was governed by a combination of the degree of flocculation and the number of mutual interactions between the flocs. Imai (1980) explained how the former is dependent on the salt concentration and the latter a function of the initial water content of the slurry. Another important factor is the type of clay that is sedimenting. Imai (1980) conducted a series of tests where the five different clays previously listed where allowed to sediment over a range of water contents and salt concentrations. The slurries were mixed to predetermined salt and water contents and poured into the sedimentation columns, ensuring that the initial slurry volume was the same.

Figure 5.4 shows the results of the tests conducted. Imai (1980) noted how the zoning presented in Figure 5.4 was likely to be a crude approximation, and instead, there was likely to be a transition between the zones rather than a distinct boundary as illustrated. The three natural bay muds show very similar behaviour, and for dispersed free settling to occur very low salt concentrations were required. In contrast kaolin clay showed no variation in behaviour with salt content. The only factor that affected the settlement behaviour was the initial water content. A low sensitivity to salt content was a feature associated with low plasticity minerals Imai (1980). Dispersed free settling did not occur under the range of water contents that were tested for kaolin clay.

From these sedimentation tests, it appears that to create a sample with a sedimented structure, the initial slurry would need to allow for particle separation to occur i.e., to be within the free or flocculated free settling regions defined by Imai (1980).

Sridharan & Prakash (1997) conducted a series of sedimentation column experiments and confirmed the four different types of settlement proposed in Imai (1980). Sridharan & Prakash (2001a) conducted a series of tests very similar to that conducted by Imai (1980) and the soils tested by Sridharan & Prakash, (2001a) are listed in Table 5.3. The tests were completed using fresh water with a pH of 7.2 and with water contents ranging from 100% to 4000%. Figure 5.5 shows the resultant sedimentation curves for the soils tested; the bentonite was omitted from this study by the authors as bentonite takes a long time (over two years) to sediment. The boundary between dispersed and flocculated settling was determined by the observed settling characteristics. Where there was dispersed settling, the soil sample steadily rose, whereas during flocculated settling the soil/sedimentation line initially rose but then became hidden in the dispersion fluid. After a period, it reappeared at a new higher level and then started to move downwards. Above the soil formation line, there was a cloudy suspension of relatively low soil concentration.

Figure 5.6 illustrates the relationship between plasticity index and critical water content (the minimum water content required for dispersed settling). For kaolinitic soils, there is a clear relationship: as the plasticity limit decreases, the critical water content increases. Hemavathi Project Soil, Kaolinite and Red Earth are likely to experience flocculant behaviour due to the presence of kaolinite, a mineral known for its flocculant fabric (Sridharan & Prakash, 2001a). Consequently, low plasticity kaolinitic soils can exhibit flocculated settling even at very high initial water contents.

Similar findings were reported by both Imai (1980) and Sridharan & Prakash (2001a) regarding the types of settlements and the characteristics associated with each. However, there was a significant variation in the initial water content required for each settlement type to occur. In the range of water contents tested by Imai (1980), no instances of dispersed free setteling were observed in the kaolin tests. In contrast, Sridharan & Prakash (2001a) reported this occurred at a water content of approximately 1300%. At this water content Imai (1980) observed zone settling. Even though the materials tested were not identical, the plasticity index of the kaolinite tested by Sridharan & Prakash (2001a) was lower than the kaolin powder used by Imai (1980). The relationship proposed by Sridharan & Prakash (2001a) suggested that the kaolinite they tested should have a higher critical water content.

Been & Sills (1981) conducted a series of sedimentation column tests to investigate the sedimented process of different slurries. During the tests density measurements of the settling

soil were obtained using X-ray and later compared to numerical predictions. The sedimentation columns used for the test series were constructed from 2m high and 102mm internal diameter acrylic tube. The test soil was an estuarine mud collected from Combwich; Somerset. To grade the material, it was sieved and the material passing the smallest sieve (75-micron) was used. This resulted in a uniformly graded silt with a 30% clay content which flocculated in tap water.

The slurry was prepared by mixing the appropriate amount of soil and tap water to achieve the desired initial water content. Before being placed into the sedimentation column, the slurry was subjected to a controlled mixing procedure. The solutions used are detailed in Table 5.4, for ease of comparison with other studies the initial densities in Table 5.4 have been converted to initial water contents and provided in Table 5.5. Throughout these tests the total stress and the pore-water pressure were recorded using pressure transducers within the sedimentation column.

There was a distinct pattern to the density profiles obtained during these tests (Figure 5.7, X-rays from Been, 1980). Figure 5.7 details the density profile for a sample with an initial water content of around 650%, however, the same trend is visible for all initial water contents higher than this. At the base of the sample, a well-defined band of high-density material formed rapidly. Above this, there was an intermediate density region that rises less rapidly, with a clear distinction between this region and the much lower density suspension above. Over time, the height of the sample gradually reduced, resulting in an increase in density. In contract, for a slurry with an initial water content of around 380% (shown in Figure 5.8), the initial water content was low enough for a stress-free state not to exist. Consequently the features described in Figure 5.7 were not present.

The method used by Been & Sills (1981) to determine whether particle size sorting and a sedimented structure had occurred was to obtained complete particle size distributions at different depths. If the particle size distribution remained constant at different horizons dispersed or flocculated free settlement had not occurred and a sedimentation structure had not developed. Figures 5.9-5.11 show particle size distribution at various depths for three sedimentation tests conducted using the same soil with different initial water contents. Figure 5.9 presents the particle size distributions of a sample sedimented from a slurry at an initial water content of 250%. There is no difference in particle size distribution at the top, middle and bottom of the sample. Where in the sample with an initial water of around 650% (shown

in Figure 5.10) there was more fine material present at the upper horizons and more coarse material present at the lower horizons.

Figure 5.11 presents the results from a sample sedimented from an initial water content of 1300% with an added dispersion agent (sodium hexametaphosphate). A greater difference in the particle sizers throughout the sample was observed, with most of the fine material at the top of the sample and most of the coarser material at the base. Been & Sills (1981) noted that the critical density or critical water content required that prevents a stress-free suspension was likely to be dependent on a variety of factors as previously stated in studies such as Imai (1980). Been & Sills (1981) created layered soil samples by sedimentation and quantified the difference between samples using particle size distribution and density profiles as opposed to using only visual observations as occurred in studies such as Imai (1980) and Sridharan & Prakash (2001a).

Sridharan & Prakash (2001b) conducted sedimentation column tests to study voids ratio with depth in soft sediments for land reclamation projects. Sridharan & Prakash (2001b) state that separation of different particle sizes during sedimentation is influenced by factors such as, the initial water content, salinity, mineralogical and environmental factors, consistent with previous research. The authors also state that this was more likely to occur in freshwater environments, where separation can be expected even at low water contents.

The sedimentation columns used in Sridharan & Prakash (2001b) were constructed from glass tubes of 61.1mm diameter. To create the slurry, the natural soils were oven dried and mixed with deionized water to form a slurry of the desired water content. The slurry was stirred in a repeatable method, similar to Been & Sills (1981). The soils used for these tests are the same as those used in Sridharan & Prakash (2001a) (shown in Table 5.3).

Figure 5.12 illustrates the variation of voids ratio with depth for two kaolinite slurries: one with a water content of 1.5 times the liquid limit and one with 4 times the liquid limit. To obtain voids ratio with depth, the water content was measured. A comparison between the variation in voids ratio with depth profiles highlighted that there was a larger variation in the sample prepared from 4 times the liquid limit. Sridharan & Prakash (2001b) attributed this to particle separation.

The sample with an initial water content of 1.5 times the liquid limit showed little variation in voids ratio and therefore it is unlikely that particle separation had occurred. In the sample prepared at 4 times the liquid limit, the lower horizons had a lower voids ratio and the upper

regions had a much higher voids ratio. Sridharan & Prakash (2001b) attributed this to particles separation and claimed this was confirmed by particle size distributions; although these data were not presented.

Sridharan & Prakash (2001b) investigated the difference in compressibility between a sample where the particle size reduced towards the top of the sample which they called a segregated sample and a sample where the particle sizes where constant with depth through the sediment, a non-segregated sediment. After sedimentation, the samples underwent seepage consolidation tests and the results are presented in Figure 5.13. It is evident that as the initial water content increases, the voids ratio at which the sample can exist also increases, consistent with findings from the literature on natural sedimented samples (i.e., Cotecchia & Chandler, 2000). Sridharan & Prakash (2001b) noted that during consolidation, the top layers of the 'segregated sediment' (sample prepared at 4 times the liquid limit) were much more compressible, resulting in a larger change in void ratio. This observation prompted the question: would there be an upper limit where any further increases in initial water content did not change the resulting structure and initial voids ratio. Furthermore, would it be possible to create samples with specific sensitivities (after Cotecchia & Chandler, 2000) by varying the initial water contents.

Sridharan & Prakash (2001b) also determined the permeabilities of the sedimented samples using falling head permeability tests. Al-Tabbaa & Wood (1987) previously reported the relationship between voids ratio and permeability. Sridharan & Prakash (2001b) investigated the same relationship in both segregated and non-segregated samples. Figure 5.14 presents the relationship between permeability and voids ratio for kaolinite samples prepared at three different initial water contents. Sridharan & Prakash (2001b) concluded that the change in permeability for a given change in voids ratio was more significant in the non-segregated samples.

Sridharan & Prakash (2001b) offered a possible explanation, in a non-segregated soil sample, there was an even distribution of particles, with the larger particles forming pore 'throats' which are blocked by smaller particles. This soil fabric creates an initially lower value of permeability and greater reductions in permeability for the same change in voids ratio compared to a segregated sample. The results from Sridharan & Prakash (2001b) suggest that segregated sediments can be created at significantly lower water contents than those previously presented in Sridharan & Prakash (2001a), Imai (1980) and in Been & Sills (1981).

Edge & Sills (1989) studied naturally occurring sediment beds consisting of interbedded sequences of turbidite sediments. These samples were taken from the seabed deposits of the Nares Abyssal Plain. They used traditional investigation techniques such as visual inspections to observe changes in colour, particle size and sedimentary structure. Spot samples were also taken to quantify changes in particle size and density. To gain a better understanding of the changes in density in naturally occurring natural samples, Edge & Sills (1989) used the X-ray equipment detailed in Been (1980), which Allowed for continuous density profiles to be obtained. Figure 5.15 presents the density profile obtained from the first 7.5m of core 19 from the Nares Abyssal Plain, revealing 27 distinct spikes in density associated with layer interfaces.

Figure 5.16 provides a magnified section showing that each layer can be split into three distinct parts. At the base of each layer there was a thin, high-density region. Moving upwards through the layer, the density gradually reduced to a minimum value, which then remained constant until the start of a new layer (Edge & Sills, 1989). Particle size distributions obtained at various points within the layers labelled 'A, B, C and D' in Figure 5.16 are presented in Figure 5.17. The regions with the lowest density corresponded to areas where the clay sized particles were dominant. Whereas the high-density regions coincided with where coarser silt and sand size particles are dominant. There is an abrupt change between these different layers suggesting that the clay at the top of this layer had sufficient strength to resist penetration of sand from the subsequent layer.

Previous sedimentation column studies have typically introduced all the soil simultaneously into the sedimentation column. Edge & Sills (1989) used the same sedimentation columns as described in Been & Sills (1981), but introduced slurry at routine intervals to create multi-layered sedimented samples. The soil used for these tests was collected 10km offshore from Sellafield, from the first 10m of the seabed, with any organic material and shells removed. Particle size distributions were measured at various depths and the material was found to consist of approximately 30% sand, 45% silt and 25% clay. The particle size distributions obtained can be seen in Figure 5.18.

To create the slurries for the sedimentation tests, the soil was mixed with artificial sea water (commercially available as instant ocean) to a water content of around 1200%. The slurry was subsequently placed at hourly intervals during working hours over a six-week period. The sedimentation columns were left undisturbed for a further 590 days, during which the consolidation of the sediment was monitored through a series of X-ray profile (Edge & Sills,

1989). The density profiles at the end of the test are presented in Figure 5.19. There was the same general pattern of both high and lower regions of density, as in the natural samples. However, a notable difference was observed: the natural samples displayed spikes of higher densities at the interfaces between layers whereas the artificially sedimented samples had regions of lower density at these interfaces. This can be seen more clearly in a magnified density profile (Figure 5.20).

Edge & Sills (1989) used the density profiles collected during the addition of soil to explain this finding. Figure 5.21 plots the development of the first soil input after an overnight break. It highlighted the relatively quick development of a high-density layer at the interface, followed by a gradually increasing density layer above. The underlying material shows signs of compression but sufficient strength to resist the penetration of the sand. In Figures 5.21 and 5.22 point A represents the high-density layer formed as the result of the initial pour of the day. Figure 5.22 provides a comparable time sequence but for the third pour of the day. Edge & Sills (1989) noted how during the later pours of the day, as opposed to the development of a high density layer, a broad zone of uniform and lower density forms. Edge & Sills (1989) also observed that as the day progressed, the dispersion fluid became increasingly turbid. This was attributed to insufficient time between slurry pours, preventing the finer materials from fully sedimenting.

Edge & Sills (1989) offered potential explanations for the variations in density profiles between the initial and subsequent layers. Firstly, overnight consolidation of samples was dismissed due to the very low excess pore-water pressures generated near the surface. Instead, Edge & Sills (1989) noted creep could explain this difference accounting for the additional strength as reported in Leroueil et al. (1985). Another practical explanation was that allowing the slurry to sediment overnight allowed for all fine material to be deposited, Edge & Sills (1989) noted this could have been significant. However, these individual effects cannot be separated.

The first sedimented layer of the day was very similar to naturally occurring sedimented beds. When sedimenting a multi-layered soil bed for use in centrifuge modelling, it is crucial to allow sufficient time between slurry additions to allow for finer material to be deposited before introducing the second batch of soil into the sedimentation column.

Stallebrass et al. (2007) sedimented samples that would later be used to perform standard element tests. The primary objective of this investigation was to determine whether sedimenting a sample within a laboratory created sensitivity (after Cotecchia & Chandler,

2000). The soil used was a bulk sample of unweathered London Clay obtained from the former Knightsbridge Crown Court site, extracted at a depth of 52m above the base of the formation.

A slurry with a water content of 1250% was prepared by combining London Clay at its natural water content with salt water of 3.51% salinity. This slurry was then poured into a 2m high acrylic tube with an 94.2mm internal diameter comprised of two 1m sections bolted and sealed together. The sedimentation column was filled with 12 litres of saltwater, and the London Clay slurry was subsequently poured into the column.

The initial water content within the sedimentation column was approximately 5800% (Stallebrass et al., 2007). The use of saltwater served as a flocculating agent, as reported by Locat & Lefebvre (1985), resulting in a more random and open soil structure. Additionally flocculation also reduced the time required for sedimentation. The entire process of mixing, pouring, sedimentation and self-weight consolidation took three days. This procedure was repeated to create multiple sedimented layers within the soil sample.

The sample underwent additional one-dimensional compression by applying dead weights to a submersible piston. This piston had positive buoyancy, allowing for the application of very small initial loads during the early stages of consolidation. The loads were gradually increased until the total axial stress applied was 70kPa. To allow for drainage during consolidation, channels were manufactured in the base of the sedimentation column. Once consolidated the base of the sedimentation column could be removed and three 38mm diameter triaxial samples obtained using a thin-walled cutter.

The laboratory sedimented samples were compared with a reconstituted sample made from the same London Clay. To create the reconstituted sample a slurry was mixed to a water content of 125%, using both water of the same salinity as the sedimented samples and distilled water. The slurry was then poured into a floating ring consolidation tube and consolidated one-dimensionally to a final vertical effective stress of 70kPa. Both sets of samples, were subsequently placed into a triaxial cell and one-dimensionally consolidated to a vertical effective stress of 400kPa. They were then swelled one-dimensionally to various stresses to create a range of overconsolidation ratios. Finally, the samples were sheared under a range of stress paths. In addition to investigating the effect of laboratory sedimented structure, using both fresh and saltwater also allowed the effect of pore chemistry be observed.

Figure 5.23 clearly illustrates the visual distinctions between the sedimented and reconstituted samples. These images were captured after being air dried and split open. In the reconstituted

samples, the fabric displays a random arrangement of particles, with larger particles evenly distributed throughout the clay matrix. In contrast, the sedimented sample shows segregation of particles sizes.

Figure 5.24 from Mašín et al. (2003), presents the relationship between specific volume and mean effective stress for both the laboratory sedimented and reconstituted samples. The observed pattern of behaviour was similar to that reported in studies on natural sedimented clays. The curves are essentially parallel and fall into two distinct categories sedimented and reconstituted samples. From Cotecchia & Chandler (2000) parallel compression lines indicates a stable soil structure. The limited scatter of the results indicate that laboratory sedimentation is a repeatable method of creating soil samples.

This offset in compression lines, can be quantified by sensitivity as defined in Cotecchia & Chandler (2000). For the data collected by Stallebrass et al. (2007) the sensitivity fell within the range of 1.5 to 1.8 and a sensitivity value of 2 for natural *in situ* London Clay was estimated. The variation in specific volume at lower stresses was attributed to a variance in water contents. This was attributed to wall friction within the sedimentation columns (Stallebrass et al., 2007). By the end of the triaxial loading, the variation in specific volume was much smaller at just 0.02. Stallebrass et al. (2007) found that pore fluid chemistry did not affect the behaviour of the reconstituted soil samples.

Figure 5.25 presents the results from the bender element measurements during one-dimensional compression and swelling. There was no discernible difference observed between the sedimented and reconstituted or between samples with saline or freshwater pore fluid. Confirming that the shear stiffness was dependent on the current state and overconsolidation ratio (Viggiani & Atkinson, 1995) and is unaffected by soil structure or fabric. However, from preliminary results this may not be true for larger strains. Figure 5.26 shows this important observation. For constant p' extension at shear strains of around 0.0002, the stiffness of the reconstituted sample was approximately half that of the sedimented sample with the same stress state and history.

Simpson (2010) using the same data as that presented in Stallebrass et al. (2007) outlined the potential significance of this observation. Figure 5.27 plots the secant moduli calculated for the same stress change in both a sedimented and a reconstituted sample. For stresses ranging from 10 and 50kPa, the ratio of shear modulus between sedimented and reconstituted samples exceeded 2, while for the remaining the stress larger than 1.5. Simpson (2010) concluded that

this could help in pave the way in understanding some of the differences between laboratory tests and field behaviour. Both authors note how this was preliminary data that deserves further investigation.

5.2 Anisotropic/layered geotechnical centrifuge soil beds

Sedimentation columns have been used to investigate the sedimented soil formation process and standard element tests have categorised the resulting samples. Laboratory sedimentation has proven to be a suitable method for creating structured samples at an element testing scale. This section outlines the existing methods of creating anisotropic/layered soil bed suitable for testing in a geotechnical centrifuge at a scale capable of simulating construction events.

Grant (1998) investigated tunnelling induced ground movements in two-layered ground on the centrifuge. To create the centrifuge soil bed in which sand overlaid clay, a kaolin clay slurry was created using one of two methods. Either, commercially available clay powder was mixed with de-aired distilled water to form a slurry to a water content twice the liquid limit, or kaolin clay used in previous centrifuge tests with a water content of around 40% was recycled by mixing with de-aired distilled water to form a slurry with a water content of twice the liquid limit.

To reduce friction between the clay and centrifuge container during consolidation, grease was applied to the strong box walls as in Mair (1979). A porous plastic filter and filter paper was placed at the bottom of the strong box to allow for water drainage but the retention of clay during consolidation. The slurry was then carefully placed into the strongbox to avoid the formation of any air pockets. A filter paper and porous plastic filter was placed on top of the sample, which was consolidated in a hydraulic press. The centrifuge samples were subjected to a maximum stress of 500kPa and subsequently allowed to swell to 250kPa. Once consolidation was complete, the drainage taps were closed to avoid water re-entry into the sample while being removed from the press.

After consolidation the soil bed was removed from the press, and the clay layer was trimmed to the correct level. The front of the strongbox was then removed, and both exposed surfaces were covered with liquid paraffin to prevent loss of moisture from the soil bed. The tunnel and observation points were then installed into the soil sample, as detailed in Grant (1998). An observation window coated in a paraffin lubricant to reduce friction was then secured in place. The sand layer, consisting of different gradings of Leighton Buzzard sand was then placed. Initially, this was achieved by pouring the sand slowly from a height of 1.5m. Subsequently, a

system was developed by which sand was dropped through a hopper and a sieve, such that the sand particles reached terminal velocity and this led to the creation of repeatable soil beds.

The model was then placed on the centrifuge and accelerated to the required *g*-level. Once the model was in hydrostatic equilibrium, the tunnel was rapidly collapsed such that the response of the clay was largely undrained. Displacements at the ground surface and the clay/sand interface were recorded by Linear Variable Displacement Transformers (LVDTs), subsurface movements were determined using close range photogrammetry. The results and implications of this study focus on differences in patterns of movements resulting from an overlying layer with a different stiffness. In summary, the introduction of a sand layer with a relatively high stiffness, compared to the clay layer, led to wider settlement troughs within the clay when compared to an all-clay soil bed.

Marshall et al. (2014) developed a novel experimental and analytical technique for assessing single and pile groups in layered ground. Within the tests conducted, a series of clay overlying sand soil beds were created, similar to the beds created in Grant (1998). The sand used was Leighton Buzzard Fraction E and the clay was a commercially available kaolin powder provided by Imerys Minerals Ltd, with a liquid limit determined to be 0.65. The soil bed was constructed in a cylindrical steel centrifuge container with a diameter of 0.49m and a height of 0.5m. The test series was conducted at 80*g*.

To minimise construction effects the, piles were installed first, and the soil bed was created around the piles (Marshall et al., 2014). For the tests in which the base of the piles were installed into the sand layer, the piles and pile caps were installed first using temporary plates and supports. The soil bed was turned upside down using an 'inverter' which attaches to ports on the side of the centrifuge container, allowing it to rotate around its centre, as shown in Figure 5.28 (Marshall et al., 2014). The base of the centrifuge container was then removed exposing the sections of the piles to be installed into the sand layer. The sand was placed by air-pluviation to achieve the desired voids ratio and layer thickness. The base was reinstalled, and the container was inverted back to its upright position, and the temporary plates and supports removed, the sand was then saturated.

To create the clay layer, kaolin powder was mixed to a slurry to twice the liquid limit and poured around the piles. This was left to consolidate under its own weight for a few days before being consolidated further on the centrifuge. To achieve the desired overconsolidation ratio,

sand was added to the top to the model and consolidated on the centrifuge. The sample making procedure took several days.

For the sand overlying clay tests the clay was mixed in the same way and poured into the centrifuge container. A dead load equal to the weight of the sand was applied on top of the slurry. The clay slurry was consolidated inflight on the centrifuge. After the clay had consolidated, the dead weight was removed and holes slightly smaller than the piles were augured into the clay to ensure a good contact between the clay and the piles was achieved. Once the piles were installed, the sand was air-pluviated to the required thickness and saturated by ports in the side of the centrifuge container.

Hossain & Randolph (2010) conducted an investigation on the deep penetration of offshore foundations into layered stiff-over-soft layered clay. A test series was completed in the drum centrifuge facility at the University of Western Australia. Model spud cans were pushed into the clay via an actuator at 100g in two different soil beds: uniform stiff-over-soft and uniform stiff-over-non-uniform.

To create the uniform stiff over soft soil beds, a homogenous slurry was prepared by mixing commercially available kaolin clay powder with water to a water content of 120% (approximately twice the liquid limit). Subsequently, the slurry was placed into a vacuum chamber and deaired. The slurry was then poured into a cylindrical container with a 394mm internal diameter, geofabric mats were connected at the top and bottom of the sample. The slurry was consolidated one-dimensionally to a final effective stress. For the upper layer of the soil bed this was either 170kPa or 500kPa, while the bottom layer was kept constant at 100kPa. Once consolidated, the clay blocks were trimmed to the size of the centrifuge container for testing. The clay layers were placed into the strongbox to create a uniform stiff-over-soft clay soil bed.

Uniform-over-non-uniform soil beds consist of uniform layers which have been subjected to a constant applied vertical stress, while the non-uniform layers which exhibit an increasing strength with depth profile. To create the underlying non-uniform layers Hossain & Randolph (2010) consolidated samples inflight on the centrifuge.

Four strong boxes were fitted symmetrically in the channel of the centrifuge drum, lined with geofabric mats, and accelerated to 20*g*. Once at 20*g*, a kaolin clay slurry prepared using the same method as for the uniform layers, was pumped into the centrifuge strongboxes. The centrifuge was then accelerated to 200*g* and left to consolidate under self-weight for

approximately 7 days. Additional slurry was periodically pumped into the strongbox to achieve the desired soil bed height. The samples were kept submerged in water to ensure they were fully saturated. After the consolidation process was complete, the samples were removed from the centrifuge, and the top 10-20mm of clay was trimmed to achieve the target layer thickness. Finally, the soil bed was completed by placing a uniform layer, created as previously described, on top of the non-uniform layer.

The research concluded that the behaviour of the foundations in stiff-over-soft clay was affected by several factors, most notably the strength ratio between the soil layers, the thickness of the upper layer relative to the foundation diameter and the non-homogeneity of the lower layer. The model making techniques allowed the observation of the response of a two layered soil bed with varying stiffnesses, similar to Marshall et al. (2014) and Grant (1998). In these soil beds, the different layers are created as two layers with varying stiffnesses and with a clear interface between them. These soil bed preparation techniques do not produce soil beds similar to those in sedimentation columns and they do not create soil beds with sensitivity or permeability anisotropy as in sedimented clays.

5.3 Sedimentation using a geotechnical centrifuge

Stallebrass et al. (2007) demonstrated that a laboratory sedimented sample exhibits sensitivity, and the images of the split samples and the presence of layers suggest that there would be increased permeability anisotropy. Divall et al. (2018) developed an initial technique for sedimenting a clay sample using Acutronic 661 beam geotechnical centrifuge at City, University of London. Sedimentation on the centrifuge offers the additional advantage of significantly reducing the time required for sedimentation, due to the increased weight of the soil particles.

A kaolin clay slurry was prepared similar to previous sedimentation column experiments however, instead of using kaolin clay powder, recycled kaolin clay cuttings were used. Phillips et al. (2014) found that when disaggregating natural and reconstituted clay cuttings are disaggregated, they do not necessarily return to their constituent parts, as detailed in Figure 5.29. Phillips et al. (2014) also found while disaggregating kaolin clay, after a certain amount of mixing time clay peds begin to aggregate back together rather than continuously breaking down. The resulting particle size distributions depend on factors such as the material, mixing speed, mixing duration and initial soil structure. It was thought that by sedimenting a slurry

consisting of recycled peds, with a more varied particle size distribution, may produce a more anisotropic sample.

To create the slurry for sedimentation, an initial slurry was prepared by mixing distilled water with commercially available kaolin clay powder (supplied by Imerys Minerals Ltd) in a ribbon blade mixer at a water content of 120%. This was placed into a container and consolidated one-dimensionally to a maximum vertical effective stress of 350kPa. After consolidation, the sample was removed from the press and cut into 50mm cubes. These cubes were then placed into a planetary mixer with distilled water and mixed to a final water-content of 1285%. Leighton Buzzard Fraction E sand was then added to the slurry and mixed until there was a smooth consistency with no visible lumps.

The slurry was poured into a centrifuge strongbox fitted with a clear PMMA window, enabling the sedimentation to be observed by cameras. The sample was accelerated to 160g and left for approximately 90 minutes. Subsequently, the centrifuge was decelerated, and samples of the dispersion fluid were extracted from approximately 25mm above the clay surface. These were dried and found to be 99.995% water, demonstrating that sedimentation had finished in a significantly shorter time than the observed in Stallebrass et al. (2007) or Edge and Sills (1989). This procedure was repeated multiple times, to create a multi layered soil bed depicted in Figure 5.30, captured during the sedimentation procedure inflight (Singh, 2017).

While this study demonstrated the feasibility of sedimenting a clay soil bed on the centrifuge, there were a few limitations. The soil beds created were relatively shallow, with each clay layer being approximately 20mm thick. In practice, deeper layers would be necessary to simulate construction events within sedimented soil samples. Additionally, the resulting clay layers were very soft due to the low effective stresses experienced, although this could be simply addressed by consolidating the sample post sedimentation.

One of the most significant limitations was that other than visual observations there were no quantifiable tests conducted to assess sensitivity, permeability anisotropy or any differences in properties compared to soil beds created using conventional techniques as described in Taylor (1995). Although the initial water content used for the slurry was comparable to studies conducted at 1*g* where achieved a sedimented structure was achieved, there was significant variability in critical water contents within those studies, as detailed in Section 5.1. Therefore is not clear that the initial water content was suitable without further investigation.

Geotechnical centrifuge modelling has been successfully employed to study the sedimentation and consolidation of soil dewatering and disposal/reclamation schemes. Sorta et al. (2012) detailed how the application of an increased acceleration field to a soft soil, or a slurry composed of fine and coarser particles could enhance its segregation capabilities. Segregation, in this context, refers to the coarser particles settling through the soft soil or slurry to the bottom of the sample. Sorta et al. (2012) outlines how researchers have acknowledged the potential and associated challenges of segregating centrifuge models. However, these have been avoided by designing models based on experience rather than well-established guidelines. Sorta et al. (2012) produced guidance on designing non-segregating geotechnical centrifuge samples.

A Ternary diagram was generated to describe various properties of a slurry and for evaluating potential strategies for tailings management. In this study, fines are defined as the mass of soil passing through a number 325 sieve (particles smaller than 0.045mm). The Ternary diagram is characterised by three axes: the base represents fines content (mass of fines/total soil mass), the left axis represents solids content (solids mass/total mass) and the right axis the fines-water ratio (mass of fines/(mass of fines+water)). An example is illustrated in Figure 5.31, with the three points of the triangle indicating 100% water (top) 100% sand (bottom left) and 100% fines (bottom right). The horizontal lines represent constant solid content, the lines from the water apex to the base indicate constant fine content, and the lines from the sand apex to the right had side represent constant fine-water ratio (Azam & Scott, 2005).

This enables the visualisation of different geotechnical behaviours, such as segregating versus non-segregating and pumpable versus non-pumpable mixtures. The segregation boundary on a ternary diagram was used to describe the behaviour of tailings over a range of soil compositions. The non-segregating region is defined as when the fine and sand particles settle together to form a uniform deposit.

Different mixes of fines and fines-sand combinations, at varying solid and fines ratios, were prepared and allowed to sediment in sedimentation columns for a month to determine the segregation boundary. Mature fine tailings obtained from Albian Sands Energy Inc. and Sycrude Canada Ltd oil sand operations were tested in this study. These are characterised in Table 5.6 and illustrated in Figure 5.32. The soil was thoroughly mixed with pond water to create the slurry, which was then poured into sedimentation columns with an internal diameter of 63mm and height of 321mm.

The same slurries were also subjected to an increased acceleration field. Twelve polyvinyl chloride (PVC) tubes of 100mm internal diameter and 220mm height were machined from solid bars and secured onto the centrifuge. The slurries were then poured into the PVC tubes and accelerated at either 60 or 100*g*. Following Taylor (1995) the centrifuge effective radius was set to one third of the column depth. The centrifuge was allowed to operate for a time equivalent in duration to 30 days if scaled by N^2. However, as explained by Taylor (1995) the centrifuge is not a time machine. The test performed at 1*g* is not N times larger than the sample test at *Ng* and therefore the tests performed at 1*g* and N*g* have not been subjected to the same levels of consolidation. Sorta et al. (2012) also state that the in-flight columns are representative of a 5m prototype height but compare the samples directly.

Two different techniques were employed to determine the segregation index (a segregation index of less than 5% is considered non-segregating Donahue et al. 2008).

$$Segregation\ index = \frac{\sum[(s_i - s_{ave}) * (H_i - H_{i+1})]}{s_{ave}} * 100 \qquad (5.1)$$

Where;

s_i is the solid content of the slice,

s_{ave} denotes the average solid content, and

$(H_i - H_{i+1})$ is the normalised height of the slice i.

After the samples were created, they were analysed from the top down. Elements were extracted and dried in an oven to determine the solid content.

Additionally, the segregation index can be found by splitting the sample into layers and wet sieving to determine fines content.

$$Segregation\ index = \frac{\sum[(f_i - f_{ave}) * (H_i - H_{i+1})]}{f_{ave}} * 100 \qquad (5.2)$$

Where;

f_i is the fine content of the slice,

f_{ave} denotes the average fine content, and

$(H_i - H_{i+1})$ is the normalised height of the slice i.

Both methods for determining the segregation index were found to be suitable, and the 5% limit proposed by Donahue et al. (2008) was considered appropriate. Sorta et al. (2012) also noted in many cases, there are noticable visual differences between a segregating and non-segregating sample.

Figures 5.33 and 5.34 depict Ternary diagrams for tests conducted at 1*g* and tests conducted under an accelerated *g* level on the geotechnical centrifuge. When the same slurry was subjected to an increased acceleration field there was an increased likelihood of segregation. Notably, a slurry which did not segregate at 1*g* could do so at increased *g*-levels. As the *g*-level increases, the boundary between segregating and non-segregating slurries shifts, allowing samples with higher solids contents or lower water contents to segregate. Sorta et al. (2012) offer a practical explanation for this, as the *g*-level increases the weight of the particles also increases, while the carrying capacity of the slurry remains constant.

Sorta et al. (2012) concluded that material composition significantly influences sedimentation behaviour, as evident in all sedimentation column tests at 1*g*. Furthermore, they found that the *g*-level to which the samples were subjected can significantly influence their segregating behaviour. While it is not possible to make direct comparisons between the samples due to scaling law interpretation, the practical explanation for the observed pattern is still valid. As detailed in Been & Sills (1981), once a slurry reaches a point where particles are in contact, only consolidation can occur. Therefore, if the samples were left on the centrifuge for an extended period, only consolidation would occur, and the fine content of each layer would likely remain the same as reported.

5.4 Summary

Sedimentation column experiments have demonstrated the feasibility of creating sedimented samples in the laboratory with characteristics similar to naturally occurring sedimented samples, specifically at an element testing scale (Stallebrass et al. 2007). These tests have revealed that the critical water content for a slurry that ensures segregation during sedimentation is dependent on a variety of factors and different authors have reported a wide range of critical water contents for very similar materials. However, the procedure for creating a sedimented soil sample remains consistent: a dilute soil slurry should be mixed and placed in a sedimentation column and allowed to sediment for several days. When creating a multi-layered sample, it is essential to ensure particles have settled prior to adding the slurry for the

second layer. This ensures the development of a soil profile comparable to a naturally occurring deposit (Edge & Sills, 1989).

Been & Sills (1981) observed that altering the initial water content of the slurry resulted in different particle size distributions. By extension, this suggested it would be possible to create geotechnical centrifuge samples with varying sensitivities and permeability anisotropies by changing the initial water content of the slurry. Additionally, Been & Sills (1981) demonstrated the potential of reducing the critical water content using a dispersion agent.

Soil beds used in Geotechnical centrifuge tests have included layers by creating two uniform layers with different stiffnesses to investigate how an overlying layer with a different stiffness affects patterns of movements (e.g., Grant, 1998 and Hossain & Randolph, 2010). However, there is a fundamental difference between such samples and a laboratory sedimented soil sample such as Stallebrass et al. (2007). Divall et al. (2018) demonstrated that it is possible to sediment a multi-layered soil bed at a scale suitable for geotechnical centrifuge modelling by following a similar procedure to Stallebrass et al. (2007). However, the resultant layers were relatively shallow being only 20mm deep with high water contents due to the geometric differences between a sedimentation column and a centrifuge strongbox. There were also no element tests to quantify the differences between the soil beds created in Divall et al. (2018) and a soil bed prepared following a typical preparation technique, such as that detailed in Chapter 4 and Taylor (1995).

As a result, an initial investigation was required using sedimentation columns to sedimented samples on the centrifuge, determine the critical water content, and assess how soil permeability and anisotropy vary with changes in initial water content. This step established an initial framework for the effect of different sample preparation techniques on key properties to be determined. Centrifuge sedimentation columns were developed and equipment to measure the vertical and horizontal permeability of sedimented samples. Detailed information on this equipment and the experimental procedure is provided in the following chapter.

6. Equipment design and experimental procedure

Prior to sedimenting a soil bed for use in a centrifuge test an initial investigation was required to develop a methodology that ensured that a sedimented structure and anisotropic permeabilities are developed in the sedimented soil. A centrifuge sedimentation column test series was conducted to evaluate sedimented soil samples consisting of different proportions of Speswhite kaolin clay, Polwhite E kaolin clay (both supplied by IMERY's ltd) and Leighton Buzzard Fraction E sand at various initial water contents. This required the development of sedimentation columns to be used on the centrifuge.

For this study, enhanced permeability anisotropy was a crucial characteristic to be recreated within a centrifuge soil bed. It also provided a means of evaluating whether a sedimented soil structure developed. This required the development of a vertical and horizontal permeameter to assess sample anisotropy. Additionally a customised Oedometer was manufactured to determine one-dimensional consolidation behaviour to assess sensitivity. These test results led to a methodology used to design a sedimentation process that would provide a soil bed suitable for centrifuge modelling with specific layer thicknesses and anisotropies.

This chapter presents the development of the various pieces of equipment necessary to conduct a centrifuge sedimentation column experiment and determine the properties of the resulting sedimented soil. The experimental procedure used to conduct this research and the restrictions imposed by the geotechnical centrifuge at City, University of London are also detailed.

6.1 Acutronic 661 geotechnical centrifuge facility, City, University of London

The Research Centre for Sustainable and Resilient Civil Engineering at City, University of London has access to an Acutronic 661 beam centrifuge, as described by Schofield & Taylor (1988). This was designed to accommodate various packages on the swing, with a maximum permissible plan area of 500mm by 700mm. In the central area between the pivots, a maximum height of 970mm can be achieved. The centrifuge has a 40g/tonne capacity, such that a 400kg package can be accelerated to 100g. This capacity decreases linearly to a capacity of 200kg at the centrifuge's maximum acceleration of 200g. The swing has a radius of 1.8m and a typical effective radius between 1.5-1.6m. A 1.45 tonne counterweight is adjusted radially on a screw mechanism whilst stationary, ensuring the centrifuge is balanced during operation.

The strongboxes used at City, University of London have internal dimensions of 550mm (L) x 200mm (W) x 375mm (H) and are made from 38.1mm thick Duraluminium. An extension can

be attached to the strongbox to create deeper soil beds. The extensions have the same plan area as the strongbox and a height of 300mm. The centrifuge is located within a circular reinforced room for safe working and aerodynamic efficiency. The centrifuge is instrumented with strain gauges, such that if the centrifuge becomes more than 15kN out of balance a spin down procedure is initiated. This allows for overnight running of the centrifuge, which is often necessary to enable pore pressures to reach hydrostatic equilibrium.

During sedimentation of samples in the centrifuge, no instrumentation or data acquisition is required. USB cameras were employed for certain tests to observe the surface of the slurry. However, no measurements were taken; a live feed of the images were used to detect any leaks in the columns. After the first two tests, the cameras were not used during the sedimentation experiments.

6.2 Apparatus development

6.2.1 Sedimentation column development

Performing a sedimentation column test on the centrifuge imposed some additional constraints. The height of the columns were restricted by the crossbeam of the centrifuge, resulting in a maximum total height of 800mm to ensure clearance across the entire package area. The sedimentation columns were required to have a minimum diameter of 50mm to enable permeability and oedometer samples to be taken.

During a test, the sedimentation columns were secured inside a centrifuge strongbox and were all situated on the centreline of the axis of rotation. Consequently, the diameter of the sedimentation columns was also constrained by the internal dimensions of the strongbox. Typically, the wall thickness of a sedimentation column at 1*g* is not a consideration. However, due to the increased pressures experienced at elevated *g*-levels the columns were designed to undergo a change of internal diameter of less than 0.5% when containing a slurry with a unit weight twice that of water and accelerated to 100g. Acrylic tubes with a 60mm outside diameter and a 3mm wall thickness were used to construct the sedimentation columns, allowing for the placement of four sedimentation columns simultaneously on the centreline of rotation.

Due to the high water contents used during sedimentation tests, the soil samples created occupy only a small portion of the sedimentation column. Therefore, the sedimentation column was designed to split into two sections; a 200mm lower section and a 600mm extension. These sections were connected by 100mm diameter annular flanges that slide over the Acrylic tubes

and allow the sections to be bolted together. A watertight connection was achieved using Nitrile rubber O-rings between the flanges and between the flange and sedimentation columns. Figures 6.1-6.2 show schematics and an image of an assembled sedimentation column. In addition to the O-rings a silicone grease gasket was also applied to all connections. Tie rods connect the base of the sedimentation columns to a capping plate to resist the uplift force applied to the underside of the sedimentation column tube.

The sedimentation columns were placed inside a centrifuge strongbox during sedimentation experiments. Due to the height of the sedimentation columns exceeding the height of the windshield on the geotechnical centrifuge, there was a potential for high wind loads to be applied. An extension was bolted onto the centrifuge strongbox to reduce the exposed height of the sedimentation column. Additionally, guides were also located at the base and on top of the centrifuge strongbox to secure the sedimentation columns during centrifuge acceleration, as illustrated in Figure 6.3.

The maximum *g*-level achievable when using the sedimentation columns was 100*g*. When the effective radius when set to one third of the sedimentation columns height, it was noticeably smaller than a typical model at City, University of London. Consequently, the geotechnical centrifuge required a higher rotational speed to achieve the same *g*-level as a typical centrifuge test at City, University of London. Due to component limits on the geotechnical centrifuge the maximum *g*-level achievable was 100*g*.

As determining the permeability anisotropy of the soil sedimented using various sample preparation techniques was essential, a reliable method of determining vertical and horizontal permeability was required. Extruding the soil samples and placing them into a separate vertical permeameter was disregarded due to the tendency to create preferential drainage paths. Therefore, the lower 200mm section of the sedimentation column was designed as a vertical permeameter.

The base of the sedimentation column featured a recess to allow a porous stone to be located within the base of the column. Two drainage channels connected the porous stone to 6mm push fittings, providing drainage from the sample. During the sedimentation procedure, these drainage channels were sealed using specially manufactured plugs.

After a soil sample had been sedimented, excess fluid was siphoned from approximately 25mm above the sample. The extension was then removed from the sedimentation column, and a top cap installed and plugs removed from the drainage channels turning the sedimentation column

into a permeameter. The top cap was a 100mm diameter acrylic cap, with a centrally located 6mm push fitting to apply a head of water. The head was applied by 10mm bored acrylic tube and measured manually. The laboratory setup was designed to allow four falling head tests to be conducted simultaneously, as depicted in Figure 6.4. The base drain system also allowed samples to be consolidated within the sedimentation columns.

6.2.2 Development and validation of a horizontal permeameter

For this study a new piece of equipment was developed to measure the horizontal permeability of the sedimented soil samples. A drainage condition was applied such that water flowed radially from the outside perimeter of the soil element to a central permeable core. Equation 3.18, proposed by Al-Tabbaa & Wood (1987), applies for outwards radial flow. Changing the limits of derivation for inwards radial flow it was determined that the same equation applied.

A critical aspect in creating a horizontal permeameter based on this principle was to ensure the outside perimeter of the soil sample (at the same elevation) was subjected to the same applied head, whilst preventing water flow over and around the sample towards the permeable core. Achieving this within the sedimentation columns themselves was deemed unfeasible. Therefore, the soil samples needed to be extracted and placed into a separate piece of equipment. The principle of the horizontal permeameter is shown schematically in Figure 6.5.

The horizontal permeameter has been designed for a 30mm tall, 48mm diameter soil element. The height of the permeameter was chosen to enable the observation of horizontal permeability variation throughout the depth of the sample. The horizontal permeameter was constructed from the same Acrylic tubing and the same flange details as the sedimentation column. Soil elements were extracted from the sedimentation column from the bottom upwards by removing the base and using a 48mm internal diameter thin-walled cutter. These extracted soil elements were then placed into the horizontal permeameter using the following method.

The extracted soil elements were wrapped in filter paper placed inside an external filter. In addition to supporting the circumference of the soil sample with a permeable material the external filter acted as a guide to trim the samples to a consistent height. It also ensured that the soil sample was always located in the centre of the permeameter, maintaining a consistent void, (which was subsequently filled with water during testing) between the soil sample and permeameter tube. The external filter was manufactured from two 49 mm internal diameter stainless steel collars each 100mm high, that locate in grooves in the top and bottom cap. These

collars were connected by a 100-micron aluminium mesh, which was adhered to a recess on the inside of the collars to create a smooth internal surface.

To create the permeable core at the centre of the horizontal permeameter, a half-inch outside diameter porous plastic tube with 70-micron pore size was used. This was installed once the sample was in the permeameter using a half-inch outer diameter thin-walled cutter to create a bore within the sample, a 12mm auger was used inside the cutter to remove any soil. The top cap was manufactured with a guide, while the bottom cap featured a recess to ensure the permeable core remained vertical and centred within the permeameter. To prevent the permeable core aiding radial flow through capillary action, the permeable core was manufactured to be at the same height as the top of the clay element and was fully saturated in a vacuum prior to installation. The head was applied from a standpipe which was connected to the horizontal permeameter using an M5 push fitting on the Acrylic tube.

During the preliminary tests using the horizontal permeameter, there were significant overestimates of permeability due to the presence of preferential drainage paths around the soil element. This was attributed to two main factors; flow of water around the external filter and along the surface of the soil element, and flow of water up through the sample and along the surface of the soil element. These potential flow paths are illustrated schematically on Figure 6.6.

To address this, Nitrile rubber gaskets were placed between the flanges and under the external filter to ensure that water did not flow around the sample and along the surface of the clay. To verify that these gaskets were effective, a solid section of pipe (rather than a soil element) was subjected to a head of water and left for 24 hours. The centre of the pipe remained dry and the applied head did not change, which demonstrated that water was not flowing around the external filter. Gorasia (2013) demonstrated that Plastidip (a spray on plastic) was an effective means of stopping centrifuge models drying during testing. Prior to testing in the horizontal permeameter a Plastidip coating was applied to the top and bottom surfaces of the soil element to create impermeable boundaries. These measures ensured that the water expelled was due to radial flow as opposed to preferential flow around the soil sample. The different components and the assembly details of the horizontal permeameter can be seen in Figures 6.7-6.13.

To remove air from the void between the external filter and the permeameter tubing a bleed screw was manufactured on the Acrylic tubing and flexible pipe was used to connect the

applied head to the horizontal permeameter. This allowed the permeameter to be positioned such that the bleed screw was at the highest point, expelling any air from the permeameter.

To check the horizontal permeameter measurement, Speswhite kaolin clay slurry was mixed to twice the liquid limit and consolidated to a vertical effective stress of 250kPa within the sedimentation columns. Subsequently, the vertical permeability of these samples was determined in the sedimentation columns.

An identical slurry was created and poured into a centrifuge strong box and consolidated to a vertical effective stress of 250kPa. The front of the centrifuge strongbox was removed, and samples were taken in the horizontal direction using the 48mm internal diameter thin-walled cutter. These horizontally trimmed samples were then placed into the horizontal permeameter, and the permeability was determined (hence measuring the vertical permeability in the horizontal permeameter apparatus). 10 samples were tested in both the vertical and horizontal permeameter. The normalised head vs time plots are presented in Figure 6.14 and the calculated value of permeability and final water content are presented in Table 6.1.

These tests demonstrated good repeatability with both techniques. However, from Figure 6.14 there was more scatter within the horizontal permeability tests, attributed to the larger change in applied head resulting in more swelling and a wider range of final water contents. Nevertheless, the calculated permeabilities of the different test procedures demonstrated a strong agreement between the two pieces of equipment with all calculated permeabilities lying within a 10% banding. This validation test series confirmed that the horizontal permeameter was a suitable and reliable measurement technique for permeability and permeability anisotropy. There were four horizontal permeameters manufactured allowing four horizonal permeability tests to be undertaken simultaneously.

6.2.3 Development of Oedometer equipment

To investigate one dimensional consolidation behavior, oedometer testing was undertaken. To minimise sample disturbance and allow for multiple samples to be taken from the same sedimentation column, bespoke equipment was developed. This allowed samples to be extruded from the bottom of the sedimentation columns directly into an oedometer ring with the same diameter as the sedimentation columns. This included the manufacture of a 54mm oedometer ring and an adapter enabling the use of the standard 75mm oedometer equipment available at City, University of London. A new loading piston with a specific mass was created to apply an initial stress of 2kPa to the sample (Figure 6.15). A PMMA holder, shown in Figure

6.16 was also manufactured to enable a simple and consistent experimental procedure for extracting oedometer samples to be followed, which is detailed in Section 6.3.6.

6.3 Centrifuge sedimentation column test procedure

Section 6.2 presented the development of the new equipment to sediment samples on the centrifuge and to determine vertical and horizontal permeability and one dimensional consolidation behaviour. Section 6.3 outlines the testing procedure followed for the centrifuge sedimentation tests and subsequent element tests.

6.3.1 Preparation of sedimentation columns

The strongbox in which the sedimentation columns were secured was typically assembled a week prior to testing. The sedimentation columns themselves were assembled the day before testing. The porous stones, to be placed in the base of the sedimentation columns, were individually subjected to a vacuum and saturated. Once saturated, the porous stones were positioned in the base of the sedimentation columns and covered with filter paper with a 7-micron pore-size. Since the filter paper was buoyant, it was secured beneath the circumference of the sedimentation column and the base of the columns were attached. To prevent the porous stone from drying overnight the sedimentation columns were filled with distilled de-aired water. Just before filling the columns with slurry, this was poured away. The volume of water left within the sedimentation columns was negligible compared to the volume of slurry, and did not alter the water content of the slurry. This was confirmed through water content measurements taken before and after the slurry was placed into the sedimentation columns.

6.3.2 Slurry preparation procedure

There were several different slurry preparation procedures investigated over a range of water contents to determine the effect on permeability anisotropy and compressibility. The objective was to increase anisotropy whilst minimising the initial water content of the slurry. The slurry preparation techniques investigated were;

1. Mixing Speswhite kaolin clay powder and distilled water.
2. Recycling Speswhite kaolin clay cuttings and distilled water.
3. Combining varying proportions of Polwhite E kaolin clay and Speswhite kaolin clay powder with distilled water.
4. Combining varying proportions of Speswhite kaolin clay powder and Leighton Buzzard Sand fraction E with distilled water.

5. Adding a dispersion agent (sodium hexametaphosphate powder) to a Speswhite kaolin clay: Polwhite E kaolin clay slurry.

Further details of the different test series and soil properties are listed in Chapter 7. For all slurries tested the same slurry preparation procedure was followed. The dry soil components (Speswhite kaolin clay, Polwhite E kaolin clay, Leighton Buzzard sand) were weighed and placed into a planetary mixer. Distilled water was subsequently weighed and added into the mixing bowl to achieve the desired water content, after which the paddle mixer was started.

The test series containing Speswhite kaolin clay cuttings used a similar method to Divall et al. (2018). A combination of previous centrifuge soil beds and consolidated Speswhite kaolin clay blocks were cut into approximately 25mm cubes. These were placed in a mixing bowl with the required amount of distilled water (accounting for the current water content of the clay cuttings) to achieve the desired water content. The clay cuttings were soaked for approximately 1 hour to soften prior to mixing.

All slurries were mixed until they reached a smooth consistency. This typically required 2 hours when using clay powder. However, when clay cuttings were used, the mixing time were generally longer ranging between 4 to 6 hours. During the process, the paddle mixer needed to be stopped periodically as the clay cuttings tended to smear around the mixing bowl and adhere to the mixing paddle. These lumps were manually broken down and the mixer restarted. This was necessary for all mixing procedures but more pronounced when disaggregating cuttings. For mixing procedure 5 the dispersion agent was weighed and added into the slurry approximately 5 minutes after starting the paddle mixer. Throughout all sedimentation tests a minimum of 3 different samples were taken from the mixer to determine the initial water content of the slurry.

After being mixed the slurry was ready to be placed into the sedimentation columns. At the geotechnical centrifuge facility at City, University London, there were two different mixers available: a Hobart 9L Planetary mixer and a 20L Metcalfe Planetary mixer. As a result, for each sedimentation test two different slurries could be investigated. Typically, a sedimentation test contained two sedimentation columns containing slurry number 1 and two sedimentation columns containing slurry number 2.

The slurry mixing procedure always commenced in the morning of the centrifuge sedimentation test, and the centrifuge was typically accelerated by 1pm. For consistency the mass of soil to be placed within each of the sedimentation columns remained constant for each

centrifuge sedimentation test. Further details of the specific slurries and test series conducted are detailed in Chapter 7.

6.3.3 Centrifuge procedure

After assembling all four columns and mixing both slurries, the slurries were transferred to the sedimentation columns. As the slurries were not homogenous, it was essential that the particle size distributions in each sedimentation column were consistent. Pouring or syphoning the slurry from the mixing bowls would not guarantee this. A cone splitter (shown in Figure 6.17) was used to split the slurry input into 10 identical sub-batches of slurry. Slurry was manually placed into the cone splitter using a measuring jug and the sub batches were collected in beakers. Details of the construction and validation of the cone splitter are given in Phillips (2014). This method ensured that the particle size distribution remained consistent between the mixer and sedimentation columns.

After splitting the first slurry into 'sub-slurries', the de-aired distilled water inside the sedimentation columns was poured out. The 'sub-slurries' were carefully poured into the sedimentation columns until the desired slurry volume was achieved. Before the second slurry was poured into the cone splitter, the cone splitter and beakers underwent thorough cleaning with distilled water. The beakers were hand dried, and the cone splitter was allowed to drip dry before compressed air was used to remove any remaining water. There was a minimal amount of water left within the cone splitter, water contents taken pre and post second slurry splitting were consistent with experimental variation (0.5%). Slurry number 2 was then carefully placed into the remaining sedimentation columns using the same procedure.

Once filled with slurry (Figure 6.18) the sedimentation columns were secured into the strongbox as depicted in Figure 6.19. The strongbox and columns were weighed, and the counterweight on the centrifuge adjusted. The strong box was positioned on the centrifuge swing with spacers to ensure the centreline of strongbox coincided with the centre of the swing. In the initial few tests, a USB camera was secured to the top of the strongbox to monitor the water level at the top of columns. If the fluid level dropped during the tests, it was clear there had been a leak in the sedimentation columns. In such cases, the tests would be halted, and the source of the leak investigated.

After the sedimentation column commissioning test, no leaks were detected in the sedimentation columns. This leak commissioning tests was attributed to a damaged O-ring. Subsequently, O-rings were routinely inspected and replaced.

All samples were sedimented on the centrifuge for 24 hours at 100*g*, which was considered sufficient to allow for sedimentation to occur. Following a similar method to Divall et al. (2018) water contents of the suspension fluid were taken at different levels above the soil. Table 6.2 presents the solid content results from the sedimentation column experiments using only Speswhite kaolin clay (the finest material used with the longest sedimentation time in this dissertation). After 24 hours there was a negligible mass of solid left within the dispersion fluid, confirming sedimentation had completed.

After 24 hours the centrifuge was decelerated, and the sedimentation columns were removed from the centrifuge. These samples were then subsequently tested to determine the effect of different slurry preparation techniques on permeability anisotropy.

6.3.4 Vertical permeability test procedure

After the columns were removed from centrifuge, the height of the sedimented samples were recorded. The dispersion fluid was siphoned from above the sample using a 10mm diameter flexible pipe. The solid content of the dispersion fluid was taken from every sedimentation column to ensure that there was minimal soil in suspension and as an consistency check between sedimentation columns containing the same slurries.

The extension is removed from the sedimentation columns and the height of the clay sample was recorded. The measurements of sample height before and after siphoning and removal of the extension assessed sample disturbance. The sedimentation columns were immediately prepared to be used as a vertical permeameter. The top cap was attached to the sedimentation columns and the permeameter was connected to the manometer. The permeameter was filled with tap water and any air was removed from the permeameter system. Samples were subjected to an applied head of approximately 1m and left for 24 hours with the drainage taps open at the base of the sample. After this period, the height of the sample was measured again, and the permeability test was initiated.

During the permeability test, the time, applied head and change of sample height (if any) were recorded at regular intervals. Measurements were taken every 10 minutes for the first hour, 30 minutes for the next 5 hours and every hour subsequently during the working day. The falling head experiment duration was a minimum of 48 hours or until a change in head of greater than 500mm had occurred. The permeability was determined from this data using Equation 4.7.

The applied head and height of the soil sample was measured using a steel rule with 0.5mm graduations. The potential errors in the vertical permeameter procedure arise from mismeasuring the sample height and the applied head. These errors are more significant in more permeable samples. Assuming a mismeasurement of 1mm in both sample height and applied head on a vertical permeability test lasting 24 hours with a change in applied head of 500mm, the resulting error in calculated permeability is less than 0.5%. Since all the samples tested were less permeable and tested over longer time periods, the potential error was negligible.

After the initial vertical permeabilities have been determined the samples can be either:

- Extruded and the horizontal permeability tested,
- Consolidated to a higher vertical effective stress and the vertical permeability tested,
- Consolidated to a higher vertical effective stress and the horizontal permeability tested, or
- Extruded and tested in an oedometer.

The initial permeability of each sample was determined, and the samples were then consolidated to 250kPa. The samples were consolidated in stages measuring the height of the samples after consolidation to a variety of different stresses, such that it was possible to determine the global compressibility of the different slurry preparation techniques as opposed to discrete layers with the oedometer tests. After consolidation the vertical permeability was retested using the same procedure. Samples at different horizons were extruded and placed into the horizontal permeameter and the procedure detailed in Section 6.3.5 followed to determine the horizontal permeability.

6.3.5 Horizontal permeability test procedure

Similar to the sedimentation columns, the horizontal permeameters were assembled prior to testing, except for the top cap. The porous plastic cores were separately placed inside a vacuum chamber to saturate prior to testing. Soil samples were extracted from the base of the sedimentation columns using a 48mm thin-walled cutter. The base of the sedimentation columns were removed, and a restraining piece was attached to prevent the soil element moving upwards during coring. The sample was then extruded from the thin-walled cutter. Samples were taken from the top and bottom 35-40mm of the sedimented soil. In cases where the total height was insufficient for two samples to be taken, a sample was taken from the bottom 35-

40mm of the sedimented soil. If a sedimented structure had developed, and particle separation occurred, the sample taken from the top will be governed by the finest material and the sample from the bottom will be governed by the coarsest material.

Once extruded from the column, the sedimented soil elements were approximately cut to size using a wire saw and the wrapped in filter paper with a 7-micron pore size. This was placed inside the external filter, which served as a guide to trim the sample to the required size (30mm) whilst ensuring it had flat top and bottom surface. Plastidip was applied to the top and bottom surfaces of the clay to create an impermeable boundary. During the application of Plastidip, the wire mesh on the external filter was covered to prevent blocking. Once the Plastidip had dried, the soil element was carefully placed into the horizontal permeameter. The gasket was positioned, and the top cap was installed. The permeameter was saturated with tap water, and any air was removed from the system and sample was subjected to an applied head of approximately 350mm.

The central permeable core was installed using a half inch internal diameter thin-walled cutter and 12mm auger system. A saturated permeable core was gently placed into the bore and similar to the vertical permeability test, the horizontal permeameter was allowed to reach steady flow, the test was then started. The tests were conducted for a minimum of 48 hours or until there was a change in potential greater than 150mm. The permeability was determined using Equation 3.18.

The applied head was measured using a steel rule with 0.5mm markings. There were two main sources of error when calculating permeability; mismeasurement of applied head and sample disturbance during horizontal sample preparation. Similar to the vertical permeameter, the error resulting from mismeasurements can be quantified. A mismeasurement of applied head of 1mm of a sample that experienced a change in head of 200mm in 4 hours resulted in a 1% error in calculated permeability.

Sample disturbance is challenging to quantify. During the development of the horizontal permeameter equipment and procedure, every effort was made to ensure that the sample preparation technique was repeatable, easy to complete and minimised potential sample disturbance. Over 100 horizontal permeability tests were conducted covering a range of different sample preparations and the variation in measured permeability was less than 10% for a given sample preparation technique. Calculated values of vertical permeability in both the horizontal and vertical permeameter were also consistent with the 10% banding. If sample

disturbance had been significant variations in horizontal permeability would have been expected. Figures 6.20-6.30 illustrate the various steps involved in extruding samples from the sedimentation columns, preparing the horizontal samples, and assembling the horizontal permeameter.

After obtaining the vertical and horizontal permeability at the top and base of the sample the permeability anisotropy was determined (defined as the horizontal permeability at the base of the sample divided by the vertical permeability). Permeability anisotropy and the variation in permeability with depth was used to evaluate sedimented samples.

6.3.6 Oedometer test procedure

Due to time constraints, it was impractical to conduct Oedometer tests for every slurry preparation techniques. Therefore, Oedometer tests were selectively performed on sample preparation techniques which exhibited the desired permeability anisotropy. These were compared to reference samples consisting of 100% Speswhite kaolin clay and Polwhite E kaolin clay. It was not possible to subject the same soil element to vertical permeability, horizontal permeability and Oedometer tests. Therefore, two sedimented samples were created using the same preparation technique and tested in the vertical permeameter. The results were compared prior to oedometer testing to ensure sample consistency. One sample was then tested in the oedometer and the other tested in the horizontal permeameter.

To extract the oedometer samples from the sedimentation columns the PMMA holder from Figure 6.31 was used. First filter paper was placed at the base of the PMMA holder to prevent the clay sample sticking during extrusion. Subsequently, the oedometer ring was placed on a shelf inside the PMMA holder. The soil element extrudes beyond the oedometer ring by 3mm allowing for the sample to be trimmed to a flat surface post extrusion (illustrated in Figure 6.32).

The base and bottom O-ring were removed from the sedimentation columns, which were then secured to the PMMA holder (Figure 6.33). An extrusion tool was used to push the soil element down into the Oedometer ring (Figure 6.34). The bolt securing the sedimentation column was temporarily removed, and a wire saw positioned between the sedimentation column and PMMA holder. The sedimentation column was resecured to the PMMA holder and the sample cut in one smooth continuous motion using the wire saw (Figure 6.35). The Sedimentation column was removed from the holder and the base reattached. The sedimentation column containing the remaining sedimented sample was filled with water to prevent drying. The

oedometer sample was removed from the holder and the excess 3mm of sample was trimmed with the wire saw (Figures 6.36- 6.37).

This procedure ensured the starting oedometer height was aways 20mm deep (equivalent to the height of the oedometer ring). The oedometer sample was covered with filter paper and placed onto a saturated de-aired porous stone. The containing ring was assembled, and another saturated de-aired porous stone and filter paper placed on top of the sample (Figure 6.38). The custom piston was then placed on top of the sample, with the manual stop on the Oedometer set such that the loading arm was in contact with the sample but did not induce any displacement until the measurement equipment had been positioned. Sample displacement was continuously recoded during the Oedometer test by a Linear Variable Displacement Transformer (LVDT) positioned on top of the Oedometer loading arm. Once in position, the water bath was filled with distilled deaired water and the manual stop was removed to initiate the Oedometer test. The applied stress was increased every 3 hours during a working day until the maximum stress was achieved (experimental set up depicted in Figure 6.39).

Following completion of the loading cycles, the water from the water bath was drained and Oedometer ring and consolidated sample were removed. The final height of the sample was measured at a variety of location with a depth gauge micrometer, and a final water content was recorded. To measure the finial water content the entire oedometer sample was measured. A combination of the final height, final water content and initial height were used to calculate the oedometer results presented in Chapter 8.

6.4 Summary

In summary this research required the development of sedimentation column apparatus to be able to sediment samples on the centrifuge. It required the development of a vertical and horizontal permeameter to determine permeability and permeability anisotropy of different sample preparation techniques. It required the development of customised oedometer apparatus to quantify the effect on compressibility and sensitivity. The experimental procedure followed for this research is summarised below:

1. Sedimentation columns and strongbox are assembled prior to the day of testing
2. On the day of testing slurry was mixed in a planetary mixer to a desired water content (typically 2-6 hours)
3. Slurry was passed through hydro splitter and placed into sedimentation columns
4. Slurry was sedimented inflight at 100*g* for 24 hours

5. Sedimented samples were removed from the centrifuge and the solid content of dispersion fluid and the initial vertical permeability was determined
6. Samples were consolidated in stages to a final stress of 250kPa noting changes in height to determine compressibility
7. Vertical permeability was determined after consolidation
8. Samples were taken from the top and bottom of the sedimented sample to determine horizontal permeability and variation in permeability
9. Permeability anisotropy assessed and sedimented samples were evaluated
10. Select soil samples were tested in the oedometer once the permeability behaviour for a particular sample preparation technique was understood.

7. Centrifuge sedimentation column tests series

This chapter provides details of the sedimentation column tests conducted. The objective of these tests were to establish a framework for determining the resultant permeability for different slurry preparation techniques. Enabling the design of a soil bed with sedimented structure that incorporates specific layer thickness and permeability anisotropies. Further details of the different slurry mixing procedures are outlined in this chapter. All slurries were consolidated to an effective stress of 250kPa and the vertical and horizontal permeabilities tested, selected samples were also tested in the oedometer.

Three different soil types were used for the sedimentation experiments: Speswhite kaolin clay, Polwhite E kaolin and Leighton Buzzard Fraction E sand. Speswhite kaolin clay is extensively used in centrifuge modelling and is the finest grade kaolin product produced by Imery's. Material properties are detailed in Table 7.1 from Le (2017) conducted at City, University of London. Polwhite E kaolin clay is another Imery's product produced from the same source material as Speswhite kaolin clay; however, it has been subjected to less refinement and possess a more varied particle size distribution. Figure 7.1 presents the particle size distributions of both Speswhite and Polwhite E kaolin clays. Combinations of Speswhite and Polwhite E kaolin clay have been used by Chan (2020) to create a range soil properties when investigating long-term basement heave on the centrifuge. The properties of both Speswhite and Polwhite E kaolin clays determined by Chan (2020) are presented in Table 7.2. Leighton Buzzard sand Fraction E (LBS E) has also been combined with Speswhite kaolin clay to produce more varied particle size distributions. LBS E was previously used by Grant (1998) at City, University of London and was described as a sub-rounded, with a grading envelope produced) and displayed in Figure 7.2 (after Grant, 1998).

7.1 Reference testing

A baseline set of permeabilities needed to be determined which subsequent sedimented sample were compared. Speswhite kaolin clay and Polwhite E kaolin clay samples were prepared by mixing dry powder (supplied by Imery's) with distilled water to reach an initial water of approximately 120%. The slurry was mixed for a minimum of 2 hours until a smooth consistency was achieved (as per Taylor, 1995). The slurries were poured into sedimentation columns (with a deaired saturated porous stone at the base) and consolidated to vertical effective stress of 250kPa. Vertical and horizontal permeability was determined using the produce outlined in Chapter 6. These permeabilities allowed for the calculation of an idealised

layered soil model, which was then compared to the permeabilities of the sedimented samples to assess the degree of particle separation. Additionally, direct comparisons were made with specific regions of the sediment samples.

7.2 Test series 1. Mixing Speswhite kaolin clay powder and distilled water

The first series of sedimentation tests investigated how the initial water content of a Speswhite kaolin slurry affected the resultant permeability anisotropy. Table 7.3 details the different slurries used for this test series. The slurries were prepared following the same methodology as the refence test slurry but with different water contents. Once a smooth slurry consistency had been achieved, the slurry was passed through the hydro splitter to ensure a consistent particle size distribution had been achieved. Subsequently, the slurries were subjected to the centrifuge and testing procedure detailed in Chapter 6.

7.3 Test series 2. Recycling Speswhite kaolin clay cuttings and distilled water

To create a sample with increased permeability anisotropy a more varied particle size distribution was required. To achieve this while still using only Speswhite kaolin, recycled cuttings from previously consolidated Speswhite kaolin clay samples were used, following research from Phillips (2014) and Divall et al. (2018). To prepare the slurries for sedimentation, a similar method to Divall et al. (2018) were adopted. Previously consolidated Speswhite kaolin clay samples were cut into 25mm cubes, and submerged in distilled water. These cuttings were soaked for approximately 1 hour to soften and then mixed in a planetary mixer until a smooth consistency was achieved, this typically took 4-6 hours. The mixer had to be stopped frequently as the clay cuttings tended to smear around the mixing bowl and adhere to the mixing paddle. These lumps were manually broken down and the mixer restarted. This was required for all mixing procedures but more prominent when disaggregating cuttings. Table 7.4 details the various slurries tested within this test series, which investigated if disaggregating cuttings influenced the resultant permeability anisotropy.

7.4 Test series 3. Polwhite E and Speswhite powder combinations

Another method of creating a more varied particle distribution is to combine different soils to form a slurry (after Taylor, 1995). In this test series, two different grades of kaolin clay powder where combined to create the slurries. Speswhite kaolin clay powder (fine) and Polwhite E power (coarse) were used. They were weighed separately and placed into the planetary mixer with the required amount of distilled water and mixed for 2 hours until a smooth slurry was

created. The slurries were passed through the hydro splitter and sedimented following the procedure outlined in Chapter 6. Table 7.5 details the different slurry combinations tested. This test series investigated how introducing a coarser sized clay influenced the resultant permeability and to determine the critical water content for the separation of particle sizes.

7.5 Test series 4. Speswhite kaolin clay powder and Leighton Buzzard Sand combinations

Similar to Test series 3, Test series 4 combined different soil types to achieve a more varied particle size distribution. However, unlike Test series 3, which combined different grades of fine grained material, Test series 4 combined a fine grained material (Speswhite kaolin clay) with a coarse grained material (LBS E). The samples created in this test series were similar to the previous work conducted by Divall et al. (2018) and provided quantified properties of the resultant sample preparation techniques. Table 7.6 details the slurries investigated.

To prepare the slurries for sedimentation, Speswhite kaolin clay slurries were mixed from clay powder and distilled water to water contents of either 400% or 800% using a planetary mixer. The slurries were passed through the hydro splitter and placed into the sedimentation columns. Immediately prior to starting the centrifuge either 15% or 30% of the total soil mass within each sedimentation column was added as LBS E. This used a funnel located at a consistent height above the dispersion fluid to pour the LBS E into the sedimentation column. The slurry was manually mixed so all solids were in suspension and the procedure outlined in Chapter 6 was followed.

7.6 Test series 5. Use of a dispersion agent (sodium hexametaphosphate)

Previous test series determined the resultant permeability and critical water content to create a sedimented soil structure. Reducing the critical water content provided several advantages when sedimenting a soil bed within a centrifuge strongbox. The lower the initial it allowed for deeper layers to be created, a reduced sample preparation time and ultimately greater flexibility when designing a sedimented centrifuge soil bed. For these reasons, the use of a dispersion agent was investigated after Been & Sills (1981).

Dispersion agents serve two common purposes in clay related applications. First, in particle size distribution analysis dispersion agents are added into the dispersion fluid to enhance particle separation. Previous research have explored the optimal concentrations of different types of dispersion agents to provide the greatest degree of particle separation. British Standard

(BSI-BS 1377-2:1990) recommends a concentration of 33 grams of sodium hexametaphosphate per litre of distilled water. However, studies such as Bindu & Ramabhadran (2010) and Maharaj & Paige Green (2014) have suggested concentrations of dispersion agents, both higher and lower than that stated in British Standard as optimal. These studies dispersed different soil slurries with various dispersion agents and dispersion agent concentrations then compared the resultant particle size distributions. The optimal concentration and type of dispersion agent were found to be dependent on the soil being dispersed.

The second application of dispersing agents is within the ceramic mining and ceramic casting sector. Various authors have investigated the addition of a dispersion agent to reduce the viscosity of kaolinite clay slurries (e.g., Zaman et al., 2003; Andreola et al., 2005; Ma; 2012; Penkavova et al., 2014). These studies have demonstrated that minimal concentrations of dispersing agent, as small as 0.006 grams per litre, can significantly reduce viscosity. Additionally, increases in concentration can lead to an increased viscosity.

The most similar application of dispersion agent is from Been & Sills (1981), where slurries were sedimented with the addition of a dispersing agent. This study demonstrated that a concentration of 4 grams of sodium hexametaphosphate per litre of slurry significantly increased the separation behaviour observed. This finding was confirmed by particle size distributions taken from different depths within the sedimented soil as previously highlighted in Figures 5.9-5.11.

As the required dispersion agent concertation to influence critical water content was unknown, a series of tests were conducted. This test utilised a slurry from Test series 3 consisting of 70% Speswhite kaolin clay powder, 30% Polwhite E kaolin clay powder, mixed to an initial water content of 500%. Varying concentrations of dispersion agent were added to the slurry wich were subsequently sedimented on the centrifuge. The dispersion agent imparts an electrical charge onto the surface of the clay particles such that they repeal each other, known as deflocculation. Sodium hexametaphosphate is a commercially available dispersion agent, sold as deflocculant to prepare kaolinite clay suspensions for the ceramic industry. Imerys Speswhite kaolin clay and Polwhite E kaolin clay products are also sold primarily to the ceramic industry and designed for deflocculation. Suggesting that it was possible to the reduce the critical water required for a sedimented structure to develop with a dispersion agent.

The slurries were prepared using the same methodology as that described in Test series 3. While the slurry was being mixed the dispersion agent (sodium hexametaphosphate powder supplied by Fischer scientific) was weighed and added into the mixing bowl. Typically, the dispersion agent was added into the slurry around 5 minutes after the mixer was started. Following the addition of the dispersion agent the mixer was left for 2 hours until the slurry was a smooth consistency. This process was repeated for a range of dispersion agent concentrations, and the details of the slurries investigated are provided in Table 7.7. This test series aimed to confirm whether using a dispersion agent can reduce the critical water content and to optimise use.

7.7 Test series 6. Determining the minimum sedimentation time required

When conducting sedimentation column experiments it was observed that sedimentation had occurred within 24 hours inflight, evident by the absence of soil within the dispersion fluid above the sedimented sample. This sedimentation time was subsequently kept constant for Test series 1-5. However, when transferring the sedimentation procedure into a centrifuge strongbox, it would limit to only one layer to be sedimented per a day. To create a multi-layered soil bed it would take several days and a significant amount of centrifuge time. To investigate if the sedimentation time could be reduced a test was conducted such that the effect of sedimentation time on sample permeability and % of solids remaining within the dispersion fluid could be measured.

This test series used a specific slurry preparation procedure from Test series 5, which consisted of 70% Speswhite kaolin clay powder, 30 % Polwhite E kaolin clay powder, 0.1 grams of dispersion agent per litre of slurry mixed with distilled water to an initial water content of 500% and is listed in Table 7.8. The slurry was mixed following the same methodology described in Section 7.5 and was placed into all four sedimentation columns using the hydro splitter. The centrifuge was subsequently accelerated to 100*g*.

Every two hours, the centrifuge was decelerated and one of the columns was removed, and the centrifuge was reaccelerated to 100*g*. The deceleration, removal of one column, and acceleration process took approximately 10 minutes. After the removal of the columns the solid content of the dispersion fluid above the sedimented clay was determined. The resultant permeability anisotropy of the samples, following consolidation to 250kPa, was also measured. This allowed the impact of sedimentation time on soil properties to be observed. Which optimised the overall model making time for a sedimented soil bed suitable for centrifuge modelling.

7.8 Oedometer tests

Due to time constraints, it was not feasible to conduct oedometer tests for every slurry preparation technique. Instead reference samples were subjected to oedometer testing, consisting of 100% Speswhite kaolin clay and Polwhite E kaolin clay powder and prepared using the same methodology as the reference permeability testing outlined in section 7.1. Subsequently, these reference tests were compared to samples prepared as outlined in Section 7.7. For all slurry preparation techniques, oedometer samples were extracted from the top and base portions of the sedimentation columns to assess variation with depth and the formation of sensitivity. Table 7.9 details the different slurry preparation procedures subjected to oedometer testing.

7.9 Summary

The purpose of Chapter 7 was to provide full details of the different slurry preparation and mixing techniques employed in this dissertation. In summary, various centrifuge sedimentation column experiments were conducted inflight at 100*g*. Investigating the influence of different slurry compositions and initial water contents on the resultant permeability. These tests established a framework for:

- What permeability anisotropies were achievable, and
- The critical water contents

For each slurry preparation technique. Additionally, a subset of slurry preparation techniques underwent oedometer testing. A combination of these results and visual observations were used to evaluate the resultant soil samples for presence of a sedimented structure and to determine the most suitable technique for creating a multi-layered soil bed with a sedimented structure suitable for centrifuge modelling.

8. Sedimentation column and standard element test results

This chapter presents the results from the various sedimentation and oedometer experiments detailed in Chapter 7. In total, 15 centrifuge sedimentation tests (60 sedimentation column samples) were undertaken, investigating 5 different slurry preparation techniques over a range of water contents and sedimentation times. Subsequently, soil from each sample preparation technique was tested in the vertical and horizontal permeameter after being consolidated to vertical effective tress of 250kPa. The overall compressibility of the samples was determined from the consolidation stages. Additionally, 2 centrifuge sedimentation tests (8 sedimentation column samples) were conducted to assess the development of sensitivity during sedimentation through oedometer tests.

8.1 Reference test results

The horizontal and vertical permeability results determined from the reference tests are presented in in Table 8.1 along with the post-test moisture contents. The permeability results for both Speswhite kaolin clay and Polwhite E kaolin clay sit within a 10% banding, highlighting the consistency of sample preparation and permeability testing procedures. Permeability anisotropy was approximately 1.2 for both materials (defined as the horizontal permeability/vertical permeability) which was significantly less than that reported by Al-Tabbaa and Wood (1987) potentially due to the different sources of Speswhite kaolin clay being used.

The average permeabilities determined from these tests were used to predict the vertical permeability of sedimented samples containing different proportions of Speswhite kaolin clay and Polwhite E kaolin clay. An idealised soil sample was considered, where the soil sedimented into two distinct layers and the relative height of each layer was equal to the distribution by mass. For instance, in the sedimented samples consisting of 70% Speswhite kaolin clay and 30% Polwhite E kaolin clay the Speswhite kaolin clay layer was 70% of the overall height. Figure 8.1 illustrates two different idealised soil samples, the relative layer thickness and permeabilities. Equation 8.1 was then used to predict the overall vertical permeability.

$$k_v = \frac{\sum_{r=1}^{r=n}(d_r)}{\sum_{r=1}^{r=n}(\frac{d_r}{k_{vr}})} \tag{8.1}$$

Where:

d is the layer thickness,

k is the layer vertical permeability,

and n is the number of layers.

To determine horizontal permeability the sedimentation columns were extracted trimmed and placed into the horizontal permeameter. Where possible samples were extracted from the top and bottom of the sedimented samples allowing for 3-5mm of trimming at the top and bottom face. Figures 8.2-8.3 illustrate where those samples were extracted from and thickness of the layers within these samples. Equation 8.2 was used to predict the horizontal permeability of each sample.

$$k_v = \frac{\sum_{r=1}^{r=n}(d_r k_{hr})}{\sum_{r=1}^{r=n}(d_r)} \tag{8.2}$$

Where:

k is the layer horizontal permeability.

During the sedimentation tests the heights of the samples and subsequent thickness of the layers varied. This did not affect the prediction of vertical permeability as this is solely dependent on the relative thickness of each layer which remained constant. The horizontal permeability prediction is however dependent on the overall sample thickness and where the horizontal permeability samples are extracted from. For each sedimentation test the sample height was recorded and an idealised soil element was created. The position of the extracted horizontal samples were overlain as illustrated in Figure 8.2-8.3 to determine the predicted horizontal permeability of each soil sample. The predicted permeability of the sedimented samples are presented on the relevant subsequent graphs. The comparison to this prediction was used as the primary indicator that particle size separation occurred and a sedimented structure had been developed.

8.2 Test Series 1 results

Figure 8.4 presents the results from the sedimented Speswhite kaolin clay powder tests and the results from the reference Speswhite kaolin clay powder tests, Table 8.2 presents the results in a tabular form with the post-test moisture contents of the samples. Figure 8.4 highlighted that over the range of water contents tested there was no correlation between increased water content and permeability. The test results also highlighted that sedimented samples are approximately 40% less permeable than the reference Speswhite kaolin clay samples. The

change in permeability suggests that irrespective of the initial water content, sedimenting a sample on the centrifuge creates an inherently different soil structure than consolidating from a slurry in a hydraulic press. From the post-test water moisture contents in Table 8.2 a trend can be seen, as the initial water content of the slurry increases so does the final post-test moisture content. This provided an indication that a more open structure had been developed during sedimentation even if there was no change in permeability. A sample was taken from the 1200% initial water content slurry and was tested in the oedometer to confirm the presence of sensitivity and presented in Section 8.7.

Literature, such as Imai (1980) suggested that kaolin requires a much higher water content than the 1200% used in this test series, for the resultant soil sample to develop a sedimented structure and potentially enhanced permeability anisotropy. Therefore, there could be a case to further increase the initial water content to increase permeability anisotropy. When sedimenting a soil bed for centrifuge modelling in a strongbox the higher the initial water content of the slurry the smaller the resultant layer would be. Using a standard strongbox and extension at City, University of London, to create a 200mm deep sedimented soil bed with a 1200% water content slurry the maximum layer thickness achievable would be 35mm. This was deemed the smallest layer thickness that would be practical to create sedimented soil bed suitable for a scaled tunnel test. Therefore, the water content was not increased further and alternative slurry preparation techniques were investigated to increase permeability anisotropy.

8.3 Test Series 2 results

Figure 8.5 and Table 8.3 present the results from sedimenting Speswhite kaolin clay cuttings with distilled water compared with the reference Speswhite kaolin clay tests. Similar to the results from Test Series 1 there was no clear trend in the variation permeability anisotropy with changes in initial water content and the permeability was on average approximately 40% less than the reference samples. The post-test moisture contents presented in Table 8.3 also follow the same trend outlined above, again indicating that although no change in permeability was observed a sedimented structure may have been developed. This sample was not tested in the oedometer as if it was true for one sample the same would be true for both.

This Test Series demonstrated that sedimented kaolin clay cuttings did not enhance permeability anisotropy as predicted by Divall et al. (2018) following Phillips (2014). As previously detailed in Section 8.2 literature such as Imai (1980) suggested that the critical water content may not have been reached in the slurries tested. For the same reason as in Series 1 the

water content was not increased further due to the practical limitation this would impose on creating a sedimented soil bed.

Following this test series it was determined that it was not possible to create a sedimented sample with enhanced permeability anisotropy using only one material, that is Speswhite kaolin clay, within the range of water contents desired. Therefore, future sedimentation tests would include two different materials with permeabilities of at least an order of magnitude different.

8.4 Test Series 3 results

Figures 8.6 and 8.7 present the results of the sedimented samples consisting of Speswhite kaolin clay and Polwhite E kaolin clay powder in different proportions. The predicted vertical permeability is illustrated on all Figures as a solid and the predicted horizontal permeability at the top and base of the samples are represented as hollow markers and the measured values shown as solid markers. Table 8.4 also presents the results and prediction in tabular form with the post-test moisture content.

Figure 8.6 presents the results from the 70:30 Speswhite kaolin clay Polwhite E kaolin clay sedimentation results. These results demonstrate how changing the initial water content of a the slurry influenced the resultant soil structure. When the water content was less than 400% the soil sample demonstrated a modest degree of anisotropy, very similar in magnitude to the reference tests. The horizontal permeability at the base and top of the sample were also similar indicating that minimal particle separation had occurred.

At an initial water content of 800%, an increase in permeability anisotropy was observed (approx. 2) and the permeabilities started to move towards the predicted values indicating that some particle separation had occurred. At an initial water content of 1200% the predicted values are very similar to those observed indicating that full particle separation had occurred and a sedimented structure had been fully developed. The permeability anisotropy measured was approximately 5 when the initial water content was 1200%. The post-test water contents in Table 8.4 also provide a similar picture, as the initial water content increased so did the final moisture content of the sample providing further evidence that a more open structure had developed.

This pattern was similar to the finding from Imai (1980) and other sedimentation column studies. As well as the measured permeabilities there were clear visual differences between the samples prepared at different water contents. Figure 8.8 shows the image of a dried split

horizontal sample taken from the bottom of the 1200% initial water content sample where particle separation was clearly visible similar to Stallebrass et al. (2007) (Figure 5.23).

Figure 8.7 presents the results from the 50:50 Speswhite Polwhite E samples which showed a similar pattern to the 70:30 samples. When the initial water content of the slurry was 1200% the observed permeabilities were comparable to the predictions and the visual layering was easily identifiable. The 1200% samples created were only approximately 55mm tall, this had two implications. Firstly, it was not possible to extract samples from the base and the top of each sample, therefore one sample was used for each. Secondly, there was an increase in Polwhite E kaolin clay present in the horizontal sample taken at the top and an increase in Speswhite kaolin clay present in the horizontal sample taken at the base. The predictions in Figure 8.7 reflect this and explain why the prediction for horizontal permeability decreased at the top of the sample and increased at the base when comparing the results for initial water contents of 800% and 1200%.

This Test Series demonstrated that it was possible to create a sample with enhanced permeability anisotropy and a sedimented structure on the centrifuge. The critical water content for particle separation to occur fully was approximately 1200% when using Speswhite and Polwhite E kaolin clay. The decision on which ratio of the two materials to use is purely down to the desired response required from the soil bed. For this dissertation, a predominantly Speswhite Kaolin clay soil bed with an enhanced permeability and sedimented structure was desired and therefore the ratio of 70:30 Speswhite to Polwhite E kaolin clay was more selected.

The only practical limitation to this procedure was the critical water content which limits the resultant soil bed layer thicknesses. At City, University of London with the strongbox and extension a maximum layer thickness of 35mm was achievable with an initial water content of 1200%. If the initial water content of the slurry to be sedimented could be reduced, it would increase the maximum soil layer thickness. This would allow for a greater variety of layered sedimented soil beds be created and for deeper soil beds to be sedimented in a reduced time scale. The aim of the further test series was to reduce the initial water content of the samples whilst still achieving a sedimented structure and enhanced permeability anisotropy.

8.5 Test Series 4 results

Figure 8.9 and Table 8.5 present the results from the sedimented Speswhite kaolin clay Leighton Buzzard sand fraction E tests. These samples showed a significant increase in permeability anisotropy, with the horizontal permeability at the base of the sample being four

orders of magnitude larger than the top of the sample. They also showed that particle separation of sand grains occurred at a significantly lower water content that with the two fine grained materials (i.e., Speswhite and Polwhite E kaolin clay).

There was significantly more variation in horizontal permeability coinciding with the sand regions. This was due to two main reasons; firstly, the process of extracting samples from the sedimentation columns and placing into the horizontal permeameter was developed for a fine-grained soil. Changes are needed to ensure consistent samples are placed into the permeameter. Secondly, due to the much higher permeability the rate at which the head dropped was significantly faster with a change in head of 300mm occurring over approximately 25 seconds. Therefore, a constant head test would provide a more reliable measurement of permeability.

In addition, there was a greater concern about the sedimented Leighton Buzzard sand fraction E, Speswhite kaolin clay samples. In all four sedimentation columns the sand layers created were not homogenous or level as can be seen in Figure 8.10. The cause of the unlevel layers were investigated. The theoretical sedimentation time of the sand calculated from Stoke's law was approximately 15 seconds. This was confirmed by measuring the dispersion time of Leighton Buzzard sand fraction E in a dilute Speswhite kaolin slurry at 1*g*. The resultant sand layers created were level and horizontal. The short sedimentation time meant that the sand layer had sedimented prior to the spin up of the centrifuge and the uneven layers were created during the centrifuge procedure. This was confirmed by spinning the sedimentation column by hand, after which it could be seen that the sand layer had slumped to the back of the column relative to the direction of rotation Figure 8.11. This test highlighted that any material used in a centrifuge sedimentation experiment needed to be in suspension during the spin up of the centrifuge. If the particles settle prior to the spin up, an uneven layer would be created. This could be overcome by adding the coarser material into the columns inflight or by mixing the slurry inflight.

Even if the sand layer created was level, this technique created a sand layer overlain by a clay layer. The clay portion of the sample exhibited the same of degree anisotropy as the reference samples and currently further work is needed to understand the influence on resultant sensitivity at these water contents. A sample with these permeability characteristics could be created without sedimentation using a method like Grant (1998). This would be a faster more efficient way of creating a soil bed with the same permeability anisotropy.

If creating a layered clay sand soil bed with sensitivity, as suggested by the post- test moisture content and as demonstrated by the oedometer tests outlined in Section 8.8 was required this could be a viable technique of creating such samples. The initial water content of the kaolin slurry may need to be increased to achieve the desired sensitivity. Further work would also be required to modify the mixing procedure to ensure all particles are in suspension during the acceleration of the centrifuge and to extract repeatable horizontal samples to refine permeability measurements.

However, as the magnitude of permeability anisotropy was larger than desired (for this dissertation) when using Leighton Buzzard sand fraction E only fine grained materials (silt/clay) were used in future sedimentation tests.

8.6 Test Series 5 results

Test Series 5 investigated if the addition of dispersion agent would reduce the critical water content of a slurry. A slurry consisting of 70% Speswhite kaolin clay powder and 30% Polwhite E kaolin clay powder was mixed to a water content of 500% and sedimented with different concentrations of dispersion agent (sodium hexametaphosphate). A 500% initial water content was selected as a nominal value that what provide the flexibility and layer thicknesses required within the sedimented soil bed needed for this dissertation. Future work should investigate if the water content can be further reduced from 500% and still achieve a sedimented structure.

Using a dispersion agent it was possible to achieve particle separation and a sedimented structure at a lower initial water content. The dispersion agent also had an additional unexpected effect on sample behaviour. The first series of dispersion agent tests used dispersion agent concentrations of 8 and 4 grams per litre. When extruding the samples from the sedimentation column following the horizontal permeability procedure, the soil had a meta-stable structure and it returned to a slurry like state. It was not possible to determine the horizontal permeability of these samples.

The next test series reduced the dispersion agent concentration to 2, 1 and 0.5 grams per litre of slurry. For these samples it was possible to extract soil samples and measure the horizontal permeability. However, with continuous agitation, it was possible to return the soil sample back to a slurry like state. During the horizontal permeability test the radial flow of water through the sample also caused the soil sample to return to a slurry like state.

Finally, the dispersion agent concentration was reduced to 0.1 grams of dispersion agent per litre of slurry. In these tests there were no signs of a meta-stable structure both during the horizontal permeability tests and when manually agitated. The results from all tests are presented in Figure 8.12. The grey marked points indicate where the resultant soil structures were not stable. There was an exponential increase in permeability with time in samples with a meta-stable structure. The results plotted are from the early stages of the permeability tests and should be treated with caution. Figure 8.13 illustrates the observed relationship between dispersion agent concentration and time for the structure to become unstable, the higher the concentration the faster the soil returns to a slurry like state. Tabular results are also presented in Table 8.6 with the post-test moisture contents for only the stable structured samples presented.

The test results highlighted that at a dispersion agent concentration of 0.1 grams per litre the horizontal permeability at the base of the sample is larger than predicted, the horizontal permeability at the top of the sample is similar to that predicted and the vertical permeability approximately double that predicted. With the change in permeability at the top and bottom of the sample and the visual observation of the dried sample it was clear that particle size separation had occurred and the critical water content had been reduced to 500%.

A slurry consisting of 70% Speswhite kaolin clay, 30% Polwhite E kaolin clay and 0.1 grams of dispersion agent per litre of slurry mixed to an initial water content of 500% was the most suitable slurry composition for sedimenting a layered soil bed with a sedimented structure and anisotropic permeability for centrifuge modelling. A lower initial water content of 500% allowed for deeper layers to be created and greater flexibility when designing sedimented centrifuge samples.

8.7 Test Series 6 results

Test series 6 investigated the relationship between sedimentation time and the resultant properties of a sample sedimented from a slurry consisting of 70% Speswhite kaolin clay, 30% Polwhite E kaolin clay and 0.1 grams of dispersion agent per litre of slurry mixed to an initial water content of 500%.

Figure 8.14 presents a curve showing the solid content left in suspension after different sedimentation times. After only 2 hours only 1.7% of solid particles are left in suspension. Figure 8.15 presents the permeability results and the predictions for the different sedimentation times (also presented in Table 8.7 with post-test moisture contents). The permeability results

remain consistent irrespective of the sedimentation time demonstrating that after 2 hours of sedimentation at 100g a sedimented structure had been created. Over the next 22 hours of sedimentation the remaining 1.7% of solid material was deposited which had a negligible effect on the resultant properties. The post-test moisture contents were also consistent with experimental scatter.

Therefore it was possible to reduce the sedimentation time per layer to 2 hours from the 24 hours used for the sedimentation column experiments. This slurry preparation technique was used to create a soil bed with a sedimented structure in a centrifuge strongbox that would subsequently be used for a tunnel construction event.

For this slurry mix the consolidation stages of the sedimentation columns were measured, it was possible to determine the overall compressibility of the samples prepared by plotting voids ratio against log vertical effective stress. A compressibility coefficient of 0.6, swelling coefficient of 0.1 and e_0 of 2.8 were observed. These properties were used to predict the resultant sedimented layer heights and described in Section 9.2. Select samples were also tested within the oedometer to determine investigate the formation of sensitivity.

8.7 Oedometer tests

Due to time limitations it was not possible to test all samples in the oedometer. Oedometer samples were taken from the reference sample prepared by mixing Speswhite kaolin clay powder and Polwhite E kaolin clay powder with distilled water to twice the liquid limit. Samples were also taken from sedimented Speswhite kaolin clay samples with an initial water content of 1200% to determine whether sensitivity was formed even though permeability anisotropy was not. Samples were also taken from the top and bottom of samples created from a slurry consisting of 70% Speswhite kaolin clay, 30% Polwhite E kaolin clay and 0.1 grams of dispersion agent per litre of slurry mixed to an initial water content of 500%. The results from these tests are presented in Figure 8.16. The black lines represent areas where Speswhite kaolin clay were dominant and the grey lines represent areas where Polwhite E kaolin clay were dominant.

Firstly comparing the sedimented Speswhite kaolin clay sample at an initial water content of 1200% to the reference Speswhite kaolin clay sample, there was a sensitivity of approximately 2. Demonstrating that although no increase in permeability anisotropy was achieved a sedimented structure was still developed. The sample taken from the top of the sedimented Speswhite kaolin, Polwhite E kaolin with dispersion agent sample (where Speswhite kaolin

was dominant) had a higher sensitivity of approximately 2.1. This larger sensitivity could be experimental scatter or attributed to the inclusion of the dispersion agent. All Speswhite kaolin clay compression curves sit level or below the reconstituted Polwhite E kaolin clay compression curve. With only the sample taken from the base of the sedimented Speswhite kaolin, Polwhite E kaolin and dispersion agent sample (region predominantly Polwhite E kaolin clay) sitting above reference Polwhite E compression curve. The sensitivity of this sample is also approximately two.

The observed oedometer response, similar to the horizontal permeability, is a function of where the samples are taken from. For samples taken from the extremities of the sedimented soil, comparisons to the reference material were sensible, however for the intermediary regions there was likely to be mix of both materials and this comparison was not appropriate. For a full understanding of the influence of initial water content and sample preparation on sensitivity a similar study would need to be conducted using triaxial testing comparing the overall behaviour rather than discrete sections as completed for this dissertation.

These results although preliminary in nature with each curve only the average of two oedometer samples, provided evidence that a sedimented structure had been developed which was not detectible by permeability testing alone (1200% water content sedimented Speswhite kaolin clay sample). This could be practically explained from Figures 2.2-2.2 anisotropy is likely to be governed by layering within a sedimented sample as opposed to changes in clay particle orientations. It also validated that the increase in post-test moisture content observed was a function of a more open structure developed during sedimentation and provided further evidence of particle separation fully occurring in the dispersion agent tests.

8.8 Element Test summary

In summary, the sedimentation column tests conducted demonstrated that it was possible to create a sedimented structure through sedimentation on the centrifuge. This was confirmed by increased permeability anisotropy, sensitivity observed in oedometer tests and finally through the visual difference between the samples.

To create a sample with enhanced permeability anisotropy required the use of two materials with different particle sizes and permeabilities i.e., Speswhite and Polwhite E kaolin clay and an initial water content that allowed for particle separation during sedimentation. This water content was dependent on the materials present in the slurry, while using Speswhite and Polwhite E kaolin clay the critical water content was approximately 1200%. When only one

material was used (i.e., only Speswhite kaolin clay) there was no enhanced permeability anisotropy developed even though there was sensitivity developed. When the slurry contained a material such as sand which settled prior to the centrifuge accelerating it would not create a level layer.

The water content required for particle separation to occur can be significantly reduced by using a dispersion agent (sodium hexametaphosphate) in relatively small concentrations of 0.1 grams of dispersion agent per litre of slurry. It was found that when the concentration of the dispersion agent was greater than 0.1 grams per litre of slurry it created a soil sample which had a meta-stable structure. When cut or agitated the sample tended to return to a slurry like state and was therefore unsuitable for geotechnical centrifuge modelling.

The minimum sedimentation time was found by sedimenting the same slurry for different durations and determining the resultant permeability anisotropy and percentage of solid particles in suspension. This found that after only two hours of sedimentation time inflight 98.3% of solid particles had sedimented and there was no subsequent change in soil permeabilities with longer sedimentation times.

Sensitivity was observed in both samples sedimented from, a slurry consisting of only one material (Speswhite kaolin clay) and from a slurry consisting of two materials (Speswhite and Polwhite E kaolin clay). Determining the resultant permeability anisotropy, dispersion agent concentration, critical water content, sedimentation time and one dimensional consolidation behaviour was essential before sedimenting a soil bed in a centrifuge strong box. As a result of the element tests conducted the slurry selected to sediment a soil bed suitable for centrifuge testing was a 70% Speswhite kaolin clay, 30% Polwhite E kaolin clay mixed with 0.1 grams of dispersion agent per litre of slurry to an initial water content of 500% which was sedimented for two hours at 100*g*.

9. Sedimenting a soil bed in a centrifuge strongbox

This Chapter describes, in detail, how the slurry and sample preparation technique used in a sedimentation column can be scaled to create a soil bed with a sedimented structure with a centrifuge strongbox. The practical changes to the sample mixing procedure and slurry placement procedure due to the increased volume of slurry and the predictive method of determining the volume of slurry required to achieve a predetermined layer thickness are also detailed in this chapter.

9.1 Sedimented soil bed constraints within a strongbox

Sedimenting a soil bed within a centrifuge strongbox has one key constraint, the geometry of the strongbox. The Research Centre for Sustainable and Resilient Civil Engineering at City, University of London have centrifuge strongboxes with internal dimensions of 550mm x 200mm x 375mm, the height can be increased to 675mm using an extension. Without using the extension a maximum layer thickness of 25mm would be achievable to create the desired centrifuge sample (detailed in Section 9.2). When using the extension the maximum layer thickness achievable was increased to 70mm, therefore, extension was used. This required minor modifications to the existing system to ensure there were no leaks from the interface between the strongbox and extension.

9.2 Designing a sedimented soil bed within a strongbox

For each sedimentation column experiments the mass of clay in each column were kept consistent and the resultant sample height was variable. However, when sedimenting a soil bed for centrifuge modelling designing the layer thickness and total height is essential. A calculation procedure was developed to determine the required slurry volume to sediment specific layer thickness for a known stress history.

Figure 9.1 shows a flow chart for the calculation procedure to design a sedimented soil bed (note the procedure outlined is for a soil bed consolidated post sedimentation i.e., overconsolidated). The soil parameters used in this procedure were taken from monitoring the consolidation stages of the sedimentation columns. These properties were a function of the constituent parts of the slurry and the initial slurry water content. If a different slurry was to be sedimented the parameters highlighted in Figure 9.1 would need to be determined.

For this research project a centrifuge model was created for a tunnel excavation test where the support pressure is reduced inducing settlement following a similar experimental procedure to

Grant (1998). Typically, at City, University of London model tunnels are 50mm diameter and tested at 100*g* representing a 5m tunnel at prototype scale. Grant (1998) first opted for this arrangement as it allowed for a cover (C) of up to 4 times the tunnel diameter (D). Since 1998 various tunnel tests have been conducted at City, University of London with different C/D ratios. For this study a C/D of 2 was selected, for an overconsildated sample with a maximum consolidation stress of 500kPa and swelled to 250kPa. A low C/D ratio was chosen to reduce the time required to sediment a soil bed, reduce the consolidation time and the time to reach hydrostatic equilibrium on the centrifuge. The ground water table was set 10mm below the ground surface at model scale representing 1m at prototype scale. A soil sample of 204mm deep was required for the centrifuge tests.

The sedimented soil bed consisted of 4 different sedimented layers. The designed soil bed geometry is illustrated in Figure 9.2, indicating the thicknesses of the four layers and the relative positions of the layers to the tunnel. The soil bed was designed such that the tunnel was situated in the centre of one of the sedimented layers. In addition to the four layers, a fifth sacrificial layer was sedimented on top. This sacrificial layer had two purposes; firstly, this fifth layer acted as insurance if the sample consolidated more than expected or if there was any clay lost through extrusion when consolidating the sample in the hydraulic press the soil bed would not be shallow. Secondly, when centrifuge soil bed are removed from the consolidation press it was impossible to remove all water from above the soil bed. The top of the soil bed can subsequently swell and become very soft, a deeper than required soil bed allowed for this to be trimmed during the experimental procedure.

9.3 Strongbox preparation procedure

Similar to the sedimentation columns the centrifuge strongbox and extension were assembled a few days prior to the day of sedimenting a centrifuge sample. To ensure that the centrifuge strongbox was sealed the strongbox and extension was filled with water and accelerated to 100*g* for 2 hours. The water level was recorded manually before and after the acceleration of the centrifuge and the water pressure was also monitored inflight using a City, University of London pore pressure transducer (Ritchie et al., 2021) which is covered in more detail in Section 10.4.1 to ensure there were no leaks.

Porous plastic and filter paper are placed at the base of a centrifuge strongbox at City, University of London to stop the base drain from blocking. This needed to be secured down during the sedimentation phases as it is buoyant. The porous plastic was bonded onto the base

of the strongbox using silicone sealant around the perimeter of the strongbox. To secure the filter paper an aluminium frame was manufactured from 3mm thick 90-degree angle aluminium. The frame was manufactured to be 2mm smaller than the plan dimensions of the strongbox. The frame sits on top of the filter paper to prevent the filter paper from floating to the surface and the filter drain becoming blocked. Figure 9.3 shows an image of the frame and filter paper placed inside the strongbox.

After placing the filter paper, the centrifuge strongbox and extension was lined with water pump grease to reduce sidewall friction during sedimentation and consolidation. Mair (1979) stated for a 300mm deep sample up to 10% of the vertical stress was lost due to side wall friction and by lining the sidewalls in water-pump grease this could be reduced. The strongbox was weighed and placed onto the centrifuge swing. As the volume and mass of slurry to be added into the centrifuge strongbox was known the counterweight could be set prior to the day of sedimentation.

9.4 Slurry mixing procedure

The sedimentation column tests typically required 2 litres of slurry per sedimentation column and an additional 3 litres for sampling. There are two planetary mixers available at City, University of London with a 9 and 20 litre capacity. The sedimented soil bed in a centrifuge strongbox required significantly more slurry to sediment a layer, 36 litres for the design selected. Therefore, a different mixer needed to be used. The same Winkworth ribbon mixer was used to mix the slurry for sedimentation as the slurries used to mix 'typical' centrifuge soil bed at City, University of London. Prior to being used for creating the slurries for sedimentation the mixer was thoroughly cleaned as seen in Figure 9.4. A total of 36 litres of slurry were required to sediment 53mm thick layer and it was decided that 50 litres of slurry would be mixed at a time to ensure the mixer was working within optimal range.

Although a different mixer was used the same mixing procedure was followed. The dry components (the Speswhite kaolin clay powder and the Polwhite E kaolin clay powder) were weighed separately and placed into the empty mixer. The required amount of distilled water was then added using 5 litre measuring jugs and the mixer was then started. The dispersion agent (sodium hexametaphosphate) was subsequently weighed and added into the mixer, typically, 5 minutes after the mixer was started. The slurry was left to mix for two hours until a smooth consistency was achieved. After the first layer had been placed into the strongbox (as detailed in Section 9.5) the mixer was emptied and cleaned thoroughly again, before the same

slurry mixing process was repeated to create the slurry for the second sedimented layer. To empty, clean and restart the mixing procedure took approximately 20 minutes.

9.5 Slurry placement procedure

When conducting the sedimentation column experiments the slurry was transferred from the mixing bowl into the sedimentation columns via siphoning slurry from the mixing bowl and passing it through a hydro-splitter. This ensured there was the same particle size distribution in the mixing bowl and sedimentation columns. Due to the increased volume required it was not feasible to pass 36 litres of slurry through the hydro splitter. The slurry was transferred directly from the dispenser at the base of the mixer into the centrifuge strongbox. While the mixer was running the dispenser was opened and slurry was placed into the strongbox using 5 litre measuring jugs until the desired volume had been placed. Using the dispenser at the base of the mixer while running ensured that a consistent particle distribution was achieved.

When placing the slurry from the measuring jug into the centrifuge strongbox, the force of pouring slurry would have torn the filter paper at the base of the strongbox and for later pours erode the surface of the underlying sedimented layer. As a result, a 'breakwater' was developed to reduce the speed at which slurry hit the underlaying filter paper or soil. The breakwater was a PMMA plate with a plan area just smaller than the internal dimensions of the strongbox attached to a rod with cross beam that could be adjusted to be fixed approximately 20mm above the filter paper or the underlying soil. The slurry was poured from a measuring jug onto the breakwater to reduce the input velocity and to protect the underlying filter paper or soil layer. Figure 9.5 shows an image taken during the slurry placement and the use of the 'breakwater'.

For the first sedimented layer, slurry was poured into the empty strongbox using the measuring jug and breakwater until the predetermined volume had been placed into the strongbox. This volume was monitored both as litres of slurry and as a height of slurry in the strongbox. Once the slurry was poured into the strongbox the centrifuge was accelerated following the centrifuge procedure detailed in Section 9.6.

After the first layer had been sedimented there was a soil layer covered by a substantial depth of dispersion fluid. This fluid was siphoned out of the centrifuge strongbox leaving approximately 50mm covering the underlying soil layer. The 50mm of dispersion fluid acted as a secondary buffer working in conjunction with the PMMA breakwater to reduce sample disturbance of the underlying soil layer when placing the next batch of slurry. Solid contents

were taken from the dispersion fluid to compare with the sedimentation column data. This process was completed until the required number of layers had been sedimented.

9.6 Sedimentation procedure

The processes of filling the centrifuge strongbox and accelerating the centrifuge took approximately 10-15 minutes. The centrifuge was accelerated to 100*g* and left for two hours as informed by the sedimentation column experiments. During the sedimentation time the next batch of slurry was prepared as described in Section 9.4. After two hours of sedimentation the centrifuge was decelerated. The excess water was siphoned off from above the sedimented sample leaving a 50mm buffer. The excess water removed was collected and weighed for the adjustment of the counterweight.

A specially made marker was placed on the surface of the sedimented layer in the back corner of the layer (relative to the centrifuge window). This marker was designed to have a specific density such that it did not float when the slurry for the next layer was inputted. The marker was also manufactured to have a specific surface area to avoid embedment into the newly formed sedimented layer. The markers were used as a secondary means of measuring the resultant layer thickness post-test if the layer interfaces were not clearly visible.

After the excess water had been siphoned and the marker had been placed onto the surface of the sedimented layer the next batch of slurry was then placed into the strongbox using the method described in Section 9.5. The centrifuge counterweight was adjusted, accounting for the weight of the next batch of slurry and the removed dispersion fluid from the previous layer. The centrifuge was accelerated to 100*g*, and the same procedure was followed for all subsequent layers. The time taken to spin down, siphon excess water, place the marker, fill the strongbox with slurry, adjust the counterweight and to reaccelerate the centrifuge took approximately 30 minutes. Therefore, the total time to sediment a centrifuge layer was two and a half hours. Practically it was possible to sediment 4 layers within a working day.

The first 4 layers of the centrifuge soil bed were sedimented in one day and the final sacrificial layer was sedimented the following day. After the sedimentation of the fourth layer (final sedimented layer of the day) the excess dispersion fluid was siphoned from the strongbox leaving approximately 50mm. The centrifuge strongbox was covered with a clean plastic sheet to stop evaporation and contamination. The following day a new batch of slurry was mixed, placed into the strongbox and sedimented following the same procedure to create the final sacrificial layer.

9.7 Post sedimentation

Following the sedimentation of the final layer the excess water was siphoned from above the sedimented soil bed, leaving 50mm to avoid any sample disturbance. The strongbox was removed from the centrifuge swing and a 7-micron pore size filter paper and porous plastic was placed on top of the sedimented soil bed. The soil bed was consolidated and treated the same as any other clay soil bed for centrifuge modelling at the centrifuge facility at City, University of London. The soil bed was placed into a computer controlled hydraulic press to maintain a constant applied stress and the soil bed was consolidated in pre-determined stages to its final stress history. Two-way drainage was allowed via drainage taps at the bottom of the centrifuge strongbox connected to the base drain and through and around the loading plate. Figure 9.6 shows an annotated image on the consolidation press and system used at City, University of London.

Figure 9.7 illustrates the stress level of the sample over time. Firstly, on day one the stress was set as low as possible (around 10kPa) to avoid any extrusion of clay. The stress was gradually increased, the height of the sample and applied stress was recorded routinely. The sample had not fully consolidated in the time between increasing the applied stress; however, the sample had consolidated enough such that clay was not extruded around the loading plate. The soil bed was increased to a maximum stress (500kPa) at least ten days prior to testing and five days before testing the pressure was reduced to its final stress (250kPa). Three days before the tunnel centrifuge test (day 14 on Figure 9.7) pore pressure transducers (PPT's) were installed into the soil bed. After the installation of the PPT's the soil bed was left in the hydraulic press for a further 48 hours to ensure the clay around the PPT's had fully consolidated. Further details on the PPT's and installation are detailed in Section 10.3.3. Importantly after the sedimented soil bed had been created it was treated in the same way as any other clay soil bed for centrifuge testing at City, University of London. The consolidation, model making procedure and construction event testing procedure remained consistent for all soil beds.

10. Tunnel Centrifuge tests

This chapter details the centrifuge test series undertaken and the different soil beds created to investigate the soils response to a tunnel construction event. To model the tunnel construction event, established equipment at City, University of London after Grant (1998) was utilised. The soil response to the tunnel construction event was measured by pore-water pressure transducers developed at City, University of London and linear variable differential transformers.

10.1 Centrifuge test series

The primary aim of this research project was to develop a method of creating a sedimented soil bed that could be used to model a construction event. The sedimentation column tests identified a suitable method of creating a soil bed with a sedimented structure. The same procedure was applied to create a sedimented soil bed in a centrifuge strongbox using the procedure outline in chapter 9.

After the creation of a sedimented soil bed it was used to conduct a of centrifuge test investigating the soil response to a tunnel construction event. A series of three tests were conducted where a tunnel construction event was modelled in soil beds with a sedimented structure and a reconstituted structure as illustrated in Figures 3.1 and 3.2. The tunnel tests modelled a reduction in support pressure in overconsolidated clay. The tunnel was idealised as a latex rubber membrane supplied with compressed air, the pressure was reduced to simulate a tunnel construction event. The tunnel, pressure reduction procedure and instrumentation remained constant for all centrifuge tests, with the only variable being the soil bed.

The three centrifuge tests conducted are summarised below:

Tunnel test 1: The clay bed was prepared by creating a 120% initial water content Speswhite kaolin clay slurry and consolidating in a hydraulic press. This test was the reference test with a sample prepared following the established procedure at City, University of London.

Tunnel test 2: The clay bed was a reconstituted from a slurry consisting of 70% Speswhite kaolin clay and 30% Polwhite E kaolin clay slurry mixed to an initial water content 120% then consolidated in a hydraulic press. This test utilised the same constituent parts as the sedimented soil bed in tunnel test 3. This test investigated the influence of using two different constituent materials prepared whilst following the same preparation technique as tunnel test 1.

.

Tunnel test 3: The clay bed was a sedimented sample as described in Chapter 9 and subsequently consolidated in the hydraulic press. This test investigated the effect of a sedimented structure on the soil response to tunnel construction.

Within each centrifuge tunnel test two different phases were compared. First, the consolidation phase of the centrifuge experiments were compared. Second, the soil response to a reduction in tunnel support pressure was compared.

10.2 Soil bed design and clay preparation

The dimensions of the soil bed required was the same as the sedimented centrifuge sample detailed in Section 9.2 (Figure 9.2). However, in the case of tunnel test 1 and 2 there were no layers present. In summary the centrifuge tests were conducted at 100g in an overconsolidated clay bed consolidated to 500kPa and swelled to 250kPa. The tunnel was idealised to a 50mm diameter cavity representing a 5m tunnel test at prototype scale. For this study a C/D of 2 was selected and the final height of soil sample required was 204mm deep.

10.2.1 Speswhite kaolin clay centrifuge soil bed preparation

For tunnel test 1 Speswhite kaolin clay powder was mixed with distilled water to an initial water content of 120% (twice the liquid limit) in a Winkworth ribbon blade mixer. This slurry was mixed until it was a smooth consistency with no lumps, this typically took 5 hours. The mixer was frequently stopped to manually break down any lumps within the slurry. The same strongbox and extension used for sedimenting a soil bed was used for all tunnel tests. The strongbox and extension were assembled prior to the day of mixing. In the base of the strongbox a sheet of porous plastic was stuck to the base using silicone sealant. This was covered with filter paper that has a 7-micron pore size, ensuring that the clay was retained and only water passes. Similar to the sedimentation procedure the side walls of the strongbox were lightly coated in water-pump grease to reduce wall friction in centrifuge samples (after Mair, 1979).

Slurry was carefully placed into the centrifuge strongbox in approximately 20mm layers and manually agitated to minimise the entrapment of air into the soil bed. This process was repeated until the desired amount of slurry was added into the centrifuge strongbox. An excess amount of slurry was input into the strongbox such that the final centrifuge soil bed was 30-40mm deeper than required, this excess was later trimmed from the soil bed after consolidation during model preparation. Once the desired amount of slurry was placed into the strongbox another

piece of filter paper and porous plastic was placed on top of the slurry. The soil bed was ready for consolidation, the same system and procedure were followed as described in Section 9.7. Once consolidated the soil bed was removed from the consolidation press and the model making procedure was started. Further details of the centrifuge model making procedure is detailed in Section 10.5.

10.2.2 Speswhite kaolin clay, Polwhite E kaolin clay centrifuge soil bed preparation

For tunnel test 2 the soil bed preparation procedure largely remained the same as the Speswhite kaolin clay soil bed. The only difference instead of only Speswhite kaolin clay powder being added into the ribbon mixer Speswhite kaolin clay and Polwhite E kaolin clay powder were added into the mixer at a 70:30 ratio. The initial water content, mixing duration, centrifuge strongbox preparation, slurry placement and consolidation procedure all remained constant as detailed previously. Before and after this slurry was created the mixer was thoroughly cleaned to ensure there was no cross contamination between slurry preparations. After consolidation the same model making procedure was followed as detailed in Section 10.5.

10.2.3 Sedimented Speswhite kaolin clay and Polwhite E kaolin clay centrifuge soil bed preparation

For tunnel test 3 the sedimented centrifuge soil bed was preprepared using the procedure detailed in Chapter 9. After sedimentation the sedimented centrifuge soil bed was treated the same as the soil beds in tunnel test 1 and 2. The only difference between the three centrifuge tests was the method of creating the soil bed.

10.3 Centrifuge Apparatus

The centrifuge tests required various pieces of apparatus to model a tunnel construction event and to establish a ground water regime within the centrifuge. Details of the apparatus required are detailed in this section.

10.3.1 Tunnel cavity and tunnel support system

The tunnel was idealised to an air supported cavity. It was necessary to be able to increase the tunnel support pressure during the acceleration of the centrifuge to balance the increase in overburden stress. It was also necessary to reduce the support pressure inflight after the sample has reached equilibrium to model tunnel construction. The latex membrane and sealing system was the same as that used in Grant (1998). The dimensions of the latex tunnel membrane were

1mm thick, 50mm outside diameter, 199mm long cylinder with a 15mm diameter opening at one end. The latex membrane was manufactured by Precision Dipping's using a mould provided by City, University of London. The tunnel fitting system is pictured in Figure 10.1, and this was placed into the opening of the tunnel membrane shown in Figure 10.2.

The tunnel membrane and fitting were installed from inside the strongbox and the tunnel fitting passed through a port in the backwall of the strongbox. The fitting was clamped into place using a nut which also created a seal between the tunnel membrane and the strongbox wall (Figure 10.3). A manifold was used such that the compressed air supply located on the centrifuge swing and an air pressure transducer were connected to the tunnel (Figure 10.4). This allowed for the tunnel support pressure to be controlled and recorded from the centrifuge control room whilst inflight. The air pressure transducer was calibrated the day prior to each of the centrifuge tests.

10.3.2 Ground water supply

A standpipe system is used at the geotechnical centrifuge facility at City, University of London to establish a ground water regime. Figure 10.5, an annotated photograph of the arrangement used at City, University of London which details the ground water control system. Tap water is supplied to the centrifuge swing via the centrifuge hydraulic slip rings into the standpipe until the water level reaches the height of the overflow pipe (central tube). The height of this overflow pipe is dependent on the water level required for each centrifuge test. For the centrifuge tests in this dissertation the ground water table was set at 10mm below the ground surface requiring an overflow height of 250mm above the centrifuge swing. The standpipe water supply was connected to the base drain of the centrifuge strongbox using 8mm pipe and standard plumbing fittings. The water pressure at the base of the standpipe was measured inflight using a new City, University of London PPT (Ritchie et al., 2021) described in Section 10.4.1 to ensure the desired ground water profile was applied.

10.4 Centrifuge Instrumentation

Centrifuge tests rely on various instruments to record the soil response to a construction event. In this series of tests, the changes in pore-water pressure were measured by pore pressure transducers and the surface settlement in response to a tunnel construction event was monitored by Linear Variable Differential Transformers (LVDT's) placed along the centreline of the centrifuge model. This section covers details of the instrumentation, their calibration, installation and use.

10.4.1 Pore water pressure transducers

To measure the response of pore-water pressure in the centrifuge models a new PPT was developed and manufactured at City, University of London as a replacement to the Druck PDCR81 transducer (Ritchie et al., 2021). The new PPT's use a TE Connectivity pressure sensor that had previously been used in centrifuge modelling at the University of Western Australia (Fiumana et al., 2018). The application was to measure changes in pore pressure while mounted on the surface of geotechnical structures. With the design of a suitable housing and the selection of an appropriate filter the same sensor elements can be used as buried PPT's for centrifuge modelling. Details of the different TE Connectivity sensitivity sensors available are provided in Table 10.1. For the City, University of London PPT's the 7-bar high sensitivity transducers were selected. The sensor dimensions are detailed in Figure 10.6 and the electrical properties are detailed in Table 10.2.

Figure 10.7 details the design of the new PPT highlighting the key features. The design of the casing ensured that the overall size was as small as possible. The Druck PDCR81 has an overall length of 19mm and a diameter of 6.4mm. The size of the City, University of London PPT has an overall length of 18mm and a diameter of 9.5mm. The City, University of London PPT was constructed from two stainless steel parts manufacture on a CNC lathe. The two parts of the PPT casing were joined using an adhesive potting compound. This construction also prevented water reaching the contact pads from the back of the transducer. To prevent water getting to the contact pads from the front of the transducer an O-ring was placed between the containing ring of the sensor and the PPT casing.

The porous stones used in the City, University of London PPT were constructed from the same material (Celleton V1) and the same size as the porous stones used in the Druck PDCR81 transducers. Celleton V1 is a silica-based ceramic with a 1 micron pore size and an air entry value of 200kPa. Manufacturing new porous stones proved difficult due to the materials tendency to fracture when machined and the specialist suppression equipment required for silica dust. A specialist ceramic supplier (Precision Ceramics) manufactured the new porous stones to an accuracy of ±0.1mm.

At City, University of London centrifuge facility instrumentation is connected to the data acquisition system using LEMO connectors. A small diameter 4 core cable was created by using 29 American Wire Gauge (AWG) strain gauge cable and heavy wall Teflon tubing with a 0.4mm wall thickness and 1.75mm outer diameter (supplied by Adtech). The strain gauge

cable was pulled through the Teflon tubing to create the cabling. The Teflon tubing pushes over the barbed detail on the boot of the PPT preventing water entry into the cable portion of the transducer. As secondary measures a sterling silver jump ring was secured over the Teflon tube and the tail of the PPT and covered with heat shrink tubing to ensure the boot of the PPT was sealed. Figure 10.8 is a photograph comparison of the City, University of London PPT and a Druck PDCR81.

Essential to getting a good response from a PPT was to ensure the porous stone had been fully deaired and saturated. A two-chamber system was developed to effectively deair, saturate and calibrate 8 PPT's at a time. The deairing and calibration equipment is illustrated in Figure 10.9. When calibrating or using the PPT's within a centrifuge test the transducers need to be sealed against the back plate of the centrifuge strongbox or the calibration chamber. To create the seal standard Swagelok plumbing fittings with a custom a rubber tube and washer on the PPT cable were used (as illustrated in Figure 10.10). When the nut of the Swagelok fitting was tightened it compressed the rubber washer onto the PPT cable. The sealing system was tested under a vacuum and a maximum applied pressure of 700kPa the system provided an effective seal in both conditions.

Prior to calibrating and using the PPT's they were thoroughly cleaned by hand with distilled water and left to dry. Once dry the PPT's were installed into the left chamber in (Figure 10.9) and isolated from the rest of the system by closing the valve connecting the two chambers. The left chamber and the PPT's were deaired using a vacuum pump. The pressure was monitored with a dial gauge and it typically took 5 minutes for the pressure to be reduced to 0.99 of a vacuum. The chamber containing the PPT's were subjected to a vacuum for approximately 30 minutes. Once fully deaired the PPT's were keep under a vacuum by closing the valve connected to the vacuum pump.

The right chamber filled with distilled water was then fully deaired by connecting the vacuum pump. This typically took 1 hour, after the distilled water had been deaired the valve was closed to maintain a vacuum. The valve connecting the two chambers was opened, which flooded the PPT chamber with deaired distilled water. The chamber containing the PPT was then isolated by closing the valve connecting the two chambers. The vacuum was then released by opening the valve to atmosphere. This saturated the porous stones with distilled deaired water. As a secondary measure the vacuum was reapplied to the chamber containing the PPT's to remove

any remaining air within the porous stone. In all tests no visible air bubbles were seen being expelled from the porous stones during this step.

Once deaired and saturated the PPT's were calibrated within the chamber using the bishop ram, which manually increased the water pressure within the chamber. The centrifuge data acquisition system was used to record the chamber pressure measured by a calibrated Druck Digital Pressure Indicator (DPI) and PPT's as an output voltage. The chamber water pressure was typically increased in 20kPa increments to a maximum pressure of 300kPa after which the pressure was reduced in 20kPa steps. Finally, a large pressure increase of approximately 200kPa was applied as fast as possible to assess the response time of the PPT's. The calibration and response time of the transducers were calculated, any transducers with an R-squared of less than 0.99 or a lag in response time greater than 1 second (the frequency that data was recorded) was deemed unsuitable for use in centrifuge modelling. In this scenario the PPT's were removed from the calibration equipment cleaned, deaired, saturated, and calibrated again. In all but one case this resolved the issues with PPT calibration. The PPT that was not fixed by cleaning had clay behind the porous stone. The porous stone was carefully removed, and the sensor was cleaned fixing the lag in response time. For the three tunnel centrifuge tests conducted for this dissertation the transducers where deaired and calibrated on the day they were installed into the clay bed.

Post manufacturing and prior to being used in a centrifuge modelling all transducers were pressure tested under 1*g* using the calibration equipment to ensure they provided stable and reliable pore-water pressure measurements. The water pressure was increased to 300kPa and the output of the transducers and the Druck DPI were recorded every minute for a minimum of 5 days. This acted as a pressure test for the water proofing of the PPT's and allowed for the stability of the transducers to observed over a longer duration than a centrifuge test. Over the 5-day duration there were less than a 2kPa variation in water pressure recorded in all the PPT's, the same change in pressure was also recorded by the Druck DPI. The average water pressure recorded by the PPT's and the DPI varied by less than 0.5kPa over the 5 day period. These tests provided confidence that the new City, University of London PPT's and the method for saturating were suitable for geotechnical centrifuge modelling.

Calibrating the new PPT's over numerous days while manufacturing and testing the transducers it could be seen that the calibration constants of all transducers changed by less than 0.5%. However, the offset could vary by a more significant amount and can be related to atmospheric

weather conditions. The difference in atmospheric pressure on the days which the calibrations were conducted were approximately the same as the difference in calibration offsets.

The accuracy of the City, University of London transducers when measuring changes in pore-water pressure during a centrifuge construction event was therefore approximately 2kPa (the variation that was observed under constant applied load). The error on absolute pressure measurements could however be larger. In London the difference in a high- and low-pressure day could be as much as 5kPa. Therefore, there could be an maximum error in absolute pore-pressure measurements of 7kPa. By noting the atmospheric pressure on the day the transducers were being used it may be possible to correct these measurements for changes in atmospheric conditions. However, for this study there was no attempt to correct pore pressure measurements with changes in atmospheric conditions as changes in pore water pressure were more relevant that absolute values. Overall, the potential errors in the new City, University of London PPT's were comparable with the Druck PDCR81 or any pore pressure transducer that uses atmospheric pressure as a reference. The new City, University of London pore pressure transducers were proven as a low-cost alternative to the Druck PDCR81 transducer.

PPT's were installed into clay soil beds for centrifuge modelling after the soil bed had been consolidated/swelled to its final effective stress in the hydraulic press (labelled on Figure 9.7). Ports were manufactured into the centrifuge strongbox walls at appropriate locations for this dissertation. These ports were sealed prior to the installation of the PPT's.

To install the PPT's the plugs were removed and a specially manufactured guide screwed into the ports from the outside of the strongbox (Figure 10.11). The guide was manufactured from brass and was 75 mm long and had an internal bore diameter of 11.2mm. A thin-walled seamless stainless-steel cutter with an outside diameter of 11mm was used to create a bore to the mid-point on the model (Figure 10.12.). After the bore had been created a small amount of deaired clay slurry mixed to twice the liquid limit was placed at the end of the bore using the 'slurry gun' (Figure 10.13). A deaired calibrated PPT was then placed into the PPT bore and in contact with the deaired clay slurry using the placement tool (Figure 10.14). The placement tool was carefully removed, and the remainder of the bore was filled with deaired clay slurry (Figure 10.15). The PPT port was sealed using the Swagelok system described previously (Figure 10.16). The same procedure was followed to install all the PPT's. The clay soil bed was left for an additional 48 hours after the installation of the PPT's to allow the slurry around

the PPT's to fully consolidate. After the centrifuge test the PPT's were immediately excavated and cleaned to avoid the porous stone getting blocked with clay.

At different stages of the PPT placement process there were potential sources errors, the magnitude and mitigation implemented for these are detailed in the following paragraphs. Firstly, when cutting the PPT bore it was possible to over excavate the bore as the target bore depth was marked by hand onto the cutter. Following a careful model making procedure the potential for over boring could be reduced and the bore depth should be within 2mm of the centre line of the soil bed for centrifuge modelling. As the centrifuge test replicated plain strain conditions and are sufficiently far away from the boundaries this should not have influenced the pore-water pressure readings.

Due to the tolerances within the guides, it was possible to excavate the bore at an angle in any direction. At the centre line of the strongbox this equated to an error of placement of less than 0.5mm which was deemed insignificant. When placing the PPT into the bore care also needed to be taken to ensure that the PPT was placed at the end of the bore and with no air pockets created. Similarly, when filling behind the PPT care was taken to ensure the void was fully filled and had created no air pockets. The impact of which is hard to assess, however when excavating PPT's there was no visible evidence of air pockets being created.

As the PPT's were installed while the sample was still in the consolidation press, at a vertical stress of 250kPa, when the clay bed was removed from the press to start the model making procedure (detailed in Section 10.5) the sample would have experienced a negative pore pressure of 250kPa. This was outside the linear range of a City, University of London PPT and higher than the air entry value of Celleton V1. There was the potential for cavitation in the porous stones and that the initial PPT readings may not provide reliable measurements of pore-water pressures.

As the centrifuge accelerates and the *g*-level increases the pore pressure rapidly increases, theoretically causing any air pockets created during cavitation to collapse. The pore pressure measurements from this point forward should be representative of the soil model. When outside of the operating range or if cavitation occurred the output should remain constant. After the pore-water pressure had increased to above the minimum operating range or to a sufficient pressure to collapse any air pockets the pore pressure response recorded should be representative of the 'actual' pore-water pressure. These issues are not unique to the new

transducers or the centrifuge facility at City, University of London. However, understanding the potential behaviour was essential to interpreting pore pressure transducer data.

10.4.2 Linear Variable Displacement Transformer

To house the Linear Variable Displacement Transformer (LVDT's) during the centrifuge test which measured the soil surface displacement a specially designed rack which spanned centrifuge strongbox. For the series tunnel tests in this dissertation 9 LVDT's were secured in the rack. One LVDT was positioned directly above the centre line of the tunnel and the reaming LVDT's were positioned at ±45, ±90, ±135 and ±180mm from the tunnel centreline. Figure 10.17 illustrates the layout of the LVDT's for the centrifuge tests. The LVDT's were calibrated and inserted into the LVDT rack the day prior to the acceleration of the centrifuge. The LVDT's were recalibrated before each of the centrifuge test to ensure reliable results were obtained.

10.5 Model preparation

After the soil bed for centrifuge modelling had been prepared and consolidated the first step in centrifuge model making process was to install the PPT's. Figure 9.7 details the timeline for creating a soil bed for centrifuge modelling and highlights when the PPT's were calibrated and installed. The procedure described in Section 10.4.1 was followed to install the PPT's and Figure 10.18 details the locations of the PPT's for the centrifuge tests conducted (the numbers associated with the PPT locations are used later when discussing the results obtained, numbers are relative to the back of the strongbox).

When the PPT's were installed, the bore was filled with a deaired clay slurry the same as the surrounding soil mixed to twice the liquid limit. Figure 10.19 illustrates the locations of the PPT's and layers and the whether the PPT is located in a Speswhite kaolin clay or Polwhite E kaolin clay region. PPT 8 although was at the top of design layer 3 in the Speswhite kaolin clay region, from the results of the initial water contents of the sedimented slurries, layer 3 had a higher water content than intended being 540% versus the 500% planned. Although it was not possible to confirm prior to completing the centrifuge test, it was predicted that this related to a 7-8mm shallower layer. PPT 8 would therefore sit at the bottom of layer 4 within the Polwhite E region and the bore was therefore filled with Polwhite E kaolin clay. The process of installing a single PPT takes between 5-10 minutes after all PPT's had been inserted into the centrifuge soil bed it was left for another 48 hours to allow the clay surrounding the PPT to consolidate.

After the sample had consolidated it was ready to be removed from the consolidation press and to start constructing the model. Before the sample was removed from the consolidation press the drainage taps at the base of the strongbox were closed and any excess water on top of the loading plate was removed to minimise soil swelling. The front of the strongbox was removed to gain access to the clay soil bed (Figure 10.20). A specially manufactured guide was attached to the front of the strongbox to trim the clay to the desired model height using a box cutter (Figure 10.21). Once at the current level Plasti-dip was applied to the surface of the clay to reduce the sample drying (Figure 10.22 after Gorasia, 2013).

The tunnel cavity was created using a guide bolted to the strongbox to ensure it was consistently located at the centreline of the model (Figure 10.23). The tunnel cavity was bored using a 50mm outside diameter, thin-walled seamless stainless-steel cutter (Figure 10.24). The tunnel union was placed inside the latex tunnel liner, and both were passed through the tunnel bore and into a port in the back wall of the strongbox (Figures 10.1-10.3). The clamping nut was tightened onto the fitting to create a seal. The manifold was installed onto the fitting to enable the compressed air and pressure sensor to be connected (Figure 10.4). The model tunnel was pressurised under approximately 10kPa to ensure there were no leaks from the tunnel union.

Next an observation window was bolted into place such that inflight images could be recorded, and the centrifuge test could be observed live. Prior to being installed the window was lubricated with a high viscosity (10cSt), clear silicone oil to reduce interface friction. The LVDT rack was secured to the top of the strongbox at the model centreline to measure vertical surface displacements (Figure 10.25). The model was weighed, placed onto the centrifuge swing and the centrifuge counterweight was adjusted.

Once the model was on the centrifuge swing final tasks were to connect the standpipe and water feeds to the centrifuge model to establish a ground water table inflight (Figure 10.5). A calibrated PPT was also placed inside the standpipe to monitor the imposed ground water profile. The PPT's, LVDT's and tunnel air pressure transducers were connected to the centrifuge data acquisition system and checked to ensure all instrumentation was working and recording correctly. The LVDT's where adjusted to ensure they were in range and close to their electronic zero. The positioning of the USB cameras and lighting were checked such that good quality images could be obtained. Final safety checks were completed. The time required to complete the procedure described above from removal of the strongbox from the consolidation press to position on the swing took approximately 3 hours.

10.5 Centrifuge test procedure

Once the model was on the swing and the final checks had been completed, the centrifuge was then accelerated to 100*g* increasing the rotational speed by 1 revolution per minute per second. During the centrifuge acceleration the tunnel support pressure was manually increased from the control room to balance the increasing overburden stress at the tunnel axis level. Once at 100*g* the model was left to reach hydrostatic equilibrium inflight for 44 hours. Data were logged and images were recorded during the spin up procedure and during the inflight consolidation. During the spin up procedure and the first hour of inflight consolidation data were recorded every second and for the next 44 hours data were recorded every 10 minutes.

After approximately 44 hours of inflight consolidation the centrifuge tunnel excavation test was ready to be conducted. The data logging and image capture frequency was changed to once per second. The tunnel support pressure was reduced manually by 80kPa from inside the control room at a target rate of approximately 100kPa per minute. The soil response was recorded during this pressure reduction and for an additional 2 hours. After the first 10-15 minutes the data logging frequency was reduced to once per minute.

After the 2 hours, the centrifuge was decelerated. The centrifuge instrumentation was disconnected, and the model was removed from the centrifuge swing, which took approximately 15 minutes. Hand shear vane readings were taken at a variety of locations using a Pilcon hand shear vane and at depths of 50mm, 100mm and 150mm below the surface level. The instrumentation was removed from the soil bed and the PPT's were quickly excavated and cleaned to prevent the porous filters from getting blocked affecting future tests.

10.6 Summary

The purpose of Chapter 10 was to provide full details of the centrifuge tests conducted, the equipment required, and the methodology followed. The centrifuge tests utilised established tunnelling equipment at The Research Centre for Sustainable and Resilient Civil Engineering at City, University of London with the addition of new pore pressure transducers. The centrifuge test series was a demonstration of the potential for using sedimented clay soil beds to observe how a sedimented structure effects the response to a tunnel or any construction event. Developing a framework for how sedimented layers effected the response to a tunnel construction event was outside the scope of this dissertation. To achieve this it would require an in-depth study.

11. Centrifuge Test Results

This chapter presents the key data obtained from the centrifuge tests. There are two main components to the results: firstly, the success of sedimenting a soil bed for centrifuge modelling within a strongbox. Secondly, the results obtained from the tunnel tests, including undrained shear strength, the response to inflight consolidation and finally the response to a tunnel construction event. Section 11.1 details the results obtained and the success of the sedimentation procedure. Section 11.2 details the results from; the equilibrium stages of the centrifuge test, response to tunnel excavation and post tunnel construction measurements.

11.1 Sedimentation sample making results

The sedimented soil bed was used to model a tunnel construction event and the differences between the soil response was observed. However, the results and ultimately the success of the sedimentation procedure was determined from the soil bed itself. The key observations were determining the soil layers thickness and comparison to the designed soil layer thickness and assessing if those layers were even across the strongbox.

Before the centrifuge test had been completed there was an opportunity to assess the sedimentation procedure. When the front of the strongbox was removed to construct the tunnel there were visible layers (photographed in Figure 11.1). Although it was not possible to get definitive layer thickness due to soil bed disturbance across the front face of the model the presence of layers provided confidence that the sedimentation procedure had been a success. No further measurements were possible prior to the centrifuge test being completed.

After the centrifuge test had been completed and the model had been removed from the swing all instrumentation was removed the clay soil bed. The soil bed was cut into sections in different directions to assess layer thickness and uniformity. Figure 11.2 is an image of a section across the width of the strongbox, where the resultant layers are clearly visible. From all the sections cut through the soil (shown in Figures 11.2-11.4.) the four sedimented layers and the different regions within them, i.e., the Polwhite E kaolin clay areas which were darker in colour and the Speswhite kaolin clay sections were clearly visible. Various measurements were taken throughout the soil bed and Table 11.1 details the measured layered thicknesses.

11.2 Tunnel centrifuge test results

Section 11.2 presents the significant data obtained from the centrifuge tunnel experiments using the three different soil beds detailed in Chapter 10. Results from the centrifuge consolidation

period, the response to the tunnel construction and results collected post centrifuge test are presented in this chapter.

11.2.1 Centrifuge spin up data

During the centrifuge acceleration procedure, the pore pressure response in the soil bed was recorded by the PPTs. Figures 11.5- 11.7 details the response of the PPT's the standpipe pressure transducer (indicating *g*-level) during the first 10 minutes for each of the centrifuge test. Figures 11.8-11.10 illustrates the pore pressure response of the same transducers over the entire inflight consolidation phase of the centrifuge test. After approximately 40 hours of inflight consolidation the PPT readings had stabilised as the model reached hydrostatic equilibrium. The final ground water tables measured from the PPT's at the end of the inflight consolidation phase are presented in Figure 11.11.

In each centrifuge test there was one (different) faulty PPT denoted with an asterisk in Figures 11.8-11.10. The faults with the transducers were caused by two different reasons. In the Speswhite kaolin clay and sedimented clay centrifuge tests the fault were caused by a blocked porous stone. In the Speswhite-Polwhite E kaolin clay centrifuge test an error during manufacturing of the PPT's lead to water egress to the sensor element damaging the transducer. Following this centrifuge test this PPT was discarded and not used in any further tests. These three transducers are omitted from any further analysis.

11.2.2 Surface settlement troughs

Figure 11.12-11.14 plots the development of surface settlement directly the above the centre line with a reduction of tunnel pressure for each of the tunnel tests. It can be observed that 200 seconds after reduction of the tunnel pressure there was minimal change in displacement observed. As the rate of unloading was different in each of the centrifuge tests, visible in Figures 11.12-11.14, the displacements were compared 200 seconds after the pressure had been reduced. Figure 11.15 plots the surface settlement data recorded by the LVDT's for the three tunnel tests at a time of 200 seconds after the tunnel support pressure had been reduced by 80kPa. A Gaussian curve were fit through this data using the difference squared method. This Gaussian curve had two variables the point of inflection and maximum settlement. These variables were iterated to produce a curve with a correlation factor as close to zero as possible (after Divall & Goodey, 2015).

11.2.3 Tunnel pressure and pore pressure response

Figures 11.16-11.18 plot the change in pore pressure over time following the reduction in tunnel support pressure for the three different centrifuge tunnel tests. All the Figures in Chapter 11 and 12 relating to the pore pressure response following the tunnel pressure reduction are presented versus the square root of time in minutes such that the initial response is clearly visible.

11.2.4 Soil bed undrained shear strength

After the soil bed was removed from centrifuge, Pilcon hand shear vane readings were conducted at different depths in the soil bed to determine the undrained shear strength. The results of the shear vane measurements recorded at different depths for the different soil beds are shown in Figure 11.19. This showed that when the three soil beds were subjected to the same stress history the Speswhite kaolin clay soil bed had the lowest undrained shear strength. The Speswhite, Polwhite E kaolin clay reconstituted soil bed had an undrained shear strength that was approximately 20% higher than the Speswhite kaolin clay soil bed. The sedimented soil bed had an undrained shear strength that was approximately 35-40% higher than the Speswhite kaolin clay soil bed.

12. Discussion

This section analyses the centrifuge sedimentation procedure and compares the results from the different centrifuge tunnel experiments. The success of the sedimentation procedure was determined through a comparison between the designed soil bed and the sedimented soil bed. The response of the soil bed to inflight consolidation and to a reduction in tunnel support pressure was compared to observe the influence of a sedimented structure.

12.1 Sedimenting a centrifuge soil bed

To assess the success of the sedimentation procedure the final soil bed dimensions were compared to the soil bed design. For the procedure to be viable, repeatable and predetermined soil beds needed to be created that were uniform across the entire strongbox. From cutting the sedimented soil bed into sections both could be assessed. Firstly, from all the images of the soil bed (Figures 11.1-11.4) there was clear layers developed during sedimentation. Each layer was clearly identifiable and within each layer the Polwhite E kaolin clay regions could also be distinguished from the Speswhite kaolin clay regions by colour. This was consistent with the images taken from the sedimentation columns tests and from previous sedimentation research by Stallebrass et al. (2007) and Been & Sills (1998).

From the various sections taken at different points in the soil bed it was possible to assess the uniformity of the layers created. Across the width and length of the strongbox the layers created were even. In some images it appeared that there were non-uniform layers (i.e., the sections highlighted in Figure 12.1). However, this was due to sample disturbance and smearing of the Polwhite E kaolin clay layer down into the underlaying layer when cutting the soil bed with a thin-walled cutter and wire saw. When a cut was made perpendicular to this region of the soil bed it revelled the 'true' material at that horizon. In Figures 11.2-11.4 and highlighted in Figure 12.2 there were indications of the clay bed 'hanging up' on the sidewalls of the strongbox due to interface friction. This effect appeared to be more significant at the top of the soil bed. During the sedimentation procedure the pump grease was applied to the strongbox sidewalls before the first batch of slurry was placed into the strongbox. Potentially during the sedimentation phases the grease on the side wall was forced down due to the increased *g*-level, subsequently increasing friction at higher horizons within the strongbox. Pump grease could be reapplied after the excess water from each layer had been siphoned off and this may reduce the effect of hanging up on the sidewall.

Figure 12.3 details the measured layer thicknesses and Table 11.1 shows the comparison between the final layer heights and the predicted layer heights. The sedimented soil bed was designed to achieve a specific layer thicknesses after consolidation to 500kPa and being swelled to 250kPa. During the establishment of the imposed ground water profile the centrifuge sample swelled by approximately 2mm. After the centrifuge test had been conducted the layer heights were determined, therefore it should be compared to the predicted layer heights after inflight swelling.

The post centrifuge test layer thickness are presented in Table 12.1. Layers 1 and 2 were the same thickness as predicted. Layer 3 was shallower than expected which can be explained as the water content of the third batch of slurry was greater than anticipated being approximately 540% instead of 495-510% for the other layers. As a result of layer 3 being smaller than designed, layer 4 was thicker to achieve the desired soil bed height.

This highlighted the relationship between initial water content and the final layer thickness and the potential accuracy achievable while sedimenting a centrifuge soil bed. It was not possible to determine the water content of the slurry before the layer had been sedimented. Therefore, every effort was made to clean the mixer thoroughly after each layer, weigh the constituent parts of the slurry carefully and to input the desired quantity of slurry into the strongbox to ensure the water content and final layer height was as designed.

Overall, there was a very close agreement between designed soil bed and measured soil bed proving it was possible to design and create a repeatable sedimented soil bed for centrifuge modelling. Uniform soil layers were created across the strongbox with minor signs of side wall friction at higher layers within the soil bed. When sedimenting future soil beds grease should be reapplied to the sidewalls of the strongbox after each layer has been sedimented to reduce this effect. It was possible to sediment a 5 layered soil bed (although in this case the fifth layer was sacrificial) in two working days. After the sedimentation of the soil bed it was treated the same as any other at City, University of London. The sedimented soil bed was then subsequently used to model a tunnel construction event but could be used to model any construction event in a geotechnical centrifuge.

12.2 Comparison of tunnel centrifuge tests results

The centrifuge tests were broken in two stages which are subsequently compared:

1. The response to inflight consolidation and establishing an imposed water table, and

2. The response to a tunnel construction event.

Before comparing the soil response during these phases, it was important to assess the reliability of measurements so that any differences recorded were due to the different soil beds rather than the instrumentation themselves. The first step in analysing the results from the centrifuge tests was to conduct a methodical check of the various pieces of instrumentation.

12.2.1 Instrumentation checks

The LVDT's and the tunnel pressure cell are assessed by monitoring the noise and scatter under a constant condition in each centrifuge test. The centrifuge soil beds swelled by approximately 2mm during inflight consolidation. To assess the stability of the LVDT's the last 2 hours of the inflight consolidation data were used as any further sweeling was negligible during this period. The LVDT's fluctuated by ± 0.01mm, there was 1 exception. During the Speswhite: Polwhite E kaolin clay centrifuge test the LVDT located at +180mm from the tunnel centreline worked intermittently due to a connection fault and therefore these results were omitted from any results analysis. The fluctuation of ± 0.01mm represented the accuracy of the LVDT measurements. Although this was a very small magnitude of movement, the LVDT's at an offset larger than 45mm away from the tunnel centreline the this fluctuation accounted for more than 10% of the total movement experienced.

The tunnel pressure transducer was subjected to a constant applied pressure for almost 48 hours having been increased as soon as the centrifuge reached 100*g*. The variation in tunnel support pressure recorded by the transducer was less than 0.5kPa. The compressed air passed through two regulators before entering the tunnel and the variation observed was therefore likely to be noise within the instrumentation rather than fluctuations in support pressure.

There was a greater possibility of errors or faults occurring when installing and using pore pressure transducers (previously detailed in Section 10.4.1). During the model making procedure and installation of the PPT's there was the potential for cavitation and air entry into the porous stones. Although a rigorous and thorough deairing process was followed the soil beds were created using non deaired water. When the soil beds were removed from the press they were unloaded by 250kPa (as shown in schematic for model making in Figure 9.7.) resulting in the soil bed being subjected to 250kPa of suction (larger than the air entry value of the porous stones 200kPa). This could potentially lead to cavitation and air entry into the pore pressure transducer.

If only cavitation occurred during the removal of the soil bed from the press, the transducers would be measuring water vapour pressure and 0 absolute pressure (-98kPa) even if the 'real' pore pressure in the surrounding soil was less than -98kPa. After the soil bed had been accelerated the pore pressure would rapidly increase, collapsing the vapour pocket relatively quickly. After this point the transducers would measure the 'real' pore pressure and the transducer should not experience any time delay between observed and 'real' pore-water pressure. Figures 11.5-11.7 plot the initial pore pressure response recorded, the initial reading of pore pressure varied between 0 and -140kPa and most of the readings around -95kPa. Values of initial pore pressure larger than -95kPa could theoretically be explained as when the front of the strongbox was removed during model making procedure the sample was disturbed by trimming and boring the tunnel, this could of released suction from the soil bed. Values of initial pore pressure being greater than -95/-100kPa in theory should be present however, due to cavitation and that the PPT would be outside of the manufactures operating range the accuracy when measuring a pressure smaller than -95kPa is unknown.

If there was any air trapped in the porous stones because of cavitation or clay blocking the porous stones this could of created a significant time delay between the transducer reading and the 'real' pore pressure in the soil bed. This was visible in the response of a PPT to the acceleration of the centrifuge. A blocked PPT with air or clay experienced a much slower increase in pore-water pressure than a surrounding unblocked PPT. It was possible for an initially slow responding PPT with air in the porous stone to be saturated during the consolidation phase of the centrifuge experiment. In this case the transducer which responded slowly to the increased acceleration field would responded immediately to the reduction in tunnel support pressure. A transducer with a large lag time was not suitable to measure the response to a tunnelling event due to the rapid change of pore pressure experienced.

To assess the reliability of the pore pressure transducer results a combination of the response to an increasing acceleration field, inflight consolidation and the response time of the transducers when the tunnel pressure was reduced were used. Within the discussion the changes in pore pressure recorded the initial response of the relevant PPT's to an increased acceleration field are also presented.

12.2.2 Comparisons during spin-up

During the centrifuge spin-up, inflight consolidation and establishment of the imposed ground water table the response of the soil was governed in part by soil permeability. The model was

connected to a standpipe and there was one dimensional drainage from the base drain. Table 12.2 summarises the permeabilities of the three different soil beds. Figure 12.4 shows the response of PPT 3 (PPT location illustrated in Figure 10.18) to the acceleration of the centrifuge and inflight consolidation. Due to the higher permeability the sedimented sample experienced a greater rate of increase of pore pressure and the final value of pore water pressure achieved also higher. This trend was consistent at all PPT locations.

Figure 11.11 plots the water table established at the end of the inflight consolidation phase. The final pore pressure distribution of the Speswhite, Polwhite E kaolin clay soil bed and the Sedimented clay soil bed were very similar. The Speswhite soil bed with the lowest permeability was furthest away from the imposed ground water profile. The largest difference occurred at the top of the sample, as it was the greatest distance away from the water supply. Subsequently, the samples had different degrees of consolidation at the start of the tunnel pressure reduction phase. The differences observed between the soil beds were supported by the permeability results obtained during the element tests.

12.2.3 Comparison of response to a tunnel construction event

To understand the differences in surface settlement and changes in pore pressure following a tunnelling event the differences in the soil beds needed to be understood. As well as having different permeabilities they also had different undrained shear strengths. All three soil beds were subjected to the same the stress history and inflight consolidation however there was a significant difference in undrained shear strength (seen in Figure 11.19). The undrained shear strength of the Speswhite, Polwhite E kaolin clay soil bed was 20% higher than the Speswhite kaolin clay soil bed. This demonstrated the effect of using different constituent soil. The sedimented soil bed had an undrained shear strength that was 15% higher than the Speswhite Polwhite E kaolin clay bed. This difference was due to the layering and the sedimented structure developed during sedimentation process supporting the sensitivity observed during the oedometer tests.

Existing literature (e.g., Cotecchia & Chandler, 2000; Stallebrass et al., 2007) have detailed a framework for the influence of soil structure on soil parameters. This included parameters such as undrained shear strength and permeability which were measured during this dissertation but other key parameters would have also changed. Although these parameters where not investigated as it fell outside the scope of this research it is important to note that the response to a construction event was a result of all soil properties. Any difference observed between the

three soil beds cannot be solely attributed to a difference in one soil property. However, any differences can be attributed to the different soil preparation procedures and the different soil structures. Particularly when comparing the Speswhite Polwhite E kaolin clay soil bed with the sedimented clay soil bed as the constituent soil components of the soil bed were the same.

To predict differences in pore pressure response following tunnel construction the method proposed in Divall et al. (2017) was adopted. This method is derived from the analytical approach of idealising the tunnel to a thick cylinder cavity contraction (Mair & Taylor, 1993). In which the magnitude of change in pore pressure is dependent of the undrained shear strength of soil. The larger the undrained shear strength, the larger the change in pore pressure. Figure 12.5 plots the predicted changes in pore pressure using the method proposed in Divall et al. (2017) versus distance from the tunnel centre in response to a tunnel pressure reduction of 80kPa. The three soil beds were idealised as homogenous soil beds with different undrained shear strengths. Although these predictions are based on a simplification of the differences it provides an indication to the differences expected.

Figure 11.15 plots the LVDT data and the Gaussian curves for the three centrifuge tests 200 seconds after the support pressure had been reduced by 80kPa. As expected, due to the lower undrained shear strength, the Speswhite kaolin clay soil bed experienced the largest surface displacement above the tunnel and the greatest volume loss of 2.25%. However, the sedimented clay soil bed had a higher undrained shear strength than the Speswhite Polwhite E kaolin clay soil bed but the surface settlement and volume loss was higher at 1.8% and 1.75%, respectively.

The difference in undrained shear strengths between the three soil beds were approximately the same. Therefore, a comparable reduction in volume loss would be expected. The additional volume loss experienced at a higher undrained shear strength was attributed to the layering present in the sedimented soil bed. Wongsaroj (2013) reported that there was an increased magnitude of displacement with permeability anisotropy when modelling long-term movements. Although the conditions of the analysis were not the same with an impermeable tunnel lining in the centrifuge test and a permeable tunnel lining in the numerical analysis there were similarities between the findings of the two studies. The sedimented layered soil bed experienced a greater volume loss than the Speswhite Polwhite E soil bed even with a higher undrained shear strength.

Mair & Taylor (1997) collated a database of tunnelling induced ground surface settlement data and found after normalising the results by maximum displacement above the tunnel centreline

to account for different soil compositions, soil strengths and total volume loss experienced there was an envelope in which all results reside. There is geometric similarity between all tunnelling events in clay. Figure 12.6 plots the normalised surface displacement for the three centrifuge tests, and the curves are essentially identical. Irrespective of whether the soil was sedimented the results were geometrically similar, and the shape of the settlement trough was the same. The only, but still significant, difference when considering surface displacements following a tunnel construction event in a sedimented and a traditional reconstituted soil bed were the magnitude of displacement and volume loss experienced. The sedimented soil bed had a higher undrained shear strength yet experiences a larger maximum displacement and volume loss.

Comparing the pore-water pressure response following the reduction in tunnel support pressure required a systematic approach. Firstly, the change in pore pressure within each test was observed and related to the spatial position (relative to the tunnel) so that a pattern of behaviour could be established. The magnitude and trends of changes in pore pressure were then compared for the three different soil beds. The initial response of the pore pressure transducers was carefully considered to determine if observations were due to real differences in soil behaviour and not a result of instrumentation errors.

Analysing the pore pressure response following a tunnel pressure reduction at radius of 75mm away from the tunnel centreline the following observations were made. Figure 12.7 plots the pore pressure response and tunnel pressure versus time for the three centrifuge tests for PPT location 8. Firstly, the initial response of the transducers were as expected and consistent in all three tests with no evidence of a blocked or a delayed transducer (Figure 12.8). In response to a reduction in tunnel support pressure there was also a similar response in the three centrifuge soil beds. After a reduction in tunnel support pressure of 25kPa there was a reduction in pore pressure. As the support pressure was further reduced the change in pore pressure increased and the time at which a maximum reduction in pore pressure occurred coincided with the time the tunnel support pressure was reduced to its minimum value. The magnitude of maximum change of pore pressure was similar in all three experiments, between 10-12kPa.

Figure 12.9 plots the pore pressure response and initial response behaviour at PPT locations 7 & 9. PPT 9 in both the Speswhite kaolin clay soil bed and sedimented soil bed were removed from the analysis as it was not responding correctly during inflight consolidation. PPT 9 in the Speswhite Polwhite E kaolin clay soil bed exhibited a large response time delay to an increase

in *g*-level (Figure 12.10). However, when the tunnel support pressure was reduced the response time of the transducer was comparable to PPT 7. All PPT's in this location recorded a change in pore pressure when the tunnel support pressure had been reduced by 30kPa. There was a time delay between the support pressure reaching its minimum value and the pore water pressure reaching its minimum value. This was not present in at PPT location 8. This time delay appeared to coincide with the soil permeability. The sedimented soil bed (the most permeable) had the shortest time delay and the Speswhite kaolin clay soil bed (the least permeable) had the longest time delay. The magnitude in pore pressure reduction was again comparable between the three soil beds falling between 12-15kPa.

Figure 12.11 plots PPT location 6 & 10 and a similar observation can be made to that at PPT location 7 & 9. PPT 10 in the Speswhite kaolin clay soil bed initially responded as expected with little response delay (Figure 12.12). However, when the tunnel support pressure was reduced it experienced a much larger response time and therefore this transducer was removed from the comparison. PPT 10 in the Speswhite-Polwhite E kaolin clay soil bed was another example of a PPT with an initially delayed response time. However, when the tunnel pressure was reduced there was a similar response time in both PPT 10 and PPT 6. After a tunnel support pressure reduction of 30kPa there was a change in pore pressure recorded by the PPT's and the maximum change in pore pressure was between 10-16kPa. There was also a similar delay between the time at which the tunnel support pressure had been reduced to a minimum value and the time at which a maximum change in pore pressure was recorded. The magnitude of this delay again appeared to be dependent on the permeability of the soil bed.

At a radius of 75mm away from the centre of the tunnel there was a similar pattern of behaviour in all three soil beds. The largest change in pore pressure was recorded at the axis level of tunnel and the smallest change was recorded above the centreline of the tunnel. The magnitude of pore pressure change was similar at all three locations and comparable to the prediction made using the method proposed by Divall et al. (2017) presented in Figure 12.4.

Figure 12.13 presents the response of PPT 1 & 5 located at the axis level of the tunnel and a radius of 40mm away from the centre of the tunnel. All the transducers showed a similar response to an increased *g*-level (Figure 12.14) and to the reduction of tunnel support pressure. There was an immediate reduction pore pressure following a reduction in tunnel support pressure and the time of the maximum pressure reduction coincided with the maximum change in pore pressure. The magnitude of the pore pressure reduction was comparable in all three

models being between 17-23kPa. All of which are less than the predictive method proposed by Divall et al. (2017).

The main difference, in terms of patterns of pore pressure response can be seen by comparing PPT locations 2 & 4 and 3. Figure 12.15 plots the response of the PPT 2 & 4 following a reduction in tunnel support pressure. All transducers respond as expected to the centrifuge acceleration apart from PPT 4 in the Speswhite Polwhite E kaolin clay soil bed as previously mentioned (Figure 12.16 plots the initial response of the transducers at location 2 & 4). There was an immediate reduction in pore-water pressure following a reduction in tunnel support pressure and the maximum change in pore pressure coincided with the time the tunnel support pressure was reduced to the minimum value. There was a much larger change in pore-water pressure in the Speswhite Polwhite E kaolin clay soil bed compared to the sedimented soil bed. This change was also larger than the predicted following Divall et al. (2017).

The change in pore pressure with reduction in tunnel support pressure is plotted in Figure 12.17 for PPT 3. In the Speswhite kaolin clay soil bed PPT 3 had an initially delayed response to an increased gravitational field (Figure 12.18) and this delay continued during the tunnel construction event and therefore was removed from any comparisons. In the sedimented soil bed there was a much larger change in pore pressure than in the Speswhite Polwhite E kaolin clay soil bed. In the sedimented soil bed there was an immediate reduction in pore water pressure with reduction in tunnel support pressure. The maximum change in pore pressure also coincided with the maximum reduction of tunnel support pressure. In the Speswhite-Polwhite E kaolin clay soil bed there was also an immediate reduction in pore pressure with reduction in tunnel support pressure however there was a small delay between the time of maximum tunnel support pressure reduction and the maximum reduction of pore-water pressure.

The sedimented soil bed experienced the largest change in pore pressure above the crown of the tunnel (PPT 3) whereas the soil bed prepared following a traditional preparation procedure experienced the largest change in pore pressure above the shoulder of the tunnel (PPT 2 and 4) both at a radius of 40mm. PPT 3 coincides with the interface between two layers and the more permeable Polwhite E band which may explain the difference in response observed. The response of the PPT's at all other locations were similar. There was a delay recorded between the maximum change in tunnel support pressure and maximum change in pore-water pressure at a radius 75mm away from the tunnel. This appeared to be related to the permeability of the soil beds (i.e., the lower the permeability the larger the time delay was).

Another observation from the pore pressure data during these tests, there appeared to be a difference in soil behaviour on the left and right side of the tunnel. The tunnel construction event simulated was symmetrical, therefore the response on the left and right side of the tunnel should have been the same. However, this was not the case as visible in Figures 12.6-12.17. This difference appeared to be smallest in the sedimented soil bed. This along with previous observations confirm that the layers created are even throughout the strongbox and the procedure of sedimenting a centrifuge soil bed was successful.

Following the reduction of the tunnel support pressure and reduction of pore-water pressure to its minimum value the pore pressure gradually increased for the remainder of the centrifuge test. This phase of the centrifuge test was similar to the inflight consolidation stage of centrifuge where it was governed in part by the permeability of the centrifuge models. The rate at which the pore pressure increased was greatest in the sedimented soil bed and lowest in the Speswhite kaolin soil bed (see Figures 12.6-12.17).

12.3 Summary

The data obtained whilst sedimenting a soil bed suitable for centrifuge models and conducting a series of tunnel centrifuge tests have been analysed and compared. First to assess the success of sedimenting a soil bed and second to understand the influence on soil behaviour following tunnel construction. The procedure developed to design and sediment a soil bed suitable for centrifuge modelling has been deemed a success by;

- Dissection of the soil bed and measuring the resultant soil layers (Figures 11.1-11.4).
- The sedimented soil bed had a higher undrained shear strength indicating that sensitivity had been developed.
- The soil bed created included layers the same thickness as designed and with even layers across.
- The variation in measured behaviour on the right- and left-hand side of the tunnel following pressure reduction was least prominent in the sedimented soil bed.

Therefore, it is possible to create repeatable sedimented soil beds suitable for centrifuge modelling containing a range of layer geometries. These soil beds can subsequently be used to investigate the influence of a sedimented structure on soil on the response to a geotechnical construction event.

For this research project three centrifuge tunnel construction event tests were conducted where the response to the same tunnel construction was observed in three different soil beds. These centrifuge tests found that although the sedimented soil bed exhibited a higher undrained shear strength there was a larger maximum surface displacement above the tunnel and subsequently a larger volume loss (Figure11.15). However, there was still a geometric similarity between the surface settlement troughs (see Figure 12.6) irrespective of whether the soil bed was sedimented.

There was also an observed difference in pore pressure response between the tests, the Speswhite kaolin clay and Speswhite Polwhite E kaolin clay soil beds experience a maximum change in pore pressure at the shoulder of the tunnel. Whereas in the sedimented soil beds there was a maximum change of pore pressure above the crown of the tunnel coinciding with the more permeable Polwhite E region (illustrated in Figure 12.3). These differences observed regarding tunnel construction are preliminary in nature and to fully understand the influence of a sedimented soil a much larger series of tests would need to be conducted.

13. Conclusions

Within this final Chapter the results and observations from this dissertation will be concluded, evaluating the success of modelling a construction event using a sedimented soil bed. The limitations of this research and recommendations for possible further work are also detailed.

13.1 Summary of work undertaken

This dissertation contains a literature review on; the effect of soil structure on soil behaviour, methods of recreating structured soil in the laboratory through sedimentation columns (i.e., Been & Sills, 1981; Edge & Sills, 1989; Stallebrass et al., 2007) and the influence of different initial slurry compositions on final soil characteristics. Previous methods of creating a structured/layered centrifuge soil beds (Grant, 1999; Hossain & Randolph, 2010; Marshal et al., 2014) focused on modelling soil structure as an interface between two uniform layers with different stiffnesses. The current literature on sedimenting a centrifuge soil bed is also presented from Divall et al. (2018) and the potential issues associated with inflight sedimentation are detailed from Sorta et al. (2012). It was clear that before attempting to sediment a centrifuge soil bed that a detailed investigation was required to determine which slurry preparation procedures do produce a sedimented soil structure.

Sedimentation column apparatus were developed for use on the geotechnical centrifuge. Additional apparatus were designed and manufactured for determining the vertical and horizontal permeability and permeability anisotropy of the resultant sedimented samples. Modified oedometer equipment was manufactured to investigate the sensitivity of sedimented samples. A series of centrifuge sedimentation tests were undertaken at 100*g* using slurries of different constituent parts mixed to different initial water contents. The resultant soil samples were tested and a suitable method for sedimenting a soil bed suitable for centrifuge modelling was determined and a sedimented soil bed design procedure was developed.

A sedimented soil bed for centrifuge modelling was designed to include specific layer thicknesses and arrangements. The designed soil bed was sedimented in a centrifuge strongbox and the soil layers were assessed. A tunnel construction event was modelled on the centrifuge at 100*g* by reducing the tunnel support pressure by a fixed amount in a Speswhite kaolin clay, Speswhite Polwhite E kaolin clay and in a sedimented soil bed. The response to inflight consolidation and a tunnel construction event were compared to observe the influence of

different soil structure. The soil response was recorded by LVDT's at the soil surface and by PPT's embedded in the soil bed. The soil response are compared and discussed in Chapter 12.

13.2 Findings from this research

Findings from this research are broken into three main sections:

13.2.1 Findings from sedimentation column experiments

1. It was not possible to sediment a sample with enhanced permeability anisotropy using only one material in the slurry (i.e., Speswhite kaolin clay irrespective of the initial water content).
2. Using disaggregated Speswhite kaolin clay or Speswhite 'peds' kaolin clay after Phillips (2014) did not alter permeability or anisotropy.
3. When using two different constituent parts in the slurry (Speswhite kaolin clay and Polwhite E kaolin clay), it was possible to achieve enhanced permeability anisotropy.
4. The degree of permeability anisotropy is dependent on initial slurry water content. when the water content was less than 400% a sedimented structure did not develop. When the initial water content was 800% some particle separation occurred and the resulting permeability anisotropy was 2.5. When the initial water content was above 1200% the permeability anisotropy was 4, and the permeability at the base of the sample was the same as Polwhite E kaolin clay (coarsest material) and the permeability at the top was the same as the Speswhite kaolin clay (finest material). This was defined as the critical water content.
5. When a significantly coarser material was added into the slurry (such as Leighton Buzzard Sand) the sand particles sedimented before the centrifuge had been accelerated. The subsequent motion of the centrifuge accelerating caused the sand to slide to the back of the column relative to the direction of motion creating an uneven sand layer. To create a uniform layer, which included sand, the sand would need to be added while the centrifuge was at speed or the slurry needed to be remixed once at speed. It was essential that all material remained in suspension while the centrifuge was accelerated to create even soil layers.
6. A dispersion agent (for this research sodium hexametaphosphate) was used in small concentrations (0.1g per litre of mixed slurry) to reduce the critical water content from 1200% to 500%.

7. When the dispersion agent concentration was increased it created a soil sample with a metastable structure that was unstable which when agitated or sheared returned to a slurry like state.
8. The critical sedimentation time was found to be only 2 hours of inflight sedimentation after which 98.5% of solid particles had been deposited. Multiple layers could therefore be sedimented in a working day. Further sedimentation time results in no further change in soil properties.
9. The samples prepared with a dispersion agent were test in the oedometer. They demonstrated the presence of a sedimented structure with samples exhibiting a sensitivity of approximately 2.
10. Before sedimenting a centrifuge soil bed an investigation was required to determine the critical water content of the slurry, the optimum dispersion agent concentration, the critical sedimentation time for the slurry and one dimensional compression behaviour.

13.2.2 Findings from sedimenting a centrifuge soil bed

1. It was possible to create a sedimented soil bed suitable for modelling geotechnical construction events. A four layered soil bed was designed and created then a tunnel construction event was subsequently modelled.
2. The method proposed was suitable for designing a sedimented centrifuge soil bed as the resultant layers were the same as the predetermined heights.
3. The sensitivity to initial slurry water content and the importance of careful slurry making and placing procedures were highlighted by layer 3, being smaller than expected, as the initial water content was greater than intended.
4. The layers created where visible when cutting the soil bed into sections and were consistent across the strongbox and the same height as predicted.
5. The sedimented soil bed had a higher undrained shear strength evidencing sensitivity.
6. A minor modification of reapplying side wall grease after each sedimented layer is recommended to reduce higher layers hanging on the sidewall due to increased friction after sedimentation.

13.2.3 Findings from centrifuge tunnel tests

1. When using a sedimented soil bed to observe a construction event it required no additional steps than a typical reconstituted soil bed. After the soil beds had been created the remainder of the test procedure remained constant.

2. Creating a sedimented soil bed did not increase the overall preparation time, although the sedimentation stages took 2 days to create a soil bed as opposed to a day in the conventional soil bed making procedure at City, University of London. A higher initial stress could be applied to the sedimented soil bed due to inflight consolidation negating the extra day required.
3. A sedimented soil bed required more researcher time to mix and manage the sedimentation procedure however it allows for a large variety of soil beds to be created.
4. The more permeable sedimented soil bed consolidated faster inflight due to increased permeability.
5. The sedimented soil bed had a higher undrained shear strength than the Speswhite Polwhite E kaolin clay soil bed however it experienced a higher volume loss and surface displacement when subjected to the same tunnel support pressure reduction, attributed to the different soil structure.
6. The sedimented soil bed experienced the largest change in pore pressure above the crown which coincided with the more permeable layer whereas in the conventionally prepared soil beds the maximum pore pressure reduction occurred above the tunnel shoulder.

13.3 Conclusions

The aim of this research project was to develop a technique for creating sedimented soil beds at a scale suitable for centrifuge testing. The findings from this dissertation can be concluded as follows:

I. To create a soil bed with a sedimented structure consisting of Speswhite and Polwhite E powder required an initial water content of 500%, a dispersion agent (Sodium Hexametaphosphate) concentration of 0.1g per litre and a sedimentation time of two hours per layer
II. The design procedure outlined in Chapter 9 (Figure 9.1) can be used to design soil beds to include specific layer geometries.
III. The sedimented soil beds were successfully used to model a tunnel construction event in both a conventional reconstituted and sedimented soil beds and there were two notable differences:

1. The sedimented soil bed had a higher undrained shear strength than the reconstituted soil bed yet still experienced a higher volume loss percentage following tunnel construction.
2. The conventional soil beds experienced the biggest change in pore pressure above the tunnel shoulder whereas the sedimented soil experienced the greatest change above the crown coinciding with the interface between the two layers.

13.4 Recommendations for further research

The sedimentation column results presented show the resultant soil properties when sedimenting a slurry containing three different constituent soils (Speswhite kaolin clay , Polwhite E kaolin clay and Leighton Buzzard Fraction E sand) at a variety of different initial water contents. They demonstrated that the critical water content could be reduced from 1200% to 500% by the addition of a dispersion agent (sodium hexametaphosphate). This enabled a method for creating a soil bed with a sedimented structure suitable for centrifuge modelling to be developed. Future work should investigate if the critical water content can be reduced further from the 500% used in this research. 500% was a nominal value chosen which provided the required layered thickness needed for the soil bed as detailed in Section 8.6.

To create a larger variety of soil beds and resultant properties similar sedimentation column tests should be undertaken covering a larger ranging of constituent soil. As well as determining the permeability, compressibility, and the undrained shear strength of the different slurry preparation techniques triaxial tests should be undertaken to determine other key soil properties to allow further analysis of the centrifuge test results. As the individual effects of each cannot be easily separated.

The observations made from the centrifuge tunnel tests are based off a small test series and possible reasons for these observations were suggested. However, a much larger series of tests is required to fully understand this behaviour. The test series within this dissertation was a demonstration to highlight the potential of using a sedimented soil bed for modelling geotechnical events on the centrifuge. Future research projects could use the proposed methodology for creating sedimented soil beds to investigate various construction events.

Existing literature such as Wongsaroj et al. (2007) reiterated the need for more long-term movement data. To achieve this from centrifuge modelling representative soil and structure permeability needs to be modelled. This dissertation outlines the process for creating a soil bed with representative soil permeabilities for centrifuge modelling. Combined with further

research to develop permeable geotechnical structures it would be possible to model the long-term behaviour following geotechnical construction events.

References

Al-Tabbbaa, A. & Wood, D. M. (1987). Some measurements of the permeability of kaolin Géotechnique, Vol. 37, No.4, pp, 499-503.

Andreola, F., Castellini, E., Ferreira, J., Olhero, S. and Romagnoli, M. (2006). Effect of sodium hexametaphosphate and ageing on the rheological behaviour of kaolin dispersions. Applied Clay Science, Vol. 31, pp.56-64.

Atkinson, J. H., Evans, J. S. & Ho, E. W. L. (1985). Non-uniformity of triaxial samples due to consolidation with radial drainage. Géotechnique Vol. 35, No. 3, pp 353-355.

Avgerinos, V., Potts, D. and Standing, J., (2016). The use of kinematic hardening models for predicting tunnelling-induced ground movements in London Clay. *Géotechnique*, Vol. 66, No. 2, pp.106-120.

Azam, S, & Scott, J. D. (2005). Revisiting the ternary diagram for tailings characterization and management. Geotechnical news. Waste Geotechnics Vol. 23 No. 4, pp 43–46.

Been, K. (1980). Stress strain behaviour of a cohesive soil deposited under water. DPhil thesis, University of Oxford.

Been, K. & Sills, G. C. (1981). Self-weight consolidation of soft soil: an experimental and theoretical study. Géotechnique Vol. 31, No. 4, pp 519–535.

Bindu, J. & Ramabhadran, A. (2010). Effect of concentration of dispersing agent on the grain size distribution of fine grained soil. Indian Geotechnical Conference 2010, pp, 275-278.

Burland, J. B. & Hancock, R. J. (1977). Underground car park at the House of Commons, London: geotechnical aspects. The Structural Engineer Vol. 55, No. 2, pp 87–100.

Burland, J. B. (1990). On the compressibility and shear strength of natural clays. Géotechnique Vol. 40, No. 3, pp 329-378.

Chandler, R. J., Leroueil, S., & Trenter, N. A. (1990). Measurements of the permeability of London Clay using a self-boring permeameter. Géotechnique Vol. 40, No. 1, pp 113-124.

Coop, M. R. & Cotecchia, F. (1995). The compression of sediments at the archaeological site of Sibari. Proc. 11th ECSMFE, Copenhagen 8, pp 19-26.

Cooper, M. L., Chapman, D. N. and Rogers, C. D. F. (2002). Prediction of Settlement in Existing Tunnel Caused by the Second of Twin Tunnels. Transportation Research Record 1814, Paper No. 2- 2729, pp. 103-112.

Cotecchia, F., Coop, M. R. & Chandler, R. J. (1997). The behaviour of layered clays within a framework for the structure-related behaviour of clays. In Proceedings of the International Symposium on Characterisation of Soft Marine Clays, Yokosuka, pp. 147-163.

Cotecchia, F. & Chandler, R. J. (2000). A general framework for the mechanical behaviour of clays. Géotechnique Vol. 50, No. 4, pp 431-447.

Divall, S. (2013). Ground movements associated with twin-tunnel construction in clay. Ph.D. Thesis, City University London.

Divall, S., Taylor, R.N., Stallebrass, S. E. and Goodey, R.J. (2017). Predictions of changes in pore-water pressure around tunnels in clay. Paper presented at the 9th International Symposium on Geotechnical Aspects of Underground Construction in Soft Ground, Sao Paulo, Brazil.

Divall, S., Stallebrass, S.E. Goodey, R.J, & Ritchie. E.P. (2018). Development of layered models for geotechnical centrifuge tests. Physical Modelling in Geotechnics pp, 143-147– McNamara et al. (Eds) 2018 Taylor & Francis Group, London, ISBN 978-1-138-34419-8.

Donahue, R., Sego, D., Burke, B., Krahn, A., Kung, J. & Islam, N. (2008). Impact of ion exchange properties on the sedimentation properties oil sands mature fine tailings and synthetic clay slurries. Proceedings of First International Oil Sands Tailings Conference, Edmonton, Alberta, Canada, pp. 55–63

Edge. M. J. & Sills, G. C. (1989). The development of layer sediment beds in the laboratory as an illustration of possible field processes. Quarterly Journal of Engineering Geology, London, Vol. 22, pp, 271-279

Fiumana, N., Gaudin, C., Tian, Y. & O'Loughlin, C. (2018). Physical modelling of active suction for offshore renewables. McNamara et al. (Eds) Taylor & Francis Group, London, ISBN 978-1-138-34419-8

Gibson, R. E., Knight, K. & Taylor, P. W. (1963). A critical experiment to examine theories of three- dimensional consolidation. Proc. Eur. Conf Soil Mech. Fdn Engng, Wiesbaden 1, pp 69-76.

Gonzalez, N., Rouaina, M., Arroyo, M. and Gens, A., 2012. Analysis of tunnel excavation in London Clay incorporating soil structure. Géotechnique, Vol. 62, No.12, pp.1095-1109.

Gorasia, R.J., (2013). Behaviour of ribbed piles in clay. Ph.D. Thesis, City University London.

Grant, R. J. (1998). Movements around a tunnel in two-layer ground. Ph.D. Thesis, City University London.

Hight, D. W., Bond, A. J. & Legge, J. D. (1992). Characterization of the Bothkennar clay: an overview. Géotechnique Vol. 42, pp 303-347.

Hight, D. W., McMillan, F., Powell, J. J. M., Jardine, R. J. & Allenou, C. P. (2003). Some characteristics of London Clay. Proceedings of the conference on characterisation and engineering properties of natural soils, Singapore, Vol. 2, pp. 851–907.

Hill, N., & Staerk, A. (2016). Long-term settlement following SCL-tunnel excavation. Crossrail project: Infrastructure design and construction- Volume 3, pp 227-248.

Hossain, M. S. & Randolph, M. F. (2010). Deep-penetrating spudcan foundations on layered clays centrifuge tests. Géotechnique Vol. 60, No. 3, pp 157-170.

Imai, G., Tsuruya, K. & Yaano, K. (1979). A treatment of salinity in water content measurements of very soft dredged clays. Soils and Foundations, Vol. 19, No. 3, pp.84-89.

Imai, G. (1980). Settling Behaviour of Clay Suspension. Soils and Foundations, Vol.20, No. 2, pp 61-77 June 1980.

King, C. (1981). The stratigraphy of the London Basin and associated deposits, Tertiary Research Special Paper No. 6. Rotterdam: Backhuys.

Larsson, R. (1981). Drained behaviour of Swedish clays. Swedish Geotechnical Institute Report, No. 12. Swedish Geotechnical Institute.

Laver, R., Li, Z., & Soga, K. (2016). Method to evaluate the long-term surface movements by tunnelling in London Clay. Journal of geotechnical and Governmental Engineering.

Leroueil, S., Kabbaj, M., Tavenas, F, & Bouchard, R. (1985). Stress-strain-stress rate relation for the compressibility of sensitive natural clays. Géotechnique, Vol. 35, pp 159-180.

Leroueil, S. & Vaugham, P.R. (1990). The importance and congruent effects of structure in natural soils and weaker rocks. Géotechnique, Vol. 40, No. 3, pp 467-488.

Little, J. A., Muir Wood, D., Paul, M. A. & Bouazza, A. (1992). Some laboratory measurements of permeability of Bothkennar clay in relation to soil fabric. Géotechnique Vol. 42, No. 2, pp 355-361.

Locat, J. & Lefebvre, G. (1985). The compressibility and sensitivity of an artificially sedimented clay soil: the Grande-Baleine marine clay, Quebec, Canada. Mar. Geotechnol. 6, No. 1, 1–28.

Ma, M., 2012. The Dispersive Effect of Sodium Hexametaphosphate on Kaolinite in Saline Water. Clays and Clay Minerals, Vol. 60 No. 4, pp.405-410.

Maharaj, A & Paige Green, P. (2014). The SCS double hydrometer test in dispersive soil identification. Proceedings of the 18th International Conference on Soil Mechanics and Geochemical Engineering, Paris 2013, pp, 389-392.

Mahasneh, B.Z., & Shawabkeh, R.A. (2004). Compressive strength and Permeability of Sand-Cement-Clay Composite and Application for Heavy Metal Stabilization. American Journal of Applied sciences Vol. 1, No. 4

Mair, R. J. (1979). Centrifugal Modelling of Tunnel Construction in Soft Clay. Ph.D. Thesis, Cambridge University.

Mair, R. J. and Taylor, R. N. (1993). Predictions of clay behaviour around tunnels using plasticity solutions. Predictive soil mechanics, Proceedings of the Wroth memorial symposium, Oxford, pp. 449-463.

Mair, R.J., Taylor, R. N. & Burland, J.B. (1996). Prediction of ground movements and assessment of risk of building damage due to bored tunnelling. In geotechnical aspects of underground in soft ground (Eds. R. J. Mair and R. N. Taylor), pp. 713-718. Rotterdam: Balkema

Mair, R. J. and Taylor, R. N. (1997). Bored tunnelling in the urban environment. Proceedings of the 14th International Conference on Soil Mechanics and Foundation Engineering, Vol. 4, pp. 2353-2385.

Marshall, A. (2009). Tunnelling in sand and its effects on pipelines and piles. Ph.D. Thesis, Cambridge University.

Marshall, A.M., Cox, C.M., Salgado, R. & Prezzi, M. (2014). Centrifuge modelling of non-displacement piles and pile groups under lateral loading in layered soils. Proceedings of the

Eighth International Conference on Physical Modelling in Geotechnics (ICPMG 2014), Perth, Australia, 2: pp 847–852.

Mašín, D., Stallebrass, S. E. & Atkinson, J. H. (2003). Laboratory modelling of natural structured clays. Proc int. workshop on geotechnics of soft soils: theory and practice, VGE, The Netherlands, pp. 491–496.

Mitchell, J.K. (1976). Fundamentals of soil behaviour. Wiley, New York.

Pane, V., Croce, P., Znidarcic, D., Ko, H.-Y., Olsen, H. W. & Schiffman, R. L. (1983). Effects of consolidation on permeability measurements for soft clay. Géotechnique Vol 33, No. 1, pp 67-72.

Paul. M. A., Peacock, J. D. & Wood. B F. (.1 992). The engineering geology of the Carse Clay at the national soft clay research site, Bothkennar. Géotechnique Vol. 42, No. 2, pp 183-198.

Penkavová1, V., Guerreiro, M., Tihon, J. & Teixeira, J.A.C. (2014). Deflocculation of kaolin suspension – the effect of various electrolytes. Applied Rheology Vol. 25.

Phillips, N.S. (2014). Disaggregation of soil during slurry pipe jacking. Ph.D. Thesis, City University London.

Powrie, W. (2014b) *Soil Mechanics: Concepts and Applications*. Boca Raton Florida: CRC Press/Taylor & Francis.

Rampello, S., Viggiani, G. M. B. & Silvestri, F. (1994) The dependence of small strain stiffness on stress state and history for fine-grained soils: the example of Vallericca clay. In Prefailure deformation of geomaterials (eds Shibuya, S., Mitachi, T. and Miura, S.), pp. 273–278. Rotterdam: Balkema.

Richards, D. J., Clark, J. & Powrie, W. (2006). Installation effects of a bored pile wall in overconsolidated clay, Géotechnique Vol. 56, No. 6, pp 411–425.

Schofield, A. N. & Taylor, R. N. (1988). Development of standard geotechnical centrifuge operations. In J. F. Corte (ed.), Centrifuge ’88: 29-32. Rotterdam: Balkema.

Shaker, A.A. & Elkady, T.Y. (2015). Hydraulic performance of sand-clay mixtures: soil fabric perspective. Géotechnique Letters 5, pp 198-204.

Simpson, B. (2010), Engineering in stiff sedimentary clays. Géotechnique Vol. 60, No. 12, pp 903–911.

Singh, L. (2017) Development of layered models for centrifuge modelling, Undergraduate dissertation, City, University of London.

Soga, K., Laver, R.G. & Li, Z. (2017). Long term tunnel behaviour and ground movements after tunnelling in clayey soils. Journal on Underground Space 2, Vol.2, No. 3, pp. 149-167.

Sorta, A. R., Sego, D. C. & Wilson, W. (2012). Effect of Thixotropy and Segregation on centrifuge modelling. International journal of Physical Modelling Geotechnics, 2012, Vol. 12 No. 4, pp 143-161.

Sridharan, A. & Prakash, K. (1997). Settling behaviour of fine grained soils, Indian Geotechnical journal. Vol.27, No.3, pp 278-309.

Sridharan, A. & Prakash, K. (2001a). Settling behaviour and clay mineralogy. Soils and Foundations Vol.41, No. 2, pp 105-109.

Sridharan, A. & Prakash, K. (2001b). Consolidation and permeability Behaviour of Segregated and Homogeneous Sediments. Geotechnical testing Journal, Vol. 24, No. 1, pp. 109-120.

Stallebrass, S. E., Atkinson, J. H. & Mašín, D. (2007). Manufacture of samples of overconsolidated clay by laboratory sedimentation. Géotechnique Vol. 57, No. 2, pp 249–253.

Taylor, R. N. (1984). Ground movements associated with tunnels and trenches. Ph.D. Thesis, Cambridge University.

Taylor, R. (1995). *Geotechnical centrifuge technology*. London: Blackie Academic & Professional, Taylor, R. N., 19-33.

Terzaghi, K. (1941). Undisturbed clay samples and undisturbed clays. J. Boston Soc. Civ. Engng, Vol. 28, pp 211-231.

Viggiani, G. M. B. & Atkinson, J.H. (1995). Stiffness of fine grained soil at very small strains. Géotechnique Vol. 45, No. 2, pp 245–265.

Wongsaroj, J., Soga, K. & Mair, R.J. (2007). Modelling of long-term ground response to tunnelling under St James's Park, London. Géotechnique Vol. 57, No. 1, pp, 75–90.

Wongsaroj, J., Soga, K. & Mair, R. J. (2013). Tunnelling-induced consolidation settlements in London Clay. Géotechnique Vol. 57, No. 1, pp, 75–90.

Zaman, A. and Mathur, S (2004). Influence of dispersing agents and solution conditions on the solubility of crude kaolin. Journal of Colloid and Interface Science, Vol. 271, No. 1, pp.124-130.

Tables

Borehole	Depth (m)	L/D	Shape factor (m)	Permeability k (m/s x10^{-11})
311	5.50	6.67	2.73	140.00
312	51.00	19.67	5.74	110.00
313	28.00	5.00	30.6	10.00
314	15.70	5.50	3.24	66.00
315	40.50	6.75	3.67	4.30
851	5.00	8.00	1.29	9.30
851	9.00	2.00	0.53	16.00
851	12.50	2.00	0.53	5.60
852	15.50	8.00	1.29	5.30
852	14.00	8.00	1.29	5.00

Table 3.1- Summary of *in situ* permeability tests, after Chandler et al. (1990)

Depth (m)	Type of test	Hydraulic gradient (i)	e_0^*	Permeability k (m/s x10^{-11})
4.06	k_v, oedometer	52	0.87	1.40
4.13	k_h, oedometer	52	0.89	2.40
10.13	k_h, oedometer	52	0.82	2.80
10.19	k_v, oedometer	52	0.82	1.10
10.29	k_h, triaxial	30	0.84	1.95-2.55
10.35	k_v, triaxial	30	0.83	1.07-1.46
14.08	k_v, oedometer	52	0.83	1.00
14.02	k_h, oedometer	52	0.84	2.70
14.5	k_v, triaxial ǂ	50	0.83	1.20-3.40
20.2	k_h, oedometer	52	0.81	1.50
20.26	k_v, oedometer	52	0.85	1.00
* Void ratios were calculated assuming S=1.0, and using G=2.72; permeability was measured at a temperature 20°C ǂ Test at City University				

Table 3.2- Summary of laboratory permeability tests, after Chandler et al. (1990)

Settling type	Designation	Distinctive features
I	Dispersed free settling	Soil particles do not flocculate but disperse, and freely settle without mutual interactions. Coarser particles settle earlier than the finer particles
II	Flocculated free settling	Soil particles flocculate and form flocs of different sizes. They settle freely with rates dependent on their sizes, therefore, no sharp interface is formed.
III	Zone settling	Flocs are formed due to flocculation, and they settle with strong mutual interaction among them. Therefore, they settle uniformly in the aggregate forming a sharp interface, of which settling rate is constant during the settling stage.
IV	Consolidation settling	Visible flocs cannot be formed. The mixture settles as a whole mainly due to consolidation

Table 5.1- Characteristic settling features after Imai (1980)

No.	Material	Specific gravity	Plastic Limit (%)	Liquid Limit (%)	Plasticity Index (%)	Ignition Loss (%)
1	Tokyo Bay mud	2.668	32.2	97.5	65.3	10.6
2	Ohsaka bay mud	2.712	30.8	101.7	70.9	12.6
3	Sendai Bay mud	2.582	32.4	124.2	91.8	13.2
4	Kaolin	2.673	29.5	45	15.5	-
5	Bentonite	2.605	31.07	123.5	91.8	-

Table 5.2a- Index properties of sediments tested after Imai (1980)

No.	Material	Mineral composition
1	Tokyo Bay mud	Chlorite, Illite, Quarts, Feldspar
2	Ohsaka bay mud	Chlorite, Illite, Quarts
3	Sendai Bay mud	Chlorite, Illite, Quarts, Feldspar
4	Kaolin	Kaolin, Illite, Pyrophyllite, Quarts
5	Bentonite	Montmorillonite, Quarts

Table 5.2b- Composition of sedimented tested after Imai (1980)

No.	Soil	Liquid Limit (%)	Plastic Limit (%)	Plasticity Index (%)	Shrinkage Limit (%)	Grain size distribution			Principle clay mineral
						Clay size	Silt size	Sand size	
1	Bentonite	393.40	50.10	343.30	13.7	65.5	34.5	0.00	Montmorillonite
2	Black cotton soil-1	100.80	51.90	48.90	13.2	70.0	28.1	1.90	Montmorillonite
3	Black cotton soil-2	76.60	35.40	412.00	9.90	55.0	32.6	12.4	Montmorillonite
4	Brown soil-1	64.60	26.60	38.00	14.5	40.0	41.6	18.4	Montmorillonite, Kaolinite
5	Hemavathi project soil	58.50	58.50	27.50	19.2	20.8	51.2	28.0	Kaolinite
6	Kaolinite-1	48.00	48.00	12.40	35.9	10.0	75.0	15.0	Montmorillonite, Kaolinite
7	Red earth-1	38.60	38.60	20.60	14.7	39.5	23.5	37.0	Kaolinite

Table 5.3- Materials tested after Sridharan & Prakash (2001a)

Experiment	Mass of soil (kg)	Initial density (kN/m^3)	Initial height (mm)	Pore pressure measurement	Duration (hours)	Comments
1	0.55	10.0	1929	-	43	For trends in settling suspension
2	1.05	10.2	1910	-	119	
3	1.60	10.4	1920	-	23	
4	1.93	10.6	1925	-	23	
5	2.57	10.9	1791	-	23	
6	1.10	10.2	1867	Standpipes	25	
7	2.04	10.7	1742	Standpipes	79	
8	5.00	12.0	1748	Standpipes	2403	
9	1.06	10.2	1800	-	240	Dispersing agent added
10	0.51	10.0	1895	Transducers	170	Intermediate phase and soil behaviour
11	1.17	10.3	1802	Transducers	315	
12	1.19	10.3	1800	Standpipes	1853	
13	1.12	10.6	1123	Transducers	144	
14	1.17	10.9	816	Transducers	144	
15	1.23	11.2	643	Transducers	848	
16	0.91	10.4	1111	Transducers	168	Prediction from 10 to 15

Table 5.4- Slurries test after Been & Sills (1981)

Experiment	Soil mass (kg)	Density (kN/m^3)	Slurry height (mm)	Initial water content (%)
1	0.55	10	1929	2766
2	1.05	10.2	1910	1416
3	1.6	10.4	1920	920
4	1.93	10.6	1925	764
5	2.57	10.9	1791	521
6	1.1	10.2	1867	1315
7	2.04	10.7	1742	647
8	5	12	1748	243
9	1.06	10.2	1800	1315
10	0.51	10	1895	2936
11	1.17	10.3	1802	1196
12	1.19	10.3	1800	1173
13	1.12	10.6	1123	768
14	1.17	10.9	816	521
15	1.23	11.2	643	378
16	0.91	10.4	1111	938

Table 5.5- Slurries tested converted to initial water contents after Been & Sills (1981)

Test number	Measurement Technique			
	Vertical Permeameter		Horizontal Permeameter	
	Permeability ($x10^{-9}$ ms^{-1})	Final Water Content (%)	Permeability ($x10^{-9}$ ms^{-1})	Final Water Content (%)
1	2.00	57.64	1.9.0	58.02
2	2.10	57.55	1.85	58.11
3	1.85	58.12	1.75	57.86
4	1.95	57.44	2.05	57.92
5	1.90	57.38	2.20	58.30
6	1.85	57.60	1.95	57.69
7	1.95	56.99	2.10	58.21
8	1.95	58.10	2.10	58.01
9	2.05	57.61	1.85	57.68
10	2.00	57.80	1.95	58.23
Average	1.96	57.62	1.97	57.96

Table 6.1-Results from validation of Horizontal permeameter, measuring vertical permeability of Speswhite kaolin clay in both pieces of apparatus

Sample Number	Solid content of dispersion fluid (%)
1	0.04
2	0.03
3	0.03
4	0.03
5	0.05
6	0.03
7	0.02
8	0.04

Table 6.2- Solid content of dispersion fluid after 24 hours inflight sedimentation of a Speswhite kaolin clay slurry

Symbol	Parameter	Value
κ	Average gradient of swelling line in v: ln p' space	0.05
λ	Gradient of compression line in v: ln p' space	0.19
M	Stress ratio at critical state (q' : p')	0.89
Γ	Specific volume at critical state when p'=1kPa	3.23
N	Specific volume on INCL when p'=1kPa	23°
φ_c'	Critical state angle of shearing resistance	16.5 (kN/m^3)
γ	Unit weight of soil (saturated for clay)	9.81 (kN/m^3)

Table 7.1- Speswhite kaolin clay properties after Le (2018)

Parameter	Speswhite kaolin clay	Polwhite E kaolin clay
κ- Average gradient of swelling line in v: ln p' space	0.0348	0.0234
λ - Gradient of compression line in v: ln p' space	0.1155	0.0965
Plastic limit (%)	33.2	30
Liquid Limit (%)	75	50
Permeability (x 10^{-11} m/s)	12	253

Table 7.2- Speswhite kaolin and Polwhite E kaolin clay properties after Chan (2020)

Test ID	Sedimented (Yes/No)	Initial Water content (%)	Consolidation stress (kPa)
S 1	Yes	120	250
S 2	Yes	400	250
S 3	Yes	600	250
S 4	Yes	600	250
S 5	Yes	800	250
S 6	Yes	800	250
S 7	Yes	1200	250
S 8	Yes	1200	250

Table 7.3- Details of the different Speswhite kaolin clay powder slurries

Test ID	Sedimented (Yes/ No)	Initial Water content (%)	Consolidation stress (kPa)
RS 1	Yes	120	250
RS 2	Yes	120	250
RS 3	Yes	400	250
RS 4	Yes	400	250
RS 5	Yes	600	250
RS 6	Yes	600	250
RS 7	Yes	1200	250
RS 8	Yes	1200	250

Table 7.4- Details of the different disaggregated Speswhite kaolin clay slurries sedimented using the geotechnical centrifuge

Test ID	Speswhite kaolin clay (%)	Polwhite E kaolin clay (%)	Sedimented (Yes/No)	Initial Water content (%)	Consolidation stress (kPa)
SP 1	70	30	Yes	120	250
SP 2	70	30	Yes	120	250
SP 3	70	30	Yes	400	250
SP 4	70	30	Yes	400	250
SP 5	70	30	Yes	800	250
SP 6	70	30	Yes	800	250
SP 7	70	30	Yes	1200	250
SP 8	70	30	Yes	1200	250
SP 9	50	50	Yes	800	250
SP 10	50	50	Yes	800	250
SP 11	50	50	Yes	1200	250
SP12	50	50	Yes	1200	250

Table 7.5 - Details of the different Speswhite and Polwhite E kaolin clay powder slurries

Test ID	Speswhite kaolin clay (%)	Leighton Buzzard Fraction E (%)	Sedimented (Yes/No)	Initial Water content (%)	Consolidation stress (kPa)
SLBS 1	70	30	Yes	400	250
SLBS 2	70	30	Yes	400	250
SLBS 3	70	30	Yes	800	250
SLBS 4	70	30	Yes	800	250

Table 7.6- Details of the different Speswhite kaolin clay powder and Leighton Buzzard Sand slurries

Test ID	Speswhite kaolin clay (%)	Polwhite E kaolin clay (%)	Dispersion agent concentration (g/l)	Sedimented (Yes/No)	Initial Water content (%)	Consolidation stress (kPa)
SP+SHMP 1	70	30	8	Yes	500	250
SP+SHMP 2	70	30	8	Yes	500	250
SP+SHMP 3	70	30	4	Yes	500	250
SP+SHMP 4	70	30	4	Yes	500	250
SP+SHMP 5	70	30	2	Yes	500	250
SP+SHMP 6	70	30	2	Yes	500	250
SP+SHMP 7	70	30	1	Yes	500	250
SP+SHMP 8	70	30	1	Yes	500	250
SP+SHMP 9	50	50	0.5	Yes	500	250
SP+SHMP 10	50	50	0.5	Yes	500	250
SP+SHMP 11	50	50	0.1	Yes	500	250
SP+SHMP 12	50	50	0.1	Yes	500	250

Table 7.7- Details of the different Speswhite and Polwhite E kaolin clay slurries with the addition of a dispersion agent (sodium hexametaphosphate)

Test ID	Speswhite kaolin clay (%)	Polwhite E kaolin clay (%)	Dispersion agent concentration (g/l)	Sedimentation time (hrs)	Initial Water content (%)	Consolidation stress (kPa)
ST 1	70	30	0.1	2	500	250
ST 2	70	30	0.1	4	500	250
ST 3	70	30	0.1	6	500	250
ST 4	70	30	0.1	8	500	250
ST 5	70	30	0.1	24	500	250
ST 6	70	30	0.1	24	500	250

Table 7.8- Details of the different slurries sedimented and the different inflight sedimentation time

Test ID	Speswhite kaolin clay (%)	Polwhite E kaolin clay (%)	Dispersion agent concentration (g/l)	Sedimentation time (hrs)	Initial Water content (%)	Initial stress state
OD1	100	0	0	N/A	120	Slurry
OD 2	0	100	0	N/A	120	Slurry
OD 3	100	0	0	24	1200	*In situ*
OD 4	70	30	0.1	2	500	*In situ*

Table 7.9- Details of the different samples tested in the oedometer

Test ID	Initial Water content (%)	Consolidation stress (kPa)	100% Speswhite kaolin clay powder			100% Polwhite E kaolin clay powder		
			Vertical permeability ($x10^{-9}$ ms^{-1})	Horizontal permeability ($x10^{-9}$ ms^{-1})	Post-test moisture content (%)	Vertical permeability ($x10^{-9}$ ms^{-1})	Horizontal permeability ($x10^{-9}$ ms^{-1})	Post-test moisture content (%)
REF 1	120	250	1.90	2.10	57.79	20.5	22.5	64.64
REF 2	120	250	1.85	2.00	57.73	22.0	23.0	64.78
REF 3	120	250	1.95	2.15	57.03	20.5	23.0	65.77
REF 4	120	250	1.95	2.20	57.24	21.5	22.5	65.71
REF 5	120	250	2.05	2.15	58.10	22.5	23.0	65.21
Average			1.95	2.10	57.58	21.5	23.0	65.22

Table 8.1- Permeability results of preliminarily testing of 100% Speswhite and Polwhite E kaolin clay samples prepared from a slurry and consolidated in a pneumatic press

Test ID	Sedimented (Yes/ No)	Initial Water content (%)	Consolidation stress (kPa)	100% Speswhite kaolin clay powder			Anisotropy (k_h/k_v)
				Vertical permeability ($x10^{-9}$ ms^{-1})	Horizontal permeability ($x10^{-9}$ ms^{-1})	Post-test moisture content (%)	
S 1	Yes	120	250	1.20	1.40	57.51	1.16
S 2	Yes	400	250	1.15	1.30	57.11	1.13
S 3	Yes	600	250	1.20	1.25	58.10	1.33
S 4	Yes	600	250	1.25	1.25	57.91	1.00
S 5	Yes	800	250	1.10	1.30	59.10	1.27
S 6	Yes	800	250	1.10	1.20	58.87	1.27
S 7	Yes	1200	250	1.10	1.30	62.81	1.23
S 8	Yes	1200	250	1.15	1.30	63.12	1.22

Table 8.2- Permeability results of 100% Speswhite kaolin clay slurries sedimented at different initial water contents

Test ID	Sedimented (Yes, No)	Initial Water content (%)	Consolidation stress (kPa)	100% Recycled Speswhite kaolin clay cuttings			Anisotropy (k_h/k_v)
				Vertical permeability ($x10^{-9}$ ms^{-1})	Horizontal permeability ($x10^{-9}$ ms^{-1})	Post-test moisture content (%)	
RS 1	Yes	120	250	1.25	1.60	57.20	1.3
RS 2	Yes	120	250	1.35	1.70	56.99	1.3
RS 3	Yes	400	250	1.20	1.35	58.33	1.1
RS 4	Yes	400	250	1.25	1.35	57.68	1.1
RS 5	Yes	600	250	1.15	1.70	59.10	1.5
RS 6	Yes	600	250	1.20	1.65	59.33	1.5
RS 7	Yes	1200	250	1.30	1.60	62.99	1.25
RS 8	Yes	1200	250	1.35	1.60	62.18	1.25

Table 8.3- Permeability results of 100% recycled Speswhite kaolin clay cuttings slurries sedimented at different initial water contents

Test ID	Speswhite kaolin clay (%)	Polwhite E kaolin clay (%)	Initial Water content (%)	Vertical permeability ($x10^{-9}$ ms^{-1})	Horizontal permeability at the top of sample ($x10^{-9}$ ms^{-1})	Horizontal permeability at the base of sample ($x10^{-9}$ ms^{-1})	Anisotropy (Horizontal at base/vertical k_{hb}/k_v)	Post-test moisture content at the top of sample (%)	Post-test moisture content at the base of sample (%)
SP 1	70	30	120	7.90	8.20	9.50	1.25	57.61	64.51
SP 2	70	30	120	7.70	8.30	9.80	1.25	57.77	65.12
SP 3	70	30	400	7.40	8.40	9.40	1.25	57.48	65.99
SP 4	70	30	400	7.60	8.10	9.80	1.25	57.52	66.21
SP 5	70	30	800	4.90	5.40	11.0	2.5	59.04	67.22
SP 6	70	30	800	5.30	6.00	11.0	2.5	59.31	67.43
SP 7	70	30	1200	2.20	2.50	12.0	4.5	63.07	69.24
SP 8	70	30	1200	2.70	2.90	13.0	4.5	63.28	68.87
SP 9	50	50	800	6.00	5.90	11.5	1.9	59.87	N/A
SP 10	50	50	800	6.20	6.50	12.0	1.8	59.67	66.87
SP 11	50	50	1200	4.20	4.15	12.0	3	63.61	69.25
SP12	50	50	1200	4.20	4.00	13.0	3	62.89	69.98

Table 8.4- Permeability results of Speswhite: Polwhite E kaolin clay slurries sedimented at different initial water contents

Test ID	Speswhite kaolin clay (%)	Leighton Buzzard Fraction E (%)	Initial Water content (%)	Consolidation stress (kPa)	Vertical permeability ($x10^{-9}$ ms^{-1})	Horizontal permeability at the base of sample ($x10^{-9}$ ms^{-1})	Horizontal permeability at the top of sample ($x10^{-9}$ ms^{-1})	Post-test moisture content at the top of the sample (%)	Anisotropy (Horizontal at base/vertical k_{hb}/k_v)
SLBS 1	70	30	400	250	3.20	53000	3.80	58.27	14000
SLBS 2	70	30	400	250	3.10	62000	3.90	58.64	16000
SLBS 3	70	30	800	250	3.40	55000	3.80	59.98	14500
SLBS 4	70	30	800	250	3.20	65000	3.70	60.21	17500

Table 8.5- Permeability results of Speswhite kaolin clay and Leighton Buzzard Sand fraction E slurries sedimented at different initial water contents

Test ID	Speswhite kaolin clay (%)	Polwhite E kaolin clay (%)	Dispersion agent concentration (g/l)	Initial Water content (%)	Vertical permeability ($x10^{-9}$ ms^{-1})	Horizontal permeability at the top of sample ($x10^{-9}$ ms^{-1})	Post-test moisture content at the top of the sample (%)	Horizontal permeability at the base of sample ($x10^{-9}$ ms^{-1})	Post-test moisture content at the base of the sample (%)	Anisotropy (Horizontal at base/vertical k_{hb}/k_v)
SP+D1	70	30	8	500	1.90	N/A	N/A	N/A	N/A	N/A
SP+D2	70	30	8	500	1.60	N/A	N/A	N/A	N/A	N/A
SP+D3	70	30	4	500	3.05	N/A	N/A	N/A	N/A	N/A
SP+D4	70	30	4	500	3.00	N/A	N/A	N/A	N/A	N/A
SP+D5	70	30	2	500	1.75	2.50	N/A	14	N/A	8
SP+D6	70	30	2	500	1.85	2.75	N/A	15	N/A	8
SP+ D7	70	30	1	500	1.75	2.60	N/A	18	N/A	10
SP+ D8	70	30	1	500	1.55	2.55	N/A	18	N/A	11.5
SP+ D9	50	30	0.5	500	1.95	3.35	N/A	16	N/A	8
SP+ D10	50	30	0.5	500	2.15	3.45	N/A	16	N/A	8
SP+ D11	50	30	0.1	500	4.55	2.65	63.88	17	68.74	4
SP+ D12	50	30	0.1	500	4.65	2.85	64.01	17	69.21	4

Table 8.6- Permeability results of Speswhite: Polwhite E kaolin clay slurries with added dispersion agent sedimented at different initial water contents. Note that highlighted rows indicate an unstable soil structure generated during sedimentation

Test ID	Speswhite kaolin clay (%)	Polwhite E kaolin clay (%)	Dispersion agent concentration (g /l)	Sedimentation time (hrs)	Vertical permeability ($x10^{-9}$ ms^{-1})	Horizontal permeability at the top of sample ($x10^{-9}$ ms^{-1})	Post-test moisture content at the top of the sample (%)	Horizontal permeability at the base of sample ($x10^{-9}$ ms^{-1})	Post-test moisture content at the base of the sample (%)	Anisotropy (Horizontal at base/vertical k_{hb}/k_v)
ST 1	70	30	0.1	2	4.60	2.65	63.92	17	68.98	4
ST 2	70	30	0.1	4	4.55	3.30	64.01	16	67.54	4
ST 3	70	30	0.1	6	4.65	2.65	63.87	17	68.44	4
ST 4	70	30	0.1	8	4.80	2.85	63.51	17	68.36	4
ST 5	70	30	0.1	24	4.55	2.65	64.25	17	69.27	4
ST 6	70	30	0.1	24	4.65	2.85	64.05	17	69.07	4

Table 8.7- Permeability results of Speswhite: Polwhite E kaolin clay slurries with added dispersion agent sedimented subjected to different sedimentation times on the centrifuge

Carrier	Full scale pressure	High sensitivity versions			High sensitivity versions		
		Product code	Full span cycle	Linearity	Product code	Full span cycle	Linearity
	1 Bar	MS5401-AM	240mV	±0.20%FS	MS5401-BM	150mV	± 0.05%FS
	7 Bar	MS5407-AM	392mV	±0.20%FS			
Ceramic	12 Bar				MS5412-BM	150mV	±0.05%FS

Table 10.1- Details of the TE connectivity pressure sensors available

Model	Parameter	Min	Typical	Max	Unit
MS5407-AM	Operating pressure ranges	0	-	7	Bar
	Full-scale span (FS)	322	392	462	mV
	Sensitivity	46	56	66	mV
	Linearity		±0.15	±0.40	% FS
	Operating temperature range	-40	-	125	°C
	Zero pressure offset	-40	0	40	mV
	Pressure hysteresis	-	-	±0.20	% FS
	Temperature hysteresis	-	0.3	0.8	% FS
	Repeatability	-	-	±0.20	% FS
	Bridge resistance	3	3.4	3.8	kΩ
	Temperature coefficient of resistance	+2'400	+2'900	+3300	ppm/°C
	Temperature coefficient of span	-1'500	-1'900	-2'300	ppm/°C
	Temperature coefficient of offset	-80	-	+80	µV/°C

Table 10.2-Electrical details of TE connectivity MS5407-AM selected for the City, University of London pressure transducer

	Measured thickness (mm)	Designed thickness (mm)
Layer 4-Top	52	45
Layer 3	47	53
Layer 2	53	53
Layer 1- Bottom	54	53

Table 11.1- Measured and designed sedimented layer thicknesses

	Measured thickness (mm)	Predicted layer thickness after inflight consolidation (mm)	Designed thickness after consolidation in pneumatic press (mm)
Layer 4-Top	52	45.5	45
Layer 3	47	53.5	53
Layer 2	53	53.5	53
Layer 1- Bottom	54	53.5	53

Table 12.1- Measured and designed sedimented layer thickness after inflight consolidation

Centrifuge model	Vertical permeability ($x10^{-9}$ ms^{-1})	Horizontal permeability ($x10^{-9}$ ms^{-1})
Speswhite model	2.00	2.20
Speswhite Polwhite E model	2.60	3.00
Sedimented model	4.60	17.0

Table 12.2- Summary of centrifuge soil bed permeabilities

Figures

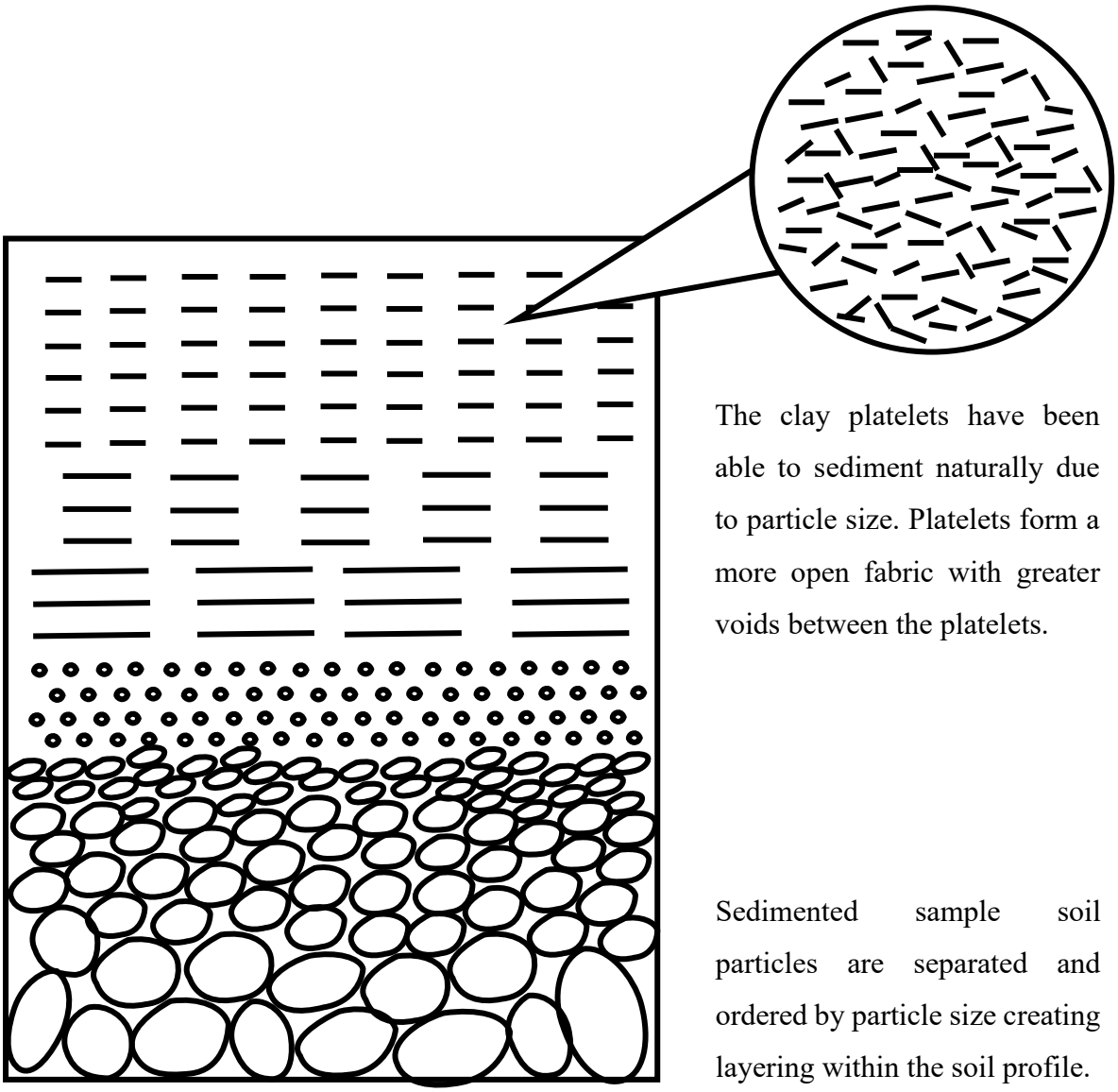

Figure 2.1- Idealised sedimented soil sample schematic

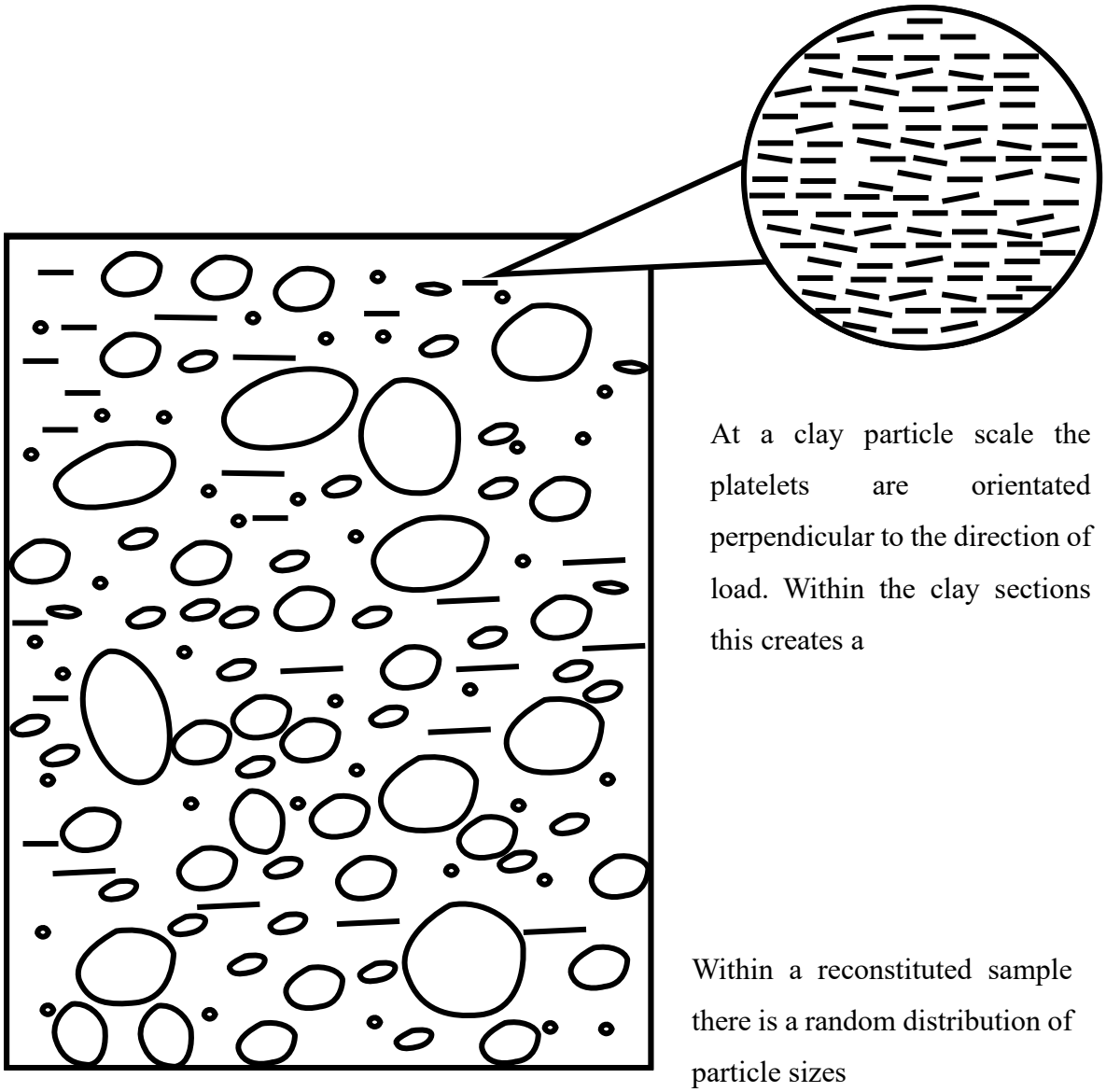

Figure 2.2- Idealised reconstituted soil sample schematic

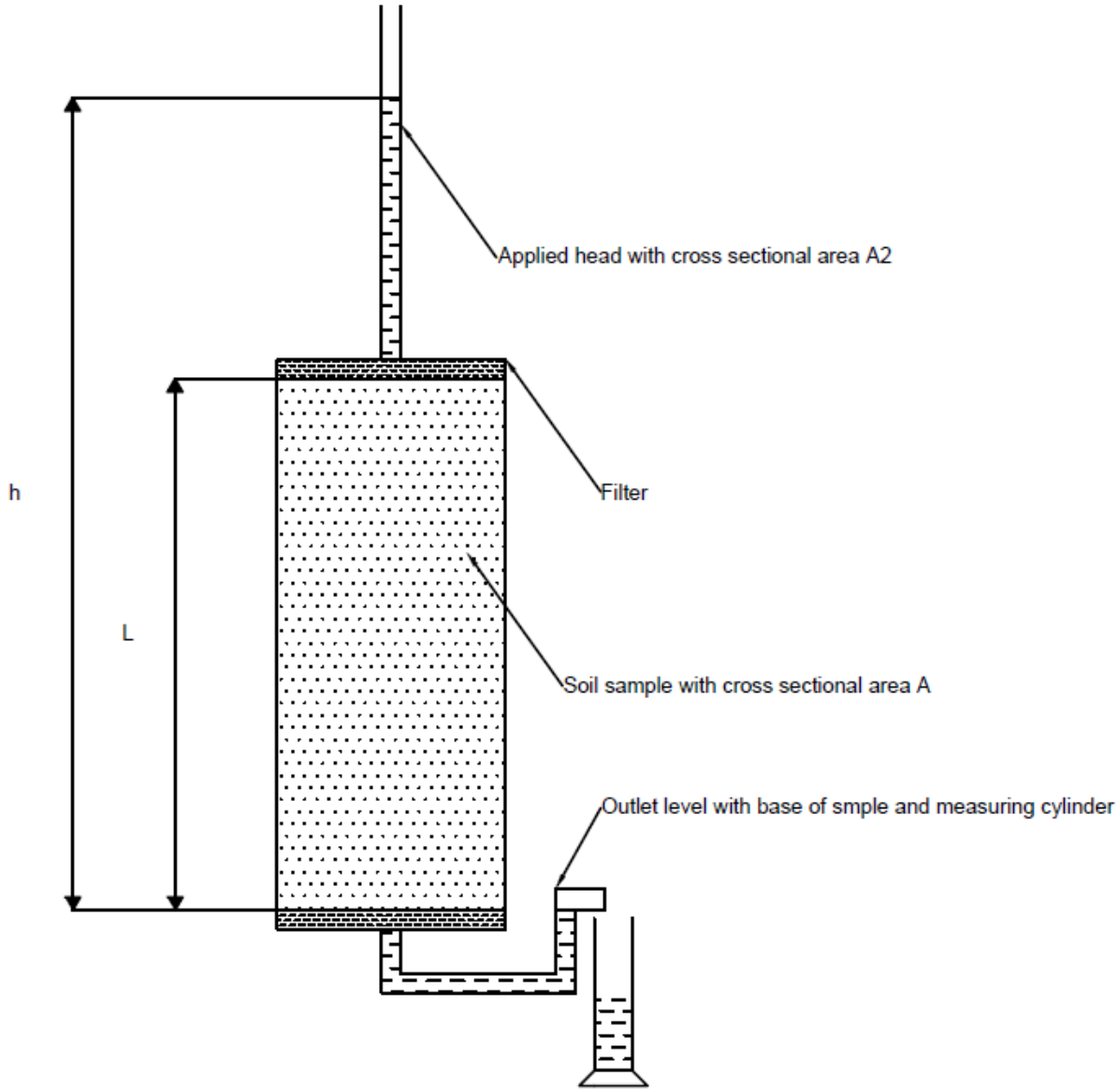

Figure 3.1- Typical Falling head permeameter, after Powrie (1997)

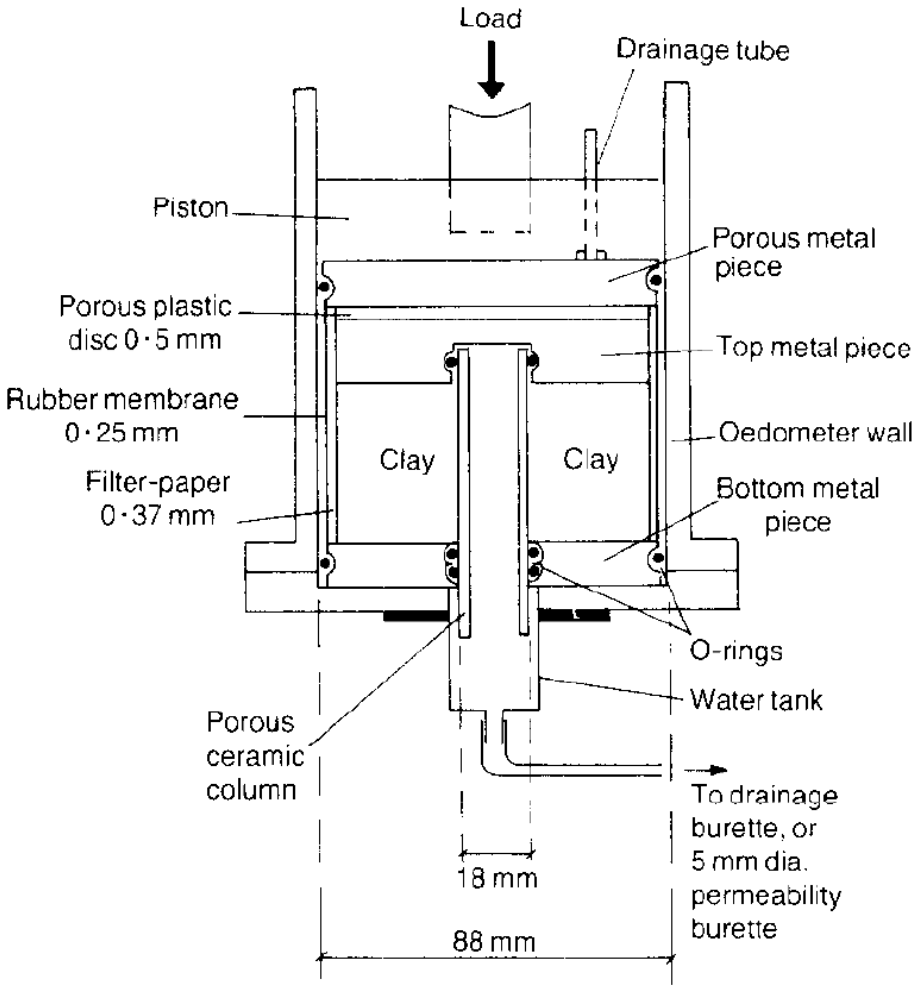

Figure 3.2- Modified oedometer cell for measuring radial flow, Al-Tabbaa & Wood (1987)

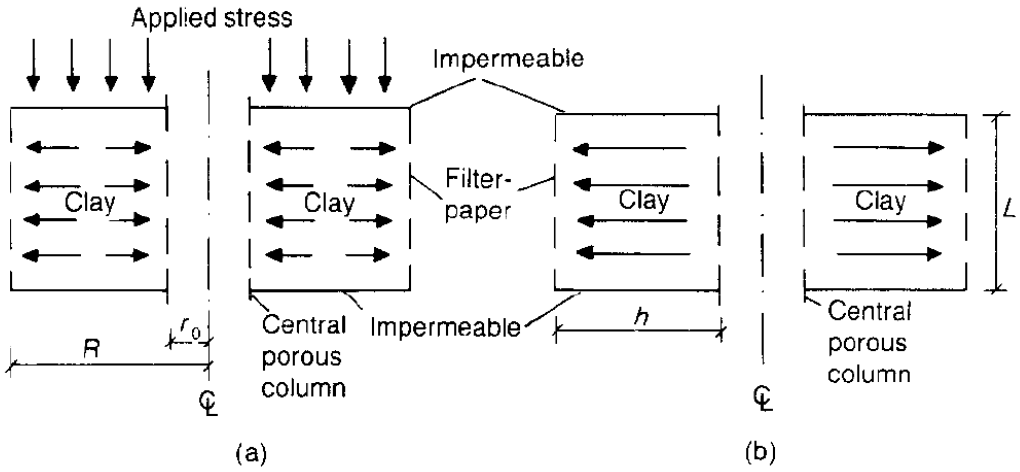

Figure 3.3- Drainage conditions during a, consolidation stage and b, horizontal permeability testing, Al-Tabbaa & Wood (1987)

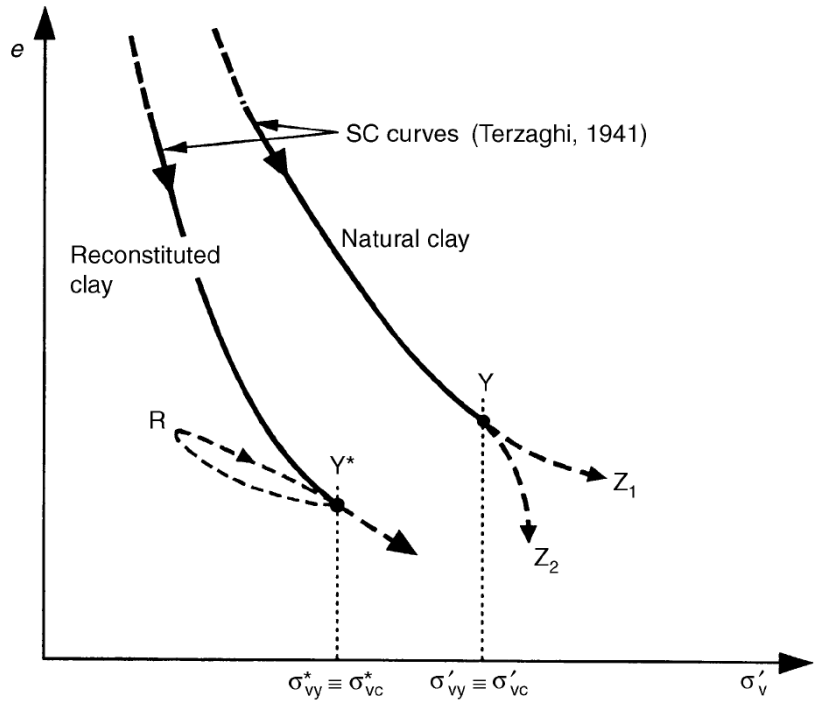

Figure 3.4- Difference in behaviour of a sedimented and reconstituted clay, Cotecchia & Chandler (2000)

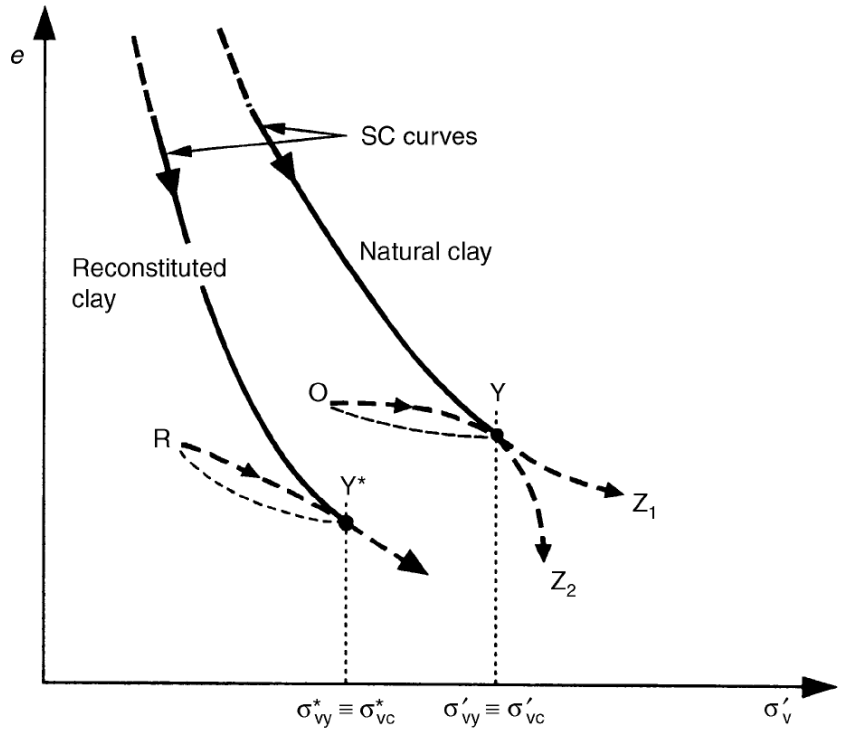

Figure 3.5 Schematic potential compression paths of a clays with post sedimentation structure, Cotecchia & Chandler (2000)

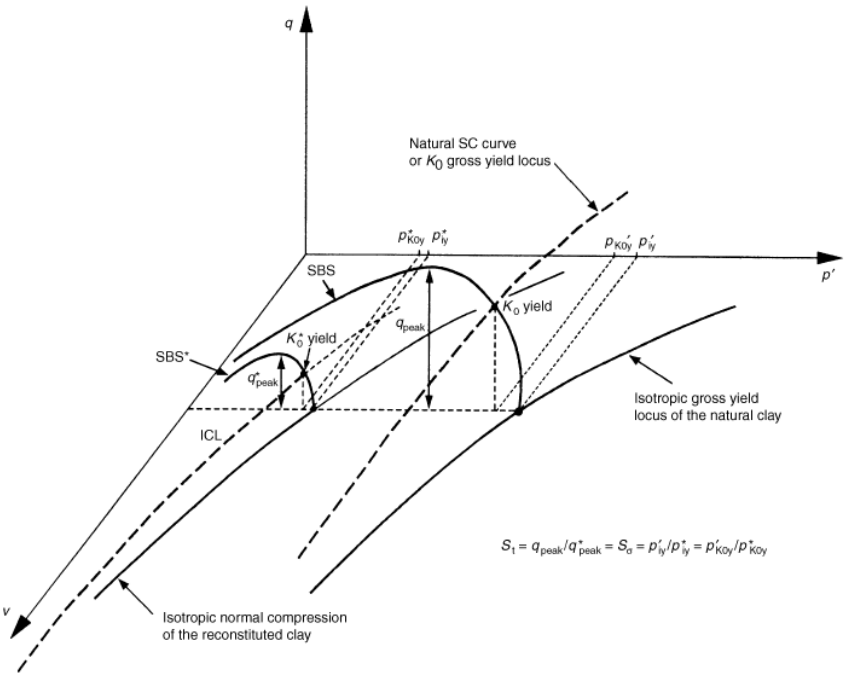

Figure 3.6- Idealised behaviour of a natural and reconstituted clay, Cotecchia & Chandler (2000)

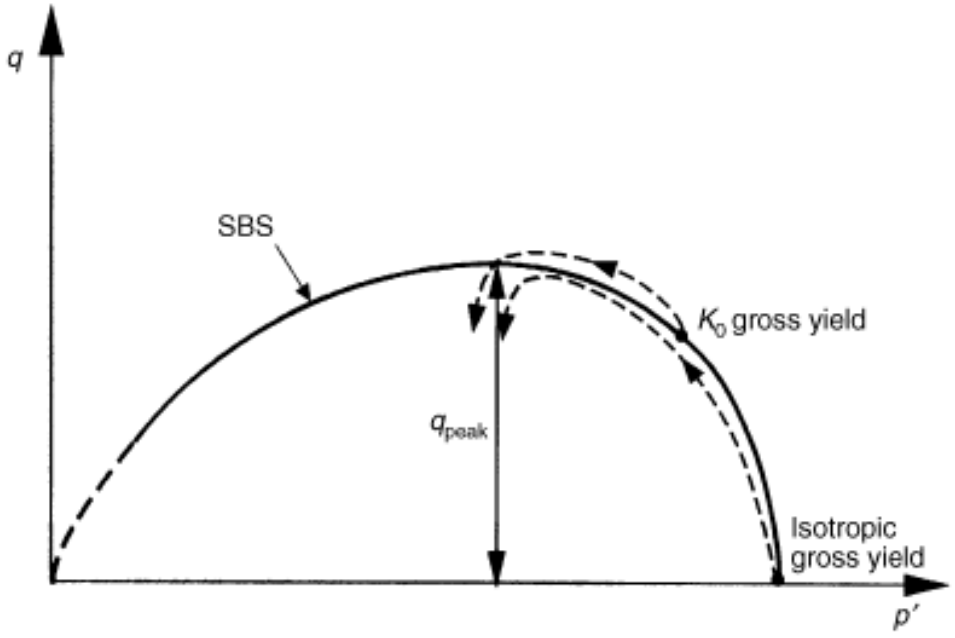

Figure 3.7- Undrained stress path of samples with a YSR of 1, Cotecchia & Chandler (2000)

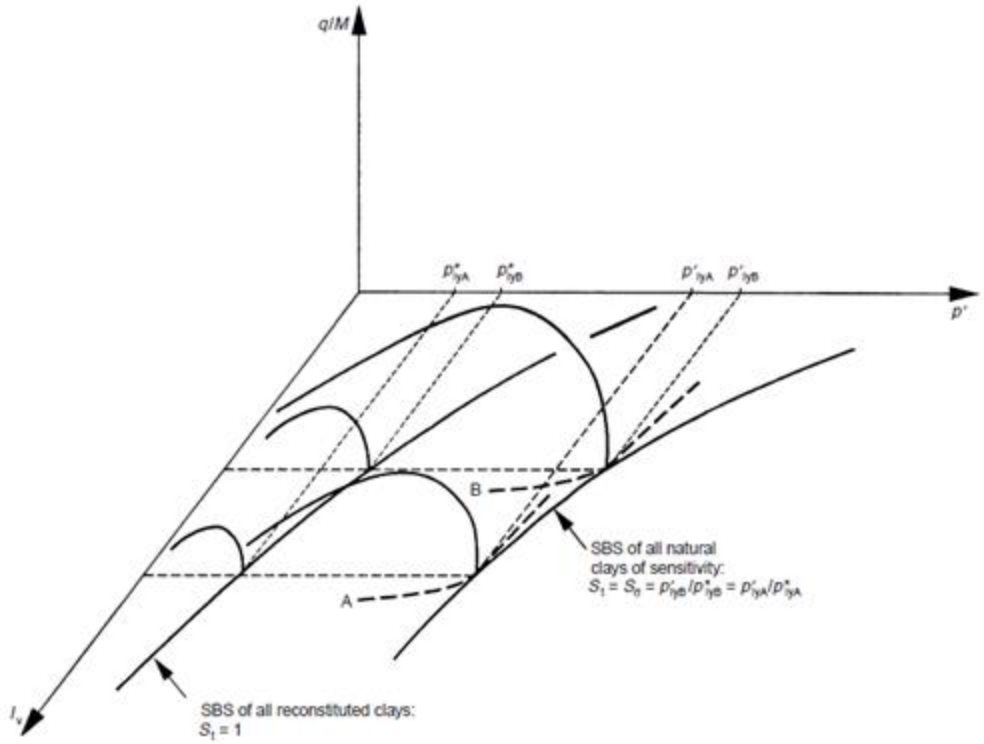

Figure 3.8- Idealised normalised behaviour of different clay with the same strength sensitivity, Cotecchia & Chandler (2000)

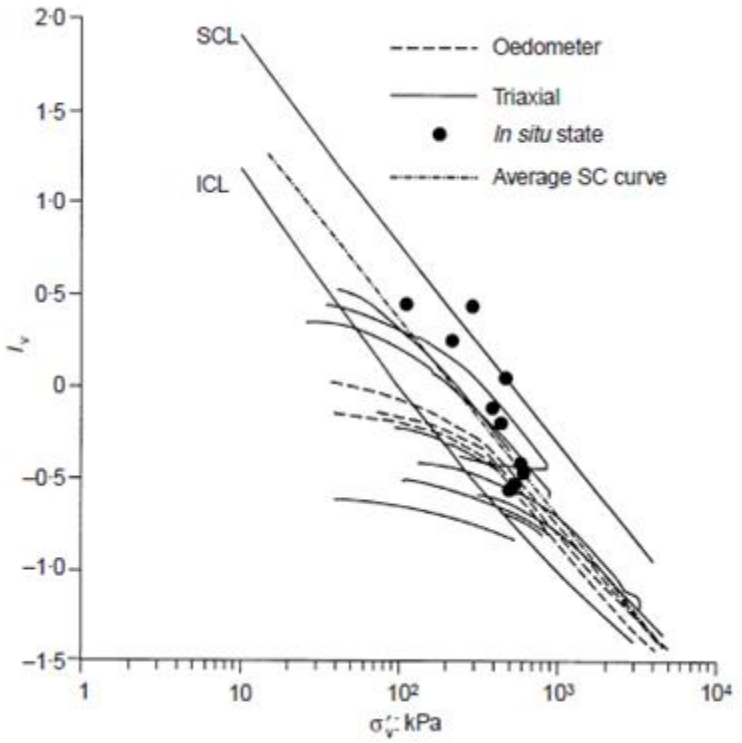

Figure 3.9- One dimensional Compression of Sibari clays, Coop & Cotecchia (1995)

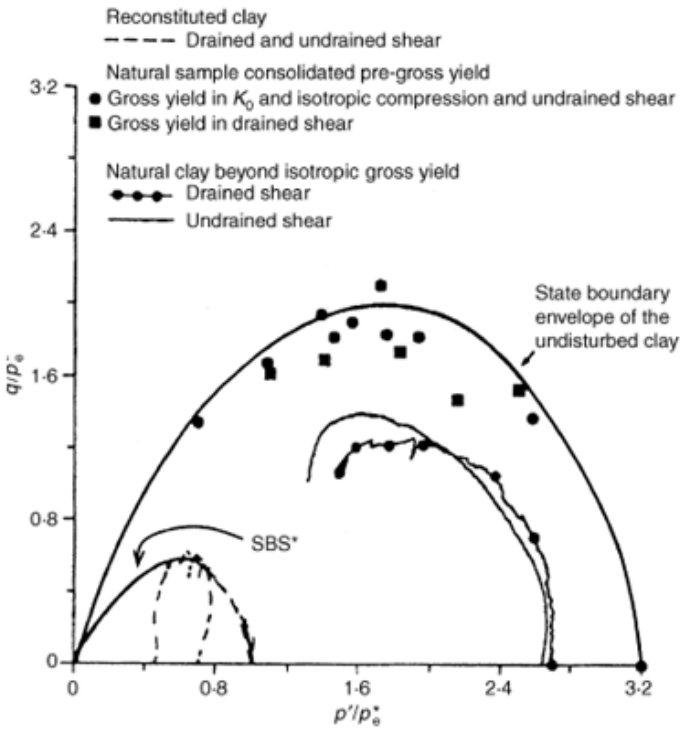

Figure 3.10- Stress paths of Pappadai clays, Cotecchia & Chandler (1997)

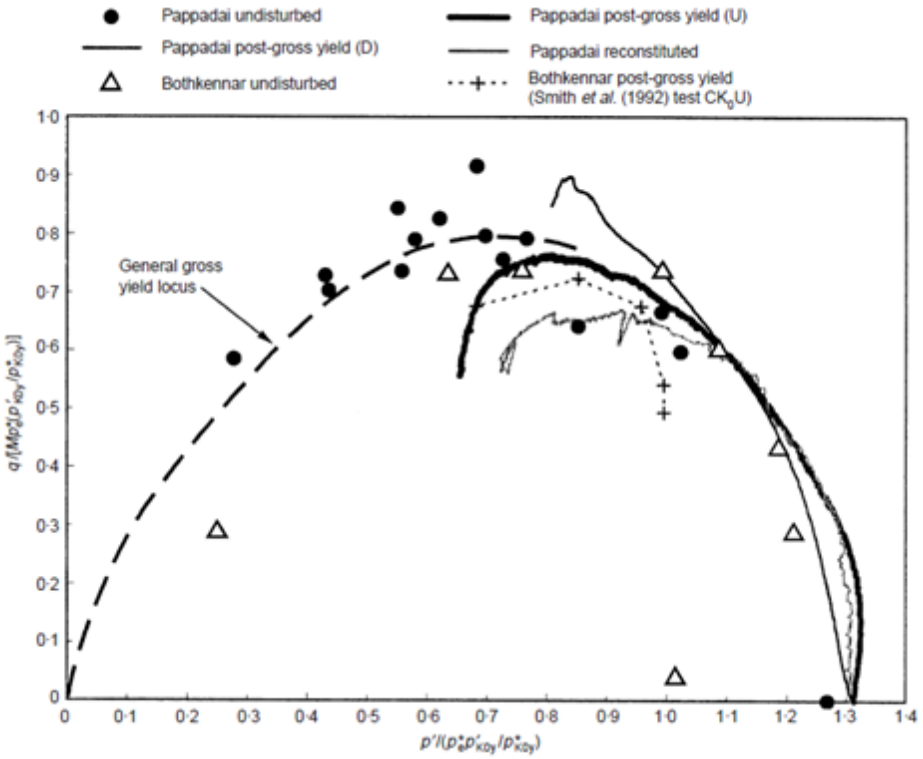

Figure 3.11- Normalised state boundary surface for a variety of clays, Cotecchia & Chandler (2000)

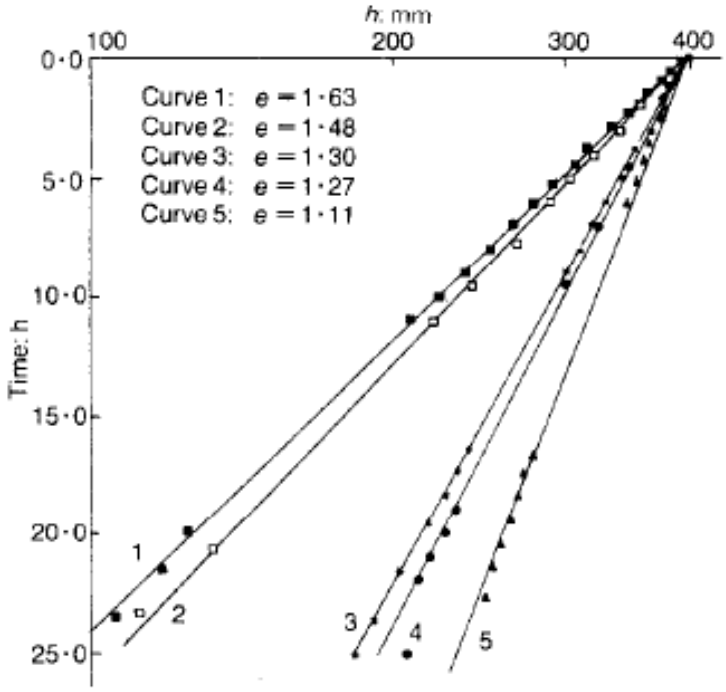

Figure 3.12- Relationship between log h and time for different voids ratios for a falling head radial flow experiment, Al-Tabbaa & Wood (1987)

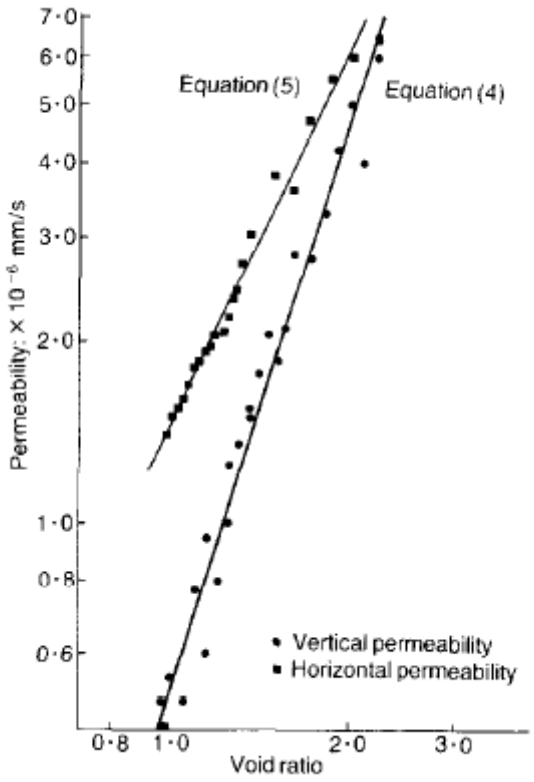

Figure 3.13- Relationship between permeability and voids ratio for normally consolidated Kaolin, Al-Tabbaa & Wood (1987)

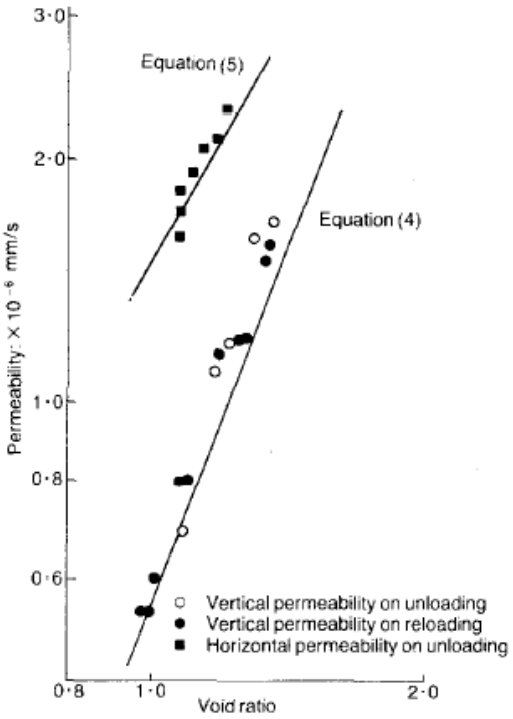

Figure 3.14- Relationship between permeability and voids ratio for overconsolidated Kaolin, Al-Tabbaa & Wood (1987)

Figure 3.15- Borehole summary of ground conditions Houses of Commons, Burland & Hancock (1977)

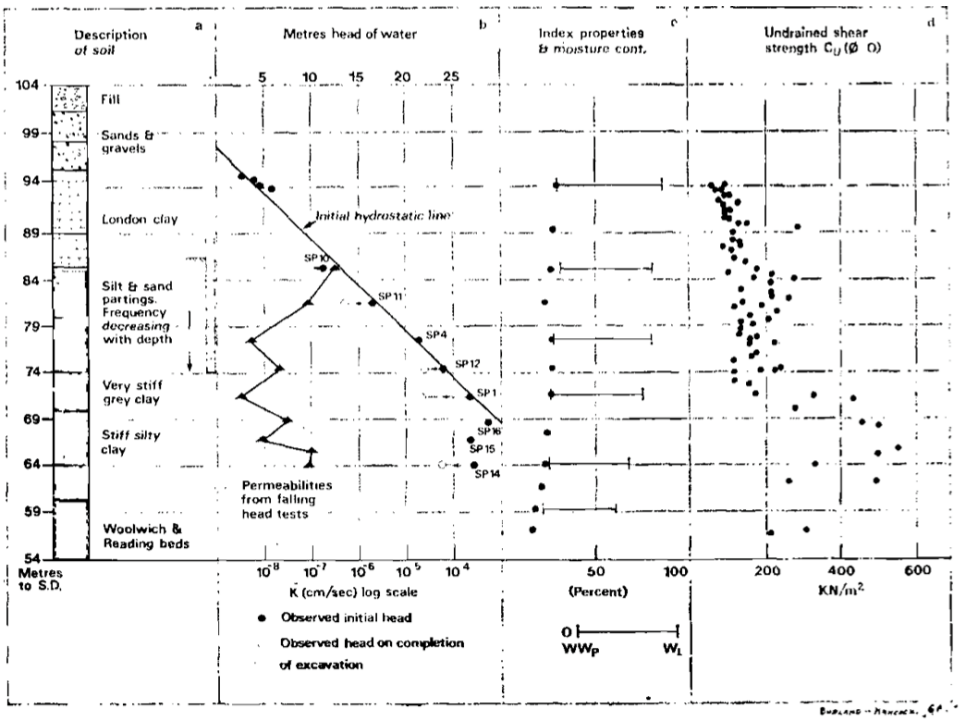

Figure 3.16- *In situ* values of permeability of London Clay, Burland & Handcock (1977)

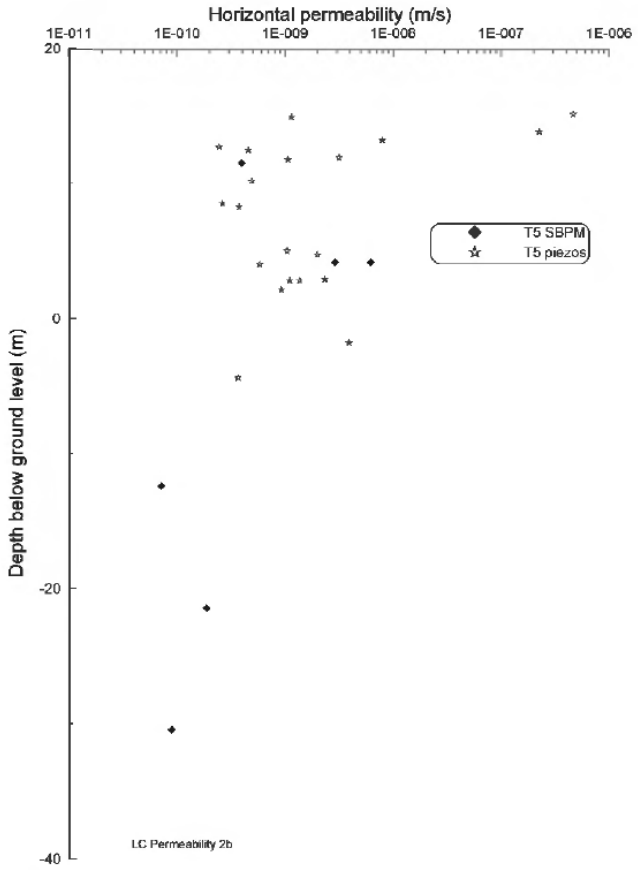

Figure 3.17- Permeability of London clay at terminal 5, Hight et al. (2003)

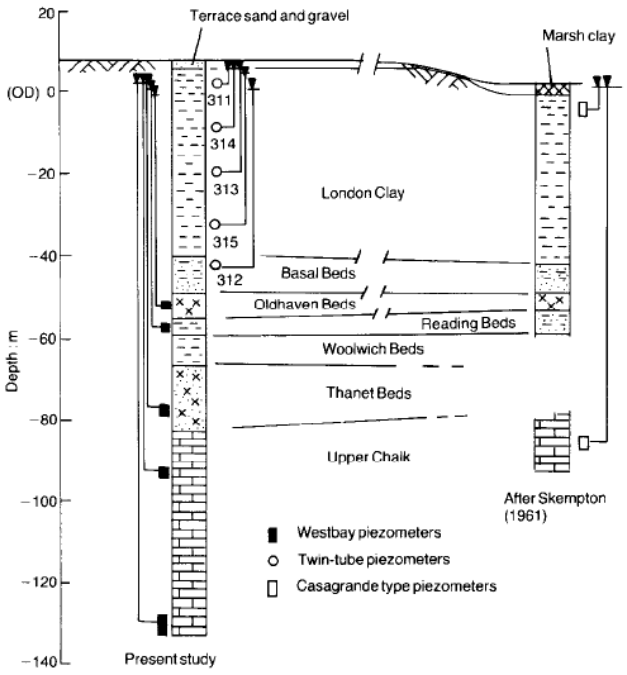

Figure 3.18- Schematic ground conditions Bradwell, Chandler et al. (1990)

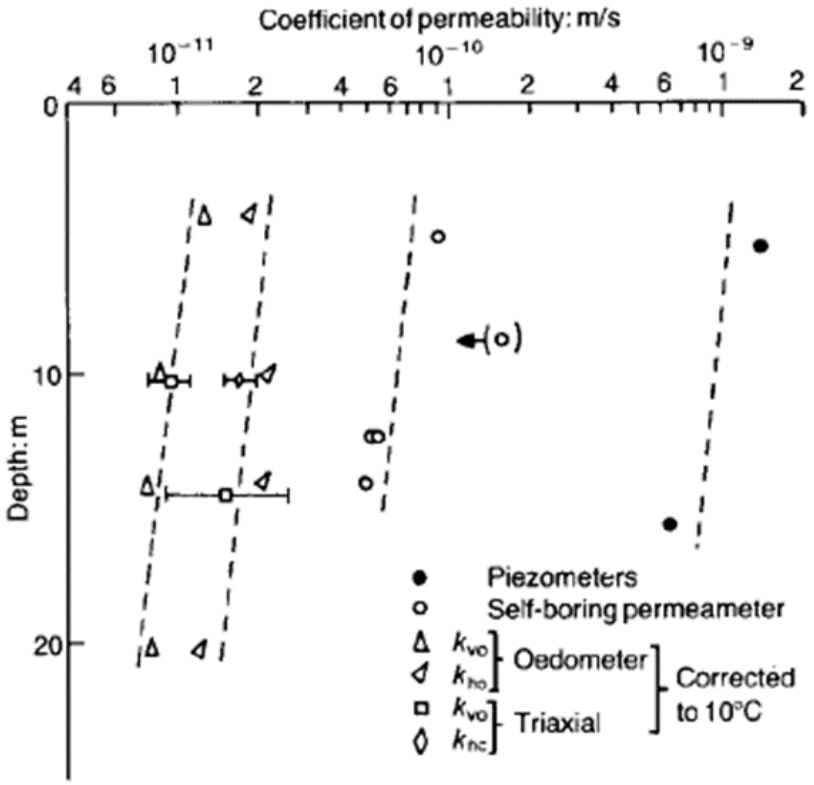

Figure 3.19- Variation in the coefficient of permeability London Clay, Chandler et al. (1990)

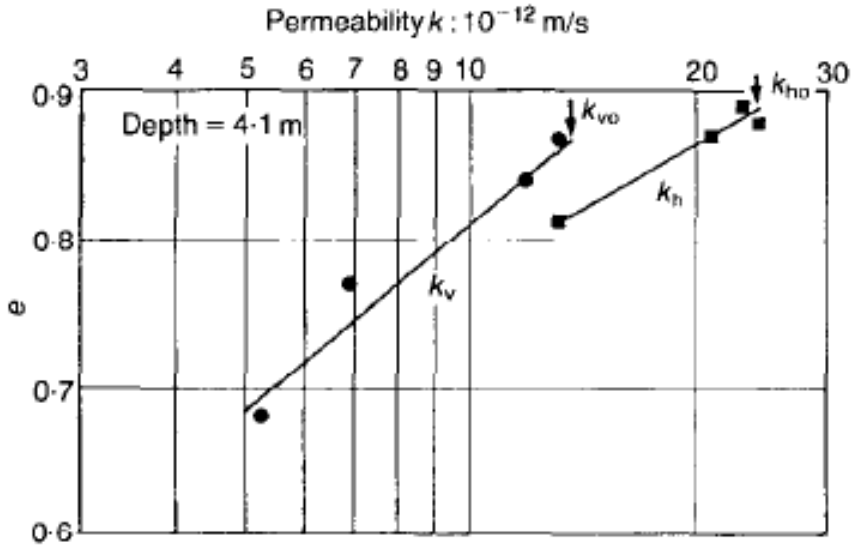

Figure 3.20- Variation of permeability with voids ratio, Chandler et al. (1990)

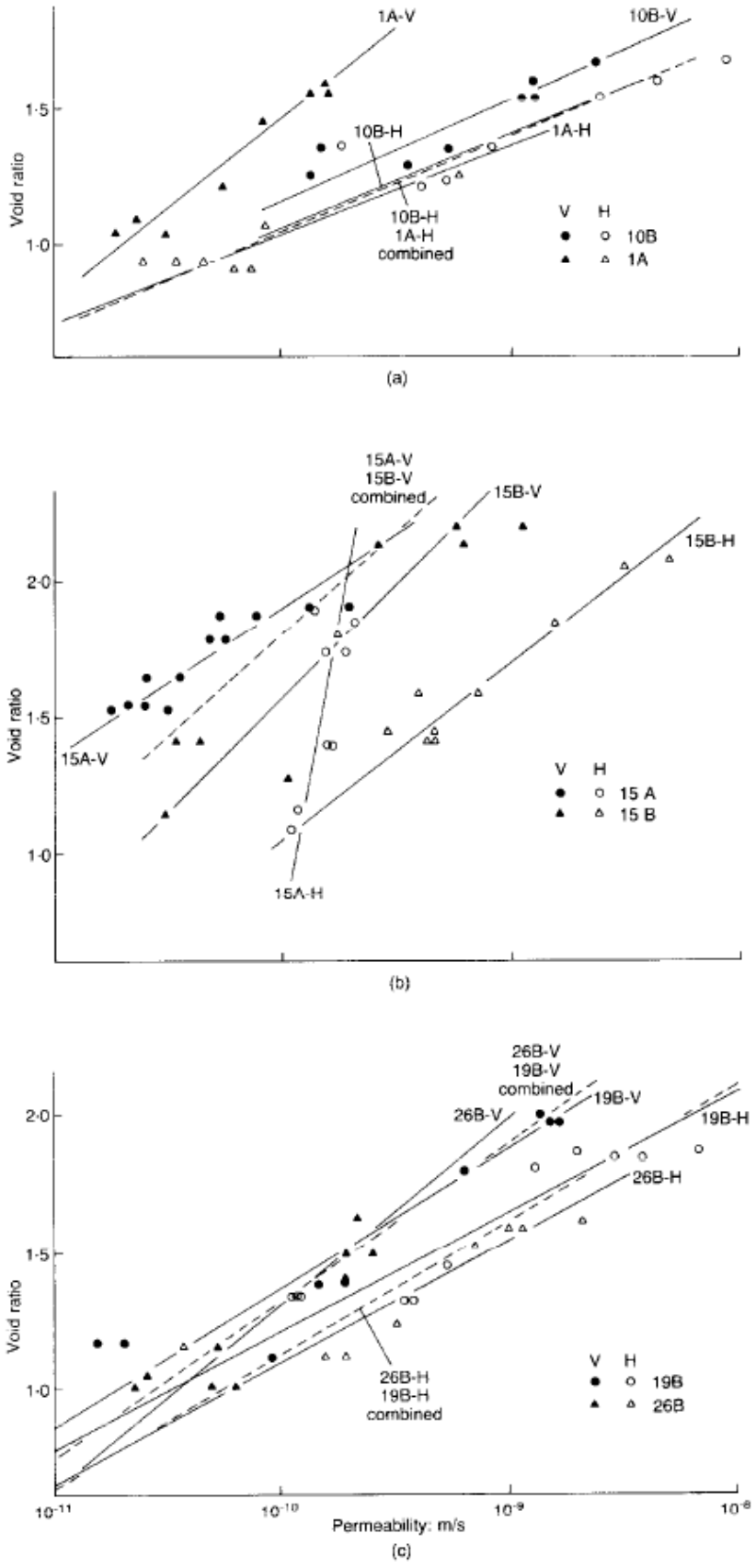

Figure 3.21-Permeability void ratio relationship of different depth Bothkennar clay, Little et al. (1992)

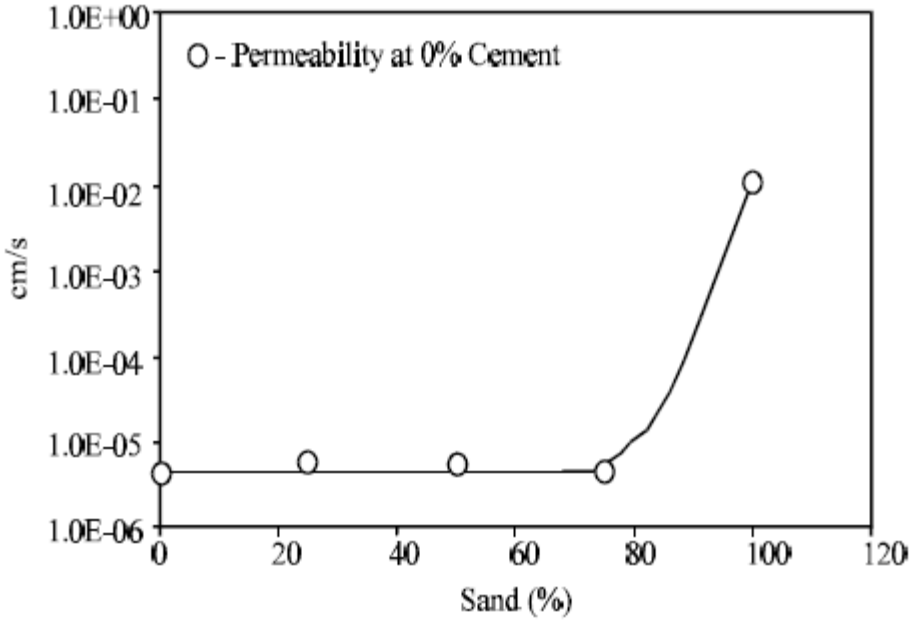

Figure 3.22- Effect of ratios of sand and clay on permeability of a homogenous mix, Mahasneh & Shawabkeh (2004)

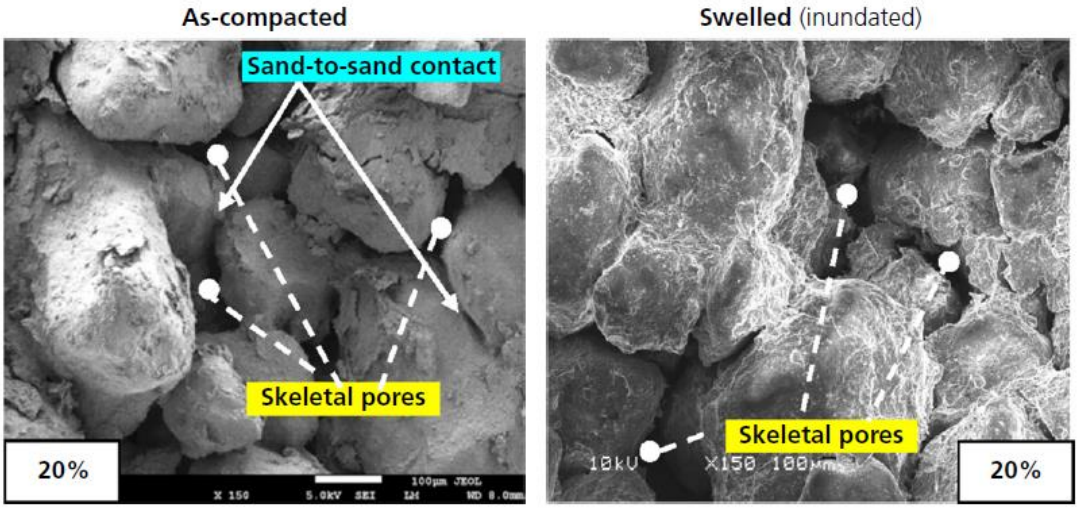

Figure 3.23- SEM of 20% clay content homogenous clay and soil mixture, Shaker & Elkady (2015)

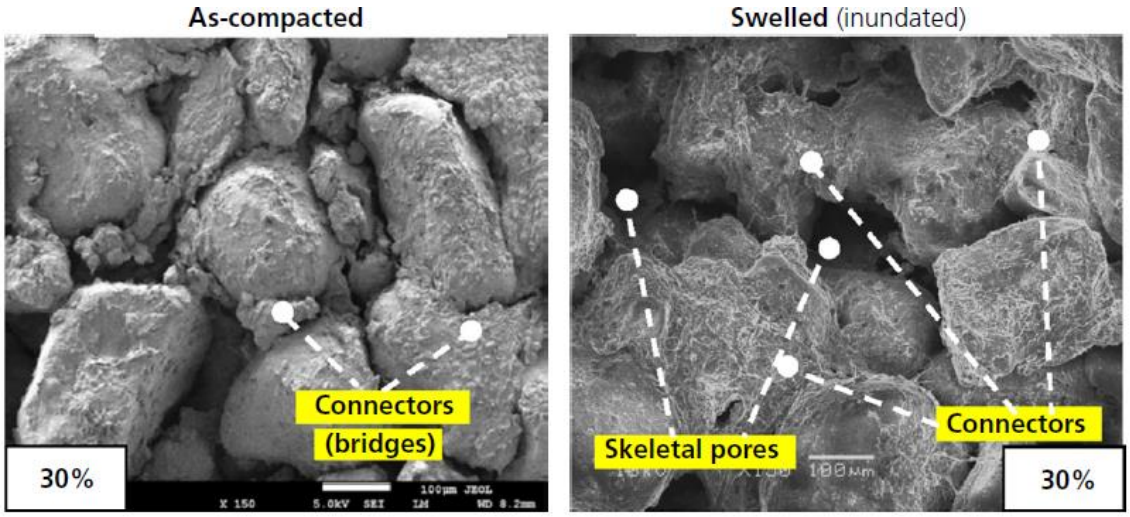

Figure 3.24- SEM of 30% clay content homogenous clay and soil mixture, Shaker & Elkady (2015)

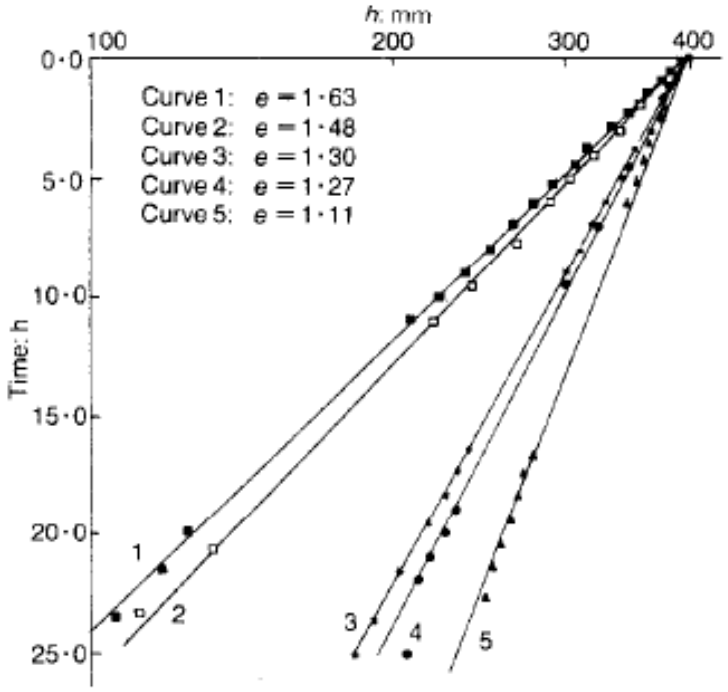

Figure 3.25- Relationship between log applied head and time for different voids ratios during a falling head radial flow experiment, Al-Tabbaa & Wood (1987)

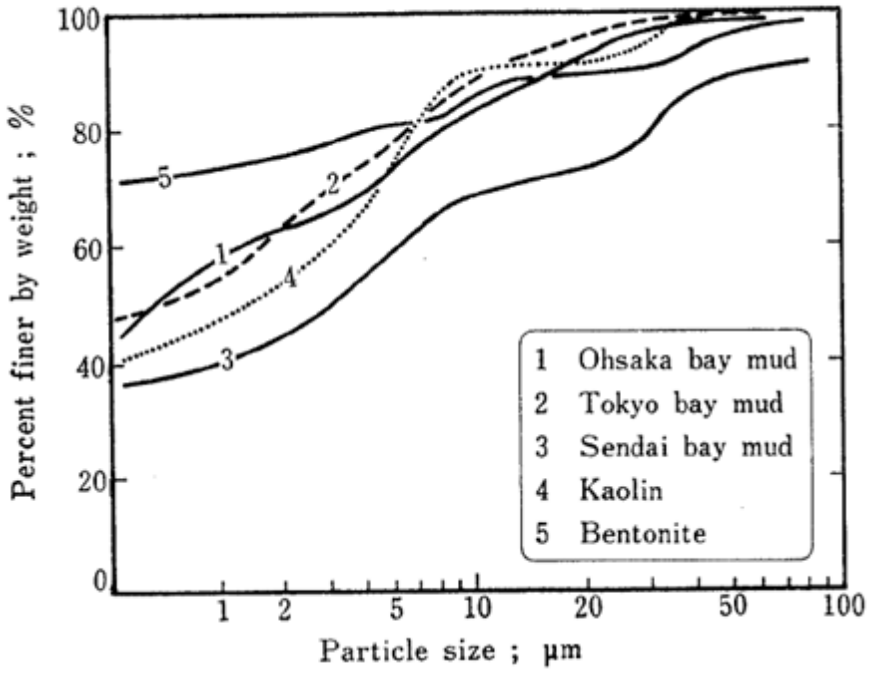

Figure 5.1- Particle size distributions, Imai (1980)

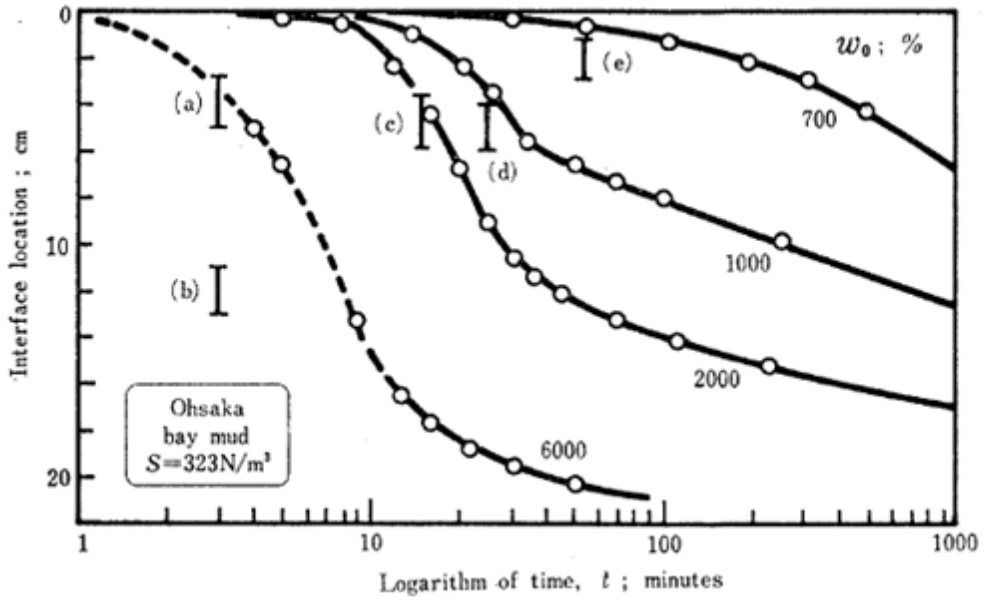

Figure 5.2- Settling curves of Ohsaka bay mud slurries with varying initial water content, Imai (1980)

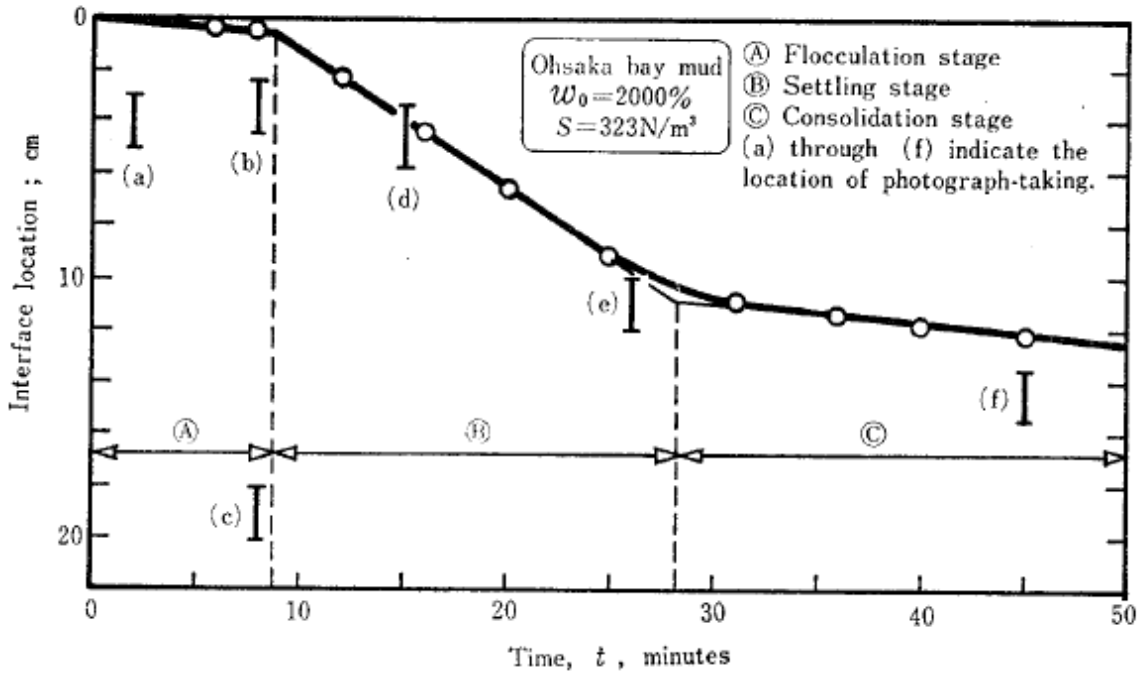

Figure 5.3- Settling curve of Ohsaka bay mud slurry with an 2000% initial water content, Imai (1980)

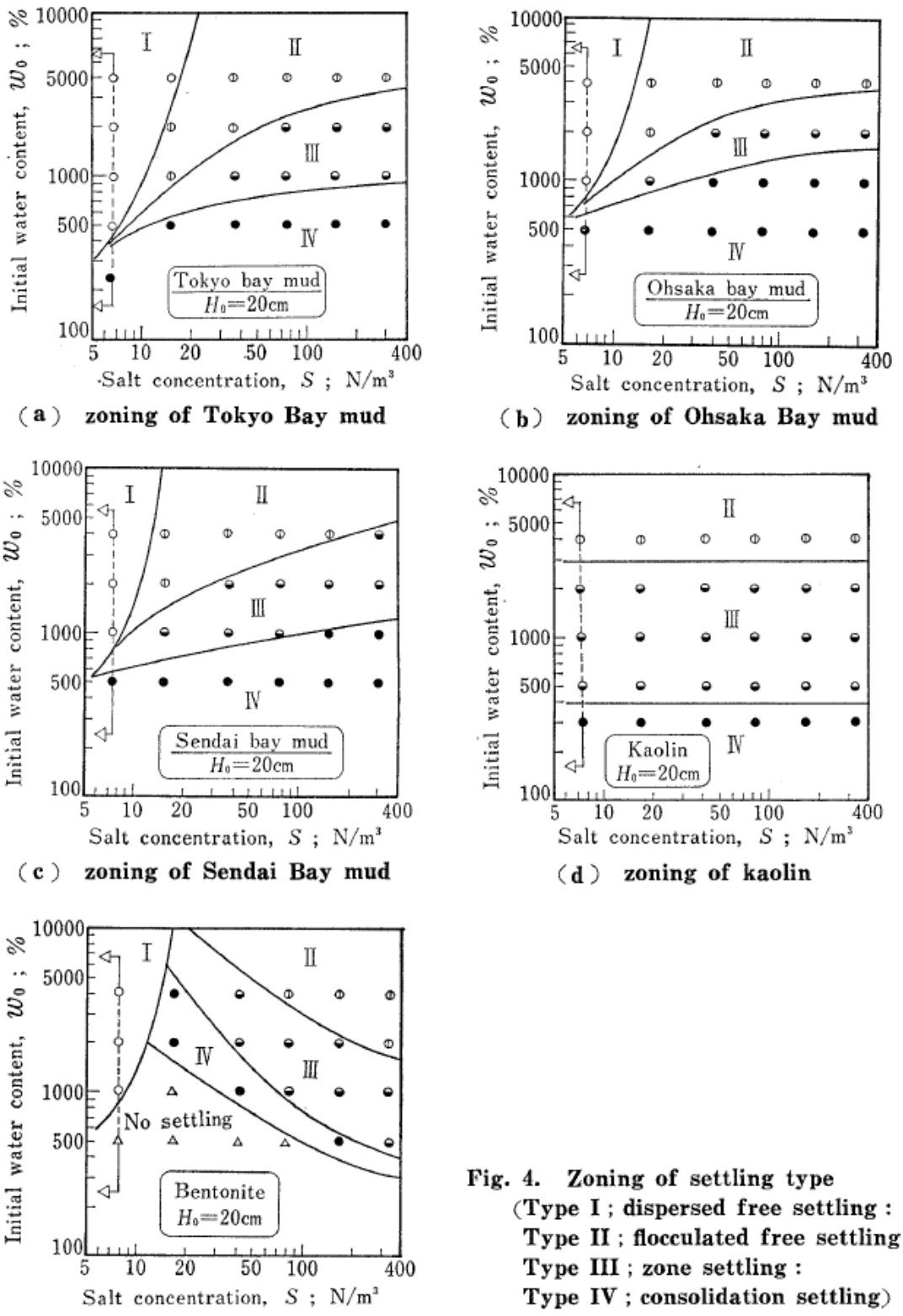

Fig. 4. Zoning of settling type
(Type I ; dispersed free settling :
Type II ; flocculated free settling ;
Type III ; zone settling :
Type IV ; consolidation settling)

Figure 5.4- Zoning of settlement behaviour of different soil compositions, Imai (1980)

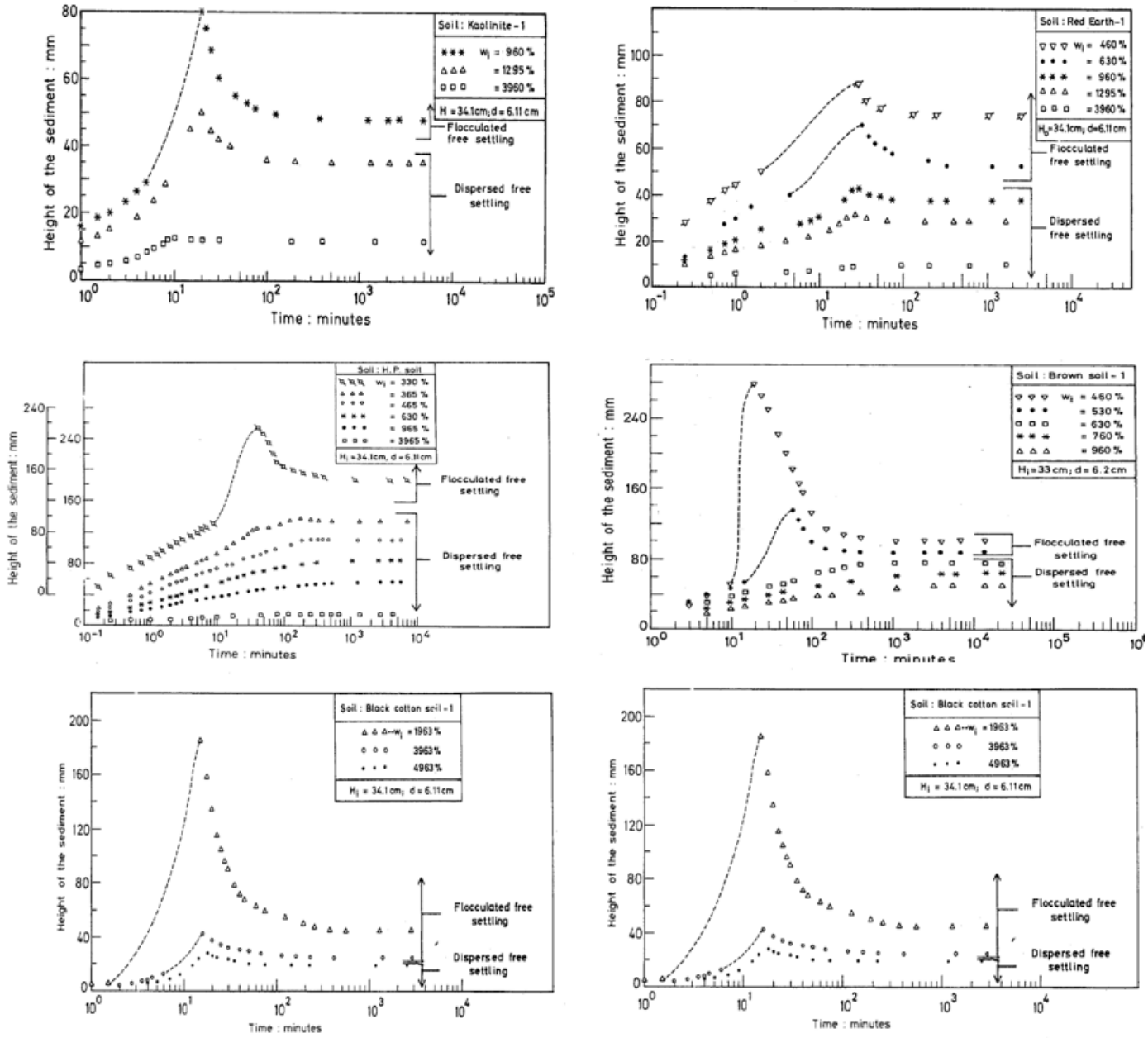

Figure 5.5- Dispersed free settling for different soil compositions,

Sridharan & Prakash (2001a)

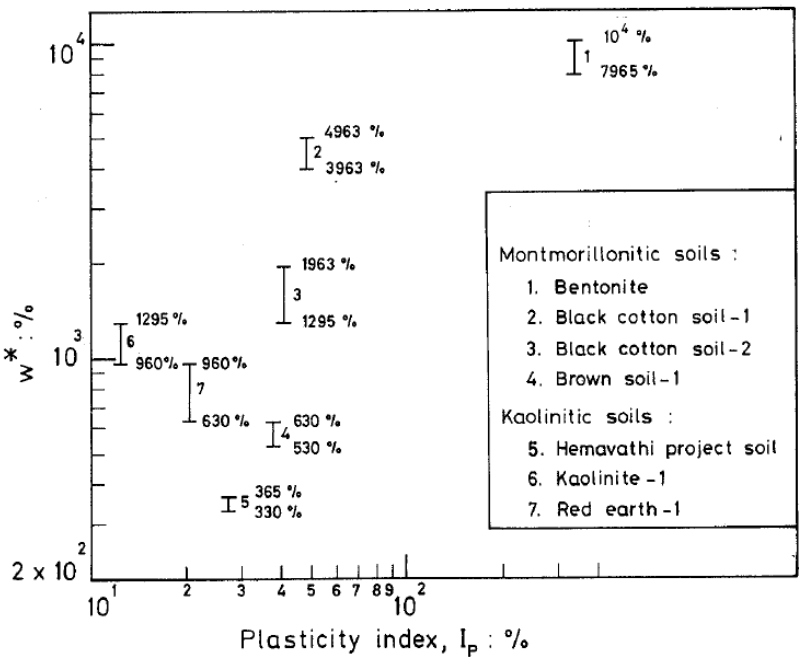

Figure 5.6- Relationship between critical water content and plasticity index, Sridharan and Prakash (2001a)

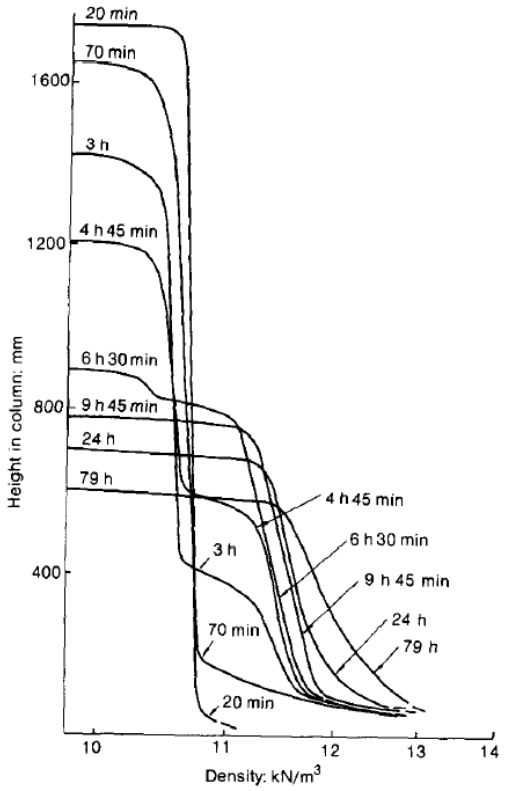

Figure 5.7- Density profiles of sedimented sample at initial water content of approximately 650% water content, Been & Sills (1981)

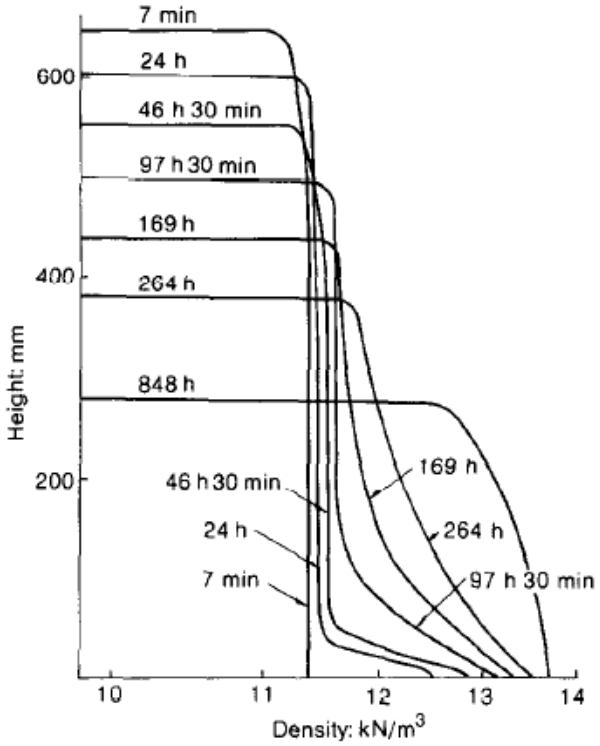

Figure 5.8- Density profiles of sedimented sample at initial water content of approximately 380% water content, Been & Sills (1981)

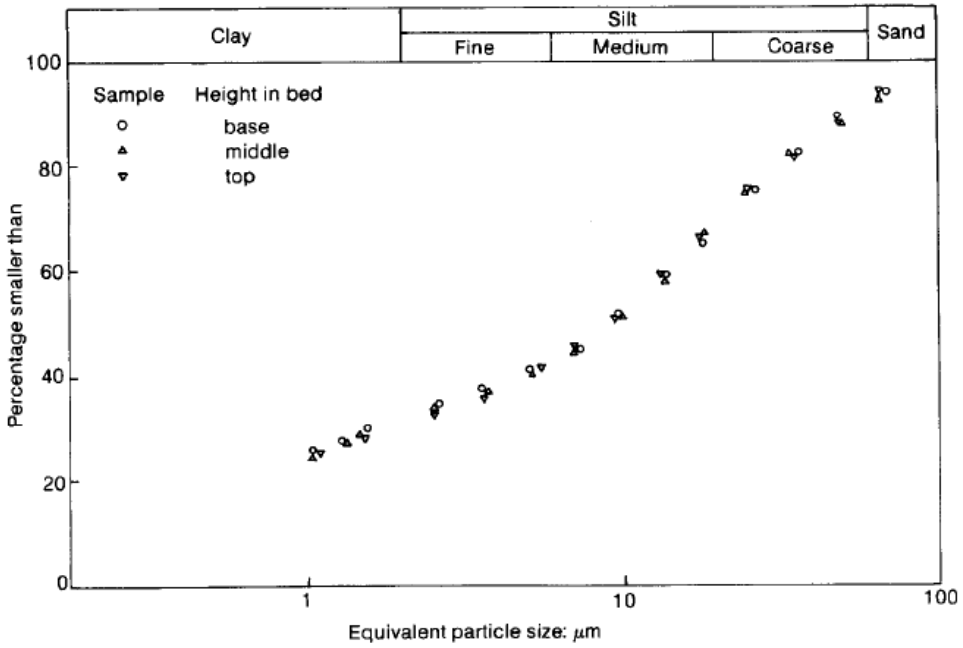

Figure 5.9- Particle size distribution of a sedimented sample at initial water content of approximately 250% water content, Been & Sills (1981)

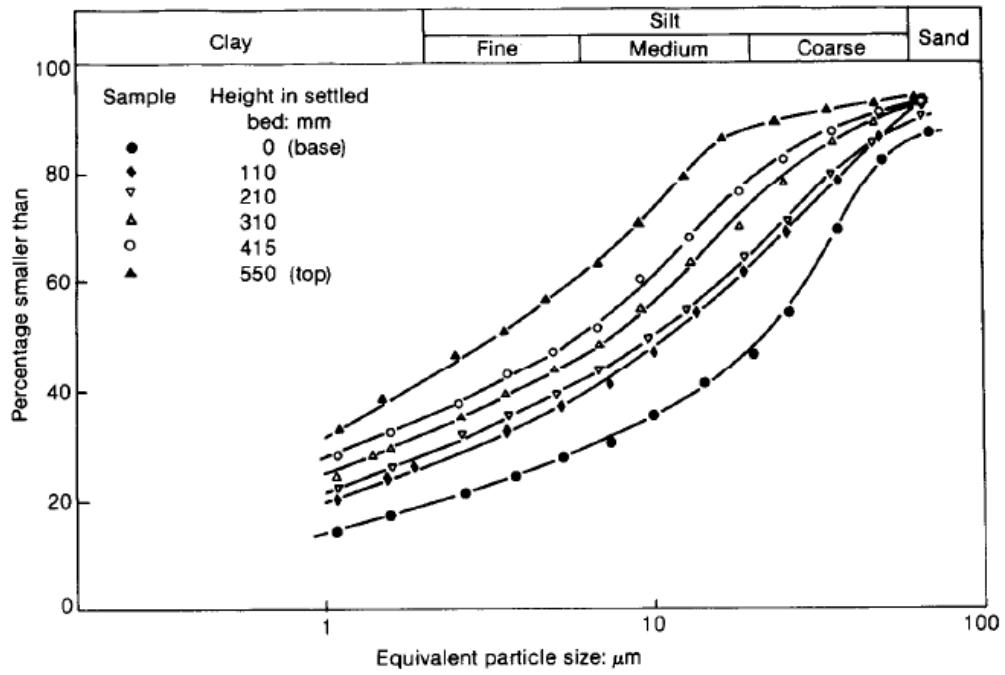

Figure 5.10- Particle size distribution of a sedimented sample at initial water content of approximately 650% water content, Been & Sills (1981)

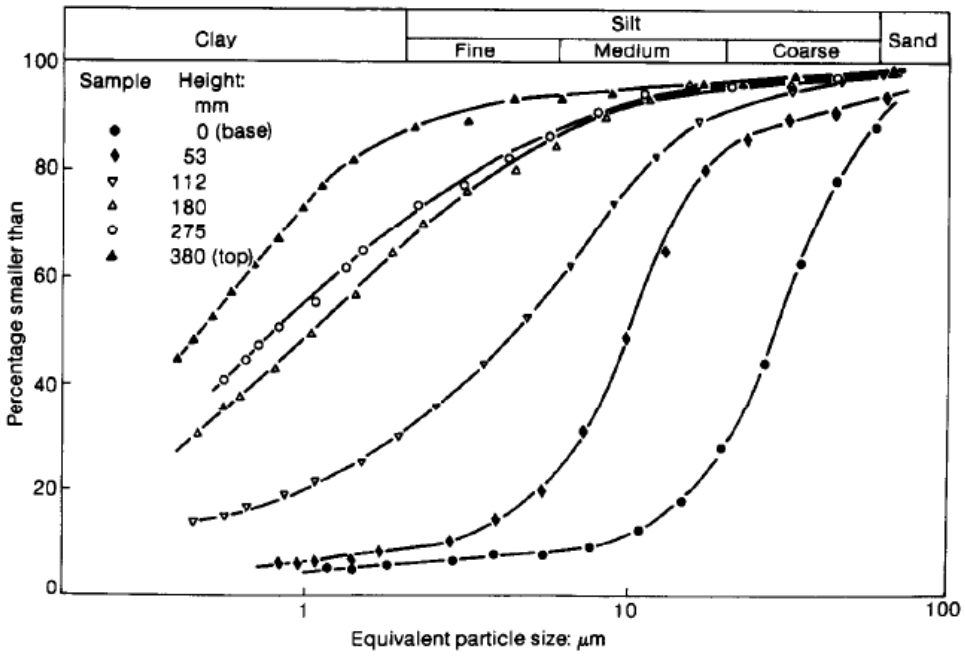

Figure 5.11- Particle size distribution of a sedimented sample at initial water content of approximately 1300% water content and added dispersing agent, Been & Sills (1981)

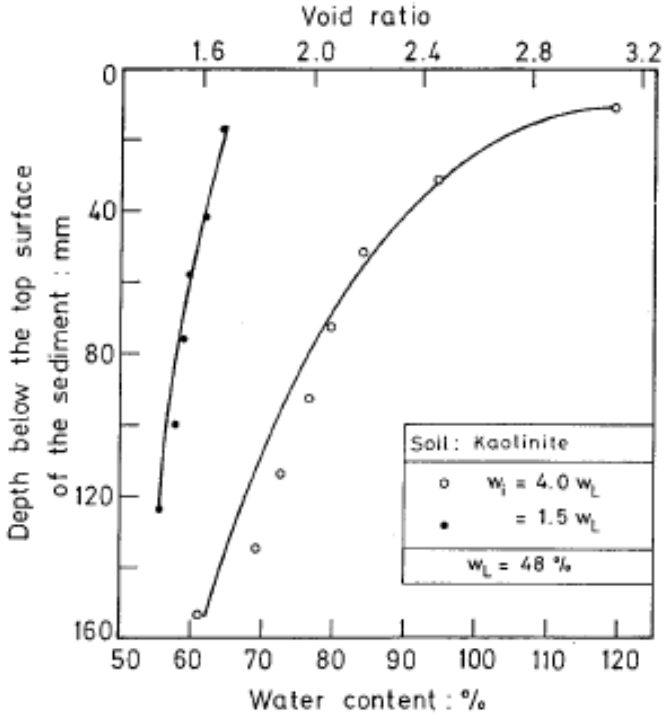

Figure 5.12- Variation in voids ratio with depth for kaolinite, Sridharan& Prakash (2001b)

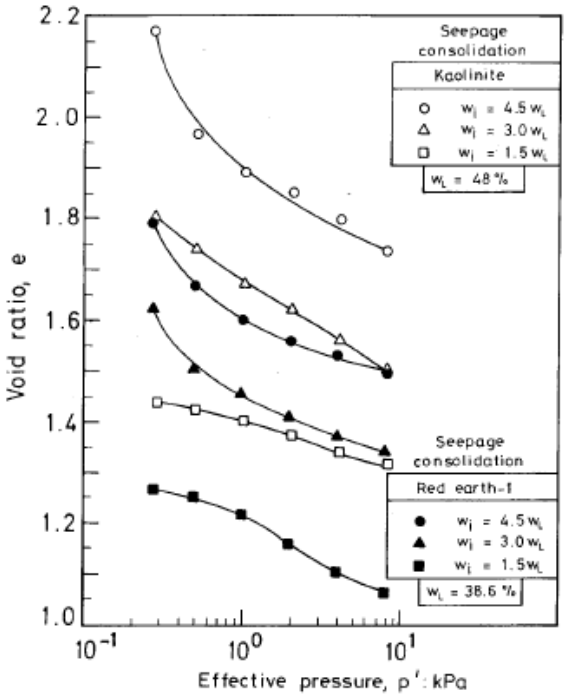

Figure 5.13- Relationship between Initial water content and compressibility, Sridharan & Prakash (2001b)

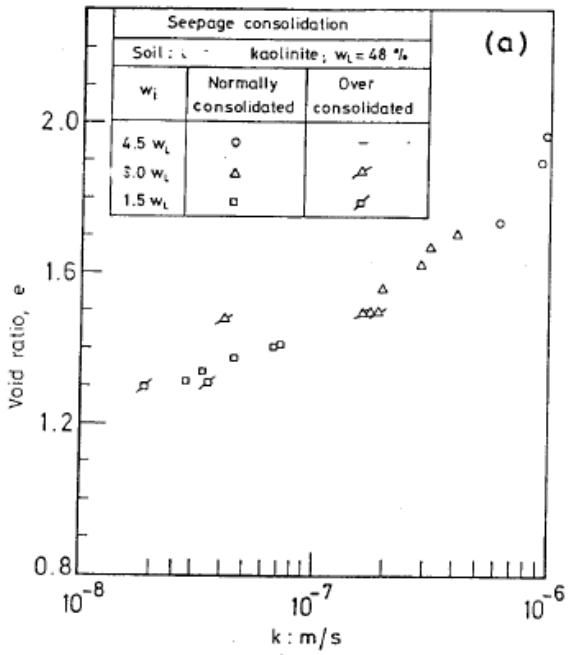

Figure 5.14- Relationship between void ratio and permeability for samples sedimented at different water contents, Sridharan & Prakash (2001b)

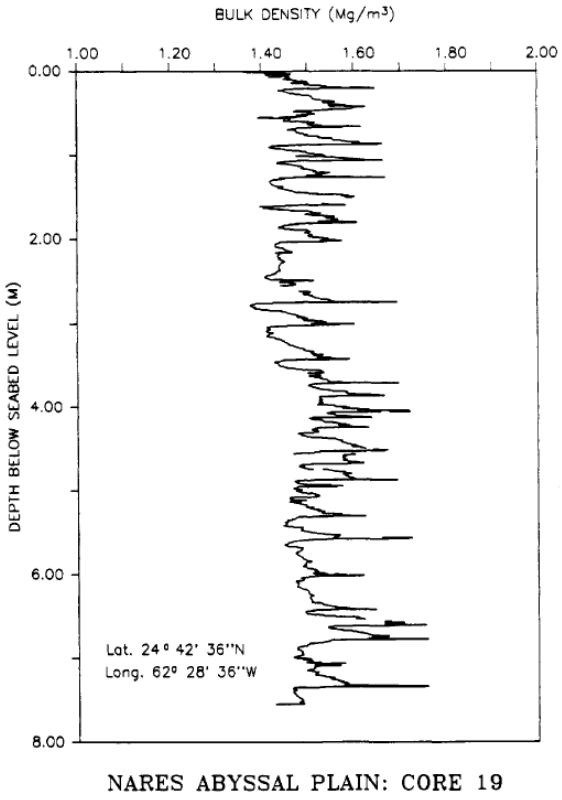

Figure 5.15- Density profile of first 7.5m of the Nares Abyssal Plain, Edge & Sills (1989)

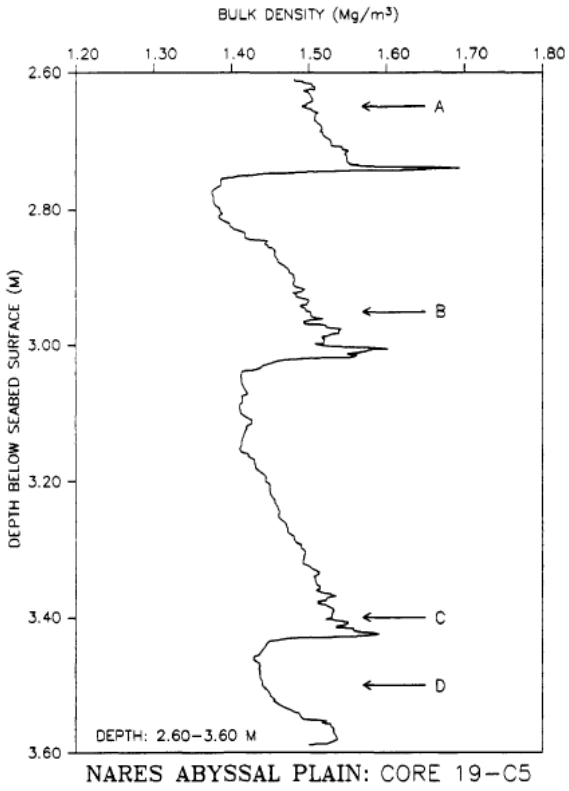

Figure 5.16- Magnified density profile of 2.6-3.6m of the Nares Abyssal Plain, Edge & Sills (1989)

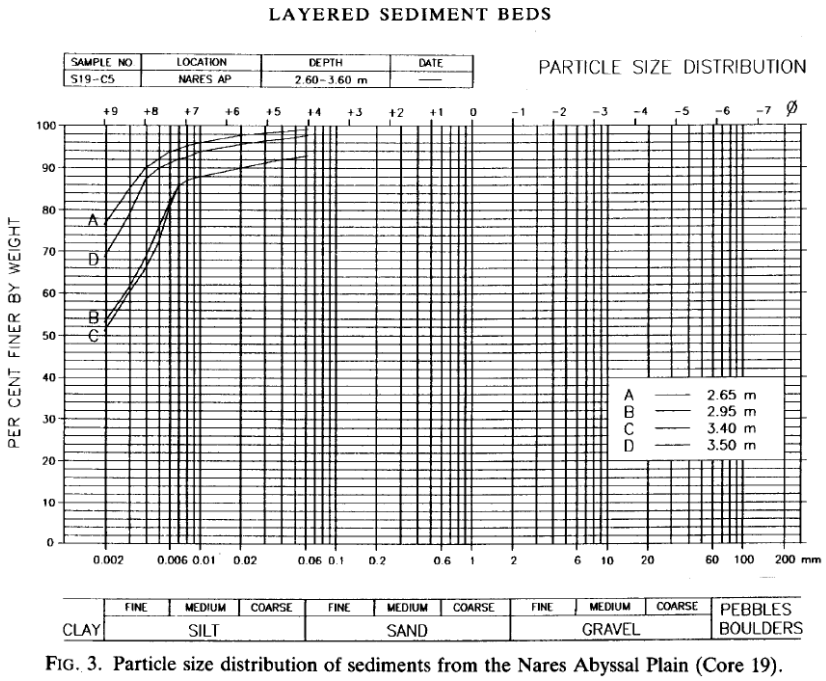

FIG. 3. Particle size distribution of sediments from the Nares Abyssal Plain (Core 19).

Figure 5.17- Particle size distribution of discrete points from the 2.6-3.6m of the Nares Abyssal Plain, Edge & Sills (1989)

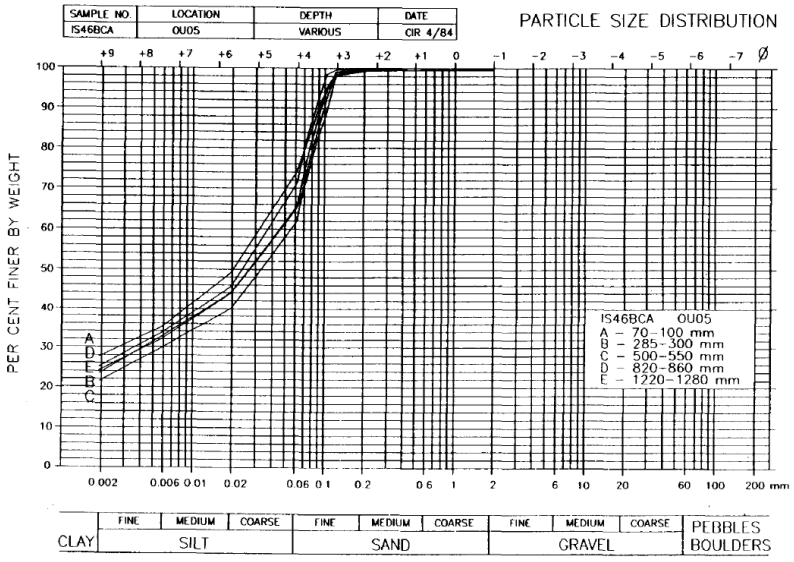

Figure 5.18- Particle size distribution of samples collected 10km offshore from Sellafield, Edge & Sills (1989)

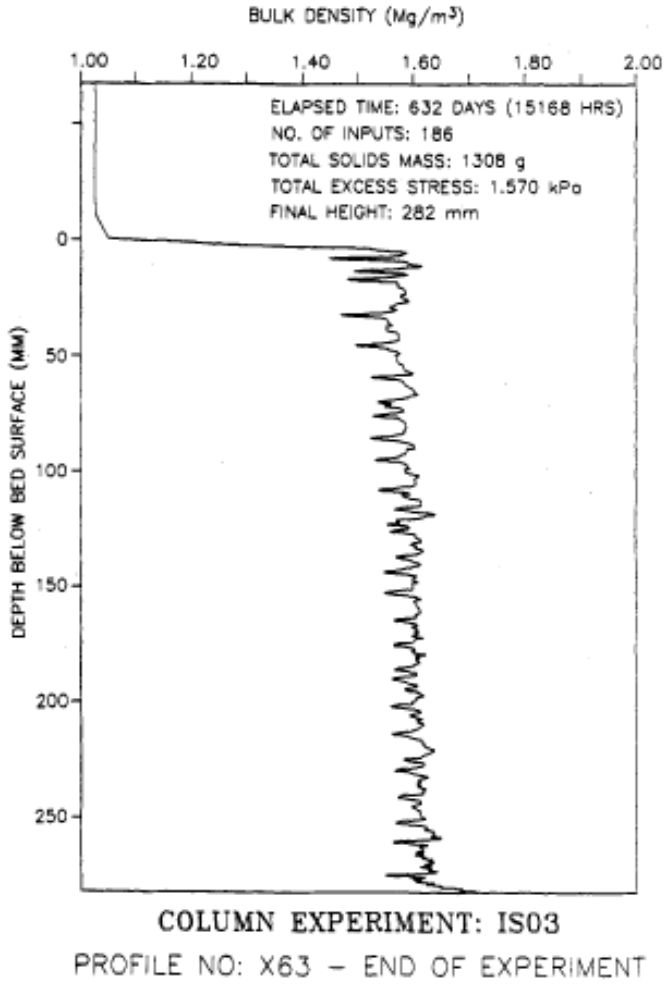

Figure 5.19-Density profiles at the end of laboratory sedimentation, Edge & Sills (1989)

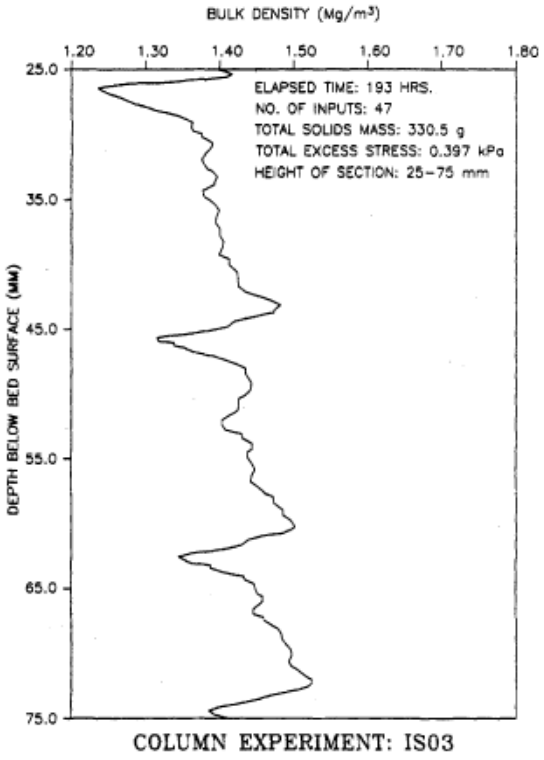

Figure 5.20- Magnified density profiles at the end of laboratory sedimentation, Edge & Sills (1989)

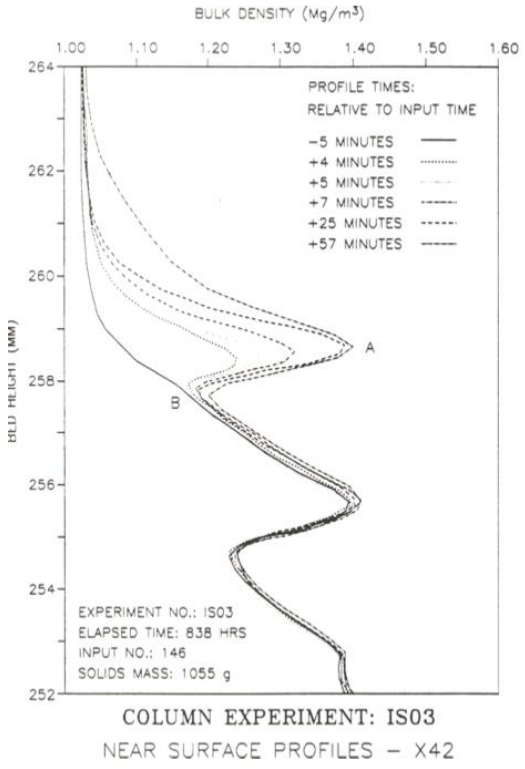

Figure 5.21- Development sediment bed (first input of the day), Edge & Sills (1989)

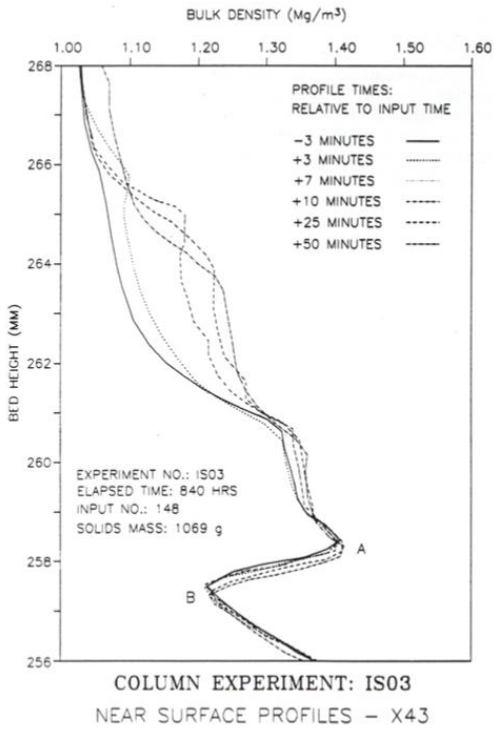

Figure 5.22- Development sediment bed (third input of the day), Edge & Sills (1989)

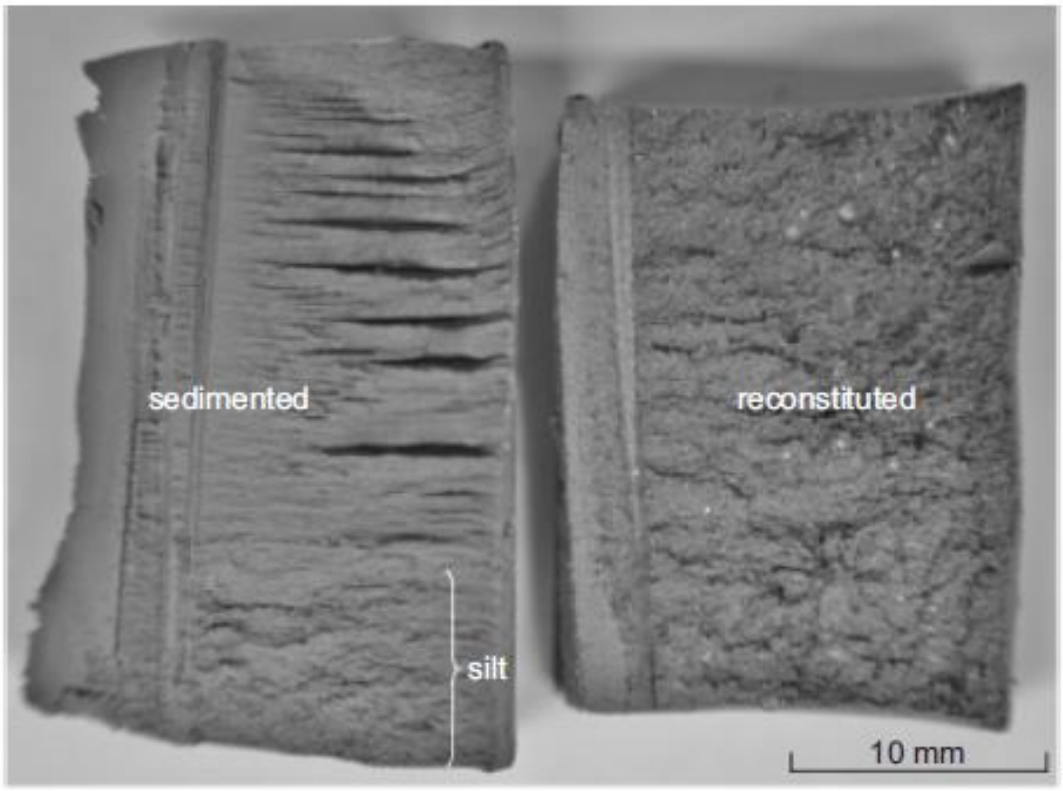

Figure 5.23- Visual difference between sedimented and reconstituted samples, Stallebrass et al. (2007)

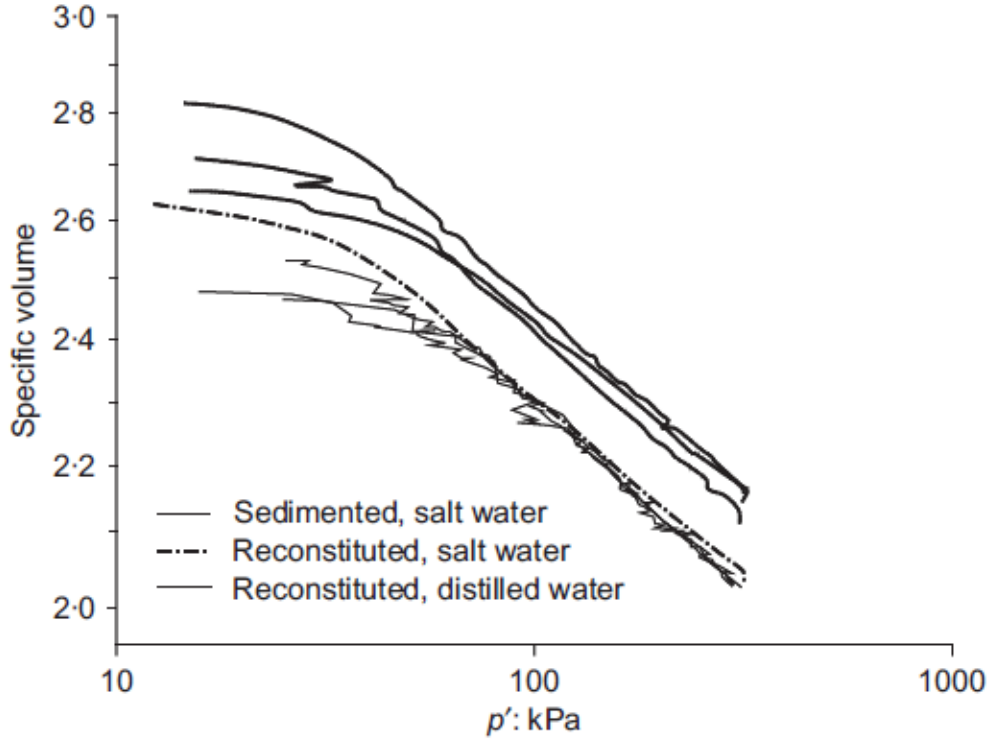

Figure 5.24- Compression curves of laboratory sedimented and reconstituted samples, after Mašín et al. (2003)

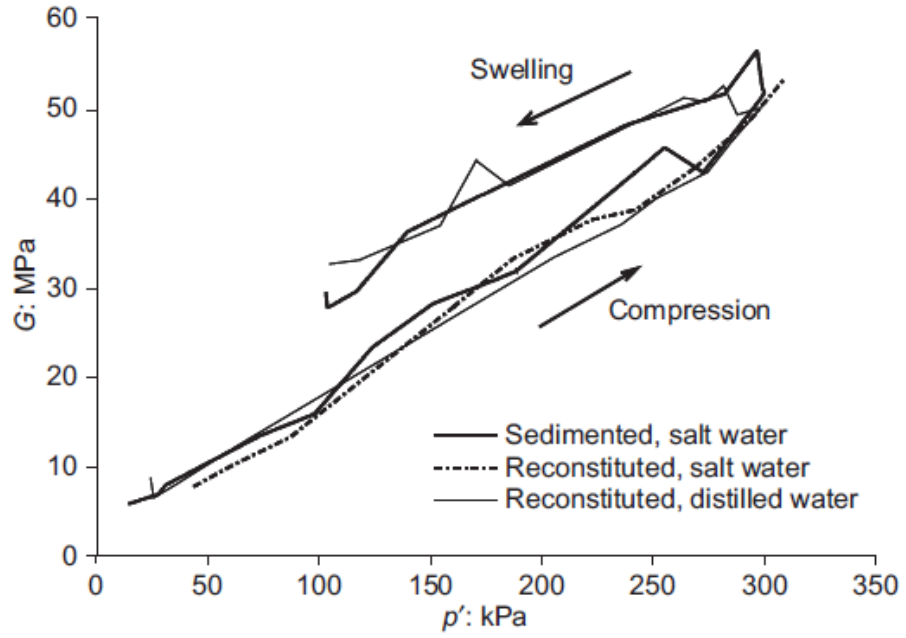

Figure 5.25- Shear stiffness obtained from bender element tests, Stallebrass et al. (2007)

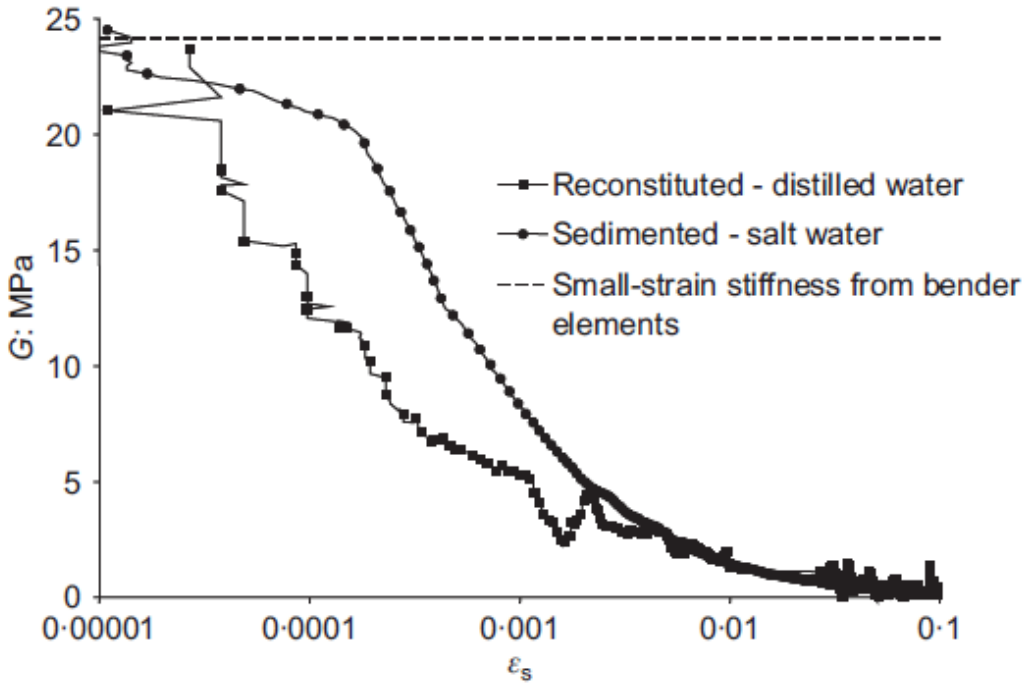

Figure 5.26- Variation of shear stiffness with strain during constant p' extension, Stallebrass et al. (2007)

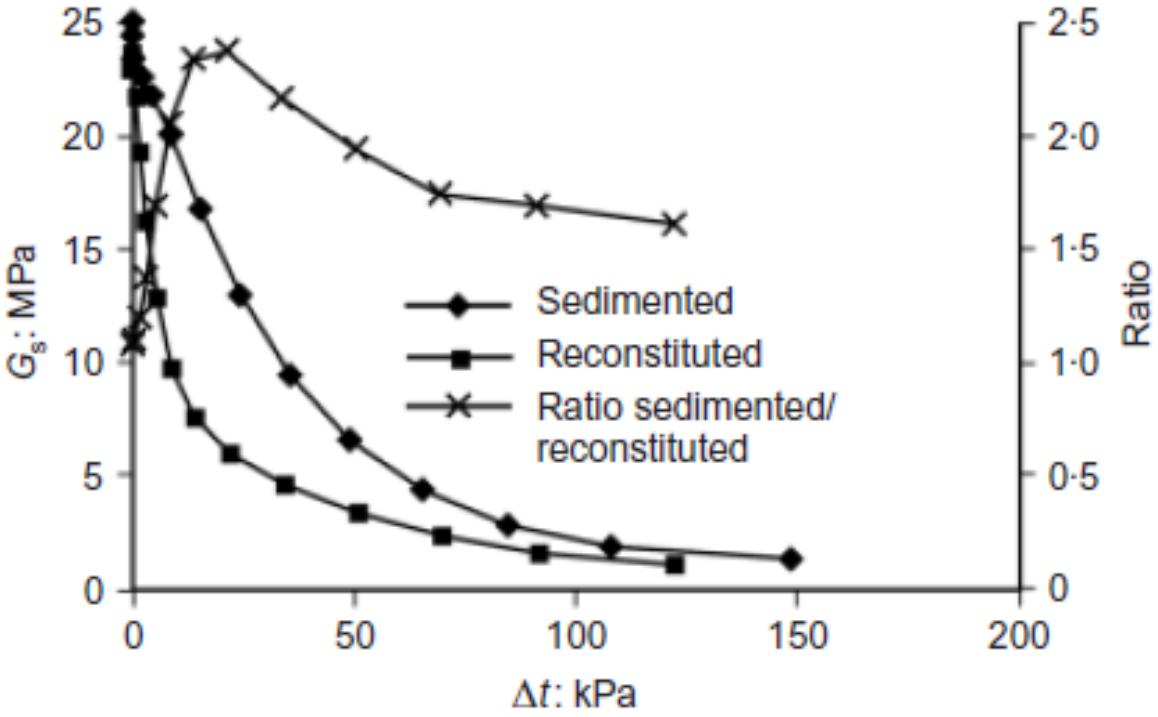

Figure 5.27- Secant moduli for the same stress change, after Stallebrass et al. (2007)

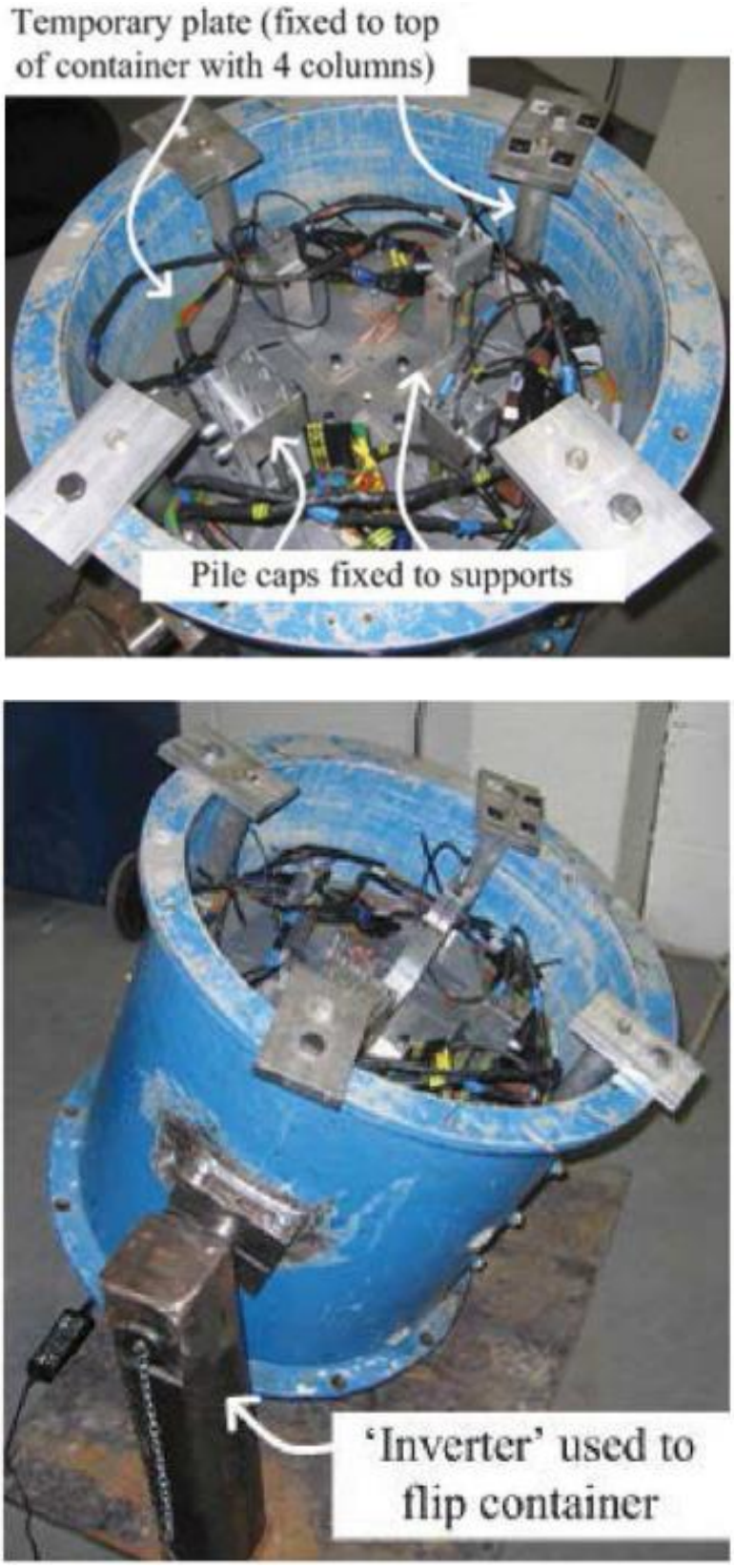

Figure 5.28-Model inverter, Marshall et al. (2014)

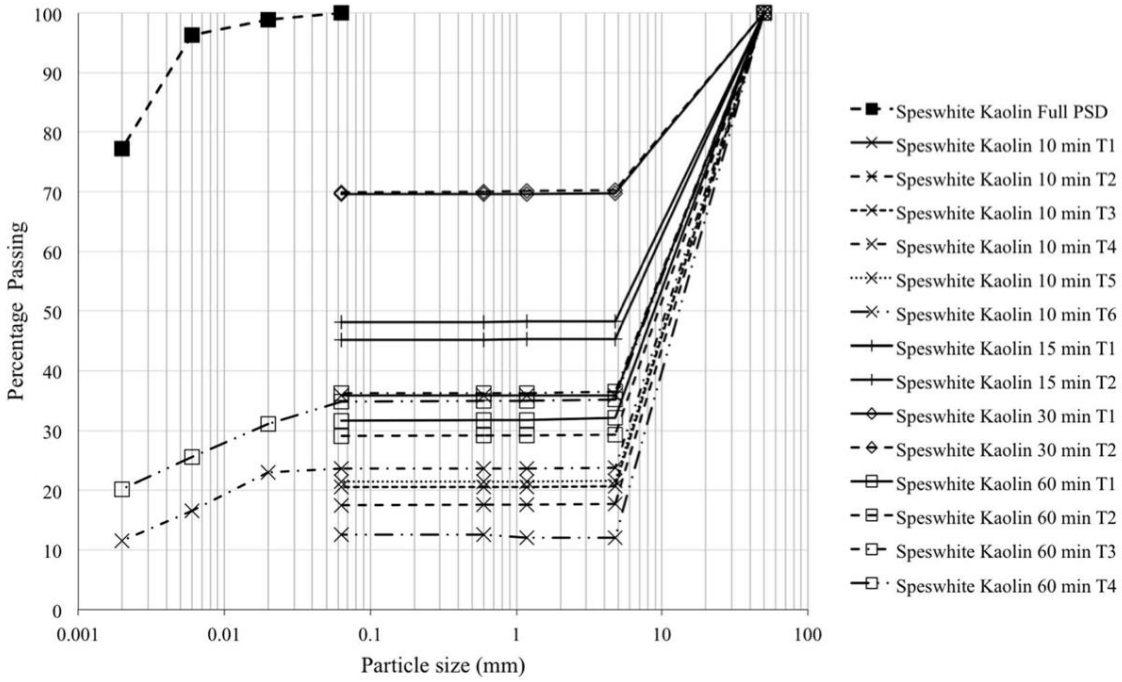

Figure 5.29- Kaolin clay particle size distribution after different mixing times, Phillips et al. (2014)

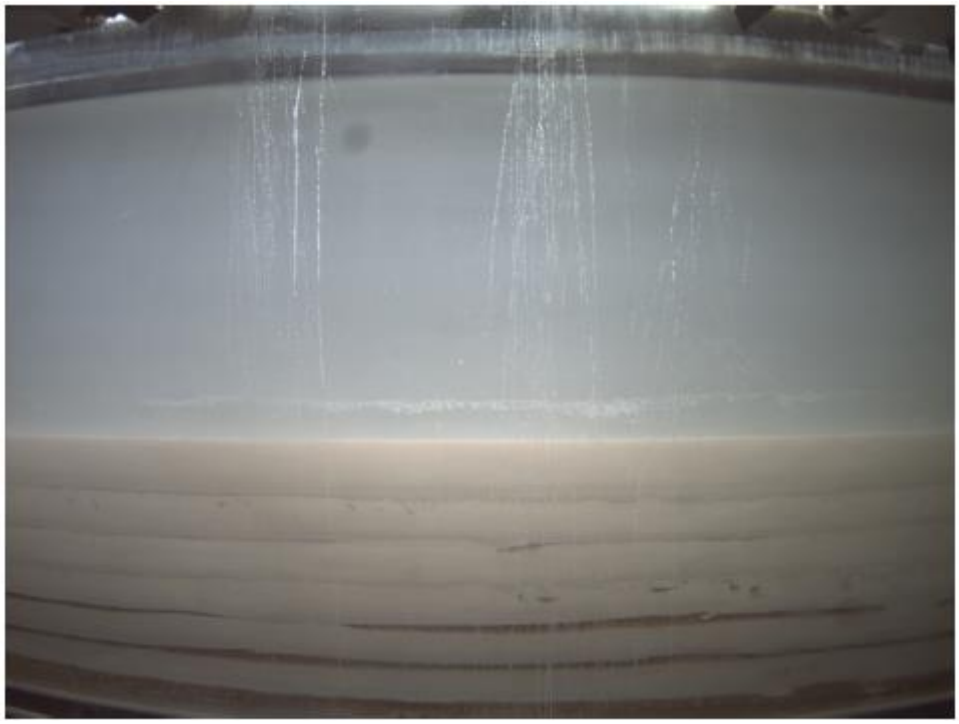

Figure 5.30- Layers created during inflight sedimentation, Singh (2017)

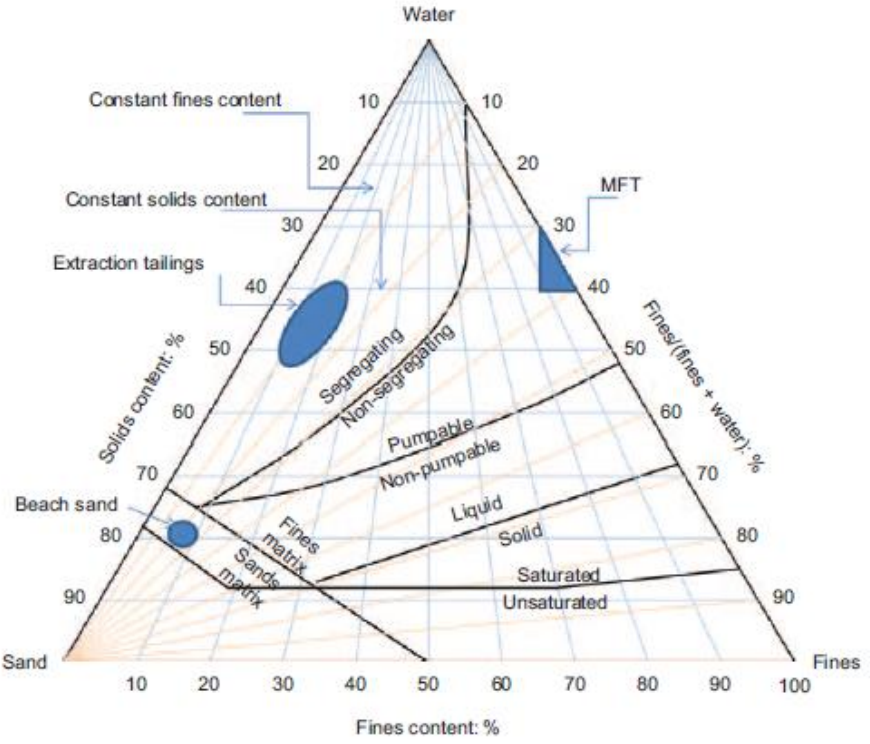

Figure 5.31- Example ternary diagram, Sorta et al. (2012)

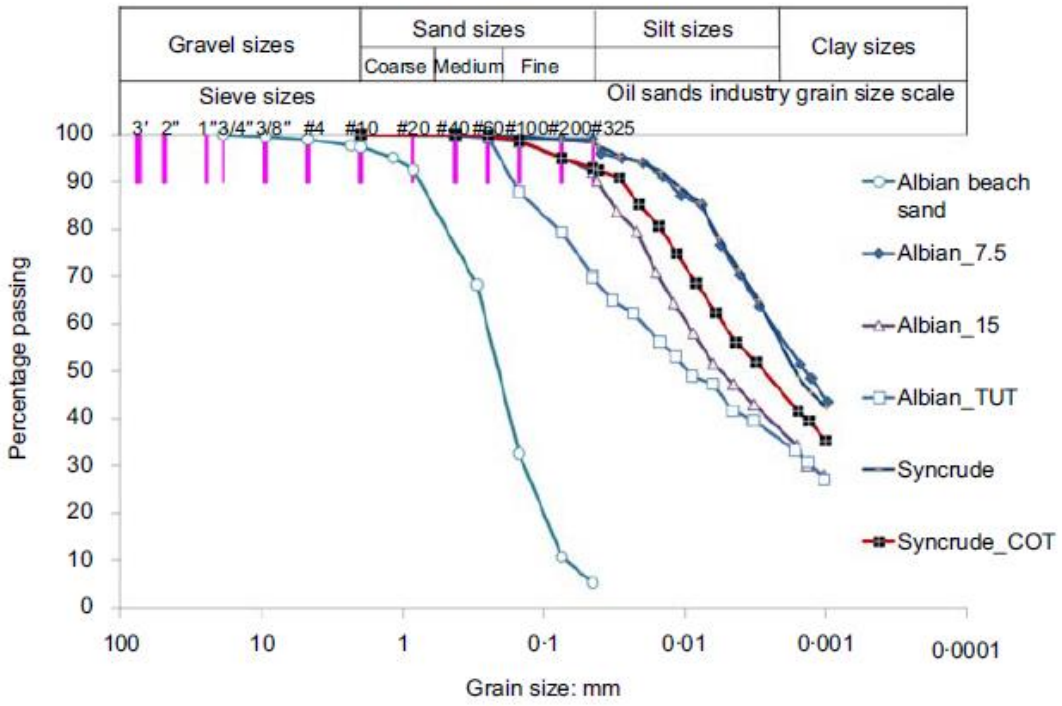

Figure 5.32- Particle size distributions of tailings, Sorta et al. (2012)

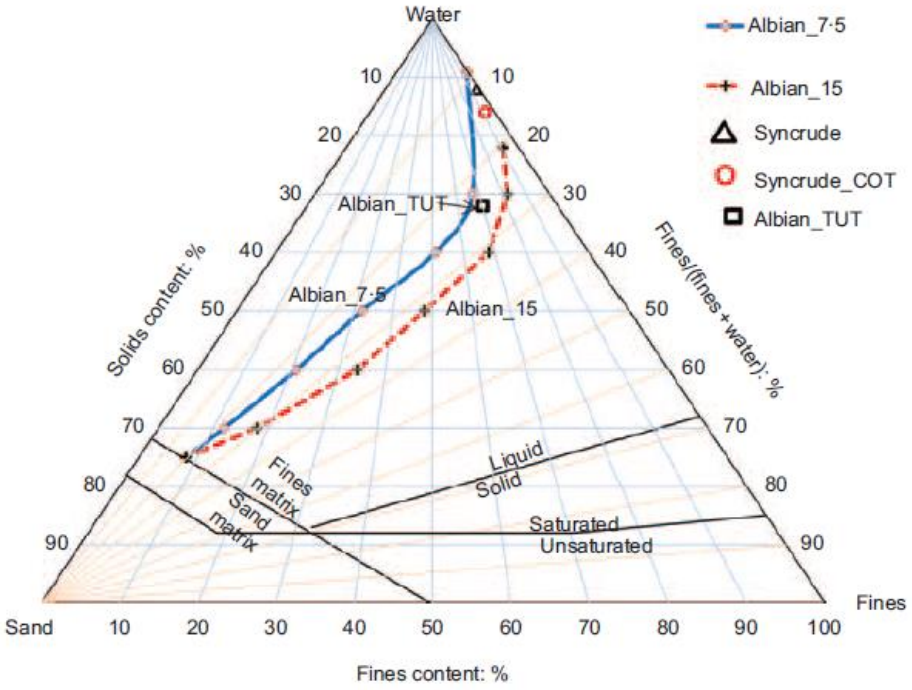

Figure 5.33- Ternary diagram for sedimentation tests at 1G, Sorta et al. (2012)

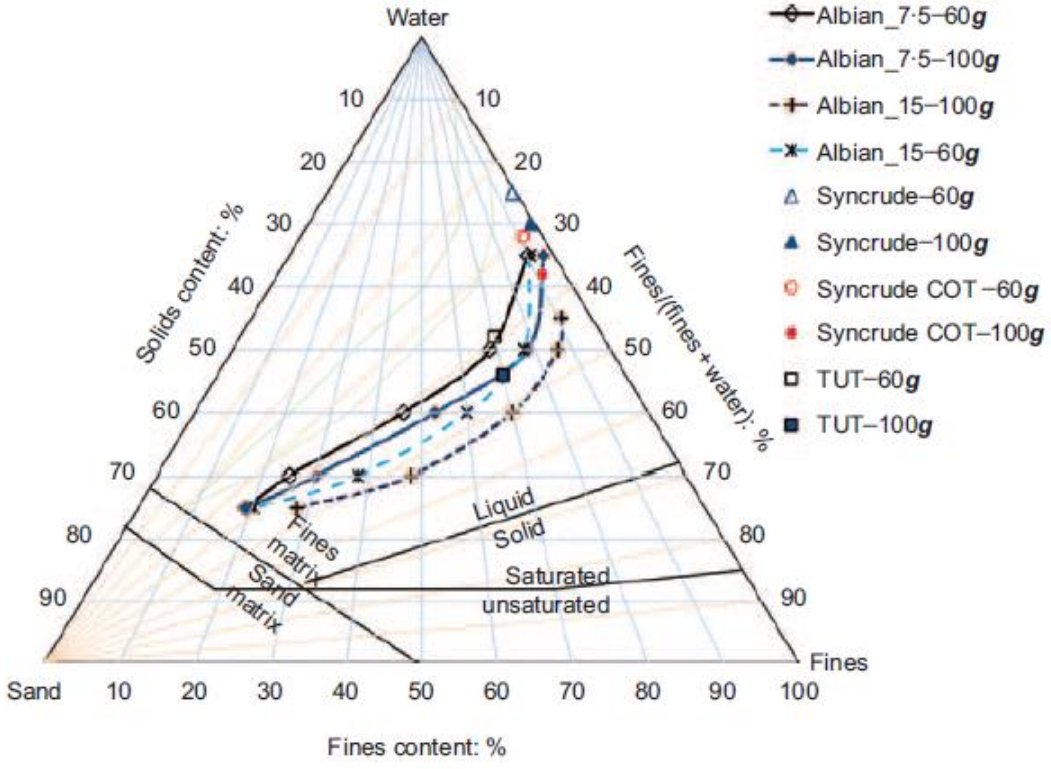

Figure 5.34- Ternary diagram for sedimentation tests in flights, Sorta et al. (2012)

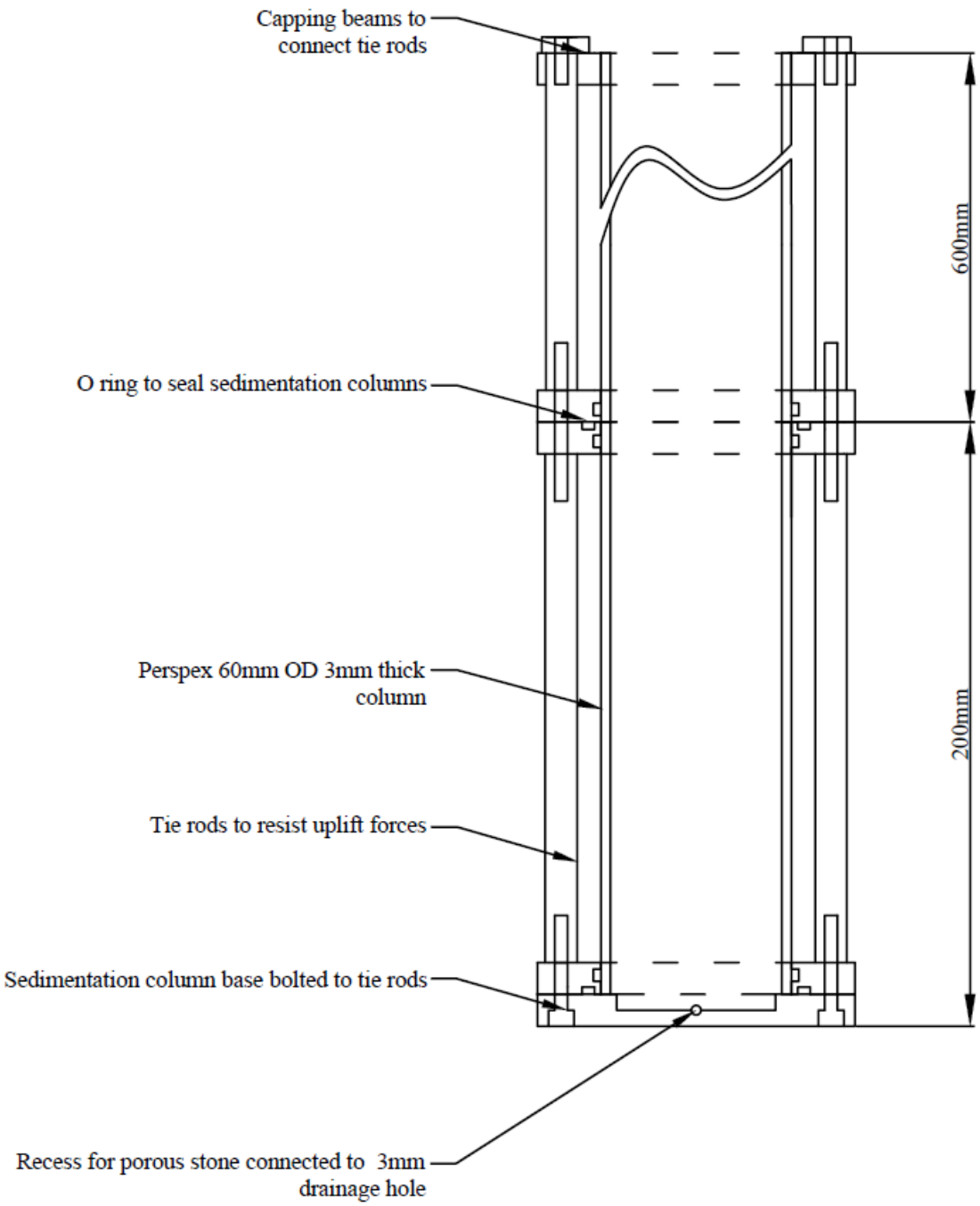

Figure 6.1- Assembly drawing of the sedimentation columns

Figure 6.2- Image of an assembled sedimentation column

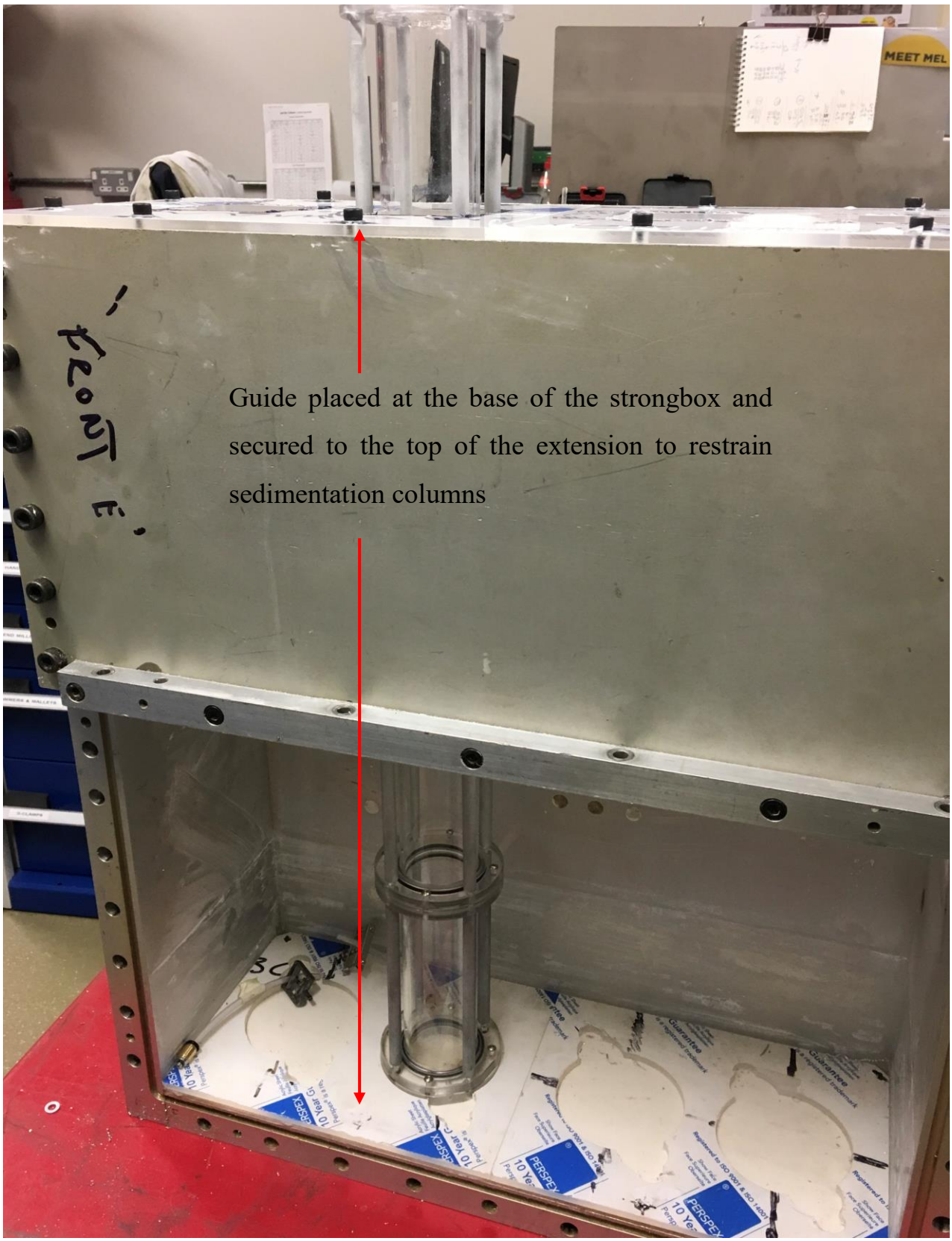

Figure 6.3- Guide secured to the top of the strongbox to keep the sedimentation columns vertical during

Figure 6.4- Falling head permeameter set up

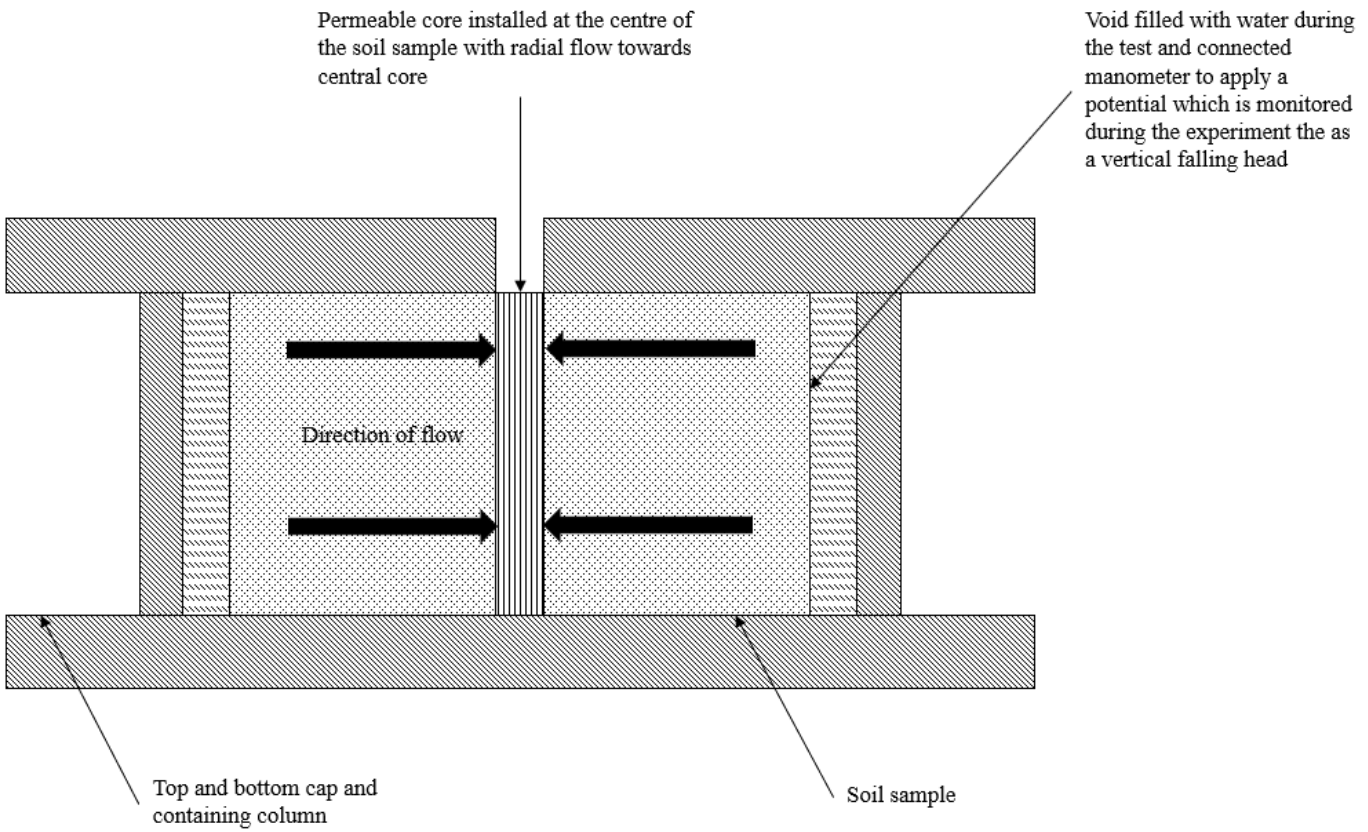

Figure 6.5- Schematic of the principle for the horizontal permeameter

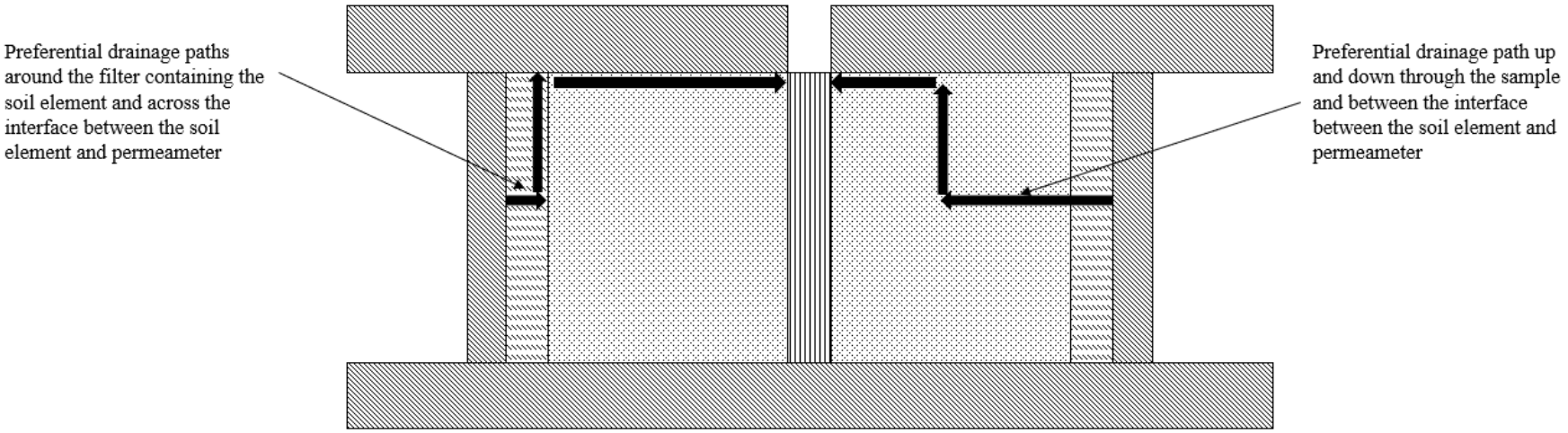

Figure 6.6- Schematic of potential drainage paths in preliminary tests

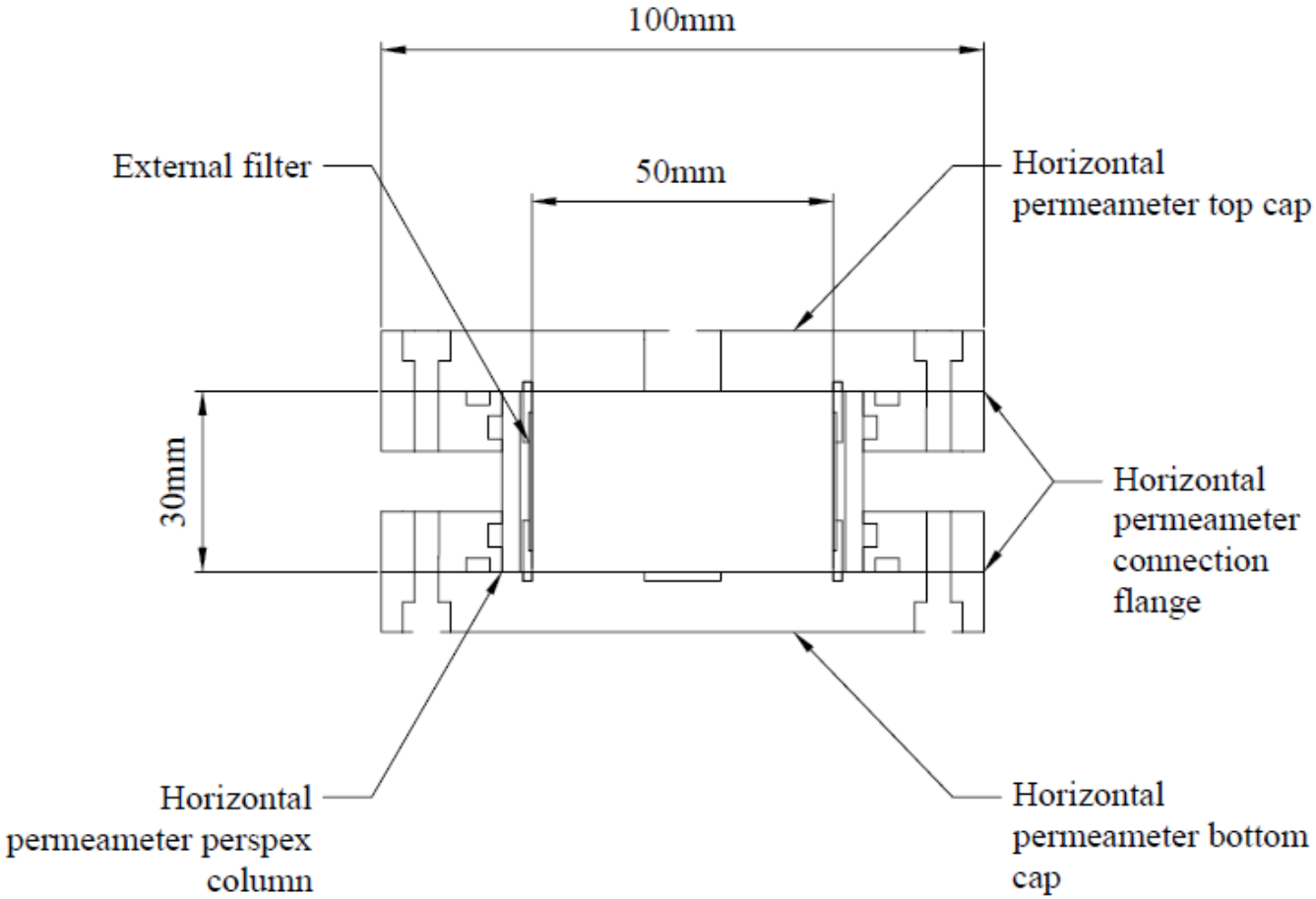

Figure 6.7- Assembly drawing of the horizontal permeameter

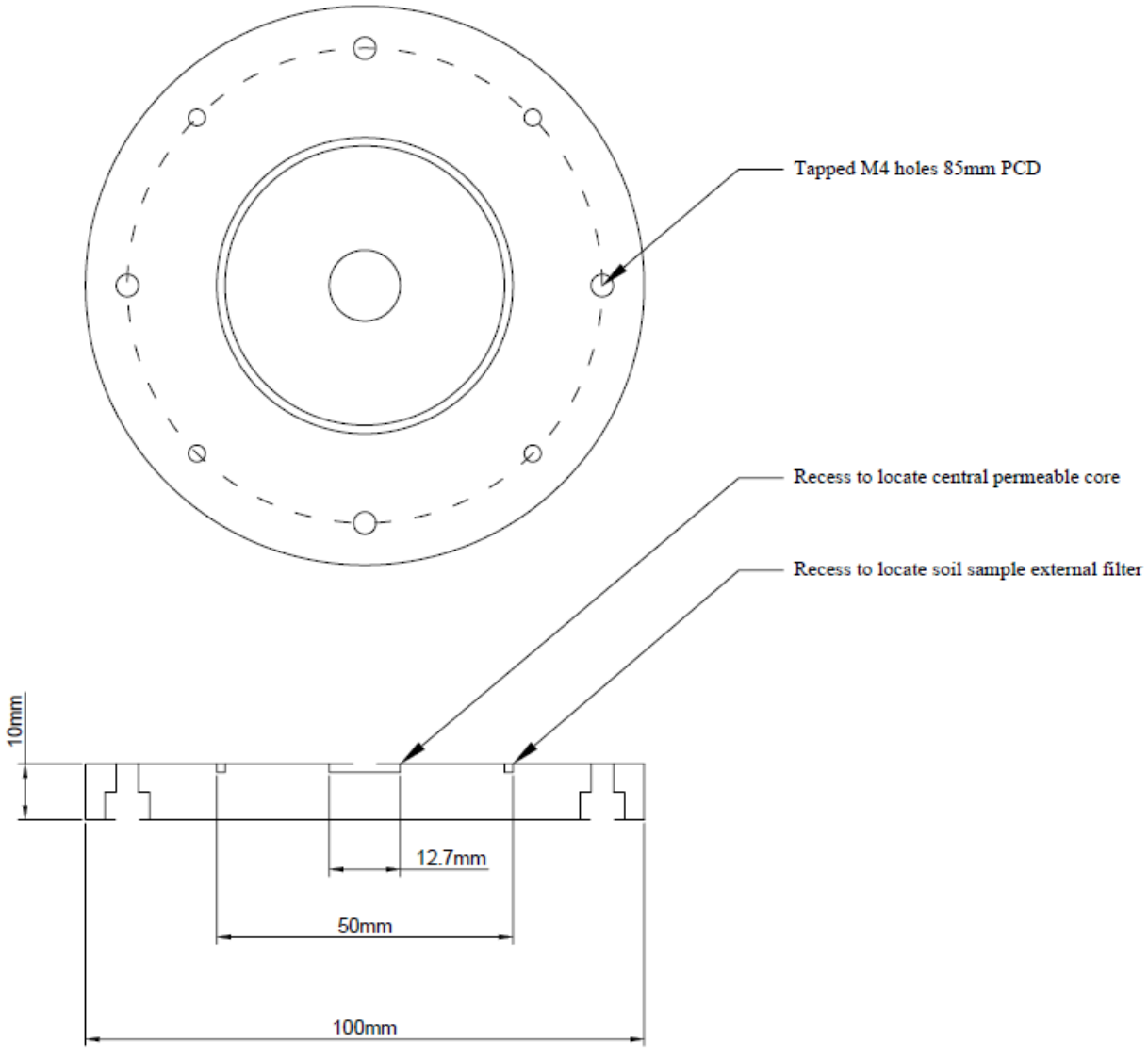

Figure 6.8- Horizontal permeameter bottom cap detail

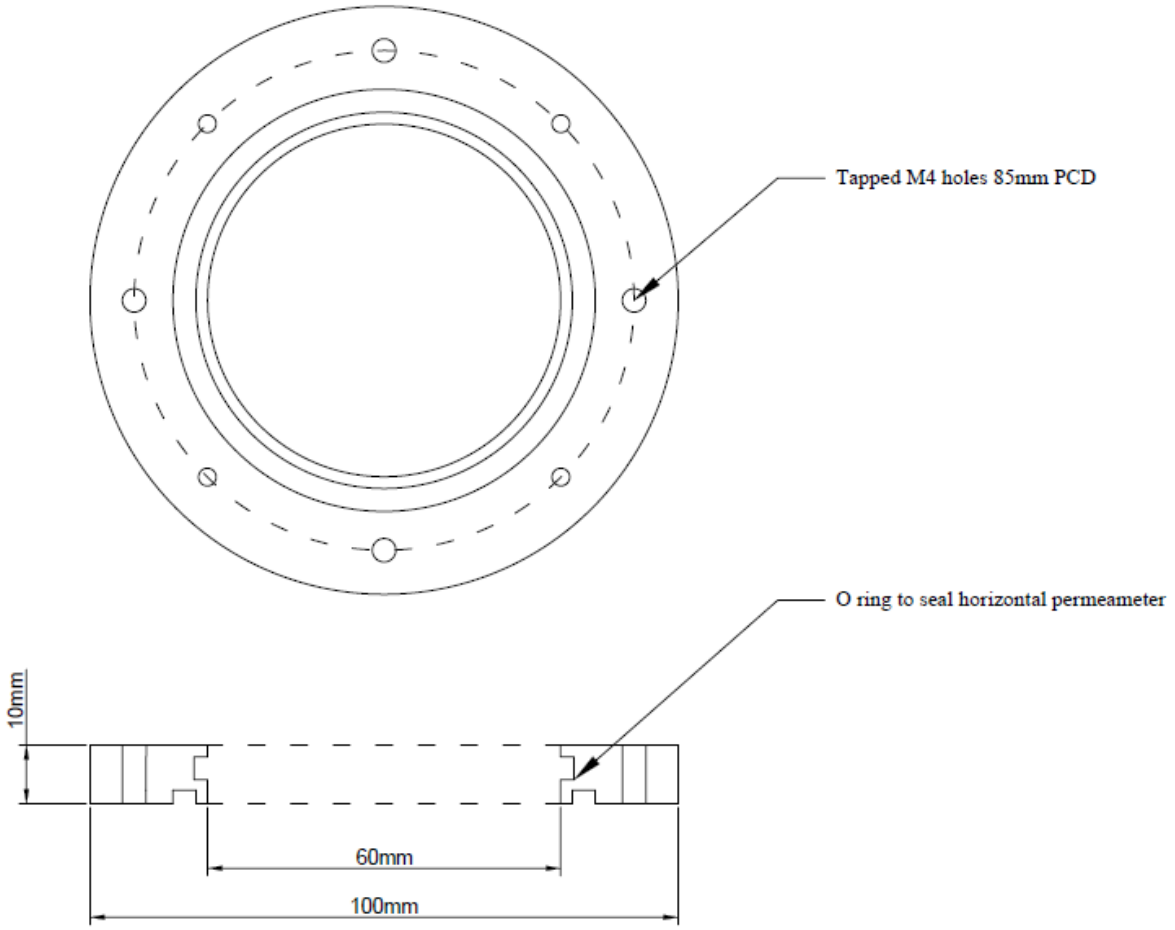

Figure 6.9- Horizontal permeameter flange detail

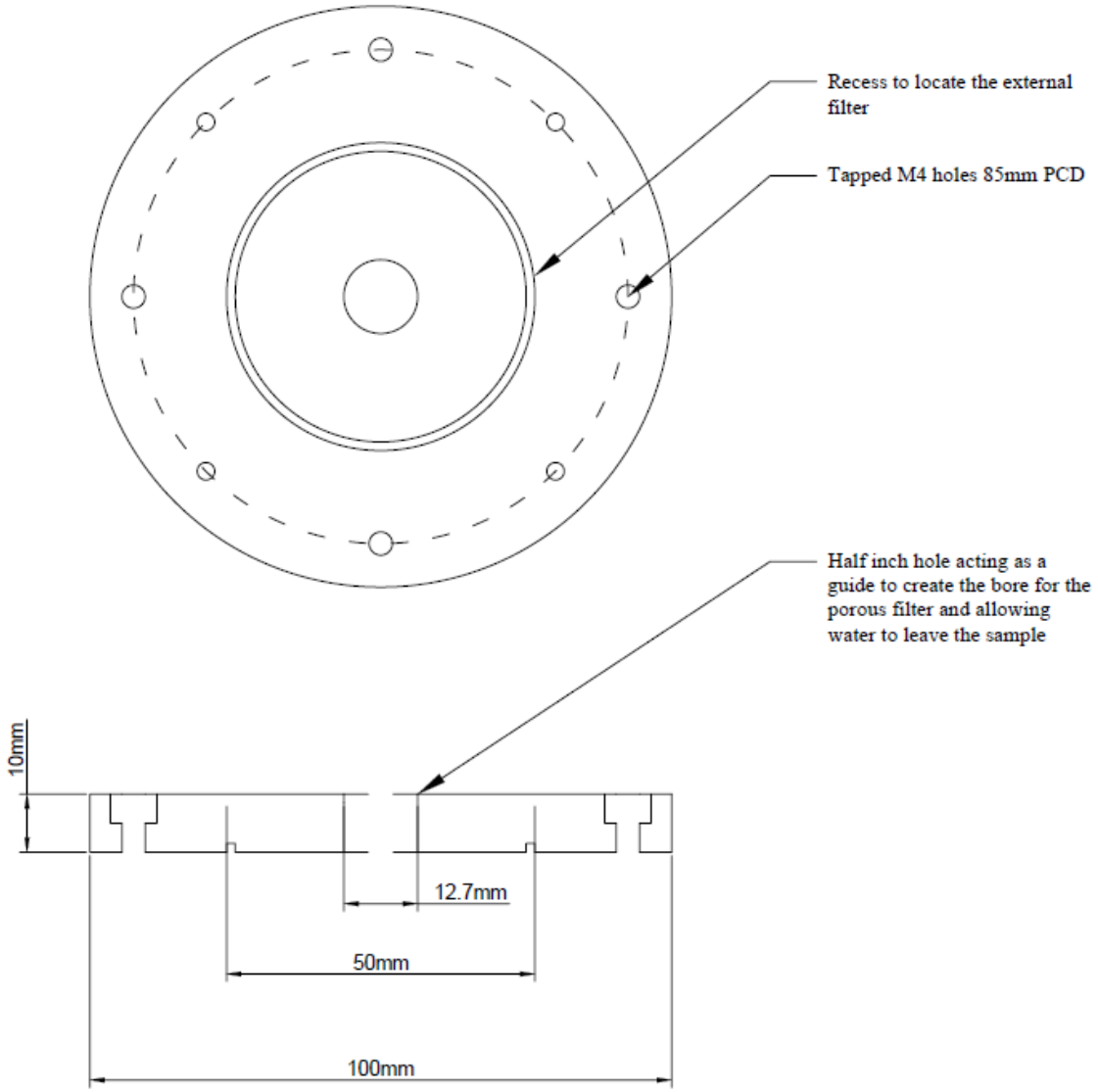

Figure 6.10- Horizontal permeameter top cap detail

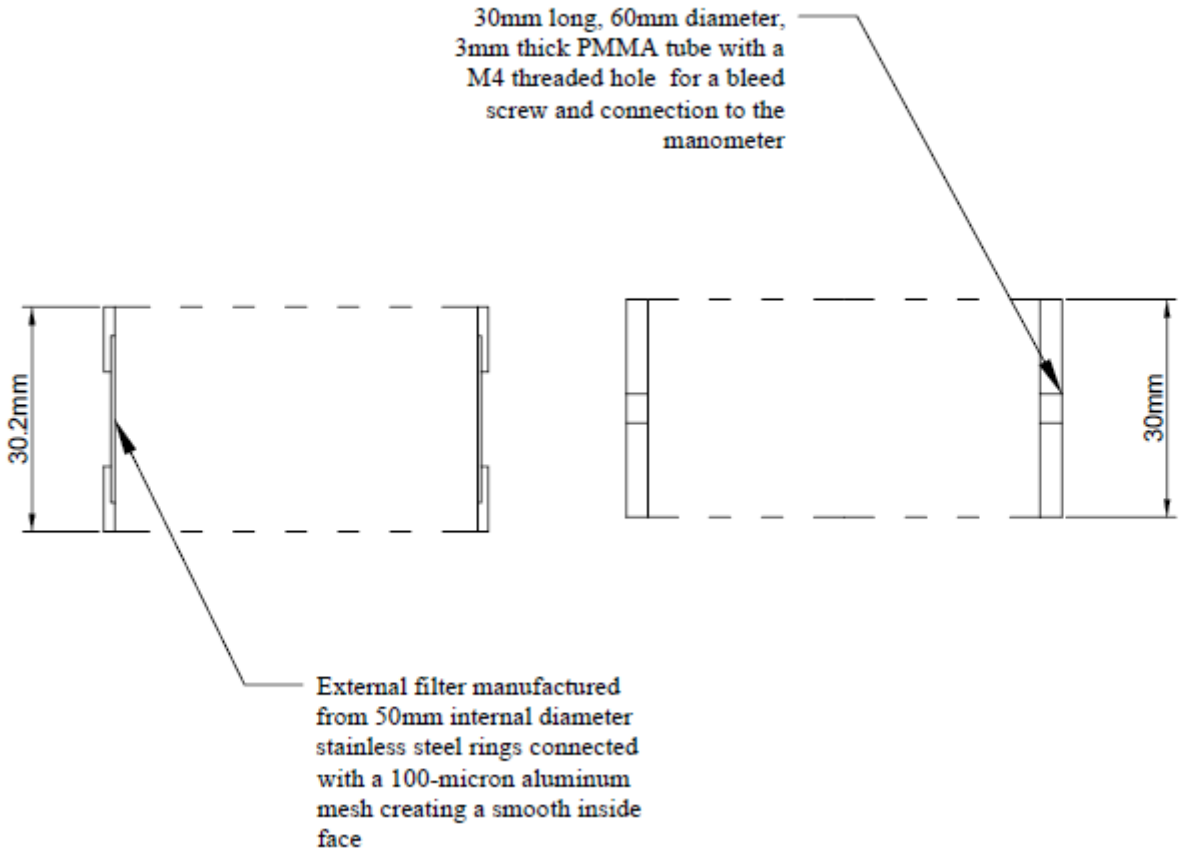

Figure 6.11- Details of PMMA column and external filter

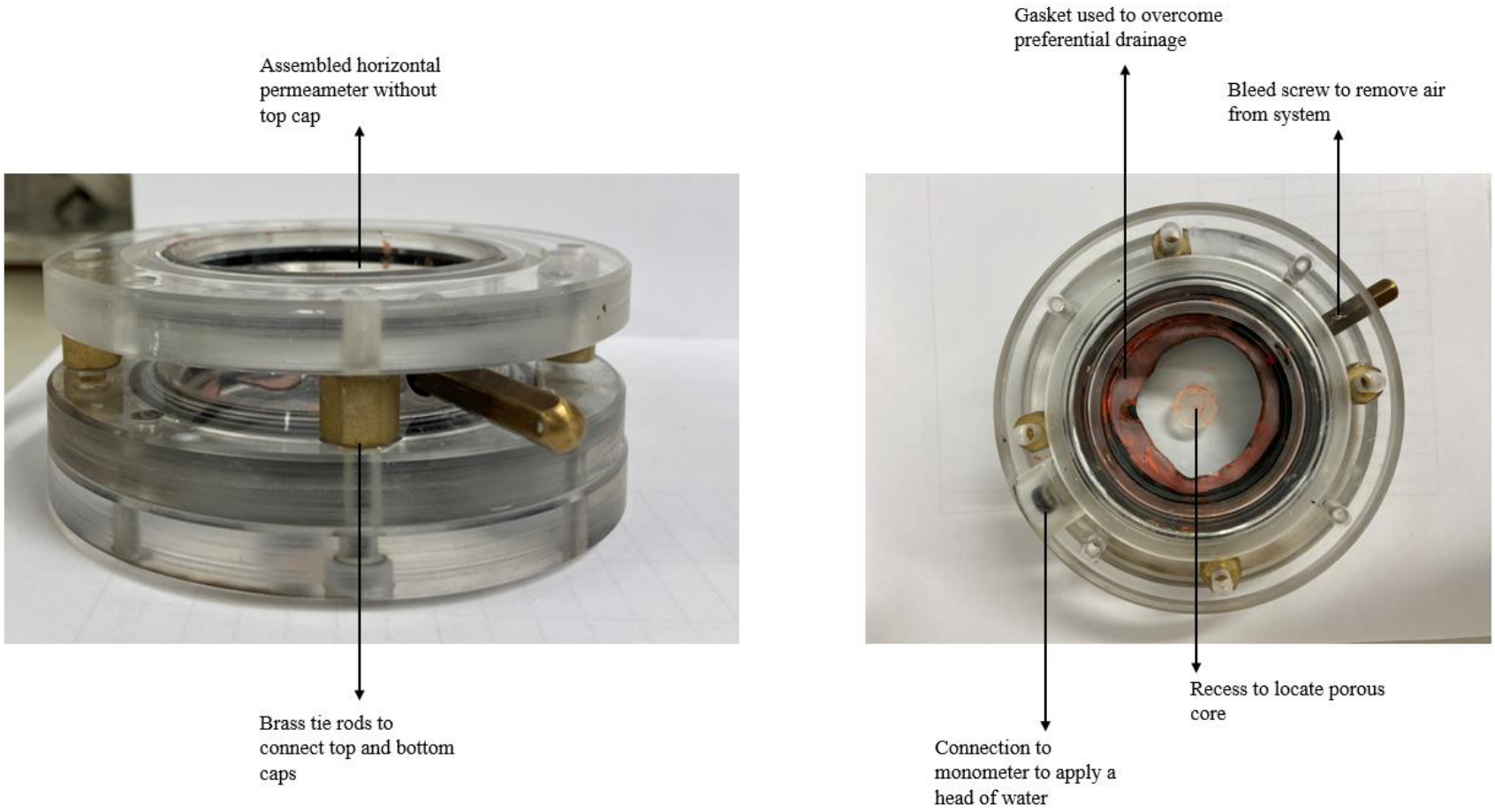

Figure 6.12 – Images of horizontal permeameter components

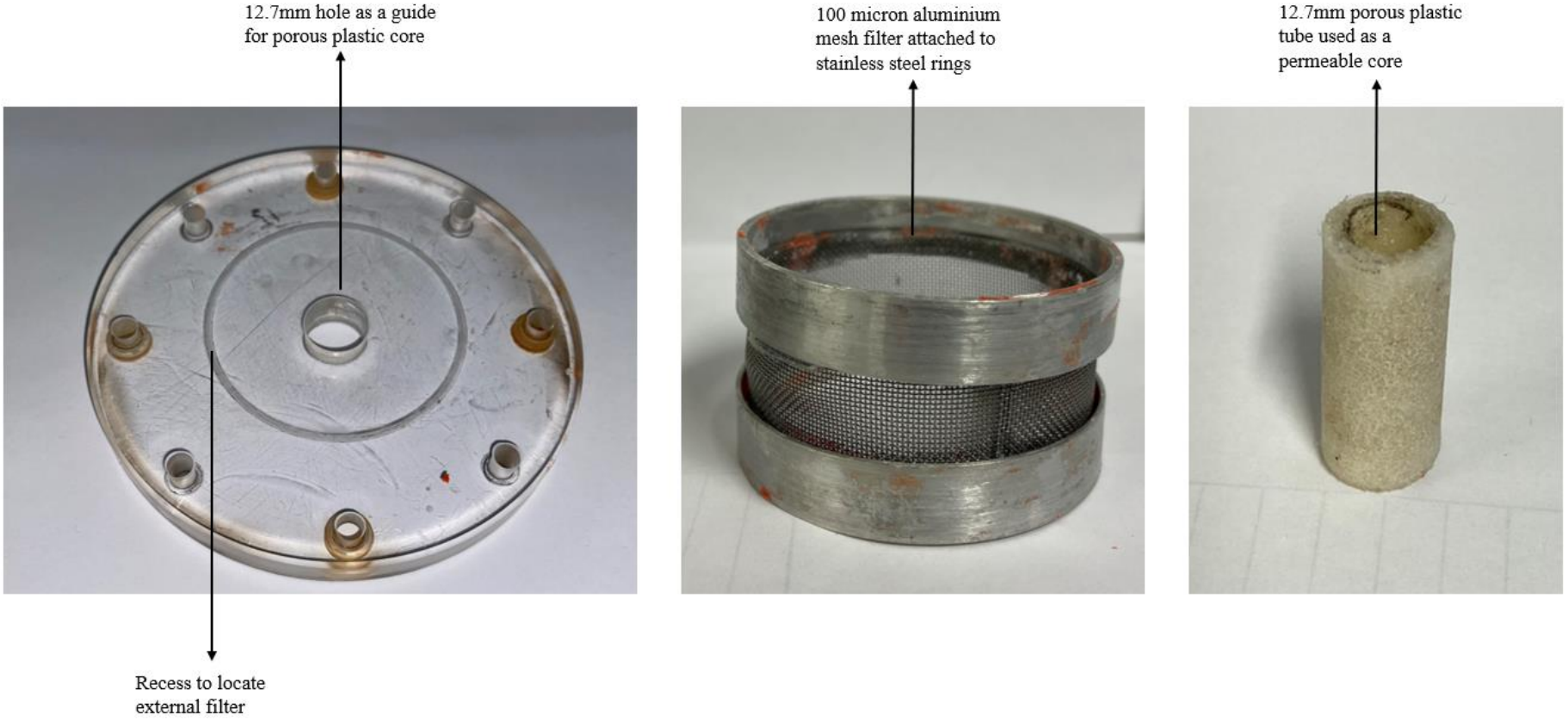

Figure 6.13 – Images of horizontal permeameter components

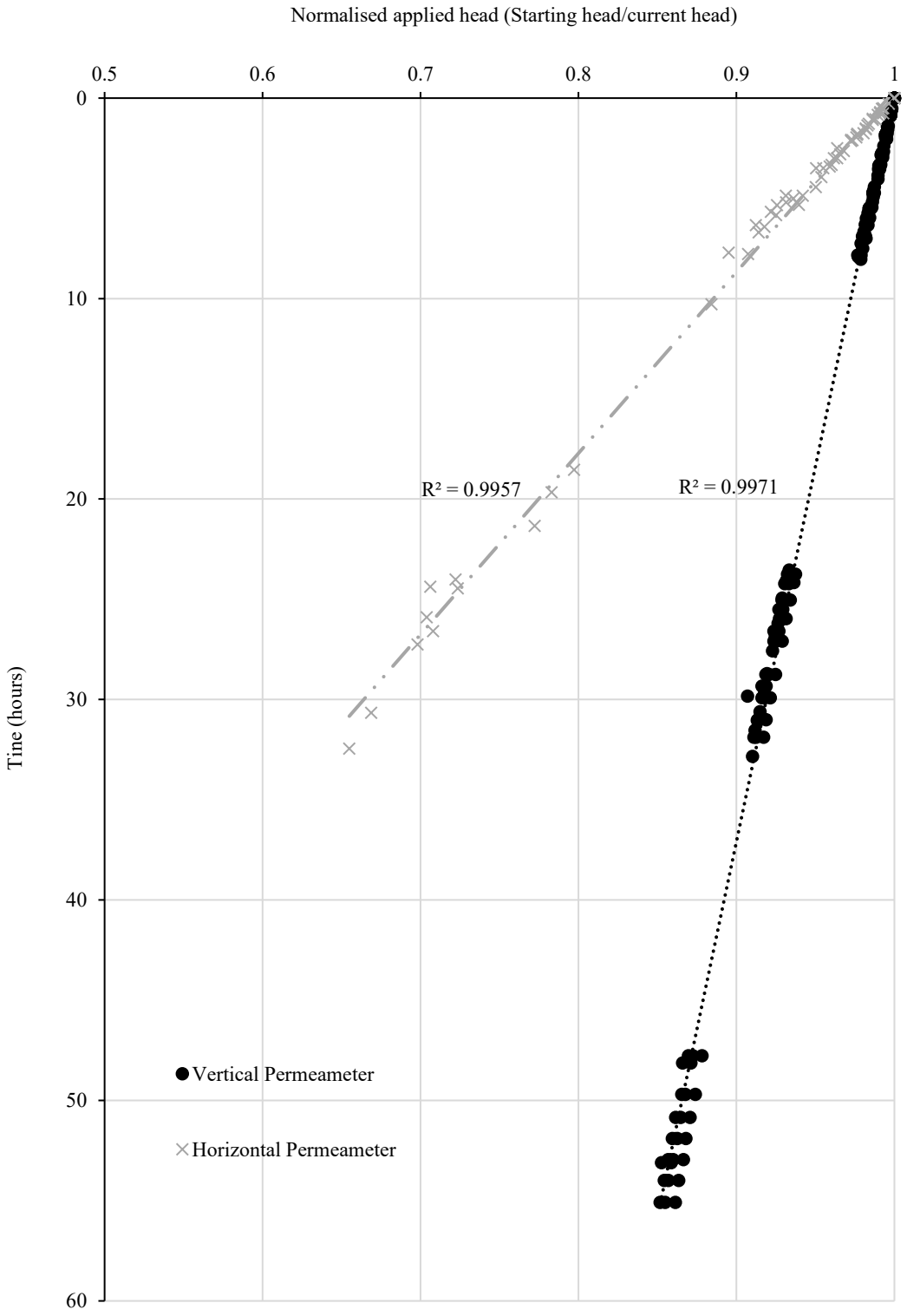

Figure 6.14 – Normalised applied head vs time comparison for vertical and horizontal permeameter

Figure 6.15- Oedometer equipment

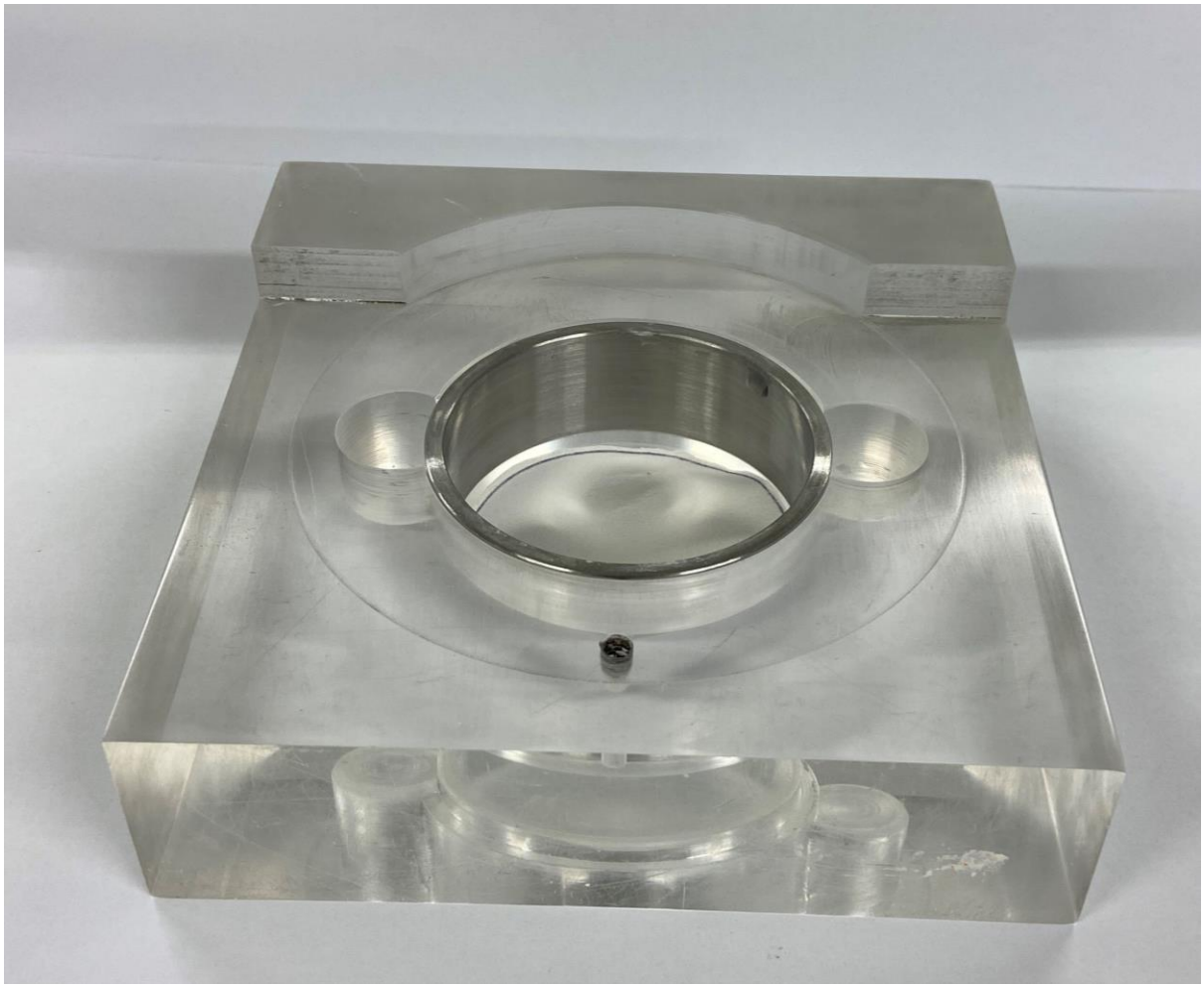

Figure 6.16- Oedometer ring holder such that sedimentation columns can be attached and extruded directly into the oedometer ring

Figure 6.17- Slurry cone hydro-splitter after Phillips (2014)

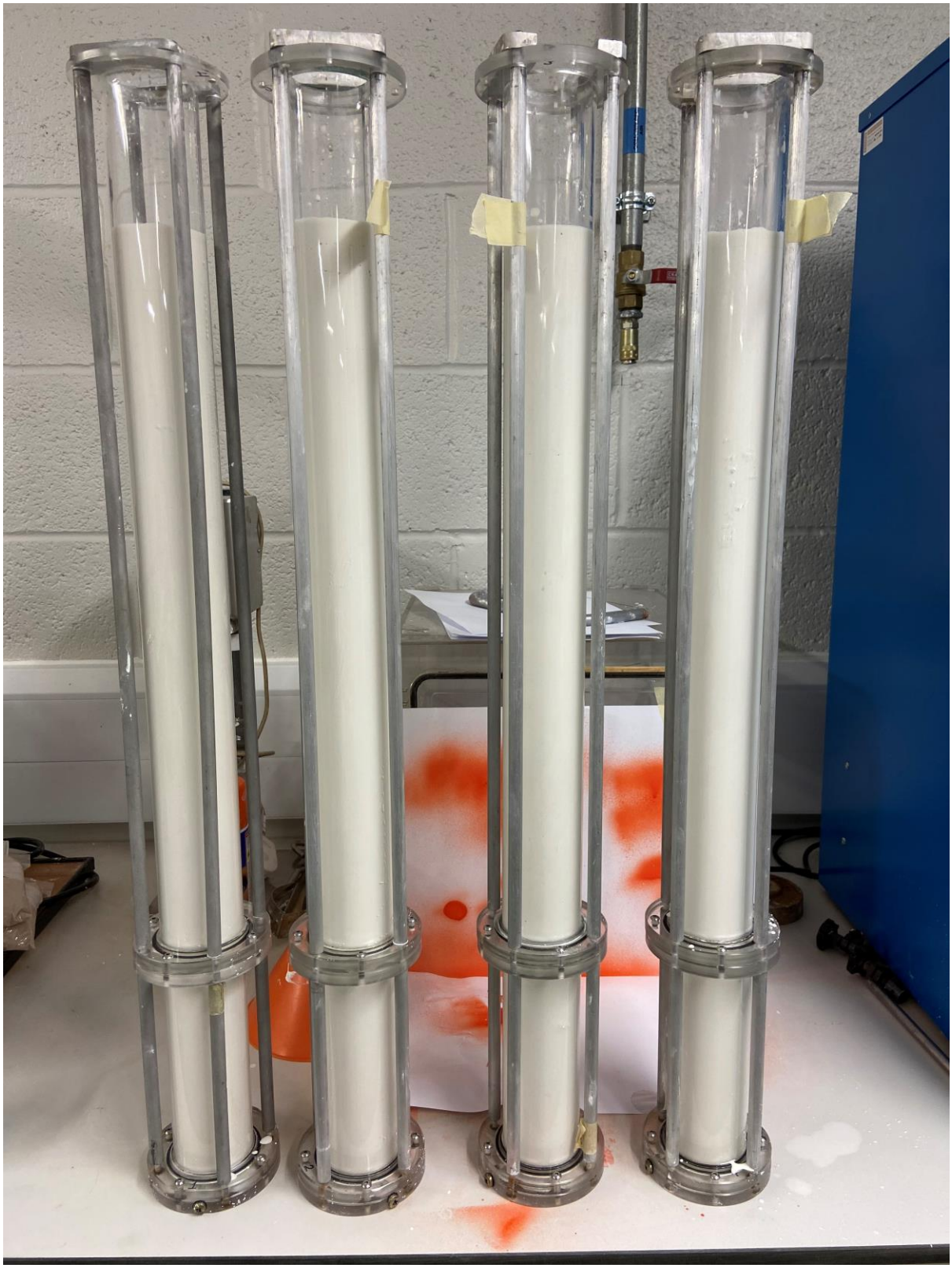

Figure 6.18- Full sedimentation columns after using the hydro-splitter

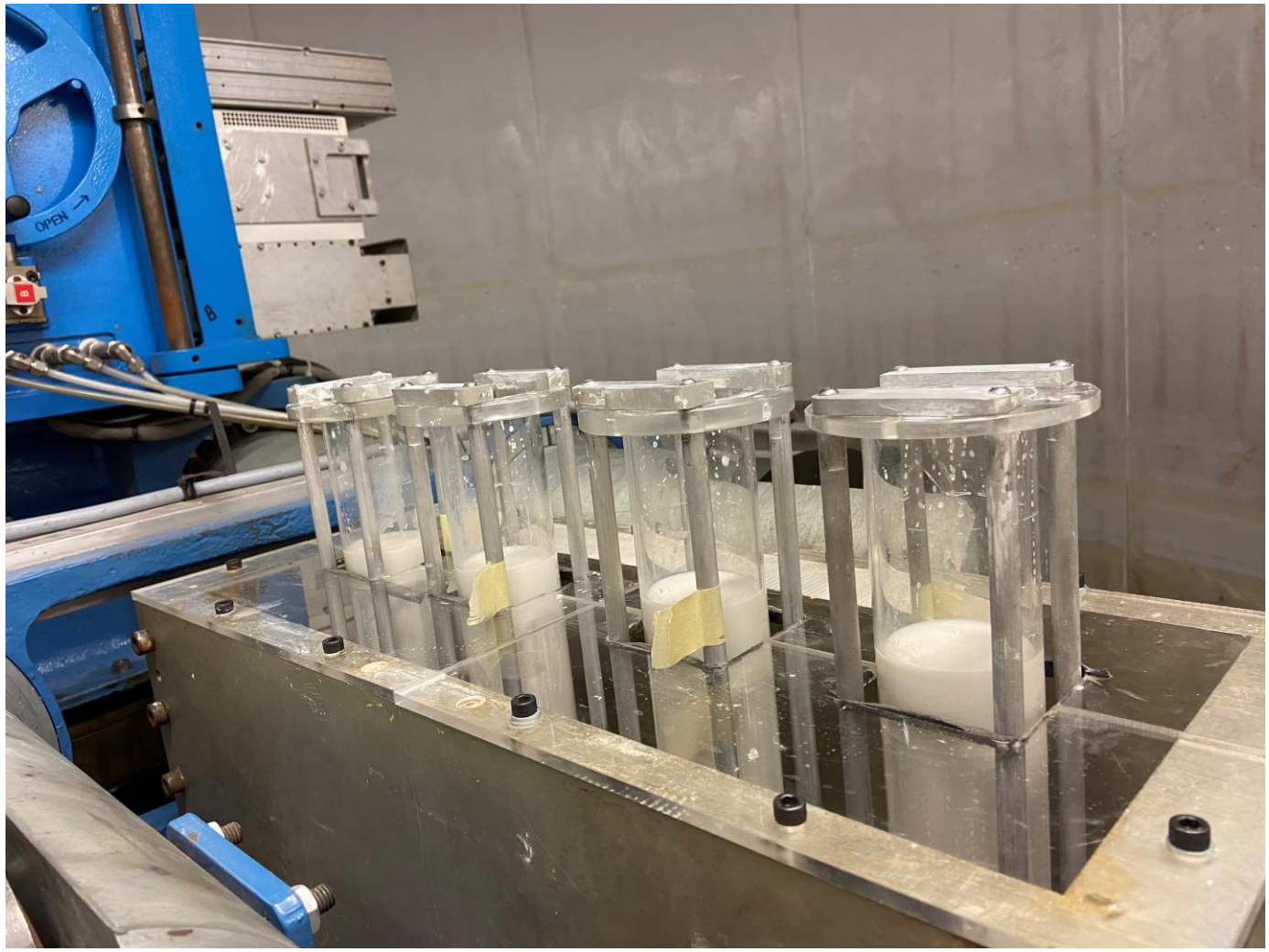

Figure 6.19- Sedimentation columns secured into the centrifgue strongbox and placed on the centrifuge swing

Figure 6.20- Step 1 of horizontal permeameter procedure: vertical permeameter top cap removed and restraining piece attached to columns

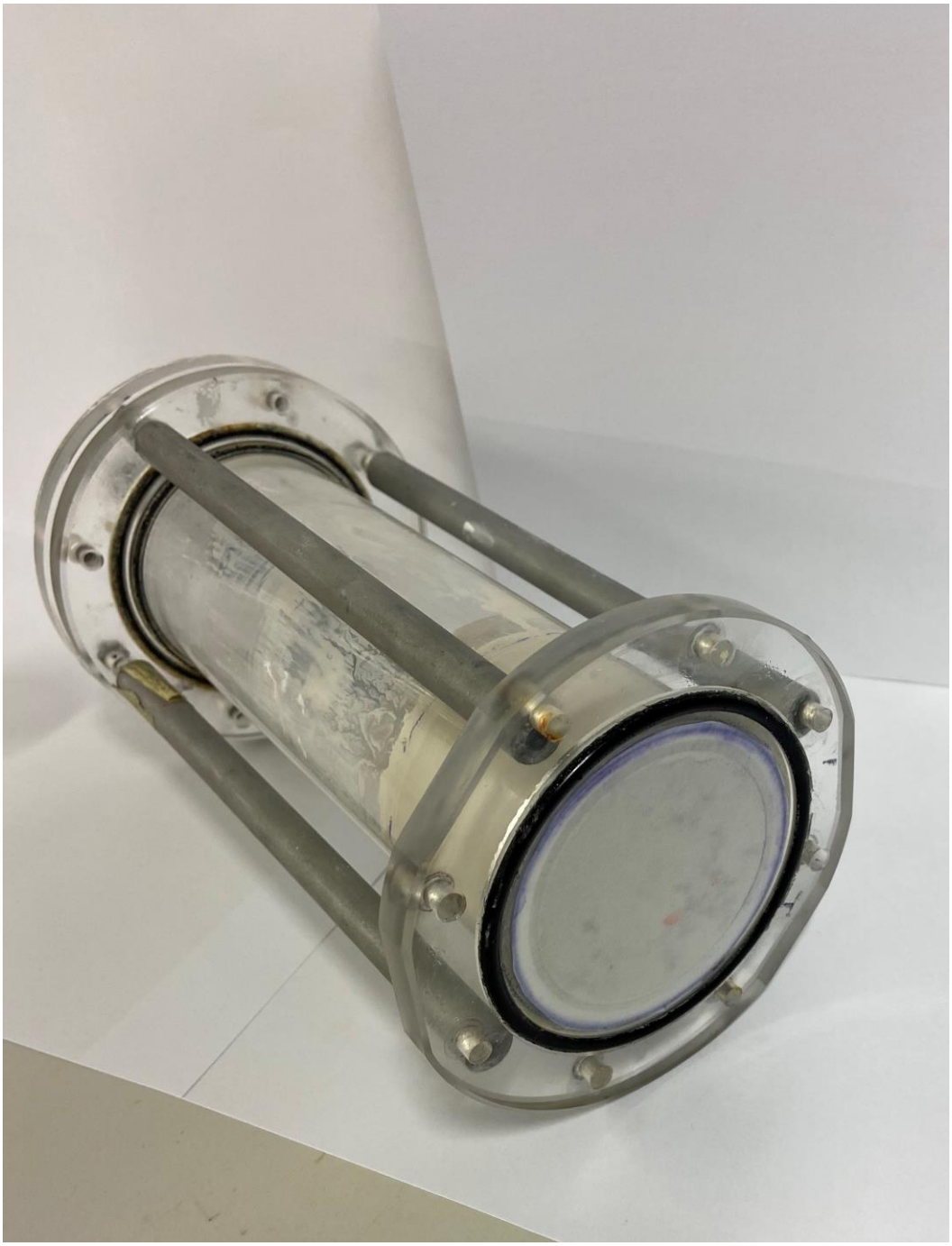

Figure 6.21- Step 2 of horizontal permeameter procedure: base of the sedimentation column removed

Figure 6.22- Step 3 of horizontal permeameter procedure: 48mm diameter core of soil taken from sedimentation column using a thin-walled cutter

Figure 6.23- Step 4 of horizontal permeameter procedure: soil sample extruded from thin-walled cutter

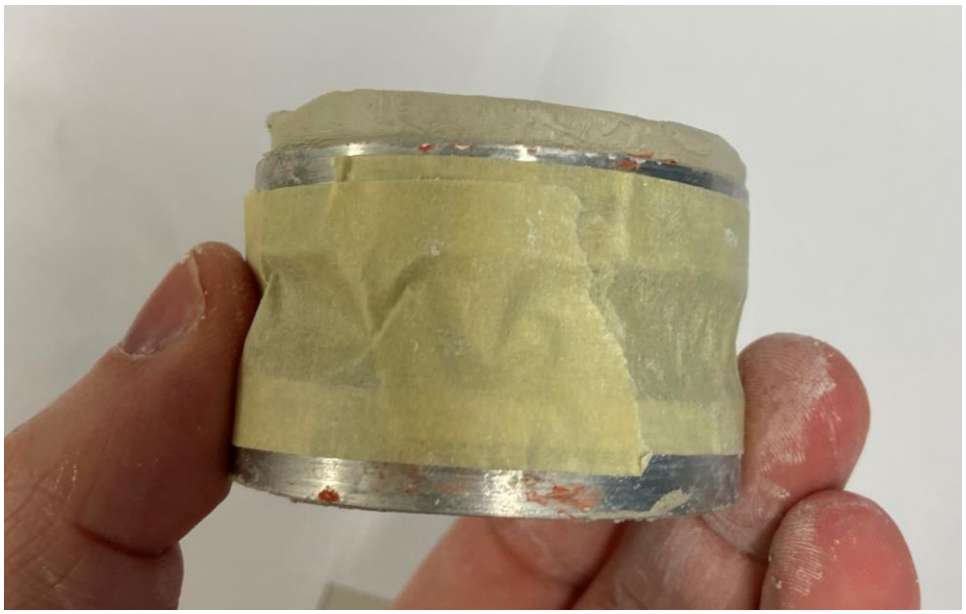

Figure 6.24- Step 5 of horizontal permeameter procedure: soil sample was approximately cut to size placed wrapped in filter paper and placed inside the external filter. The filter had been already covered with tape to avoid getting blocked with Plastidip.

Figure 6.25- Step 6 of horizontal permeameter procedure: soil sample is made flat using a wire saw

Figure 6.26- Step 7 of horizontal permeameter procedure: the top and bottom surfaces of the clay sample are sprayed with Plastidip to create impermeable boundaries

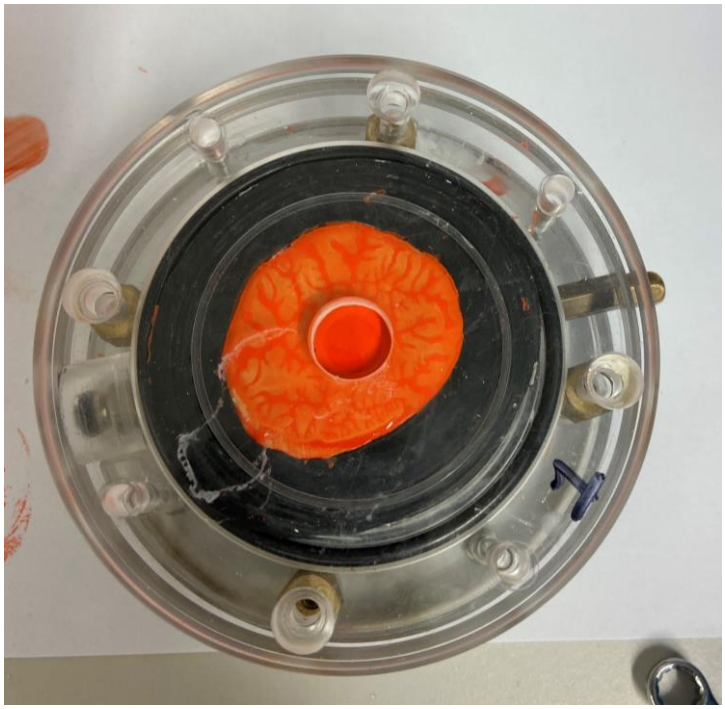

Figure 6.27- Step 8 of horizontal permeameter procedure: the gasket was placed over the external ring and the top cap was secured.

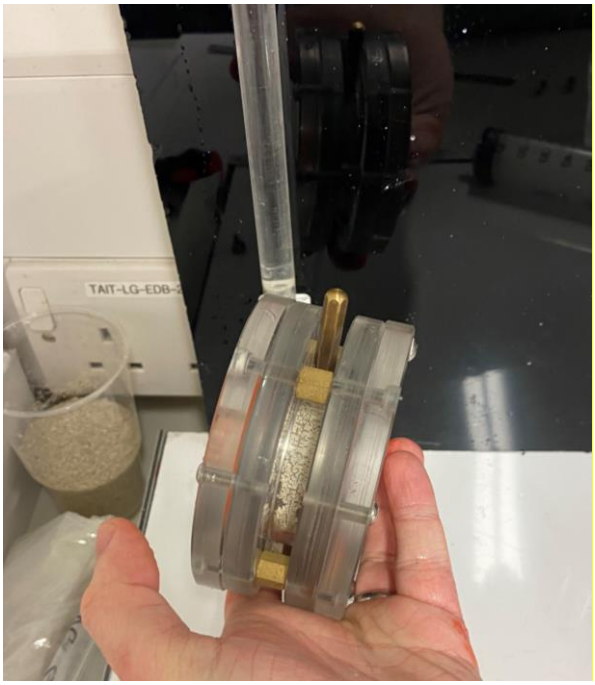

Figure 6.28- Step 9 of horizontal permeameter procedure: the permeameter was filled with water and any air was bled from the system by positioning the bleed screw at the highest point

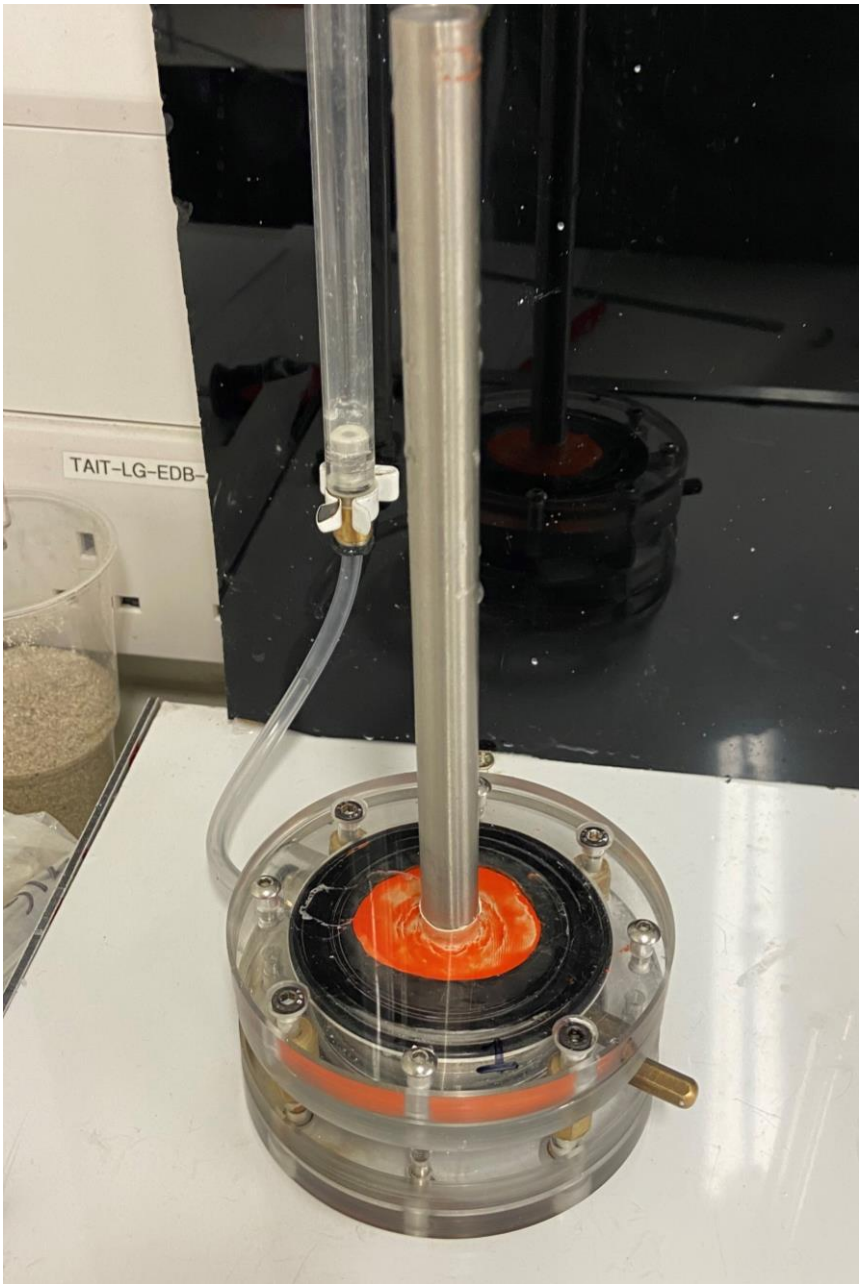

Figure 6.29- Step 10 of horizontal permeameter procedure: bore made for central permeable core using the top cap as a guide

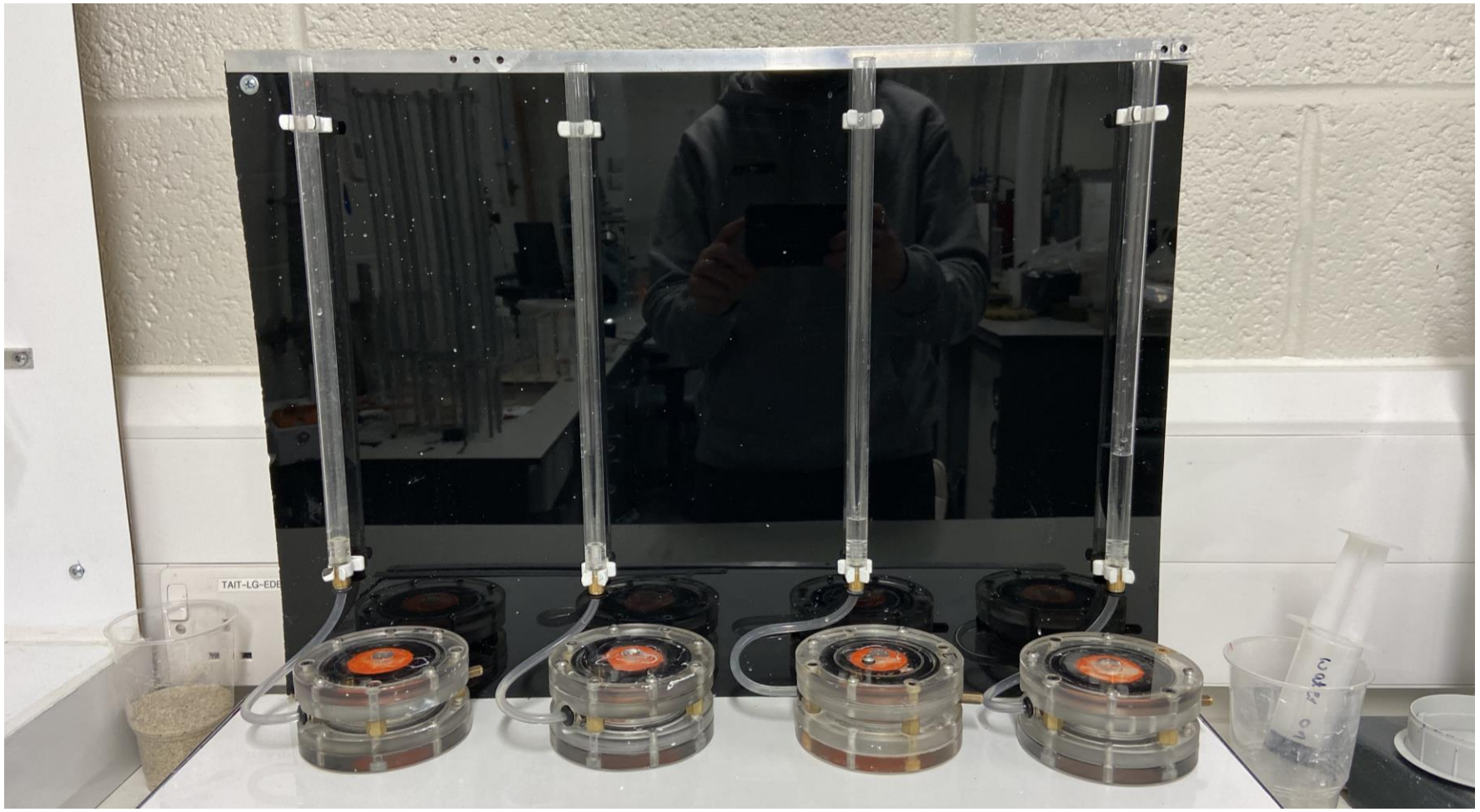

Figure 6.30- Step 11 of horizontal permeameter procedure, permeable core pushed into bore and the horizontal permeability test is ready to be conducted

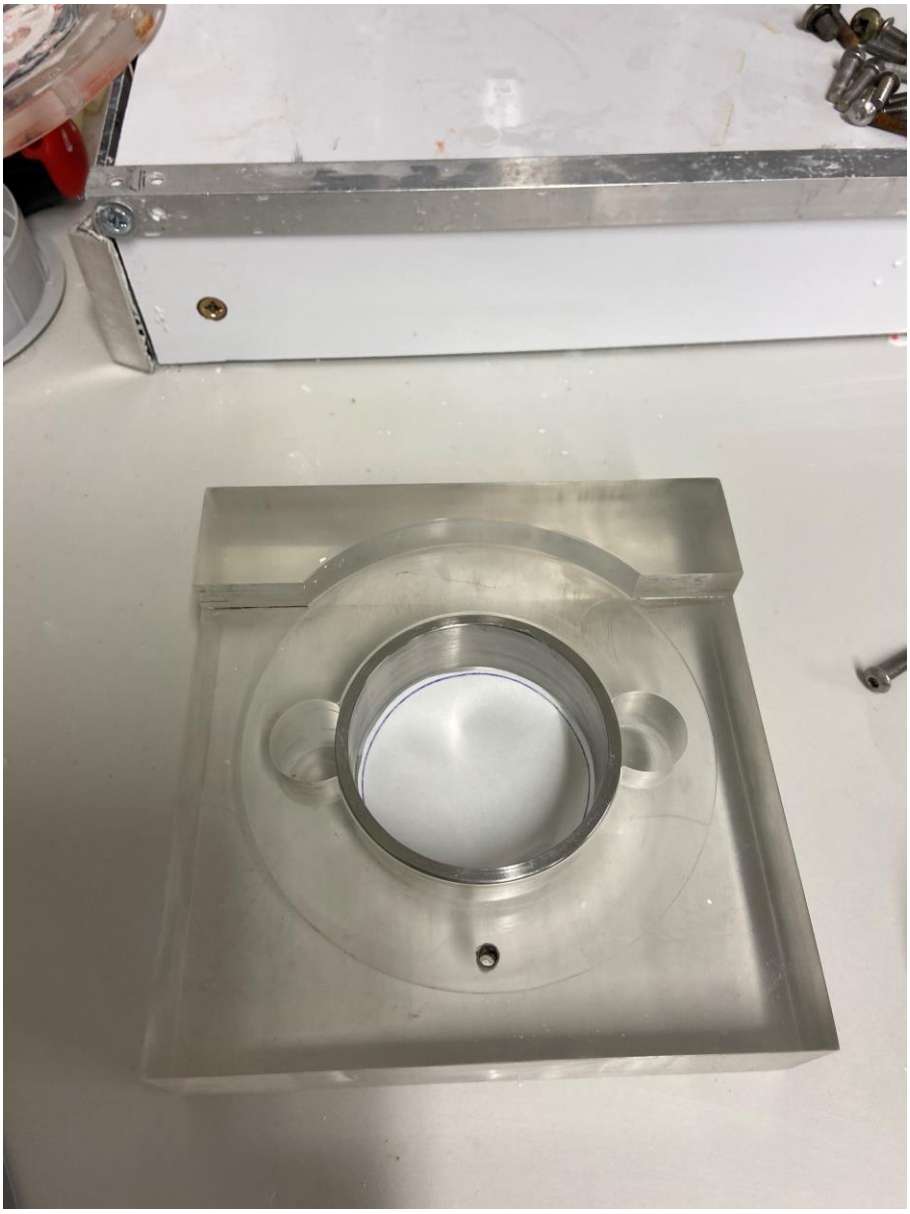

Figure 6.31- PMMA holder with filter paper placed

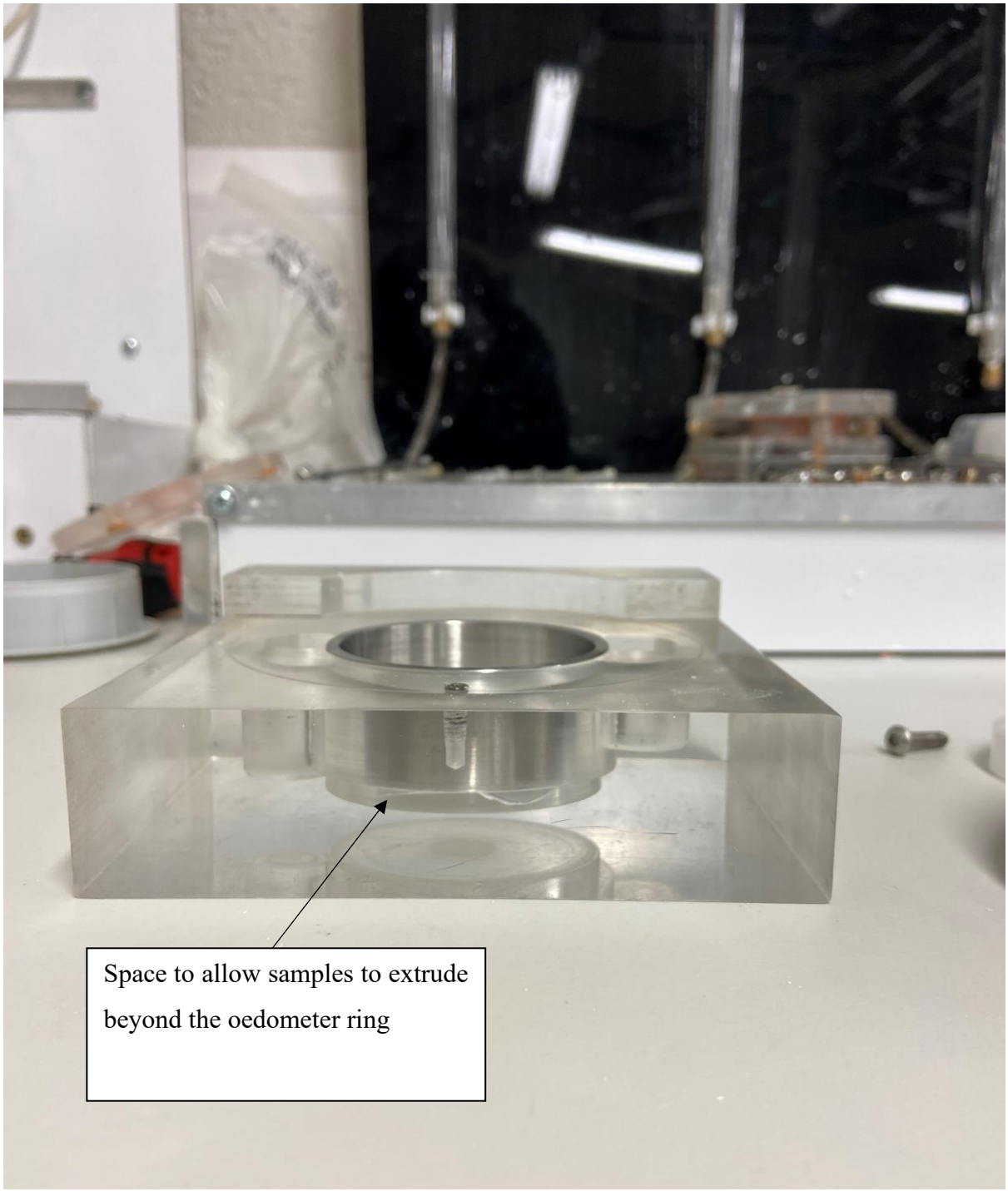

Figure 6.32- PMMA holder with oedometer ring in place

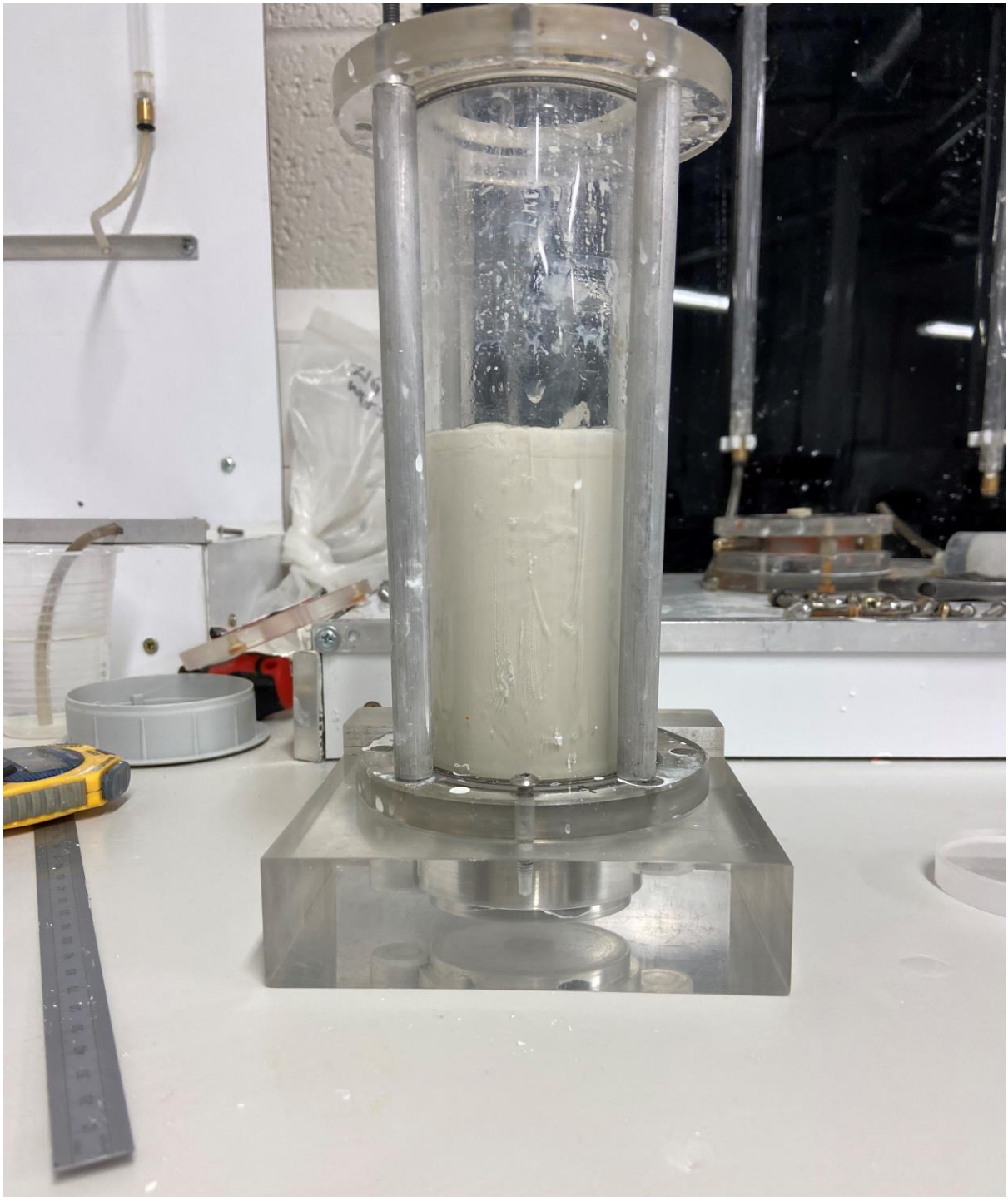

Figure 6.33- Sedimentation colum secured to the to the PMMA holder

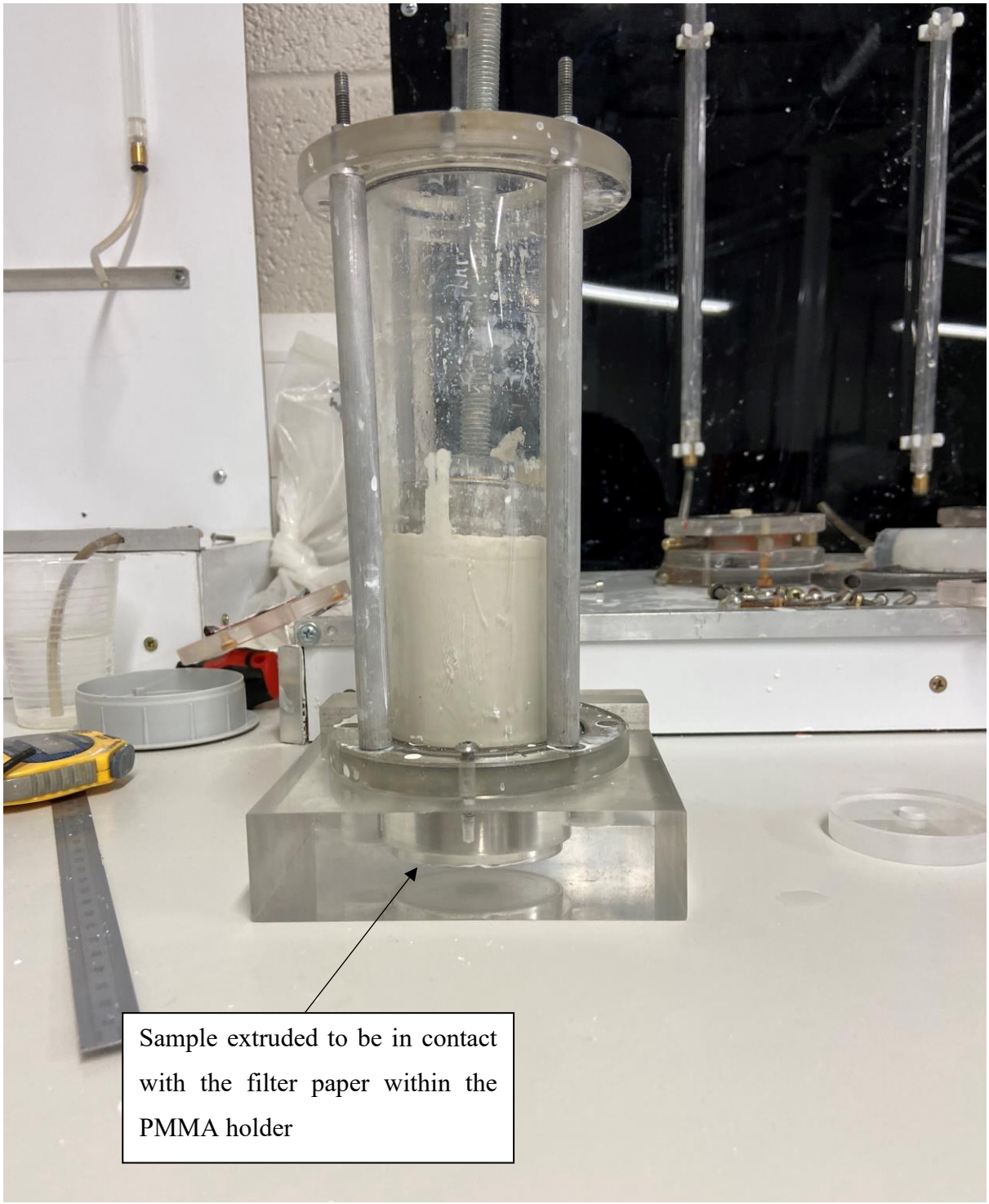

Figure 6.34- Odeometer sample extruded into the oedomter ring

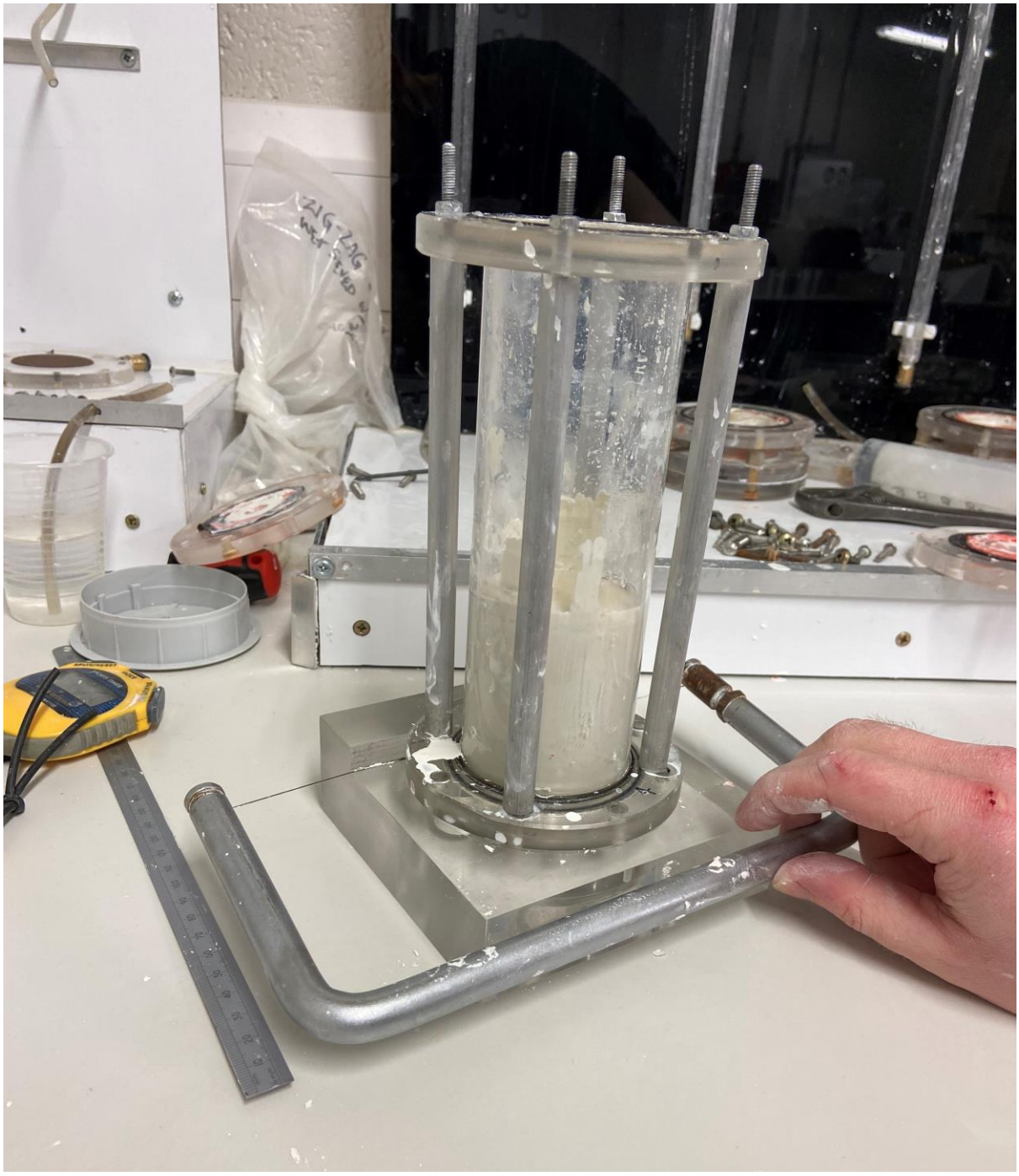

Figure 6.35- Triming oedometer sample with a wire saw

Figure 6.36- Oedometer sample post removal from PMMA holder

Figure 6.37- Oedometer sample trimmed to achieve flat top and bottom surfaces

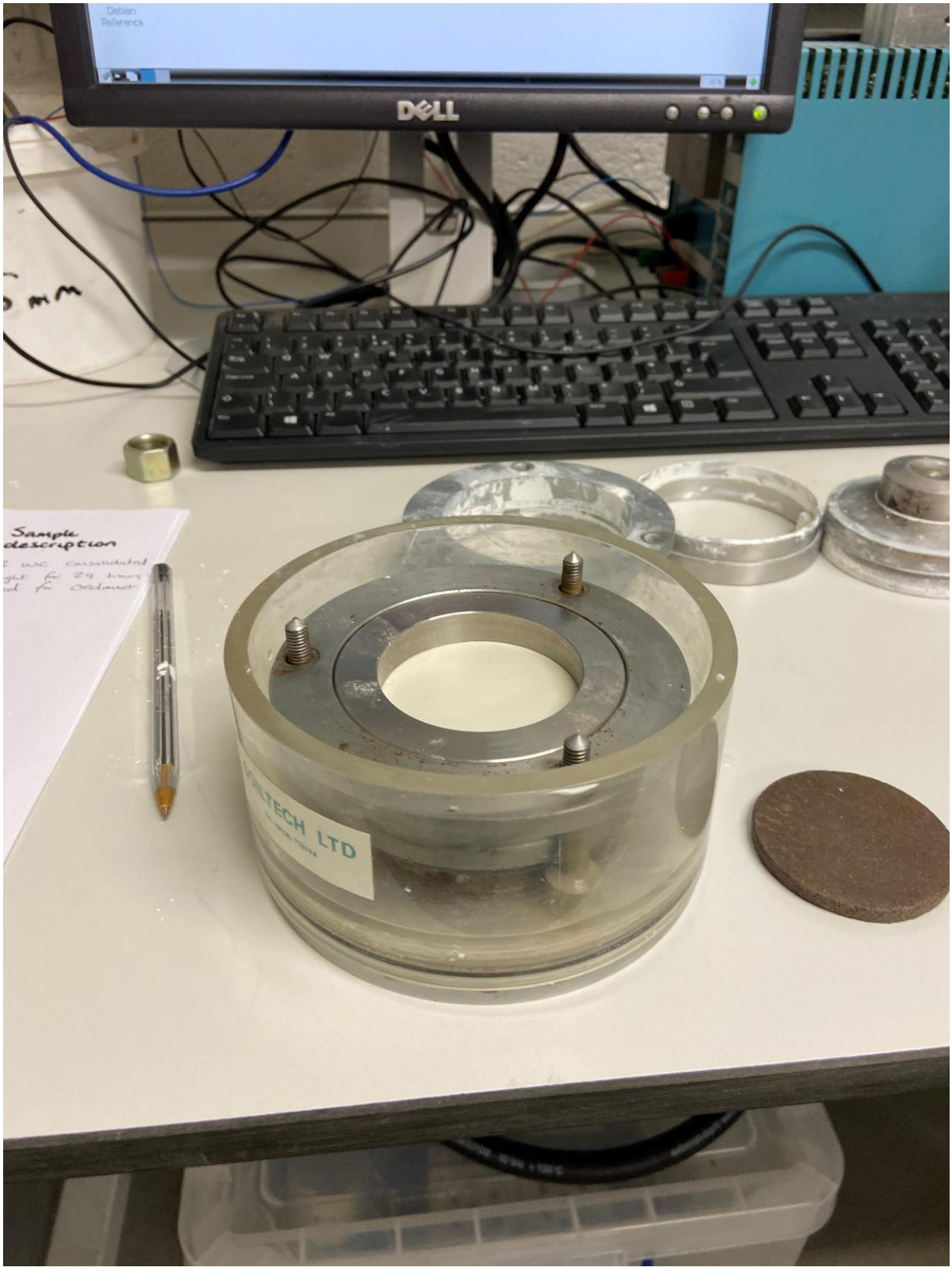

Figure 6.38- Assembled oedometer equipment prior to placing the top porus stone

Figure 6.39- Photograph of the oedometer equipment

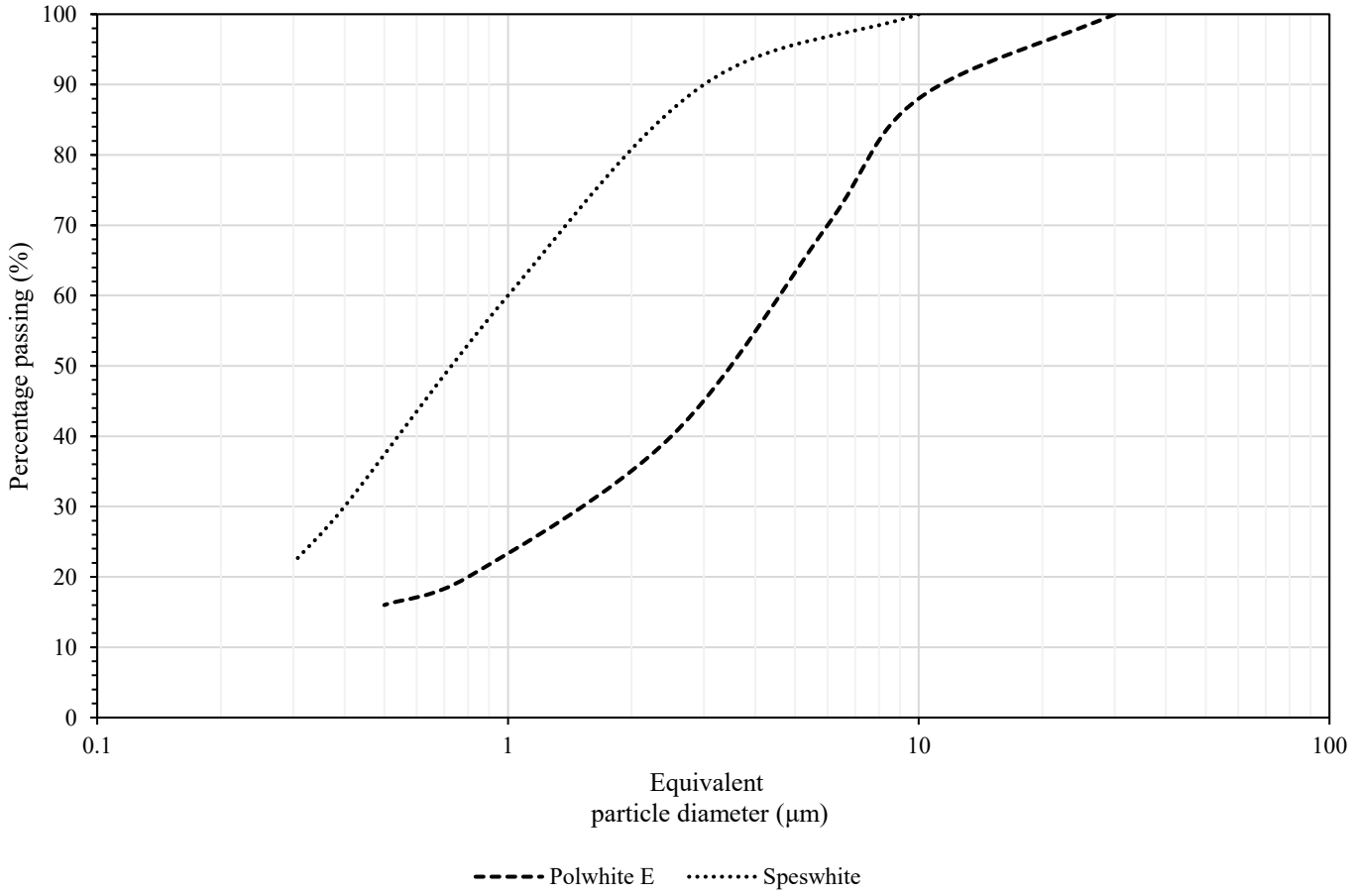

Figure 7.1- Particle Size Distribution of Speswhite kaolin clay and Polwhite E kaolin clay powder supplied by Imery's ltd

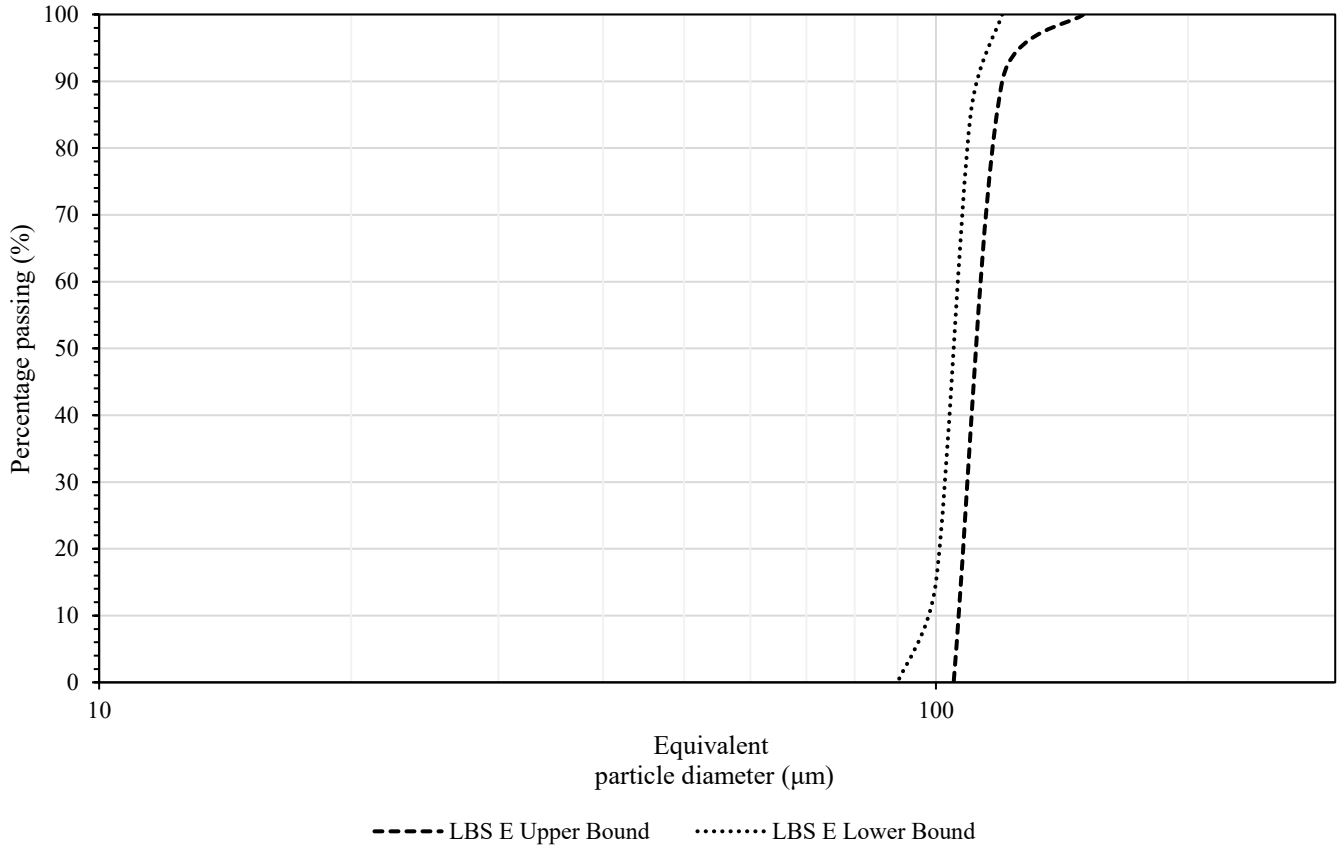

Figure 7.2- Particle size distribution of Leighton Buzzard sand fraction E, after Grant (1998)

Idealised Sedimented 70:30 Speswhite: Polwhite E kaolin clay sample

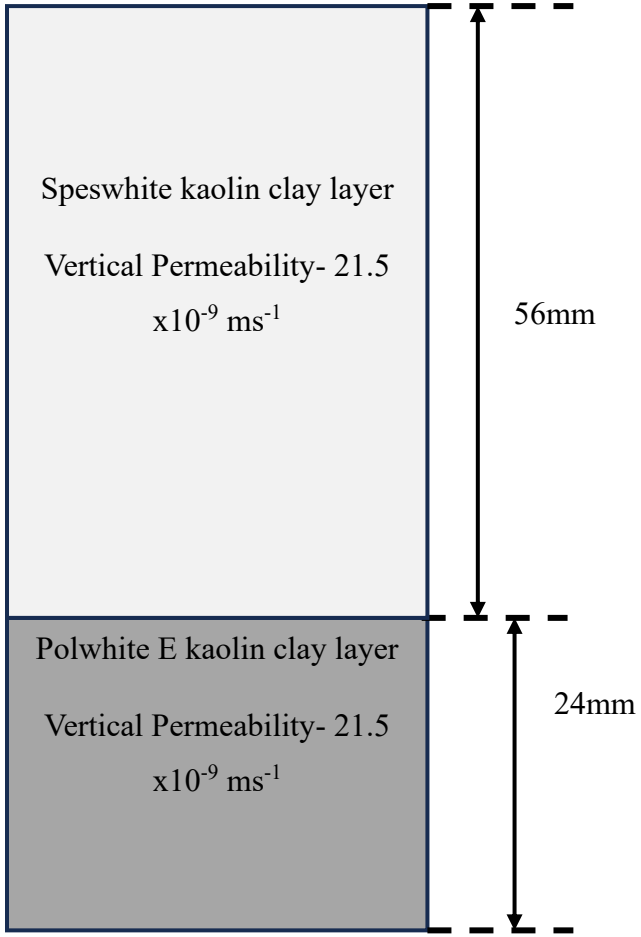

Idealised Sedimented 50:50 Speswhite: Polwhite E kaolin clay sample

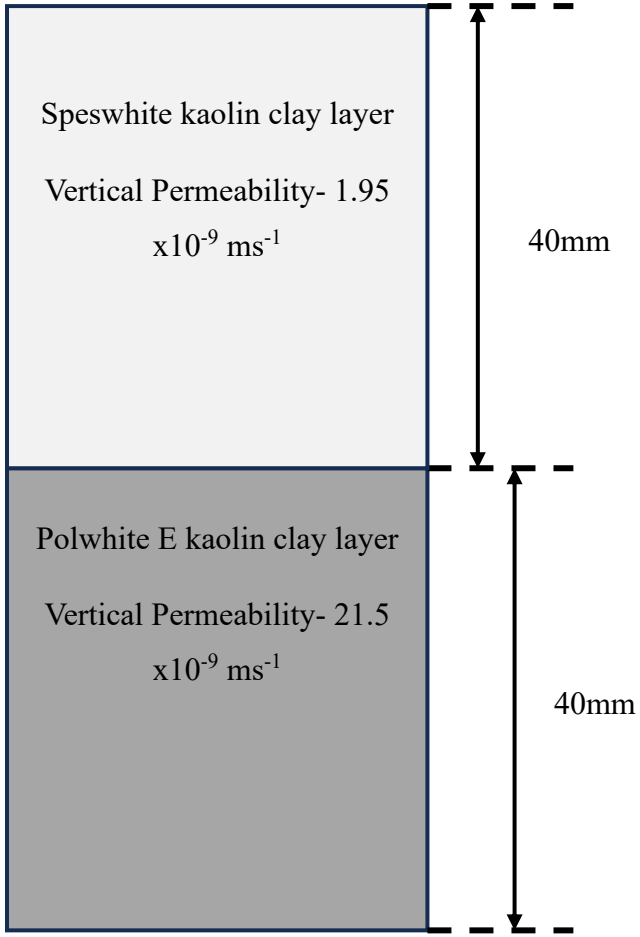

Figure 8.1- Idealised sedimented soil samples for vertical permeability predictions

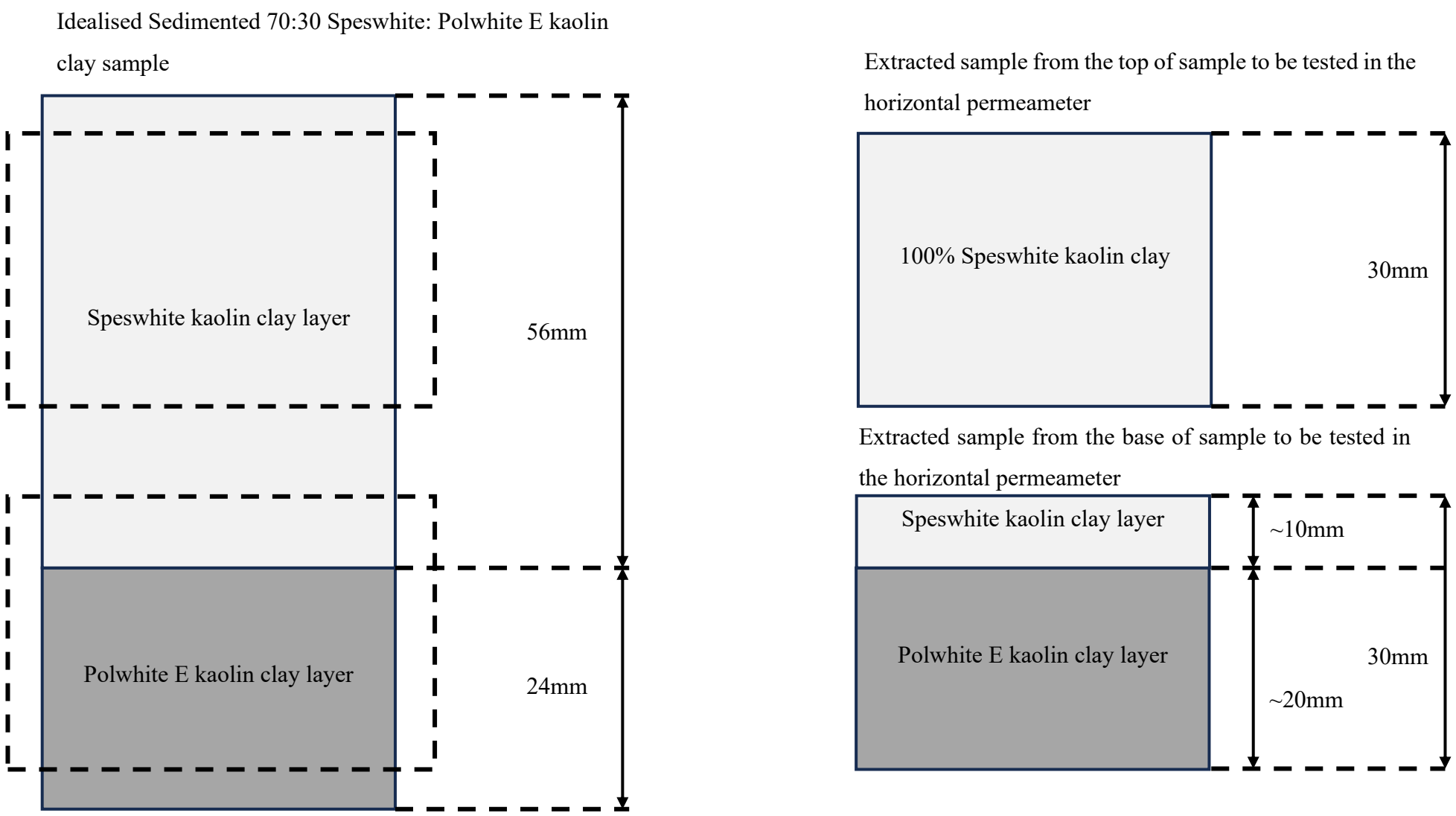

Figure 8.2- Idealised sedimented soil samples for horizontal permeability predictions

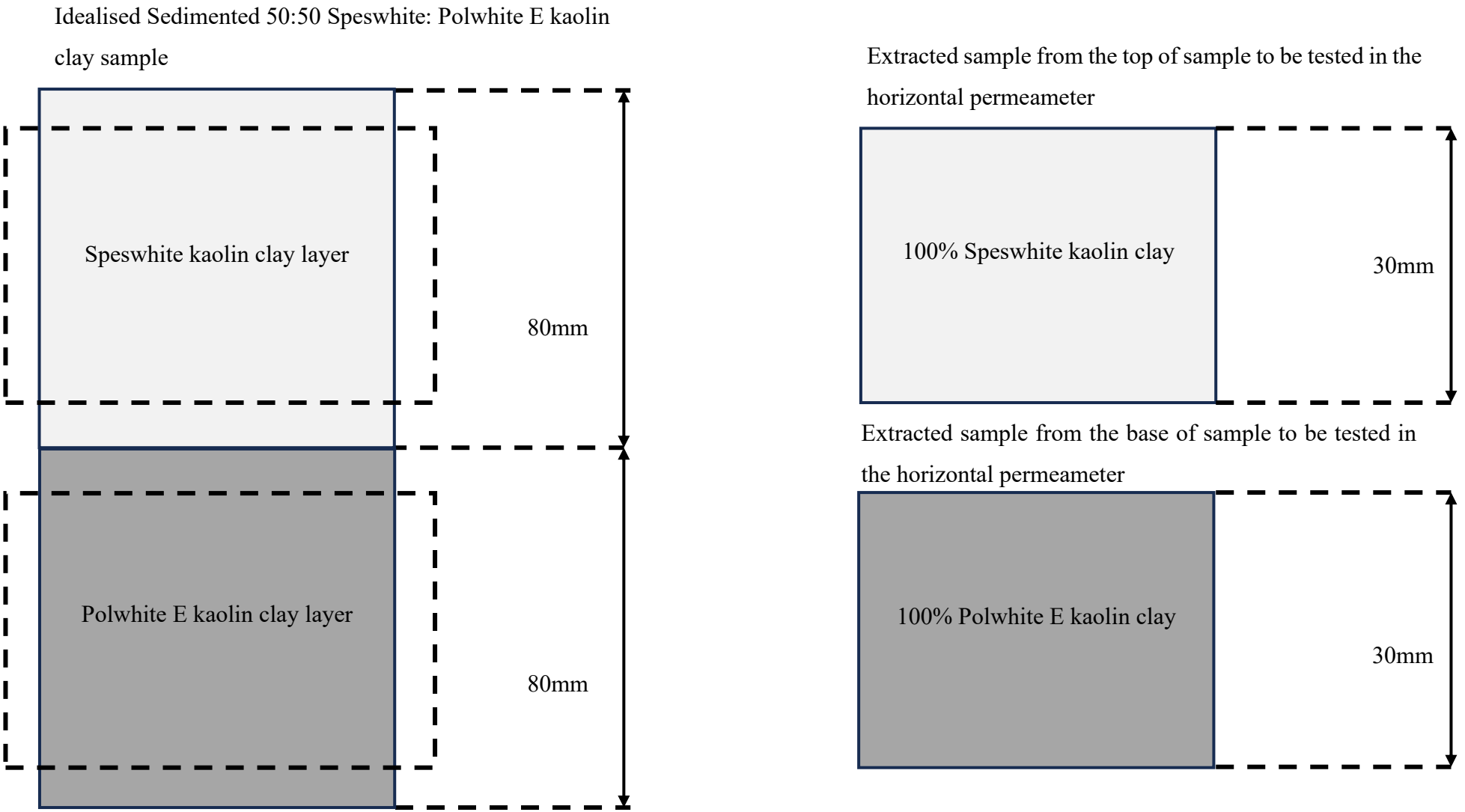

Figure 8.3- Idealised sedimented soil samples for horizontal permeability predictions

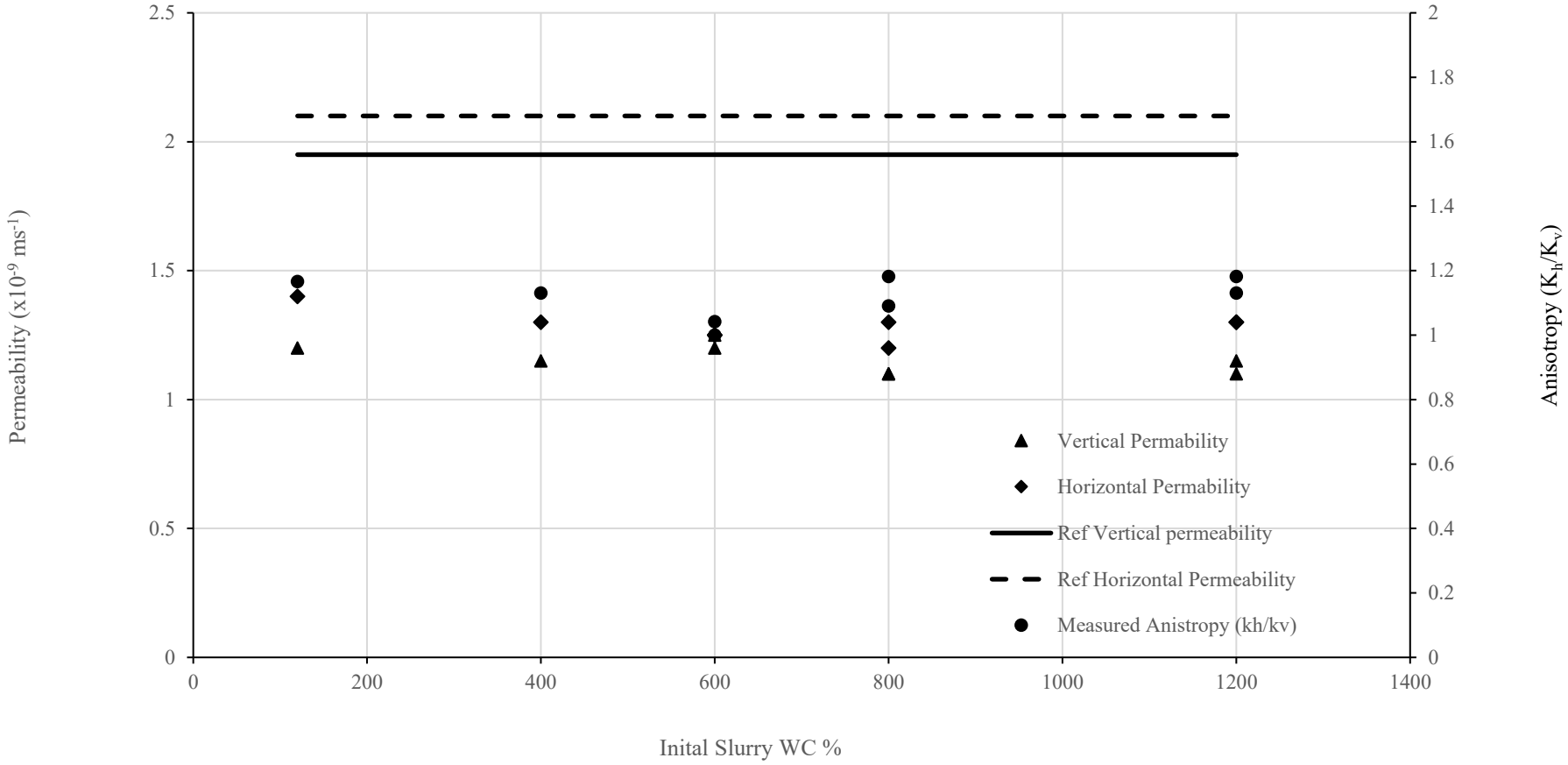

Figure 8.4- Permeability results of 100% Speswhite kaolin clay slurries sedimented at different initial water contents

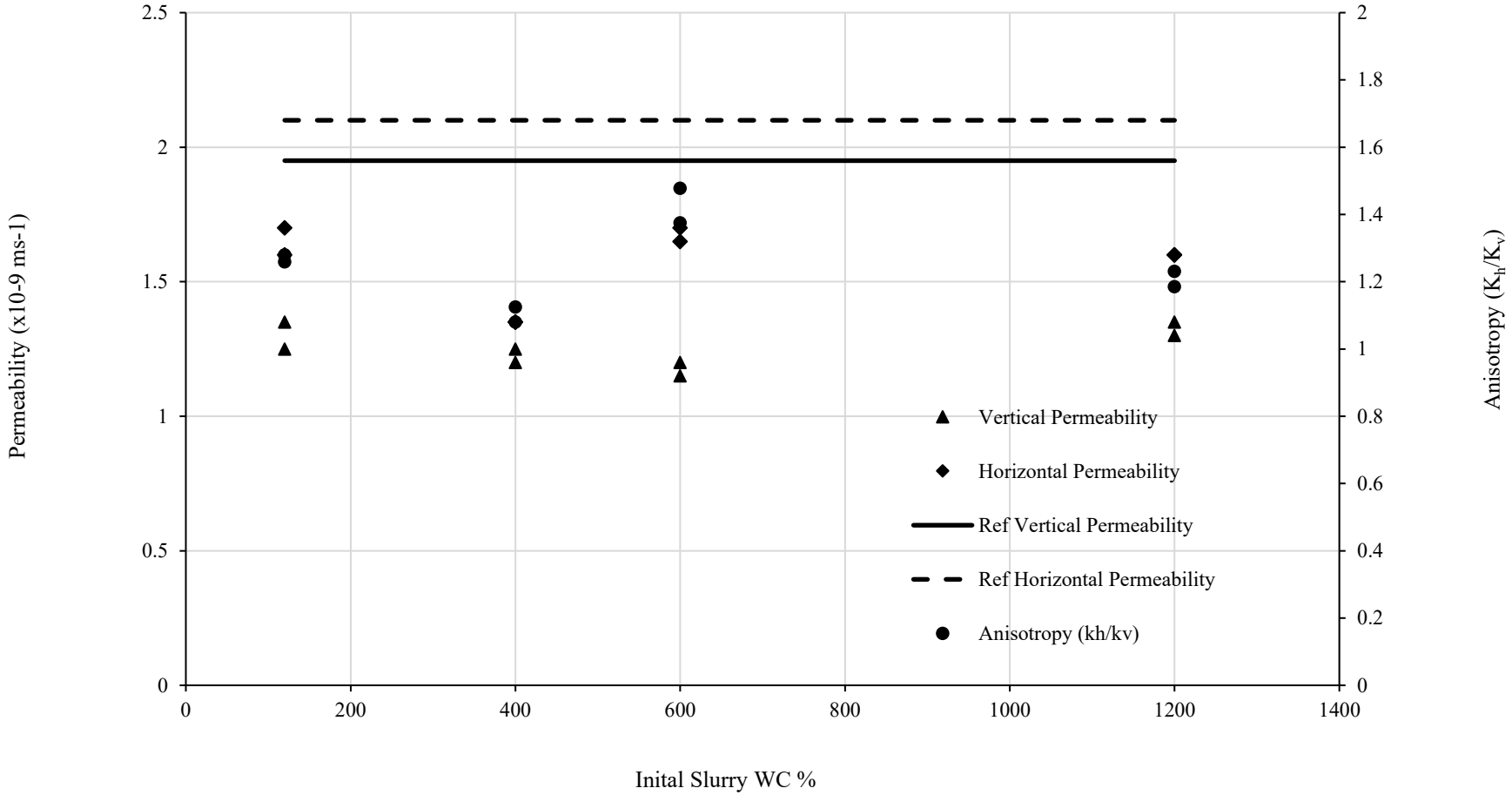

Figure 8.5- Permeability results of 100% recycled Speswhite kaolin clay cuttings slurries sedimented at different initial water contents

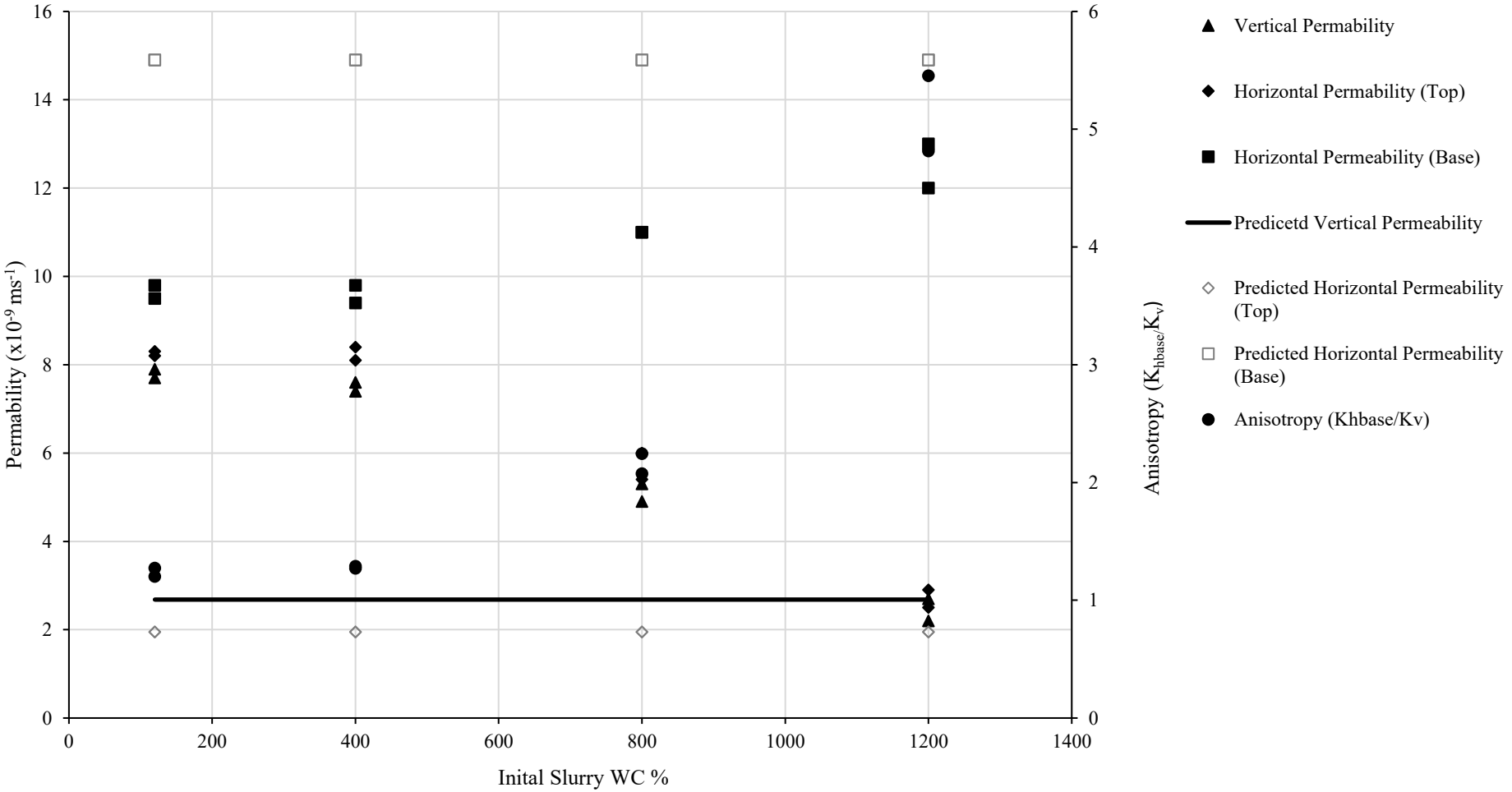

Figure 8.6- Permeability results of 70% Speswhite, 30% Polwhite E kaolin clay slurries sedimented at different initial water contents

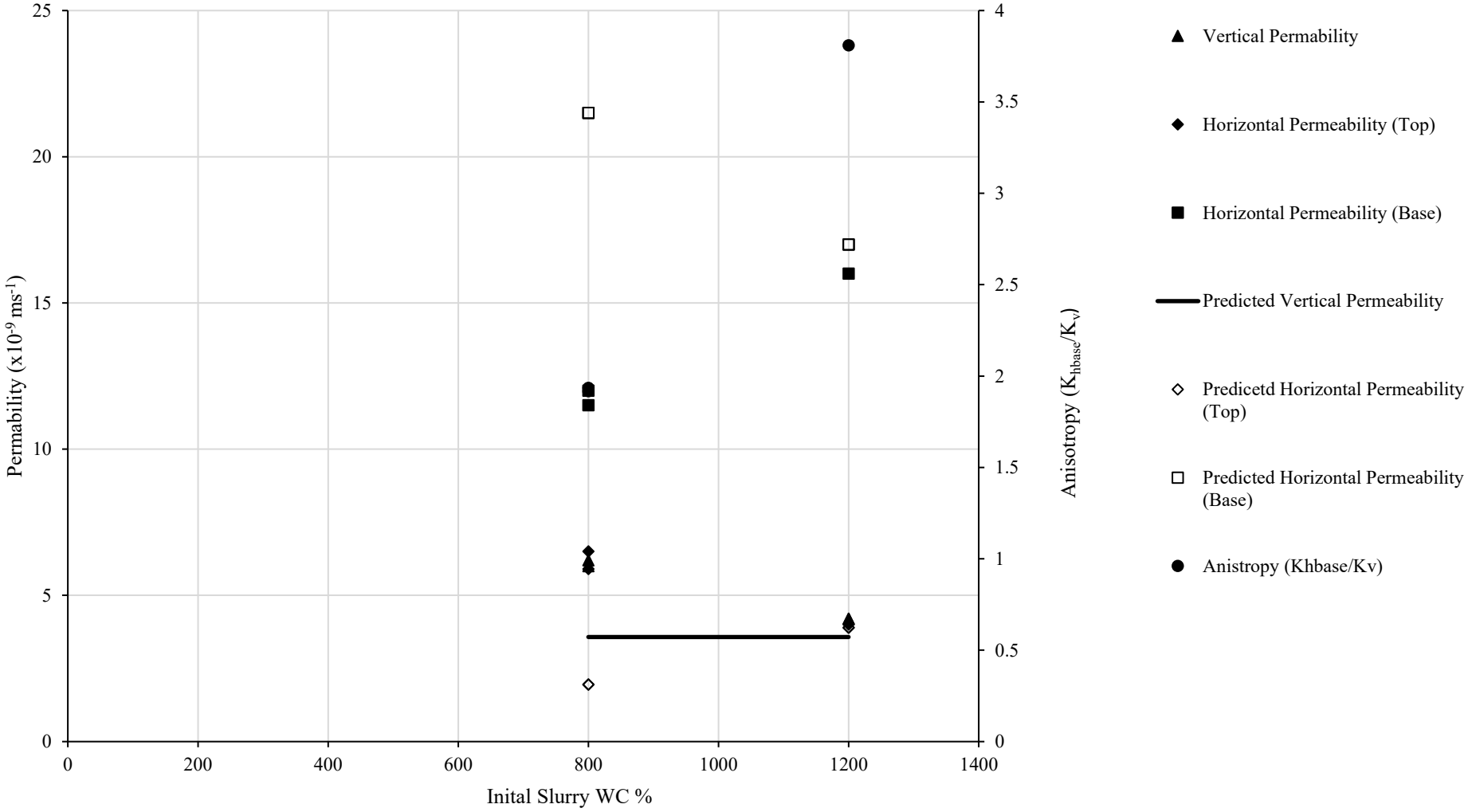

Figure 8.7- Permeability results of 50% Speswhite, 50% Polwhite E kaolin clay slurries sedimented at different initial water contents

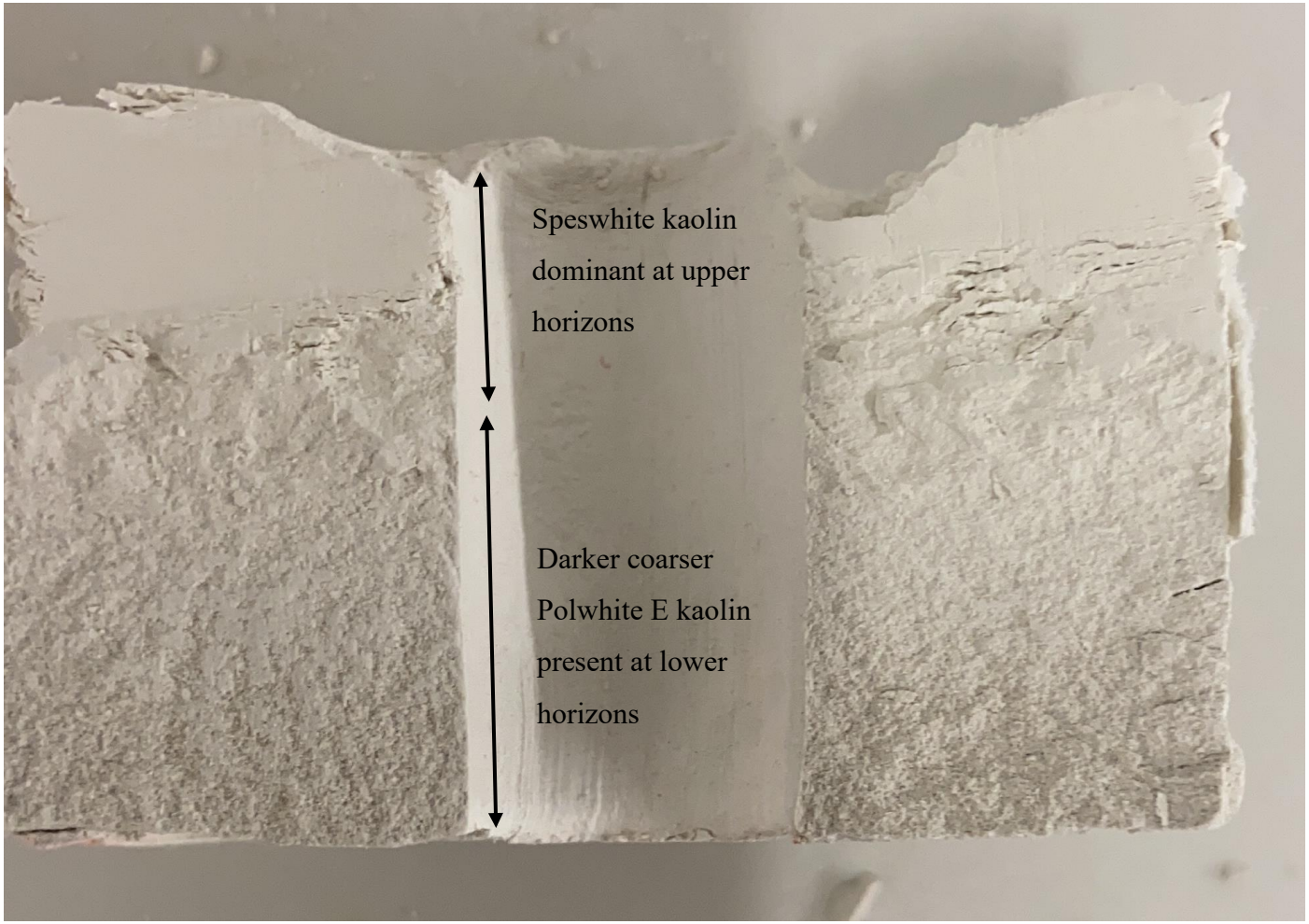

Figure 8.8- Dried split sample from the bottom section of a 70% Speswhite 30% Polwhite E kaolin clay sample sedimented with an initial water content of 1200%

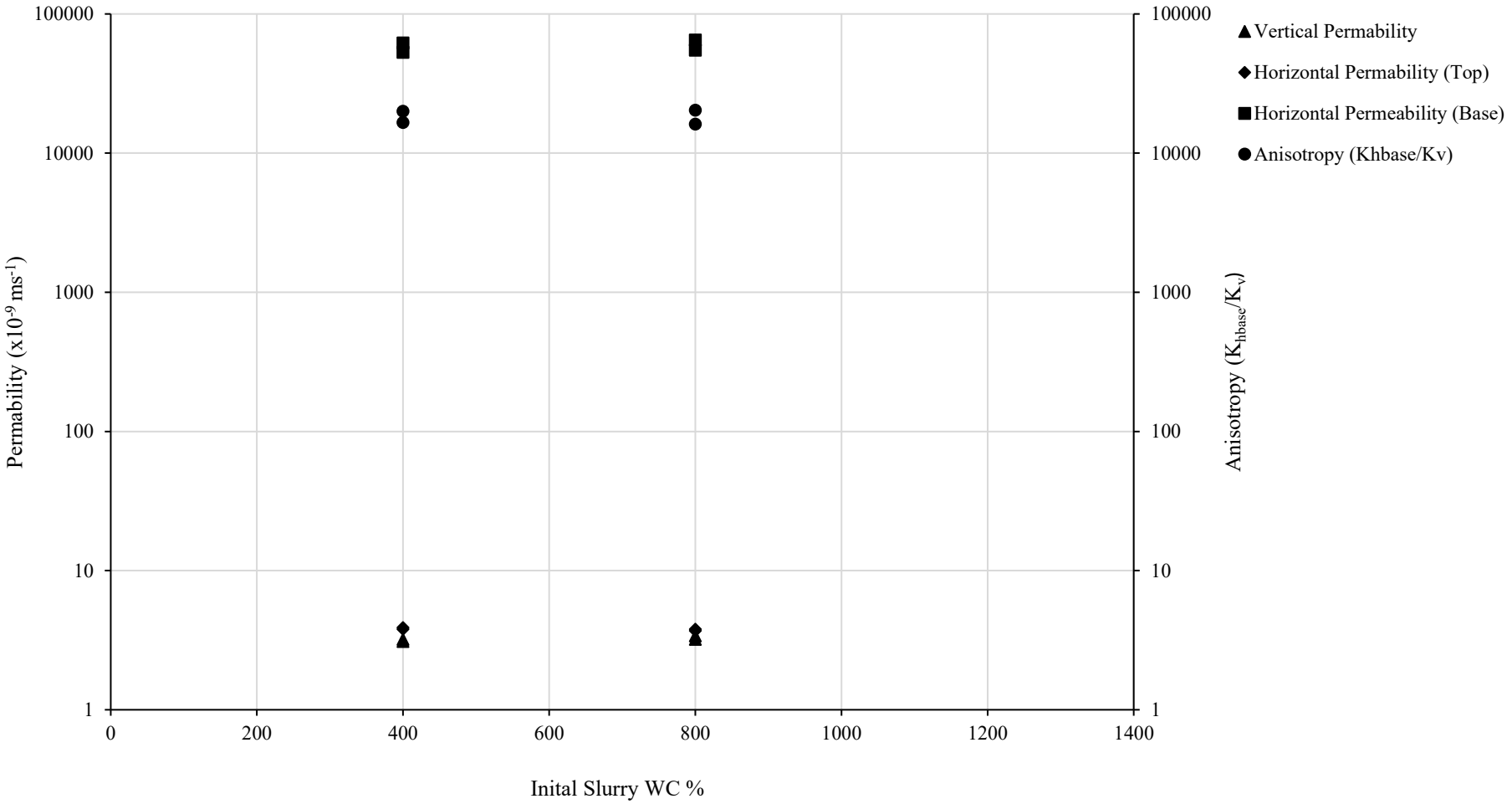

Figure 8.9- Permeability results of 50 % Speswhite kaolin clay 50% Leighton Buzzard sand slurries sedimented at different initial water contents

Figure 8.10- Uneven sand layer created during centrifuge sedimentation

Figure 8.11- Uneven sand layer created during radial acceleration

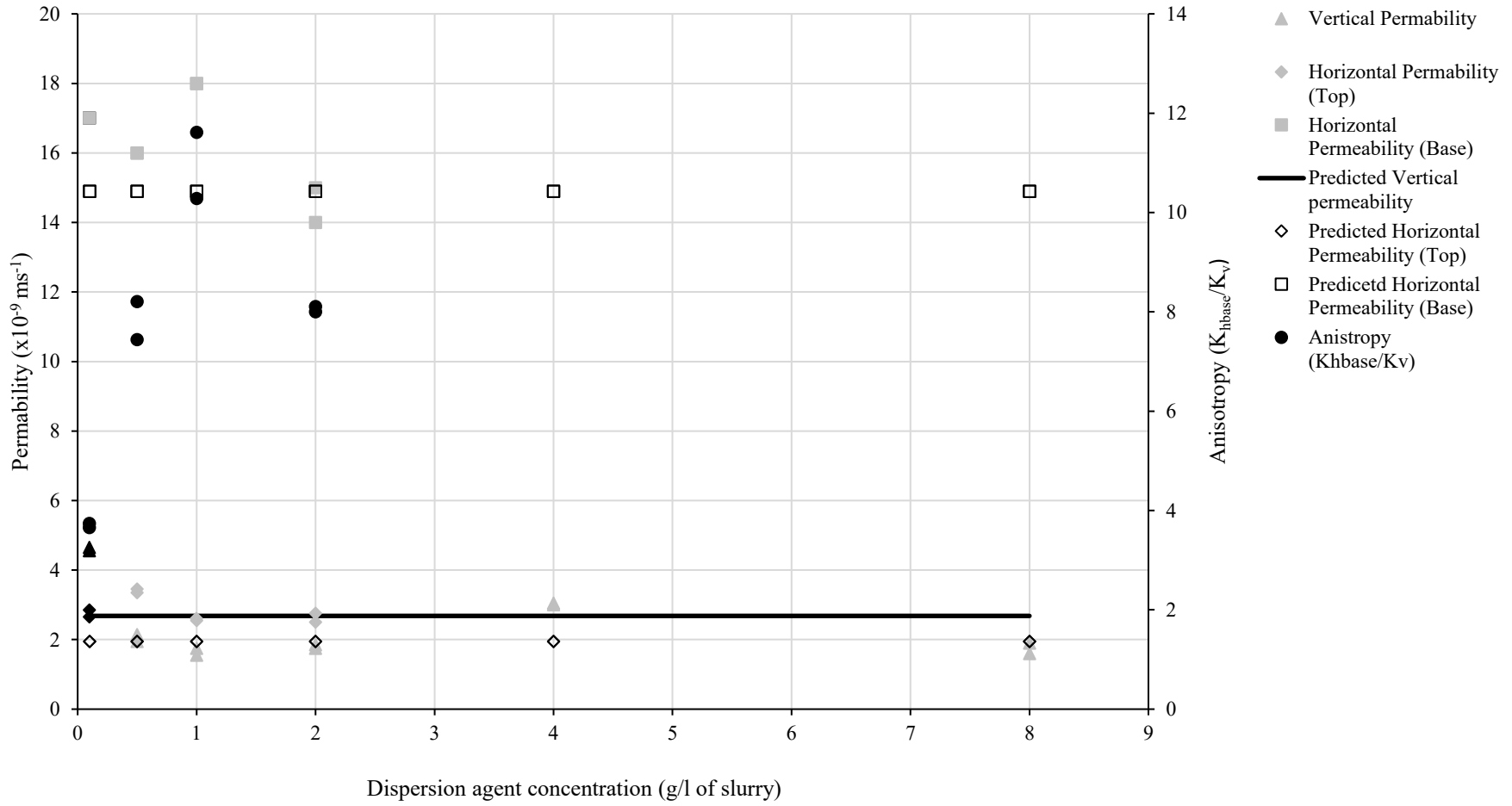

Figure 8.12- Permeability results of Speswhite: Polwhite E kaolin clay slurries with added dispersion agent sedimented at different initial water contents. Note that grey markers indicate an unstable soil structure generated during sedimentation

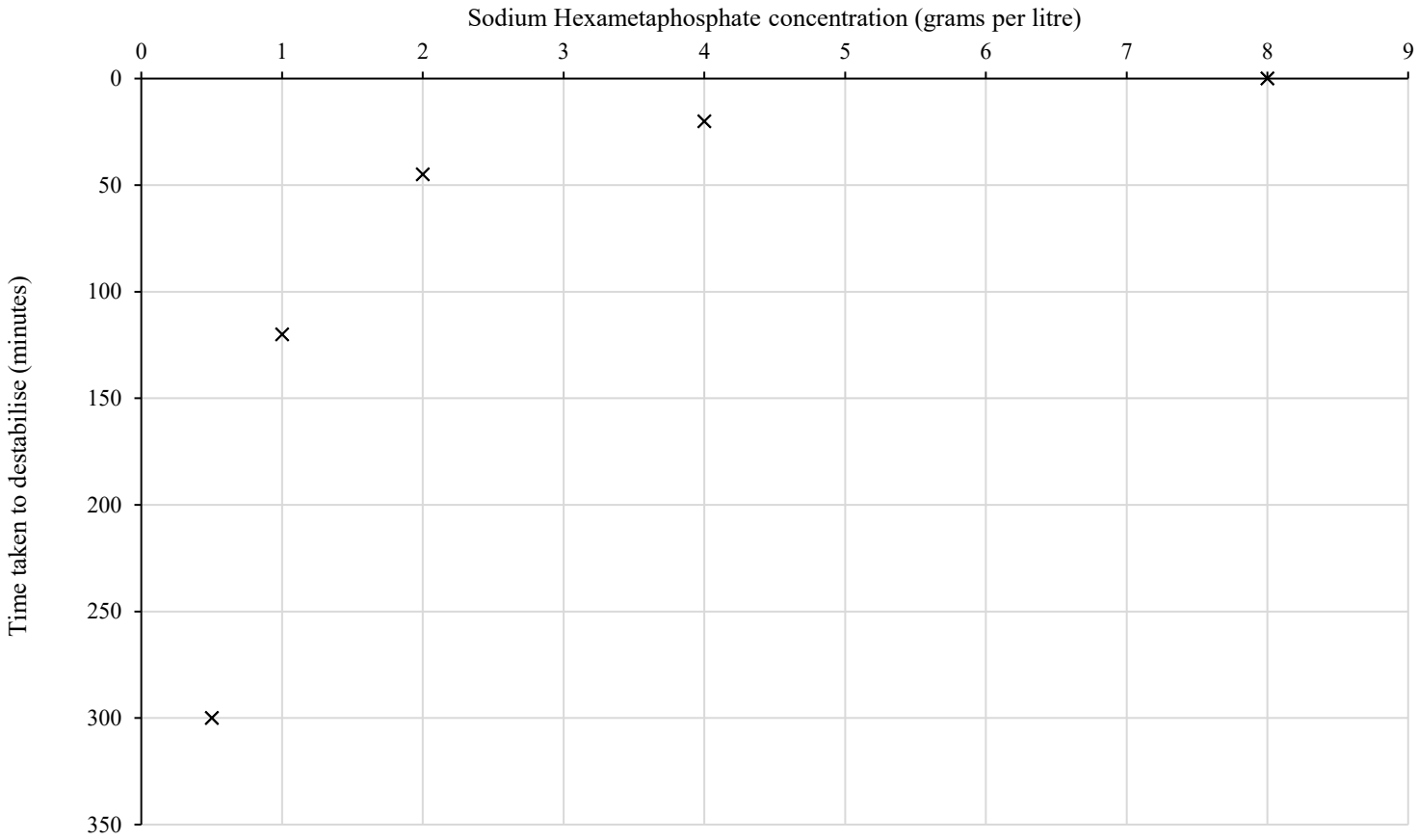

Figure 8.13- Time for horizontal samples to destabilise during horizontal permeability testing

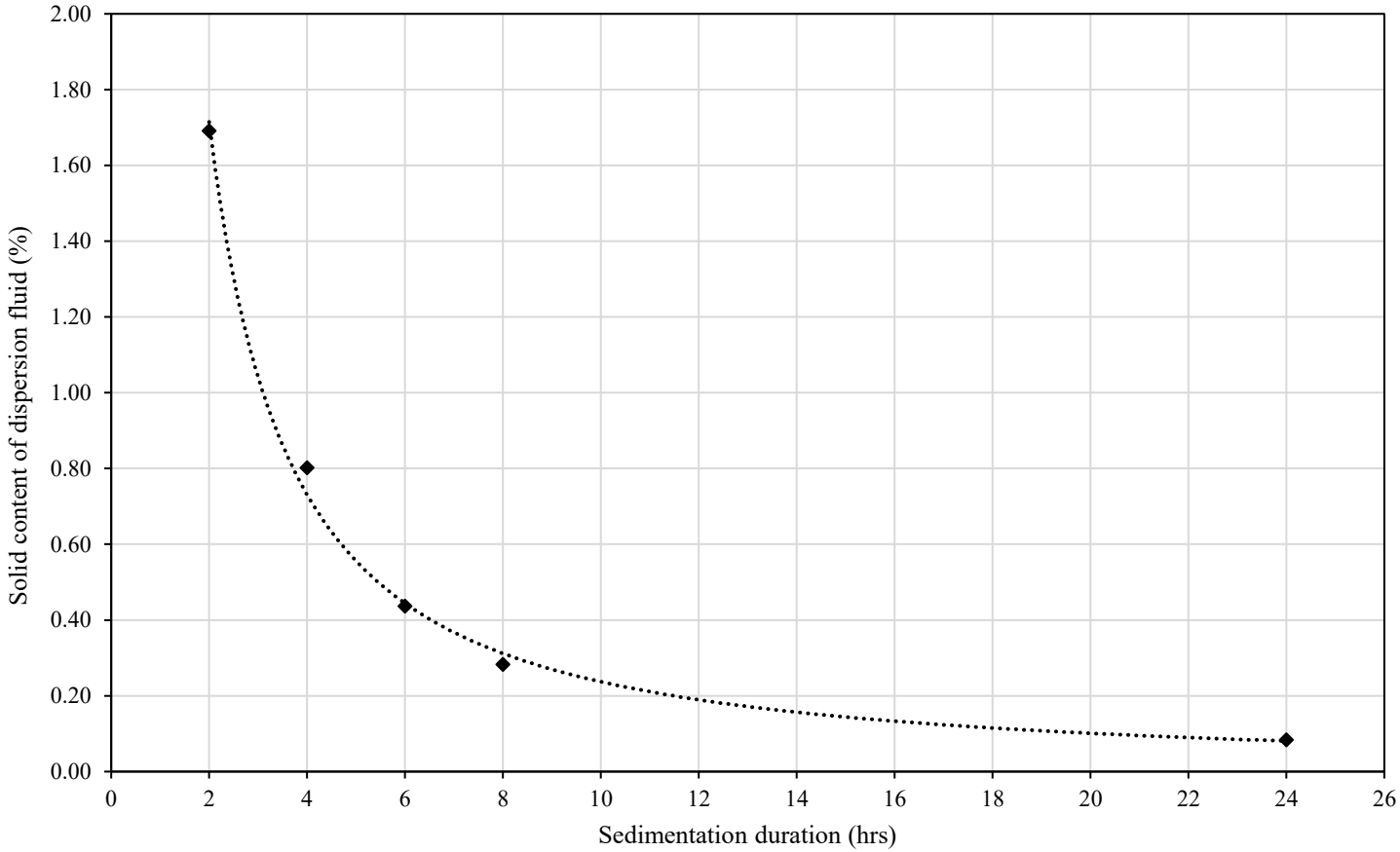

Figure 8.14- Centrifuge sedimentation time against solid content of dispersion fluid

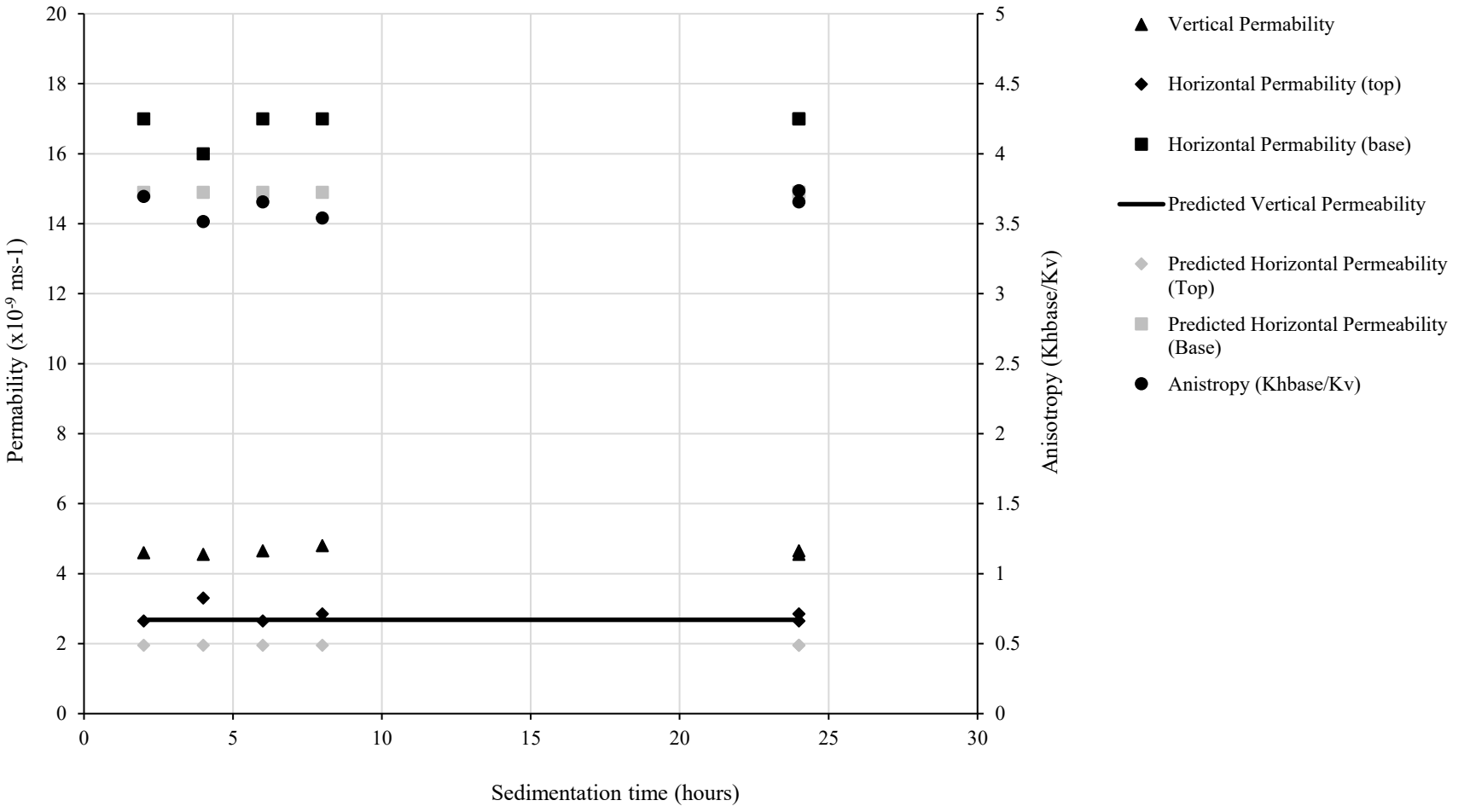

Figure 8.15- Permeability results of Speswhite Polwhite E slurries with added dispersion agent sedimented at 500% initial water contents for different sedimentation times

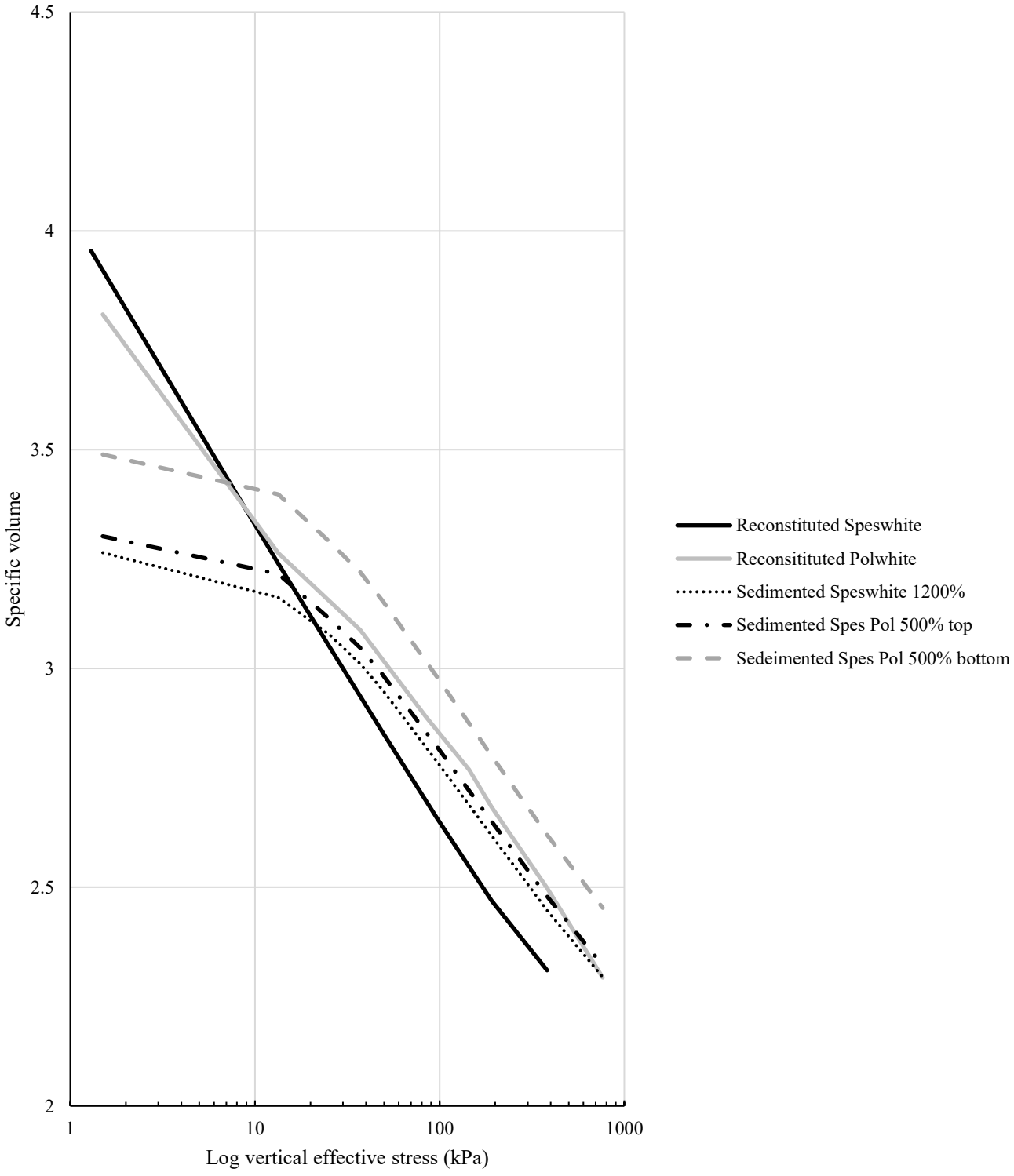

Figure 8.16- Oedometer test results from reference samples and select sedimeted samples

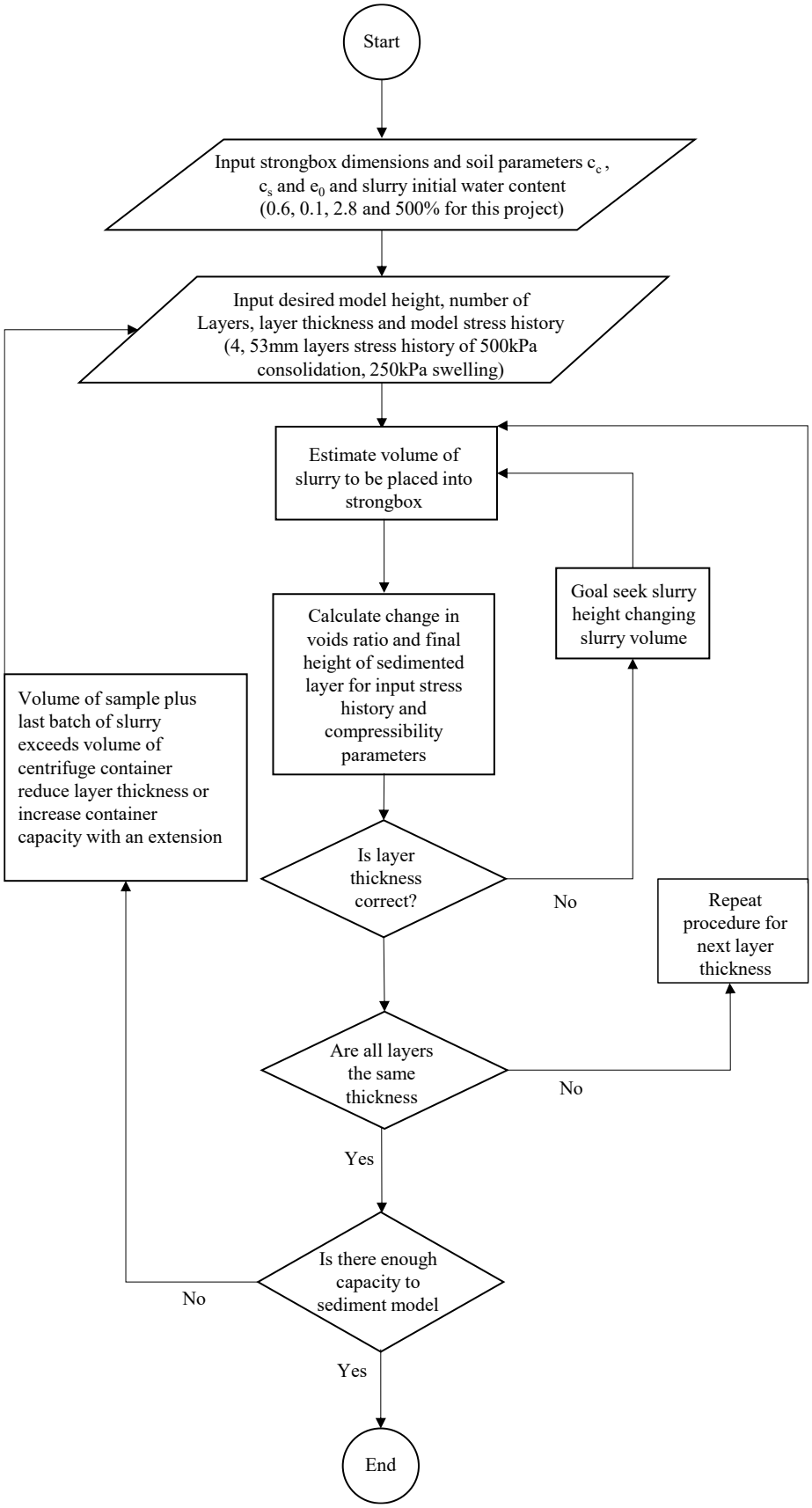

Figure 9.1- Flow diagram outlining the design procedure for the sedimented soil bed suitable for centrifuge modelling

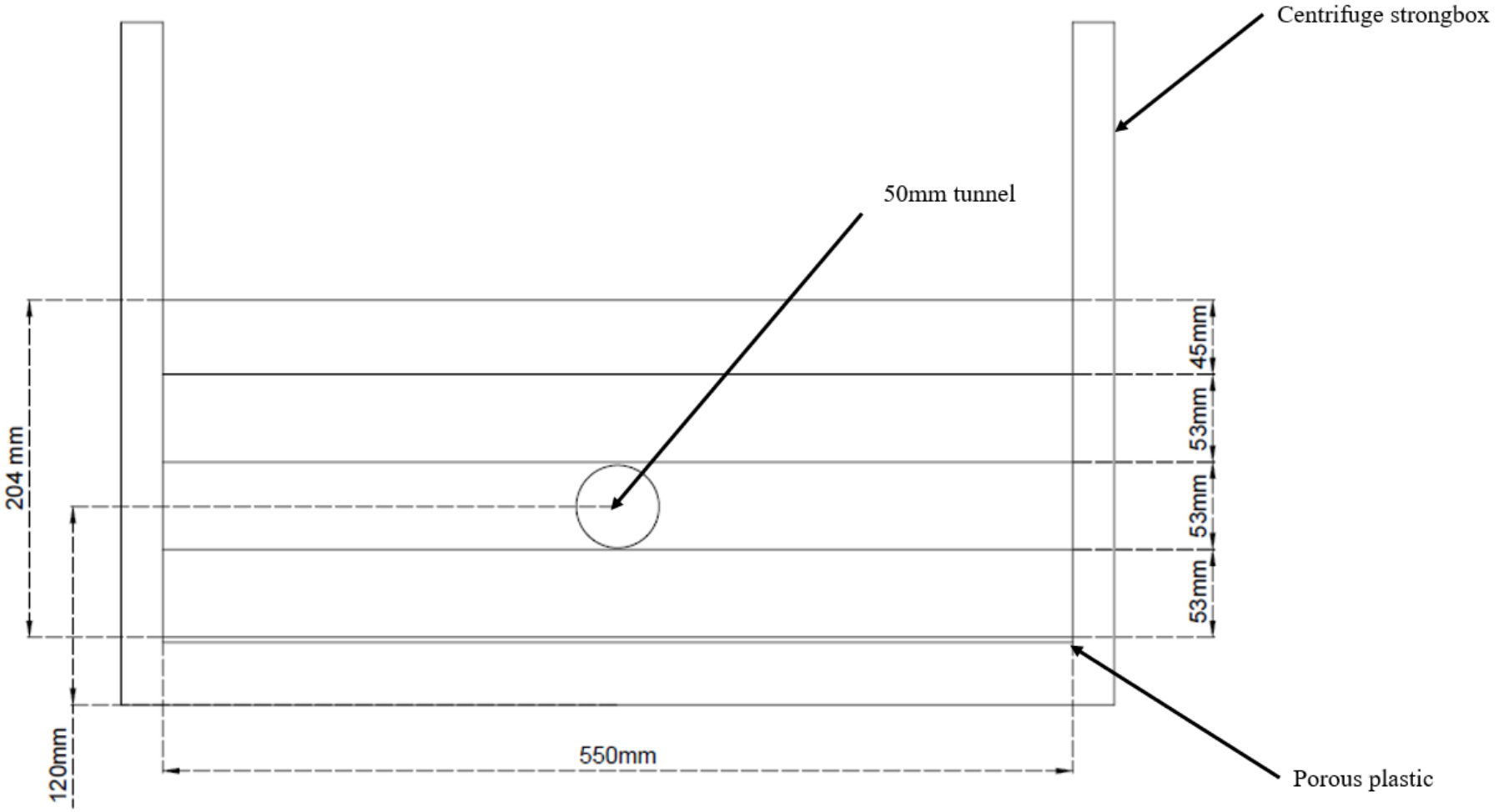

Figure 9.2- Designed sedimented soil bed geometry

Figure 9.3- Frame to secure filter paper during inflight sedimentation

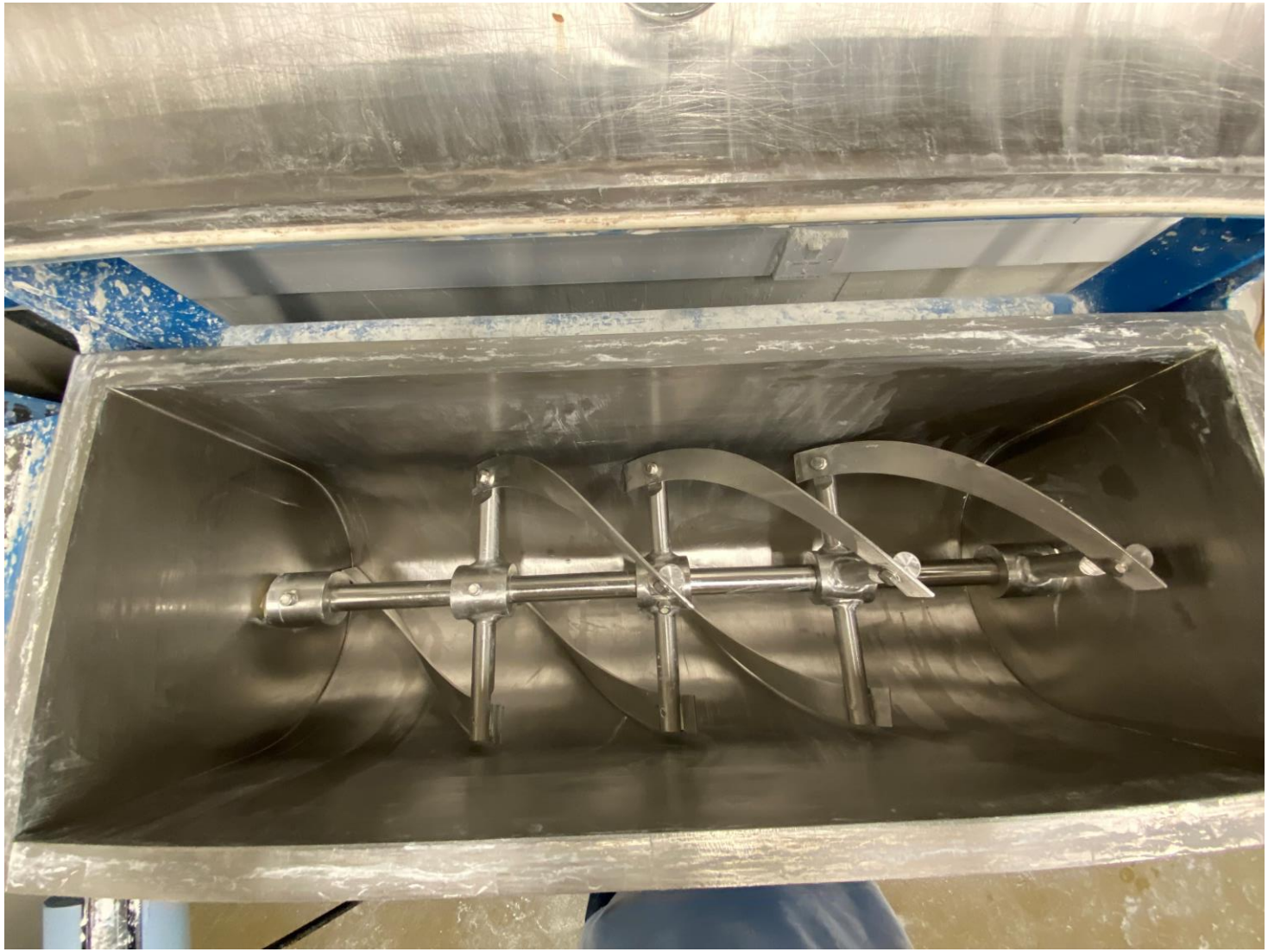

Figure 9.4- Thoroughly cleaned ribbon mixer completed before mixing a batch of slurry for sedimentation

Figure 9.5- Image taken during the slurry placement procedure; slurry being poured onto the breakwater in the strongbox

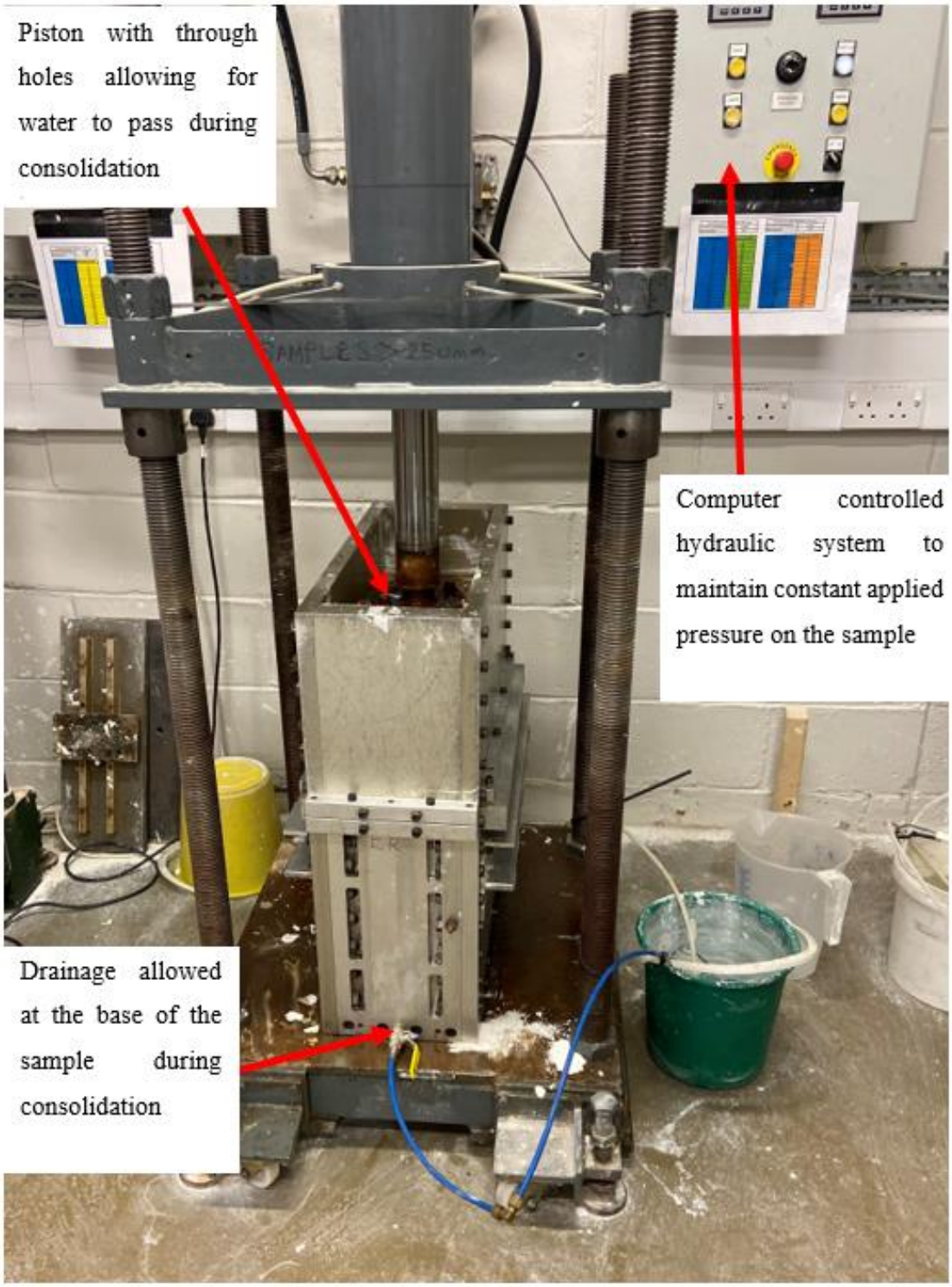

Figure 9.6- Centrifuge soil bed consolidating in the hydraulic press at City, University of London

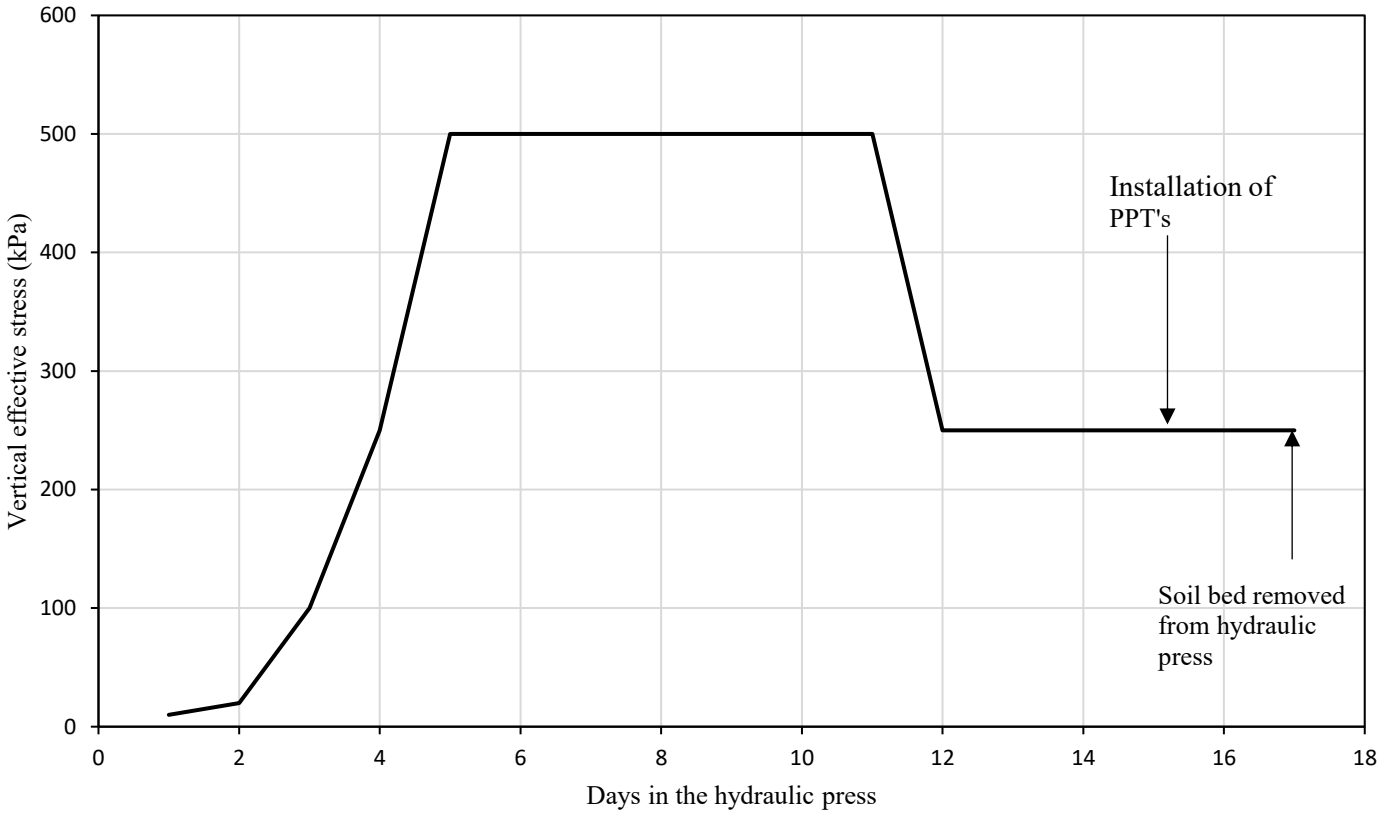

Figure 9.7- Stress history of the centrifuge soil beds

Figure 10.1- Tunnel fitting system

Figure 10.2- Tunnel fitting placed inside tunnel membrane

Figure 10.3- Tunnel fitting and membrane passed through centrifuge model and nut tightened to create an airtight seal

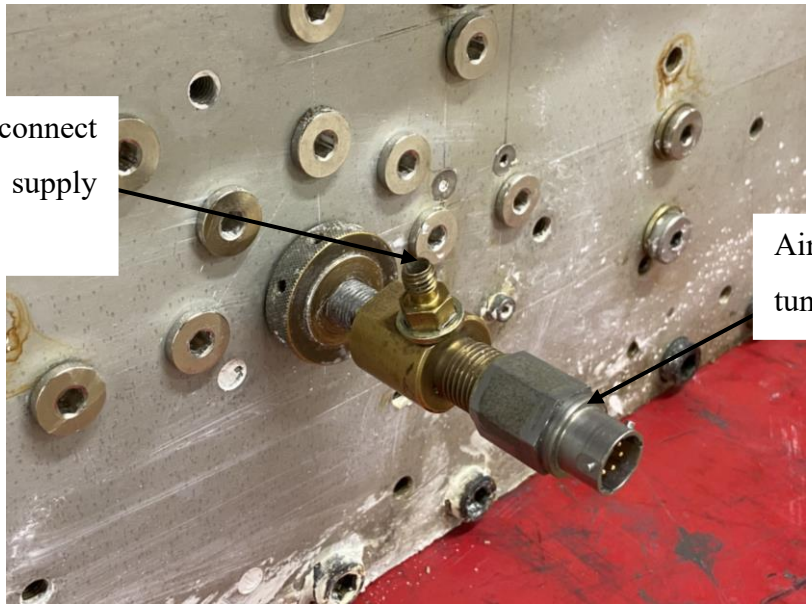

Figure 10.4- Tunnel manifold installed with an air pressure transducer and a fitting for airline so tunnel support pressure could be applied

Figure 10.5- An annotated image of the ground water table system used at the geotechnical centrifuge at City, University of London

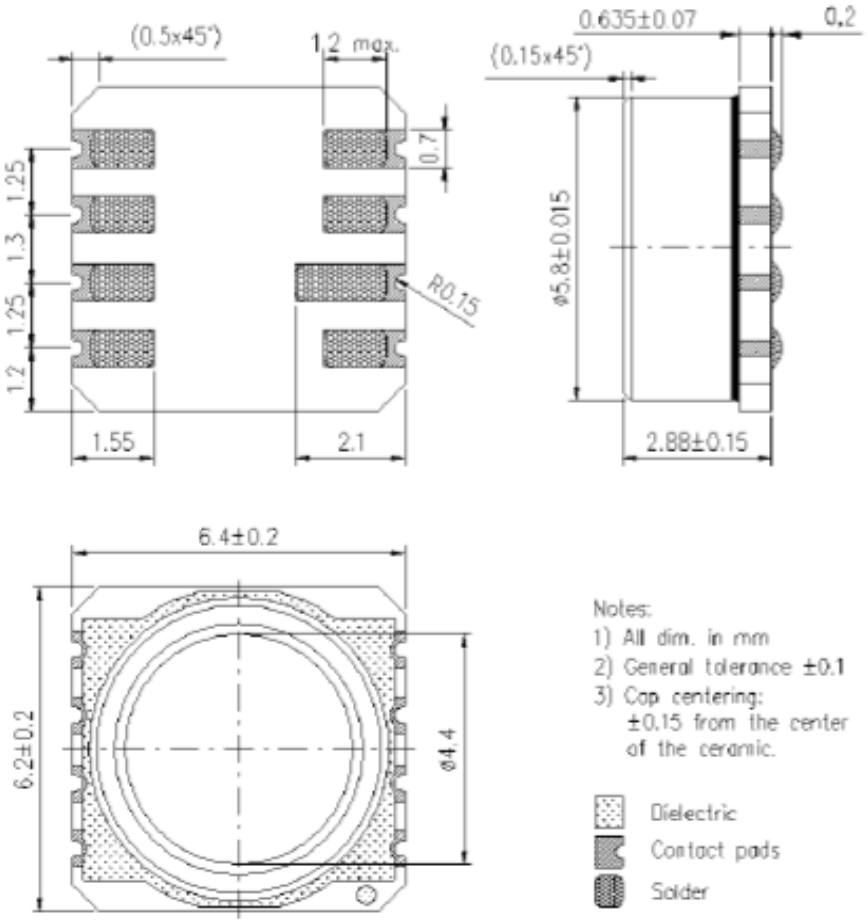

Figure 10.6– Details of the TE connectivity MS5407-AM selected for the City, University of London pore pressure tansducer

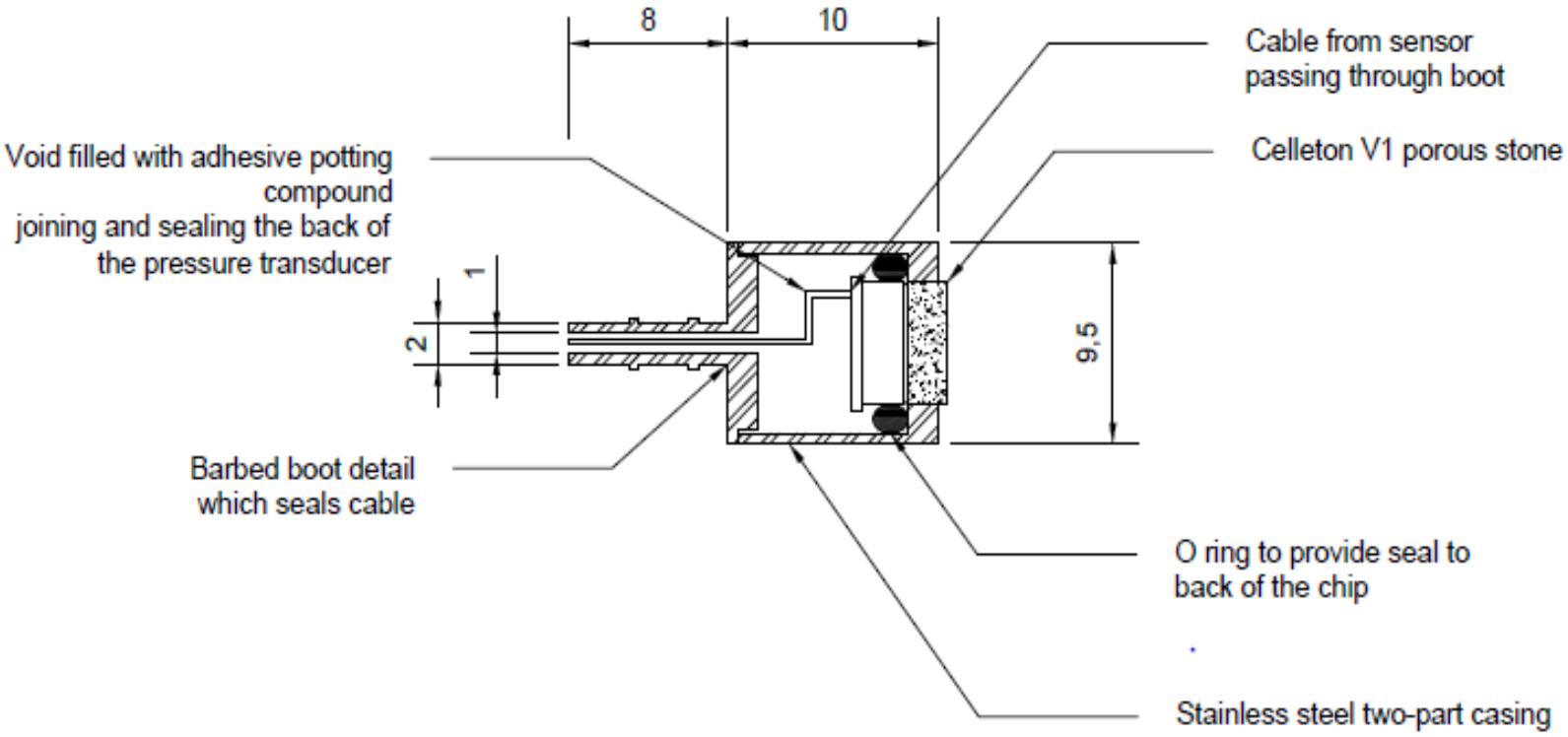

Figure 10.7 - A cross section through the City, University of London pore-water pressure transducer highlighting key features, note that the dimensions shown are in millimetre

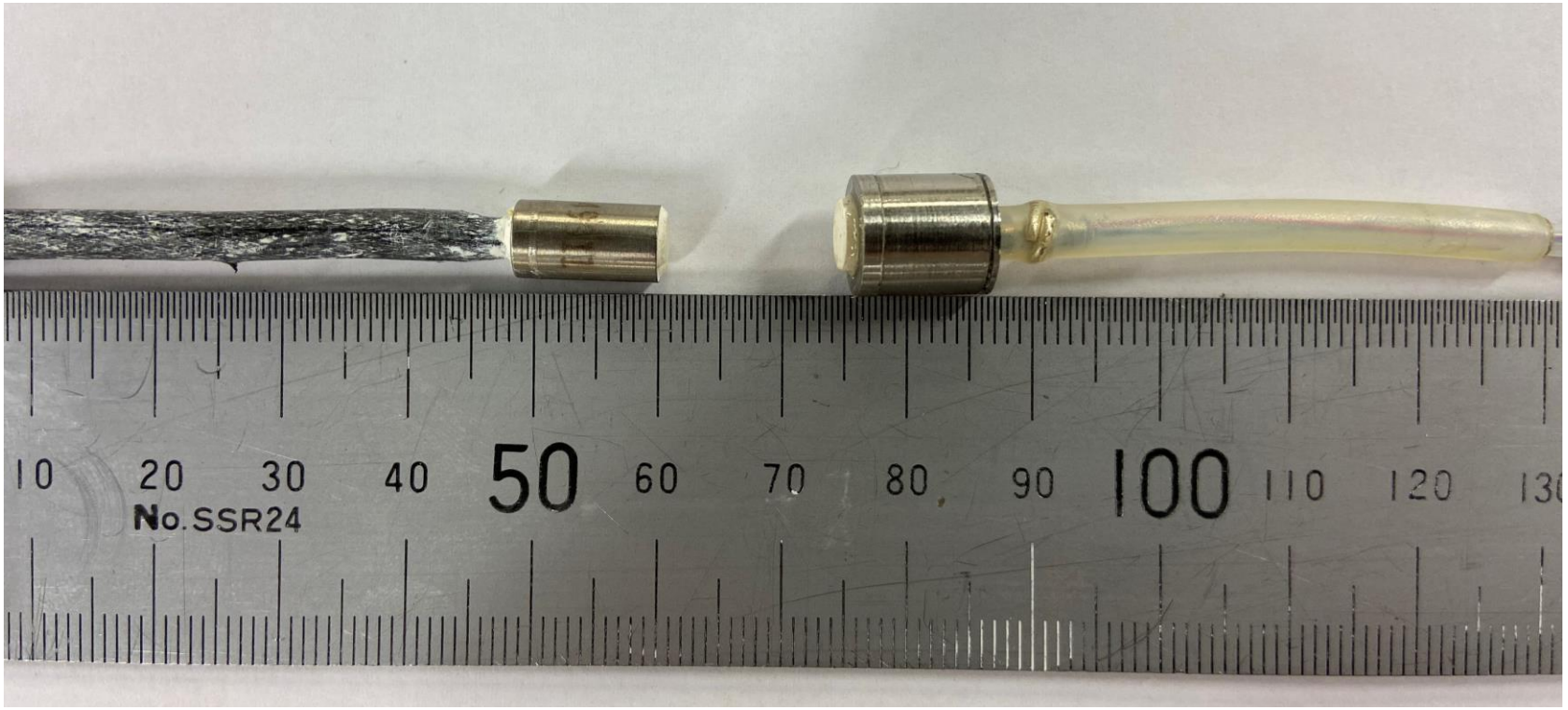

Figure 10.8– A side-by-side photograph comparison of a Druck PDCR81 pore pressure transducer and the new City, University of London pore-water pressure transducer

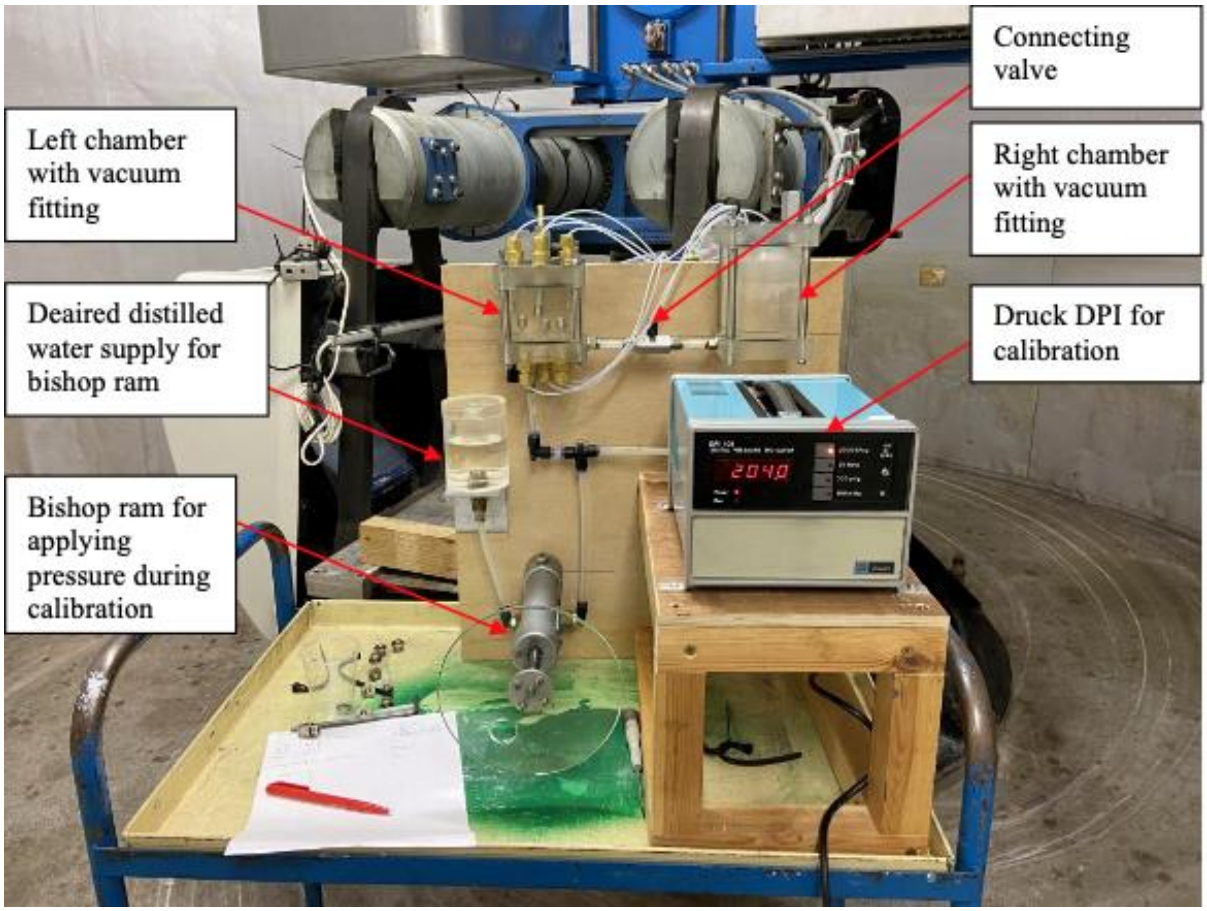

Figure 10.9 - A photograph of the PPT calibration system highlighting the key components of the system

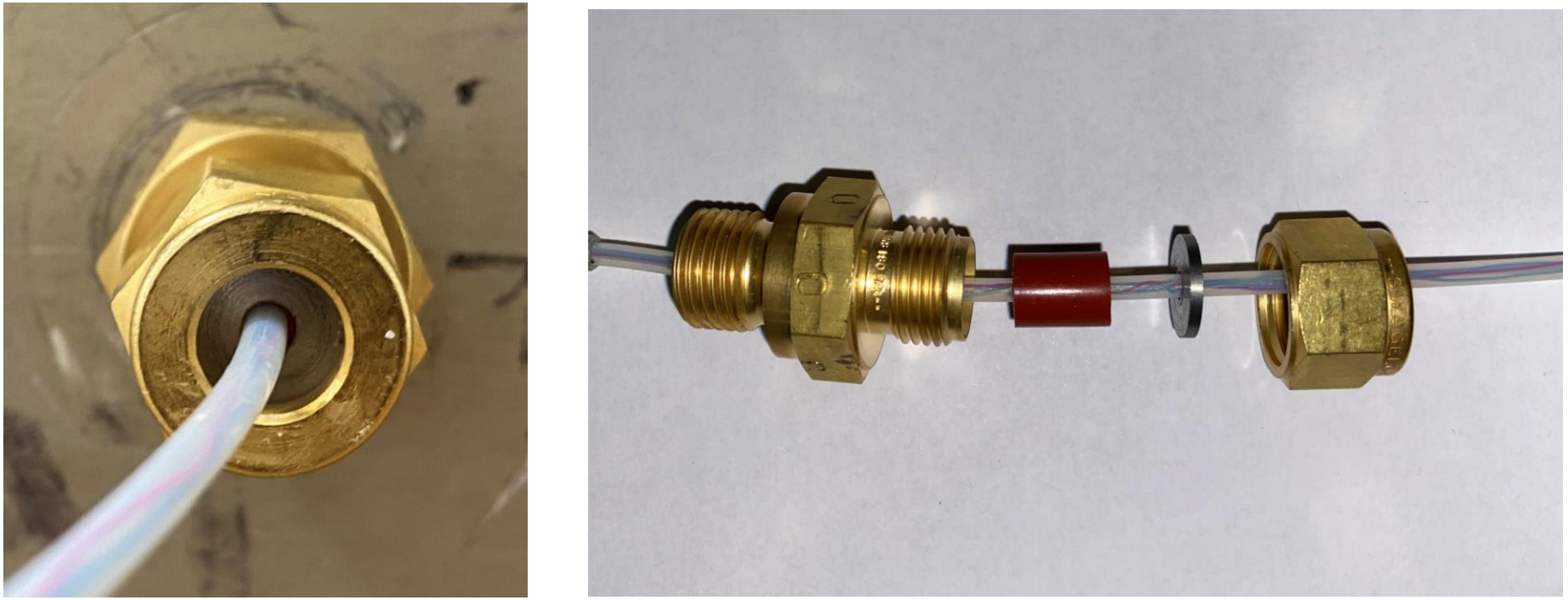

Figure 10.10- Shows a photograph of the of the Swagelok sealing system assembled and connected to the strongbox (left) and the components of the sealing system (right)

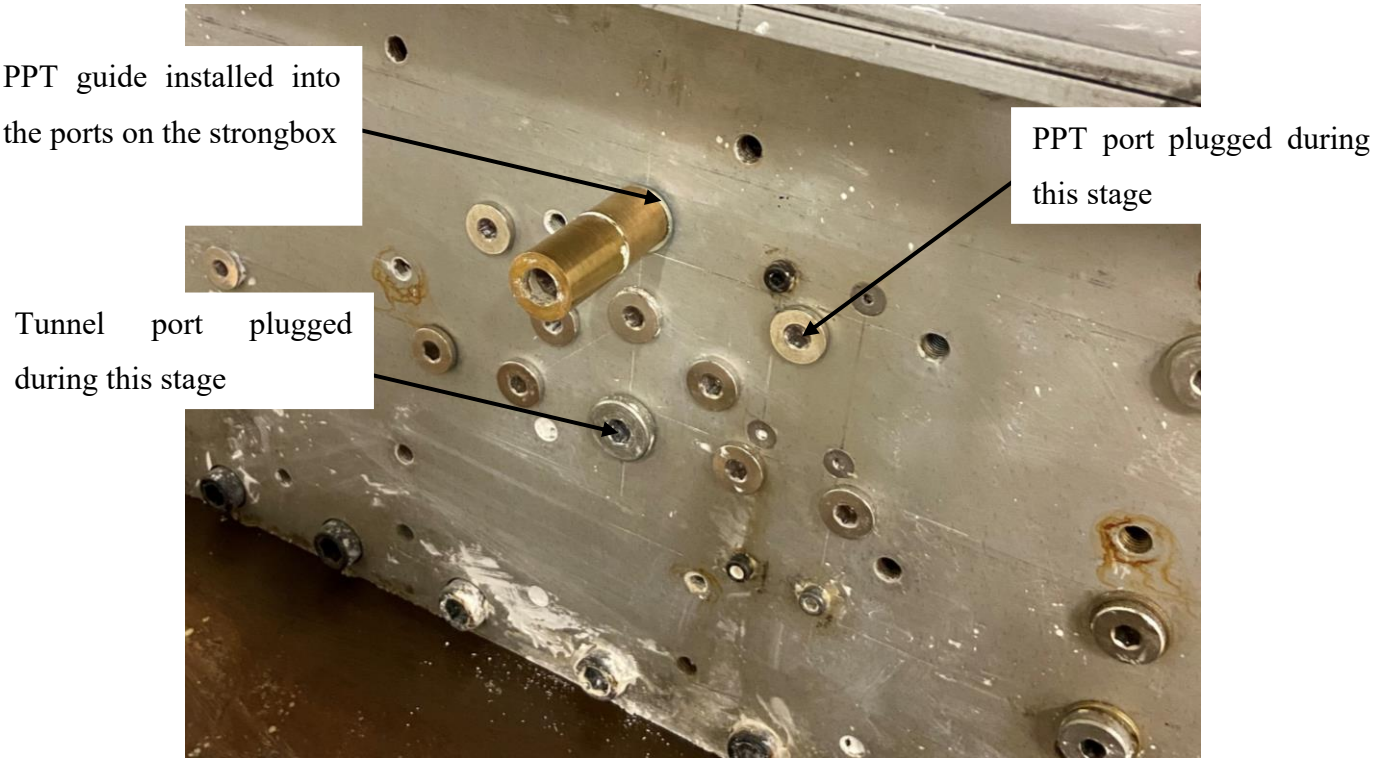

Figure 10.11- First step of installing a PPT into a centrifuge soil bed: installing the PPT guide into a PPT port

Figure 10.12- Second step of installing a PPT into a centrifuge soil bed: create a bore to the midpoint of the model using a thin-walled seamless cutter

Figure 10.13- Third step of installing a PPT into a centrifuge soil bed: place a small amount of deaired slurry at the end of the bore

Figure 10.14- Fourth step of installing a PPT into a centrifuge soil bed: place a saturated calibrated PPT into the placement tool

Figure 10.15- Fifth step of installing a PPT into a centrifuge soil bed: place PPT at the end of the bore, remove the placing tool and fill behind the PPT with deaired slurry

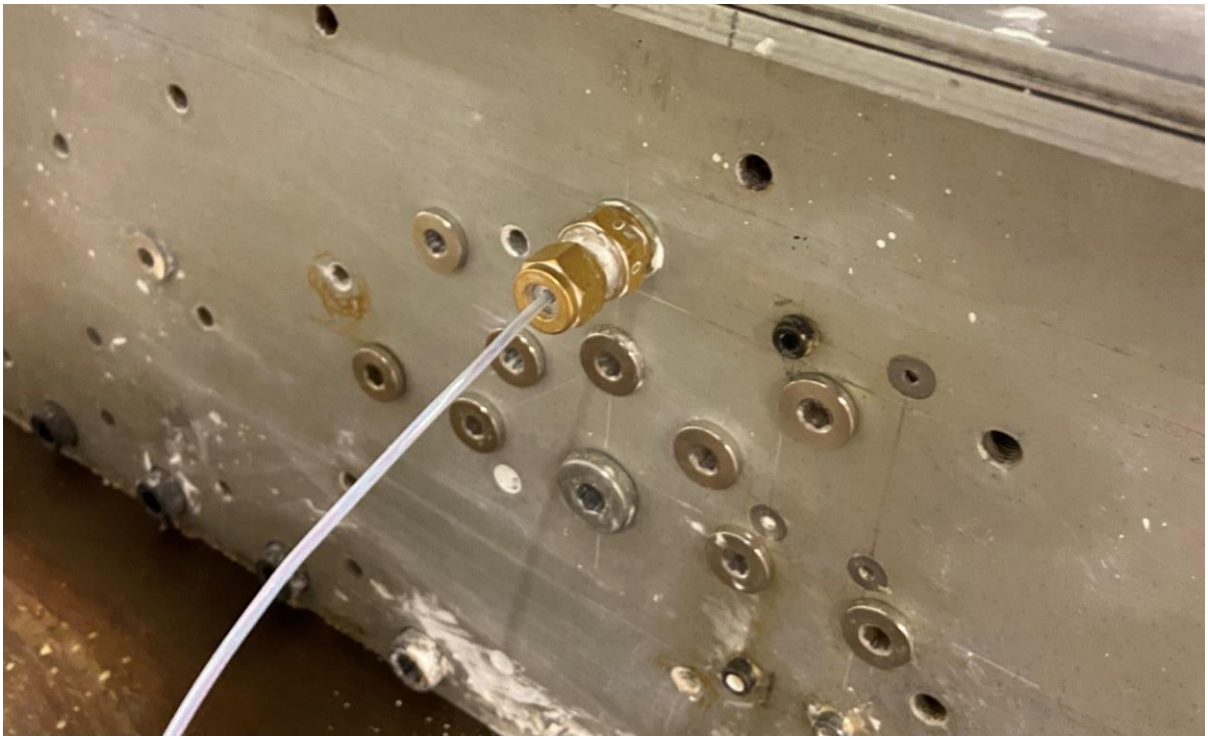

Figure 10.16: Sixth step of installing a PPT into a centrifuge soil bed, PPT was sealed using the Swagelok system

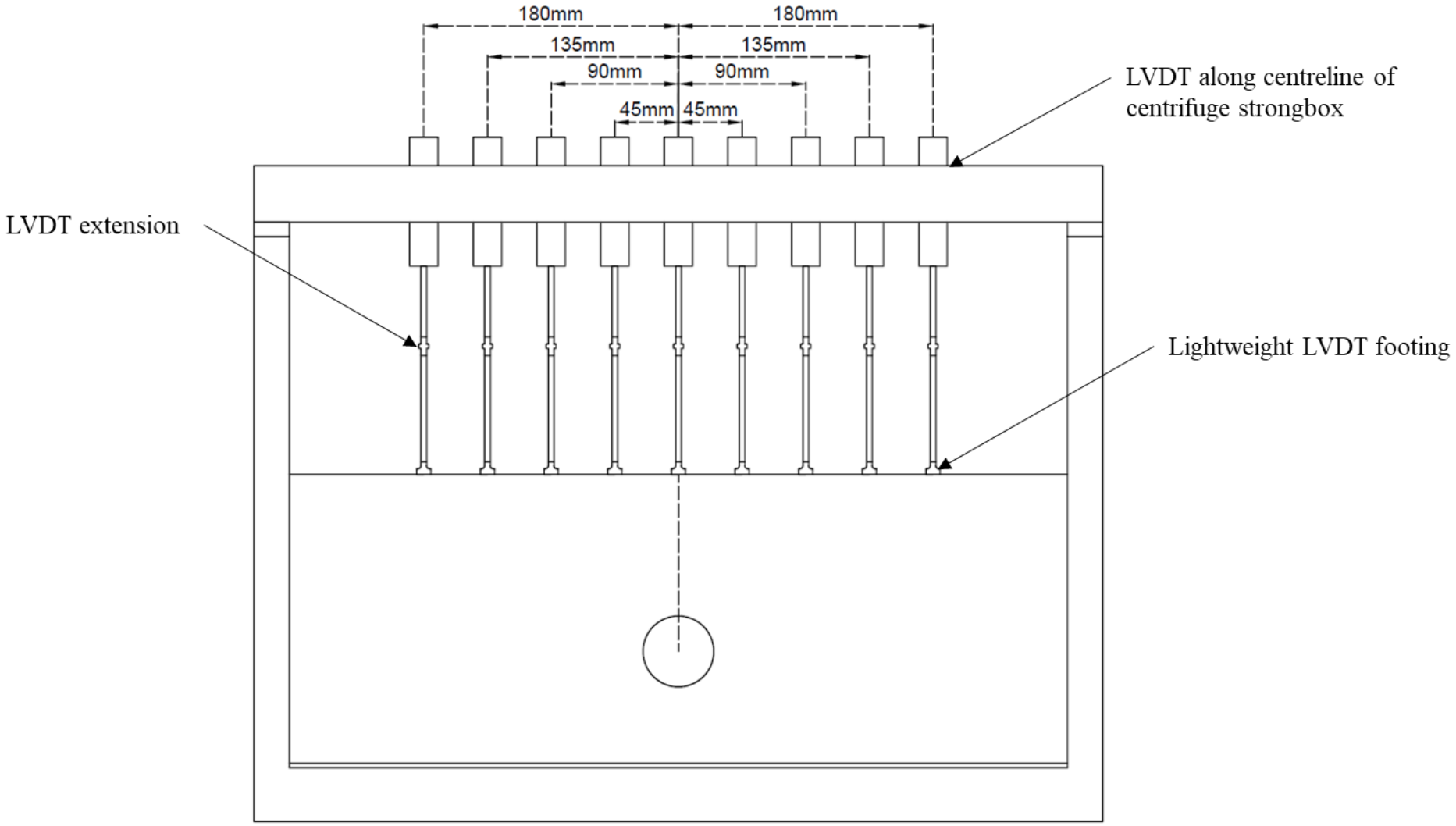

Figure 10.17- Schematic of the LVDT rack arrangement used in the centrifuge tunnel tests

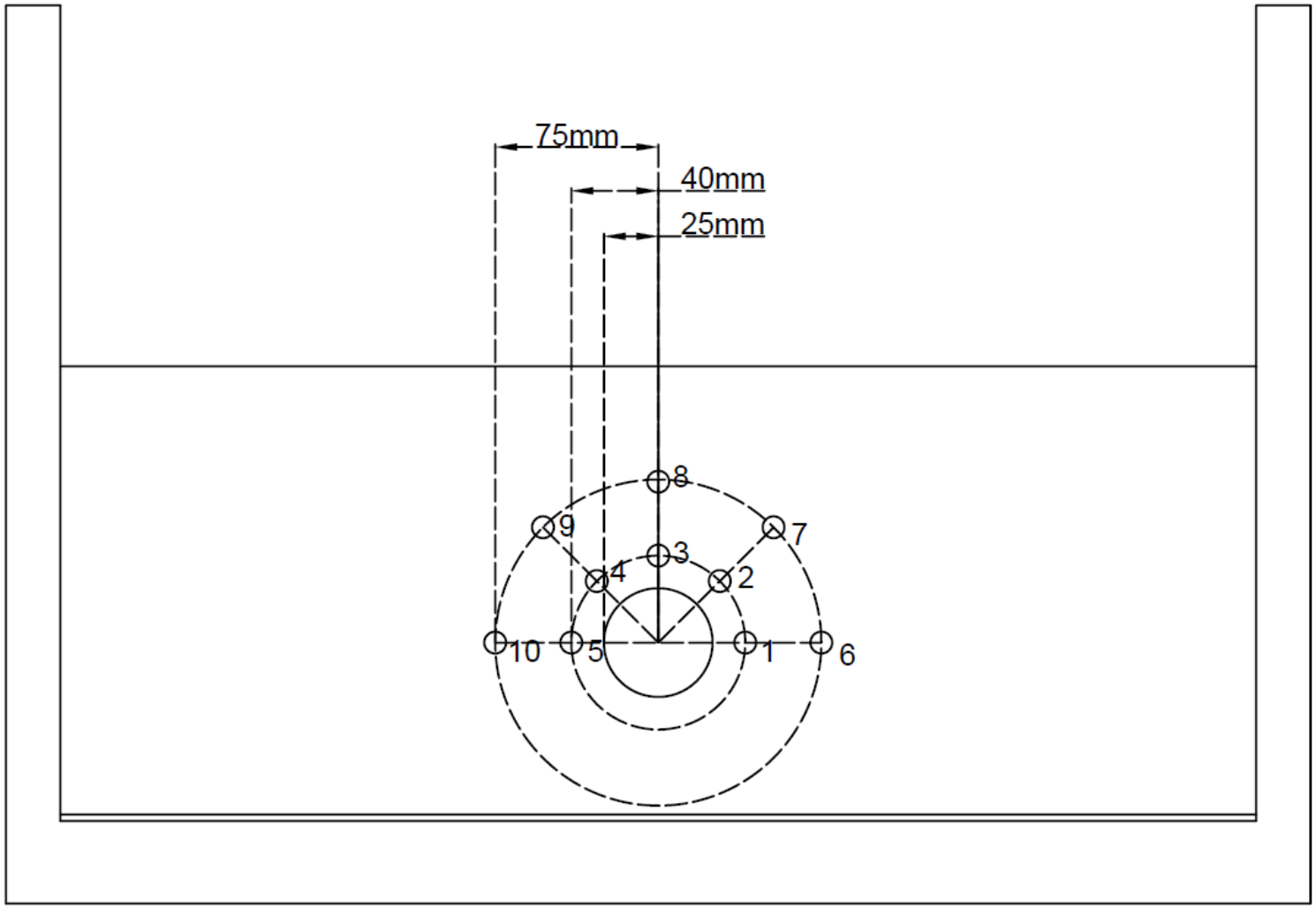

Figure 10.18- PPT locations and corresponding port numbers when looking at the back of the centrifuge strongbox

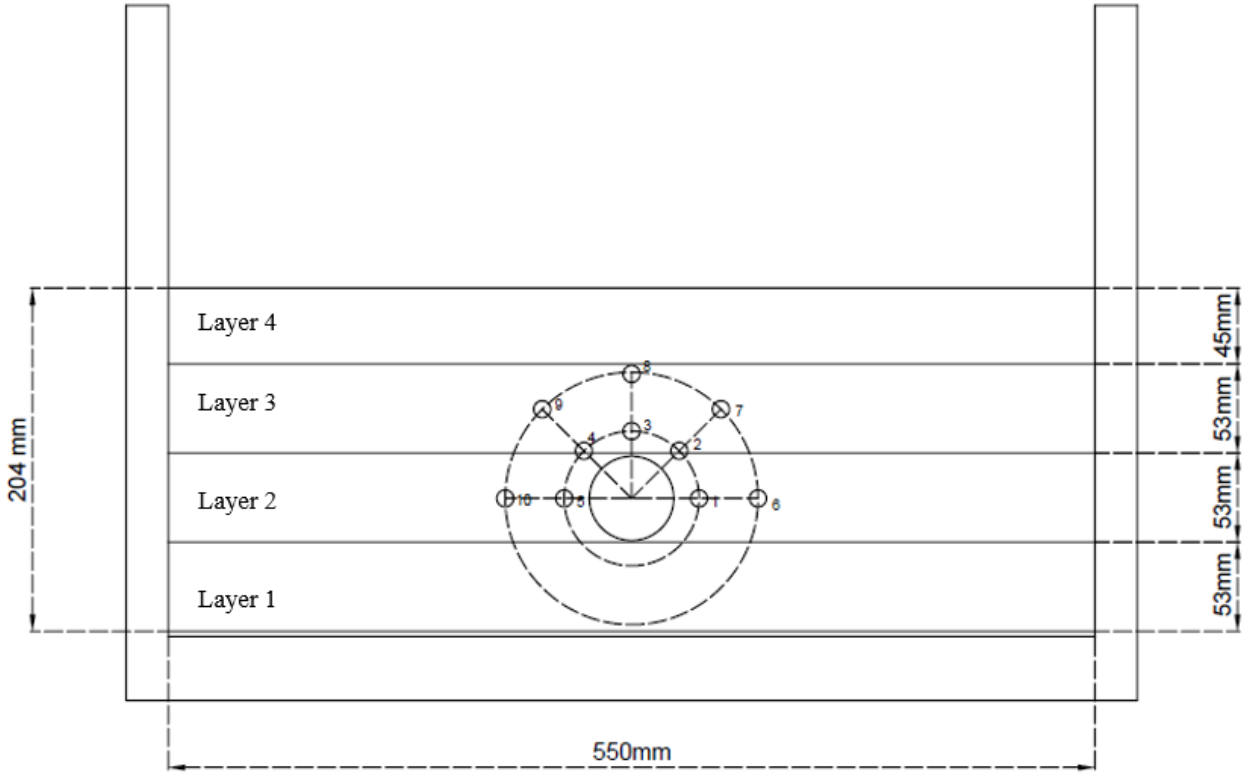

PPT number	Bore filled with
1	Speswhite
2	Polwhite E
3	Polwhite E
4	Polwhite E
5	Speswhite
6	Speswhite
7	Speswhite
8	Polwhite E
9	Speswhite
10	Speswhite

Figure 10.19- PPT's in the sedimented soil bed and details of which bores were filled with a Speswhite or Polwhite E kaolin clay slurry

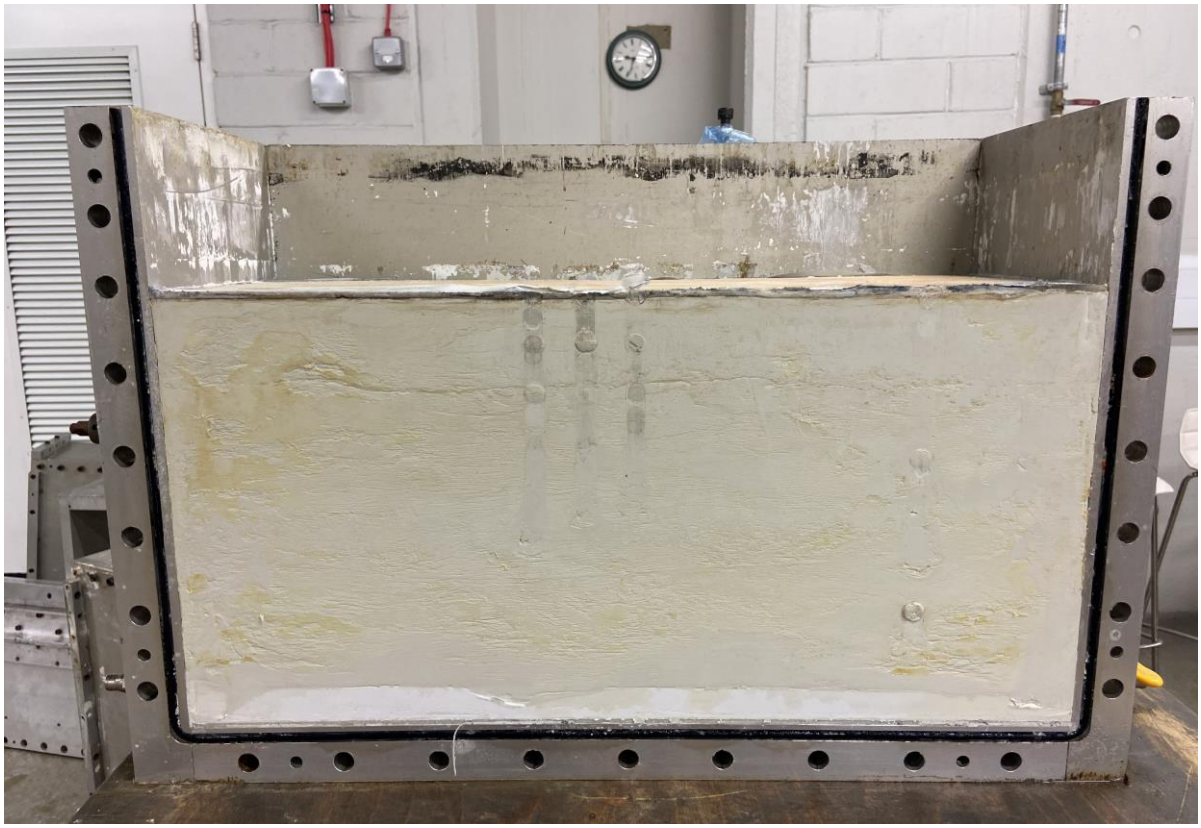

Figure 10.20- Front wall of the centrifuge strongbox was removed to gain access to the soil bed

Figure 10.21- Centrifuge soil bed trimmed to correct height using a guide and box cutter

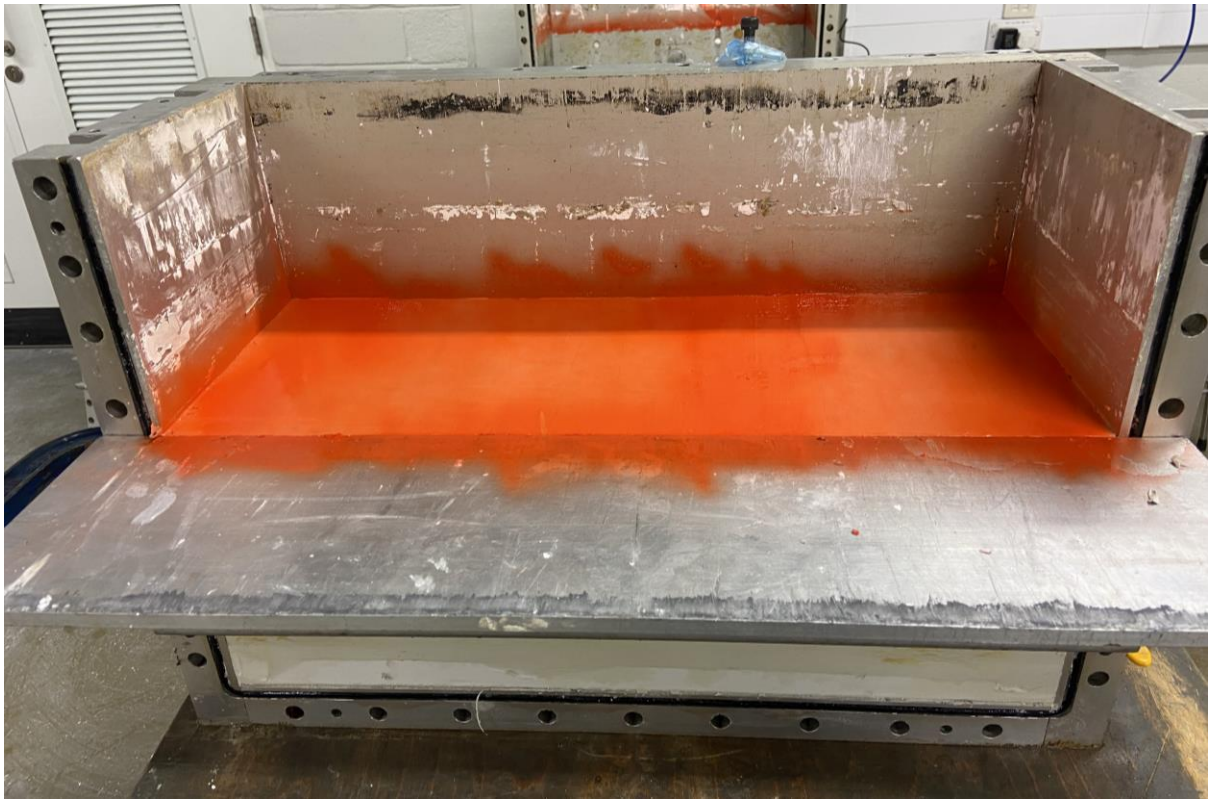

Figure 10.22- Centrifuge soil bed trimmed to correct height and surface sprayed with Plastidip to prevent drying

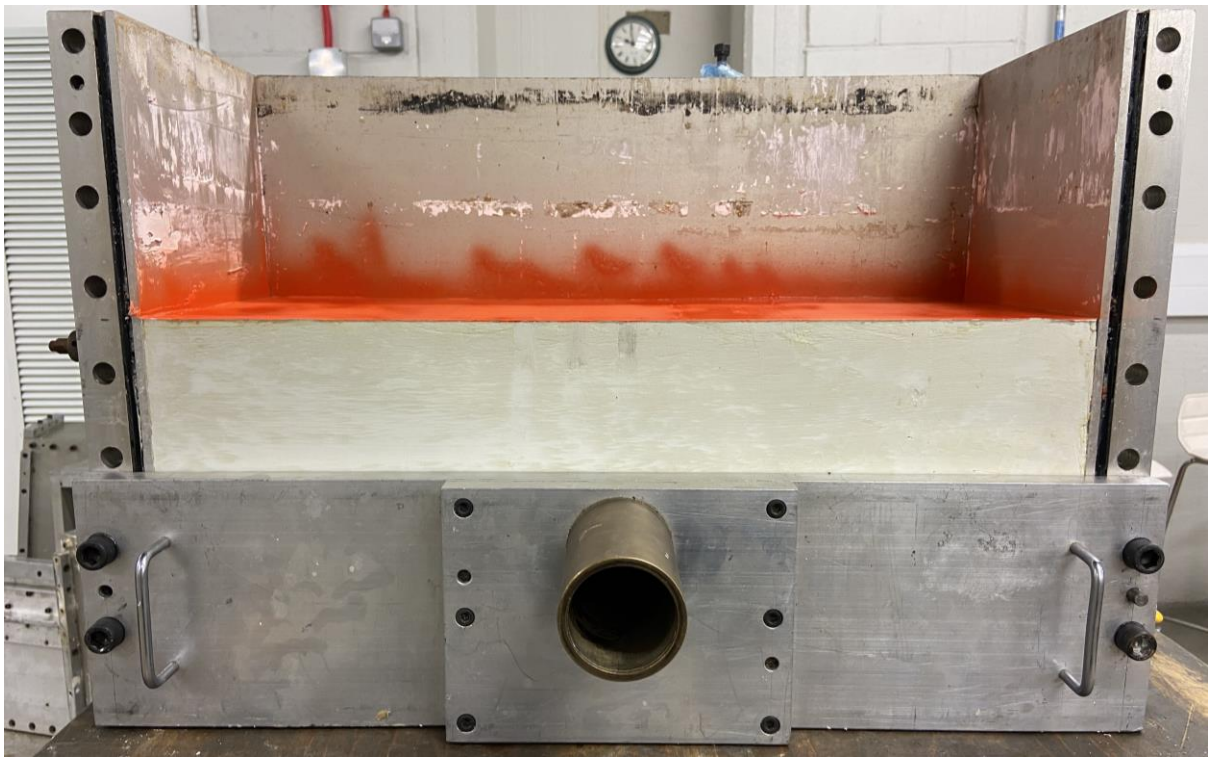

Figure 10.23- Tunnel guide installed to ensure that the tunnel bore was located in the correct location

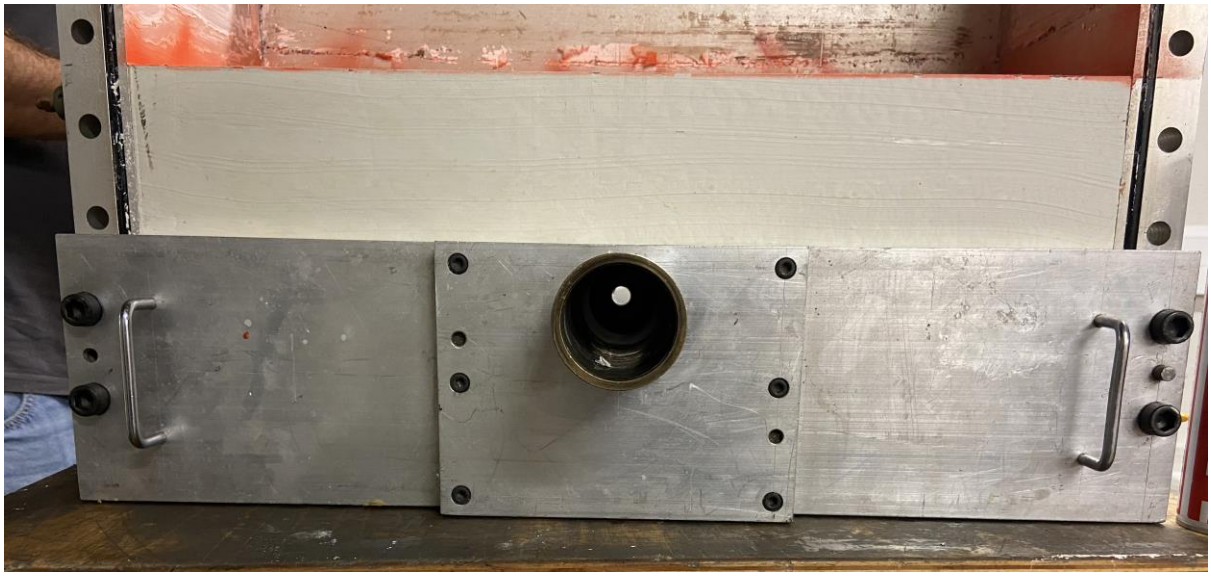

Figure 10.24- After the tunnel cavity has been bored into the soil, tunnel port was visible at the back of the bore

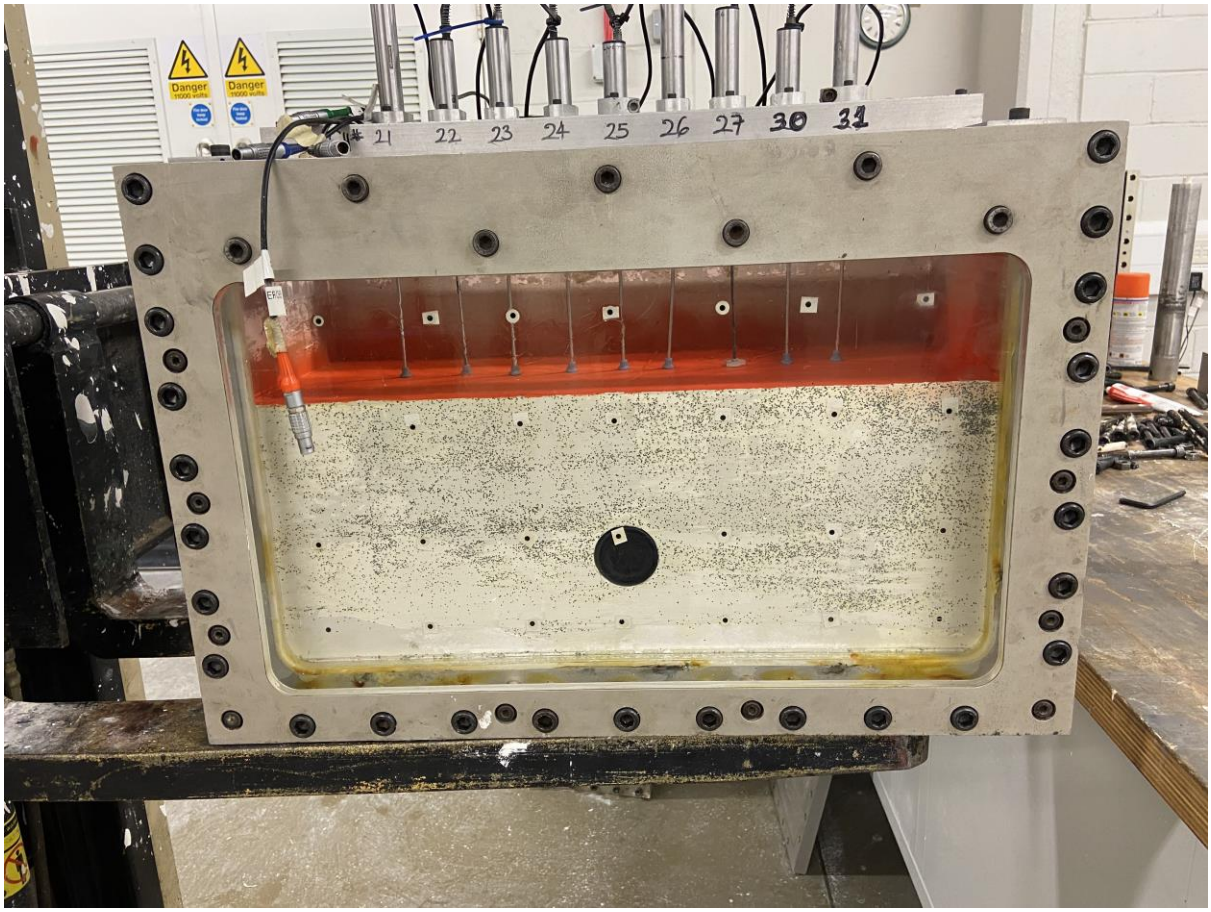

Figure 10.25- Tunnel membrane and union were installed; observation window was secured and the LVDT rack was secured to the strongbox

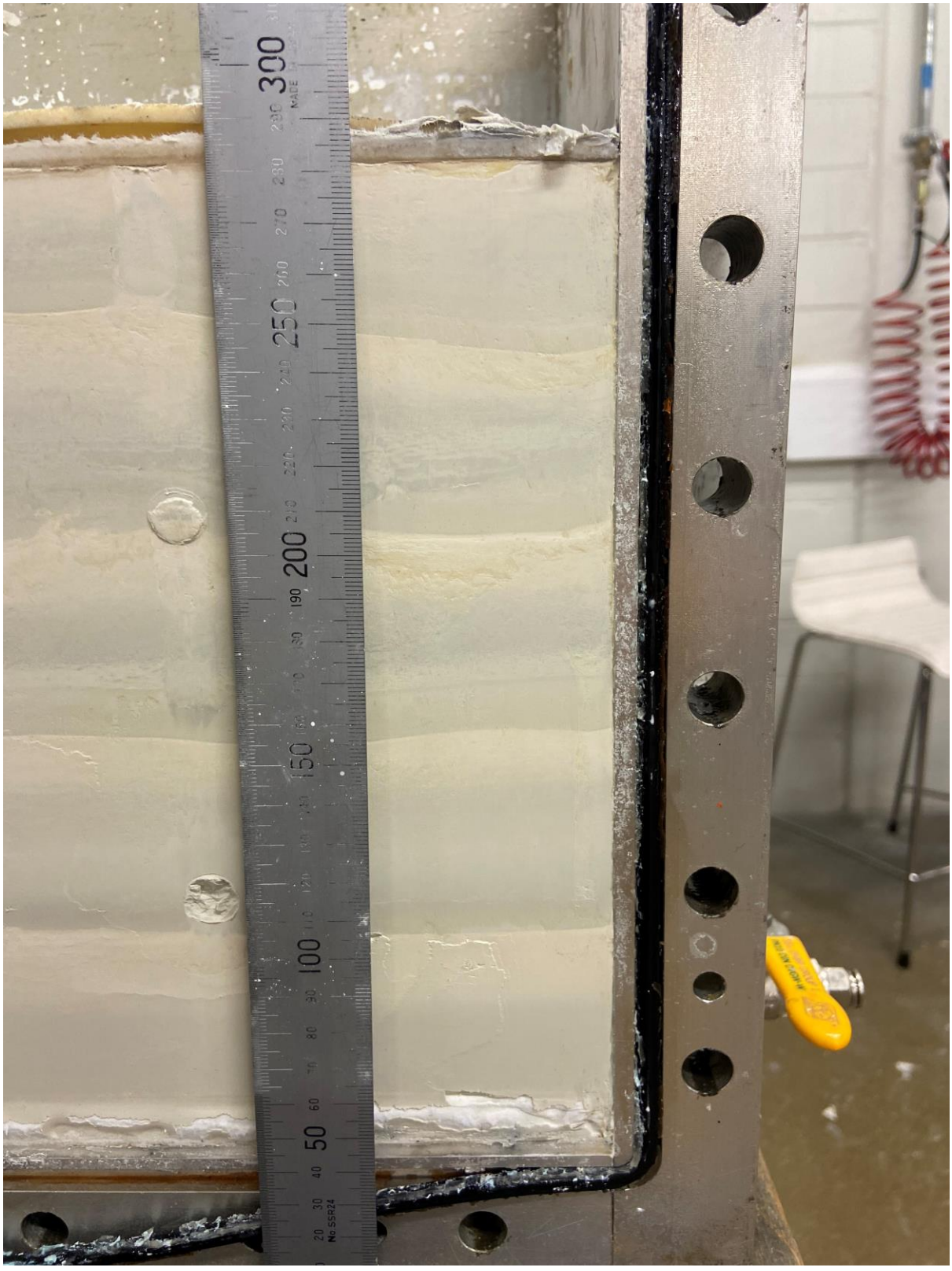

Figure 11.1- Five visible layers when the front of the strongbox was removed during the model making procedure

Figure 11.2- Photograph of sedimented soil layers across the width of the strongbox taken post centrifuge test

Figure 11.3- Sedimented layers visible approximately 10mm behind front face of the soil bed

Figure 11.4- Section through the sedimented centrifuge soil bed

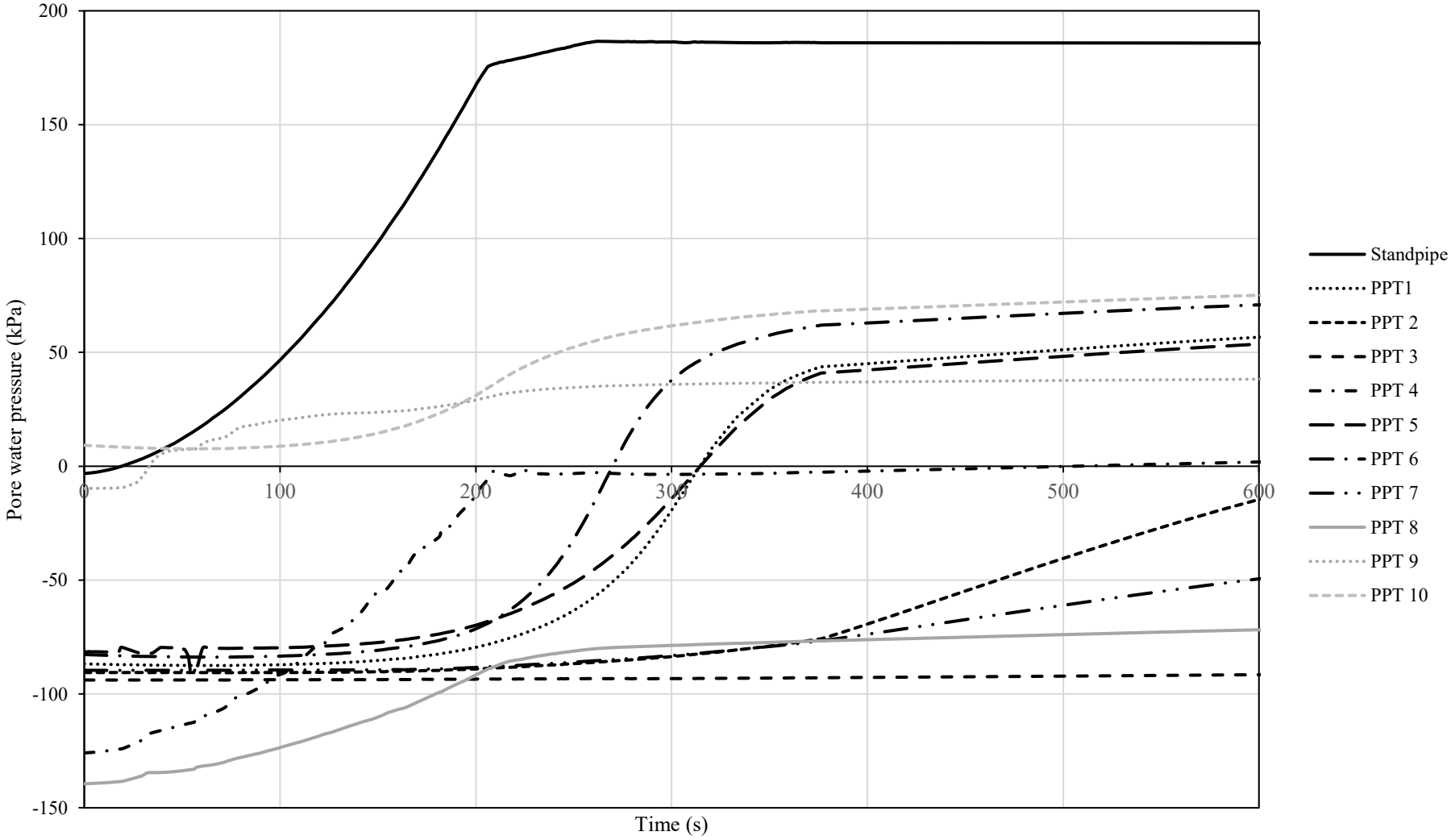

Figure 11.5- Initial response of the PPT within the Speswhite kaolin clay centrifuge soil bed

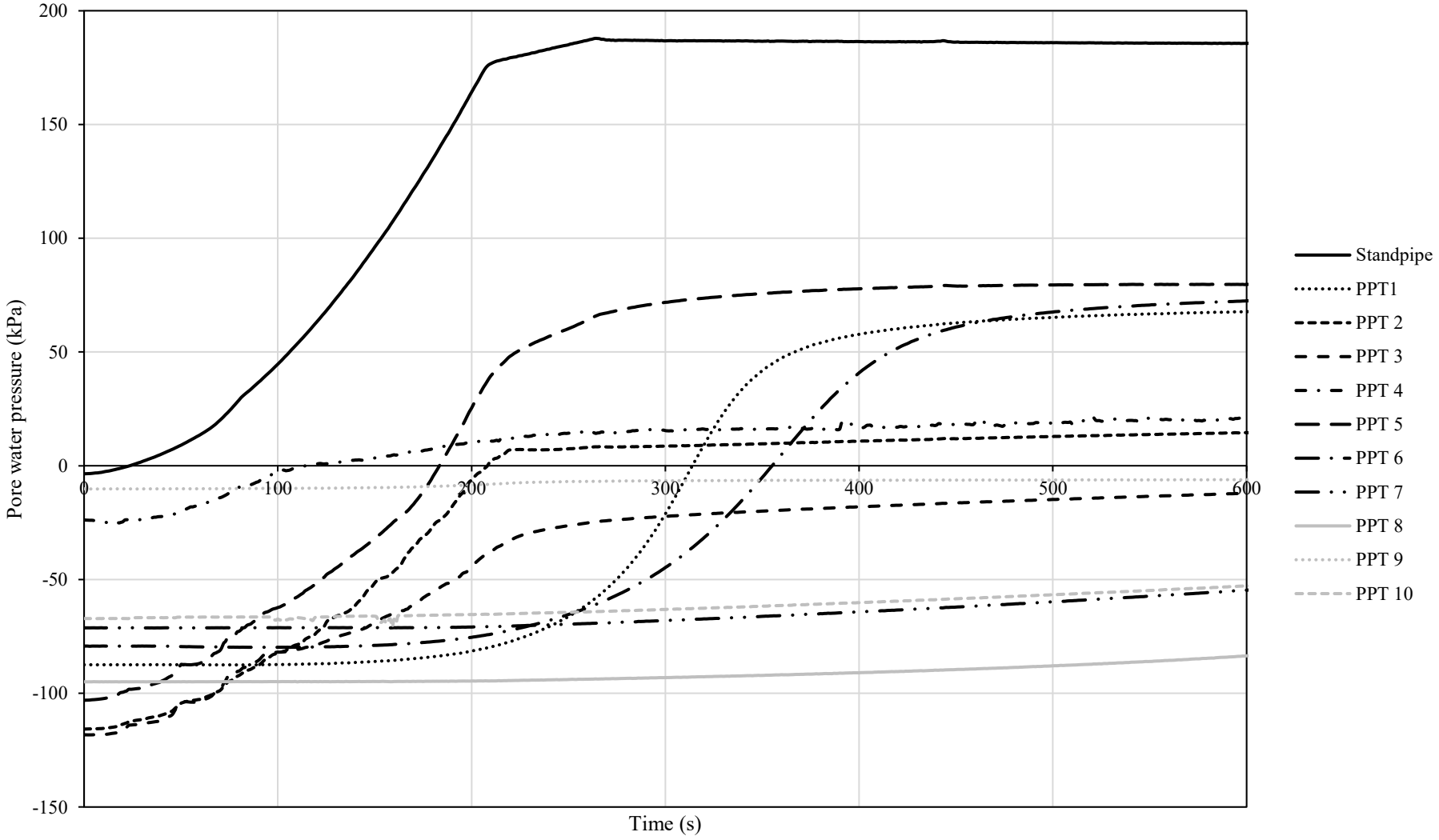

Figure 11.6- Initial response of the PPT within the Speswhite: Polwhite E kaolin clay centrifuge soil bed

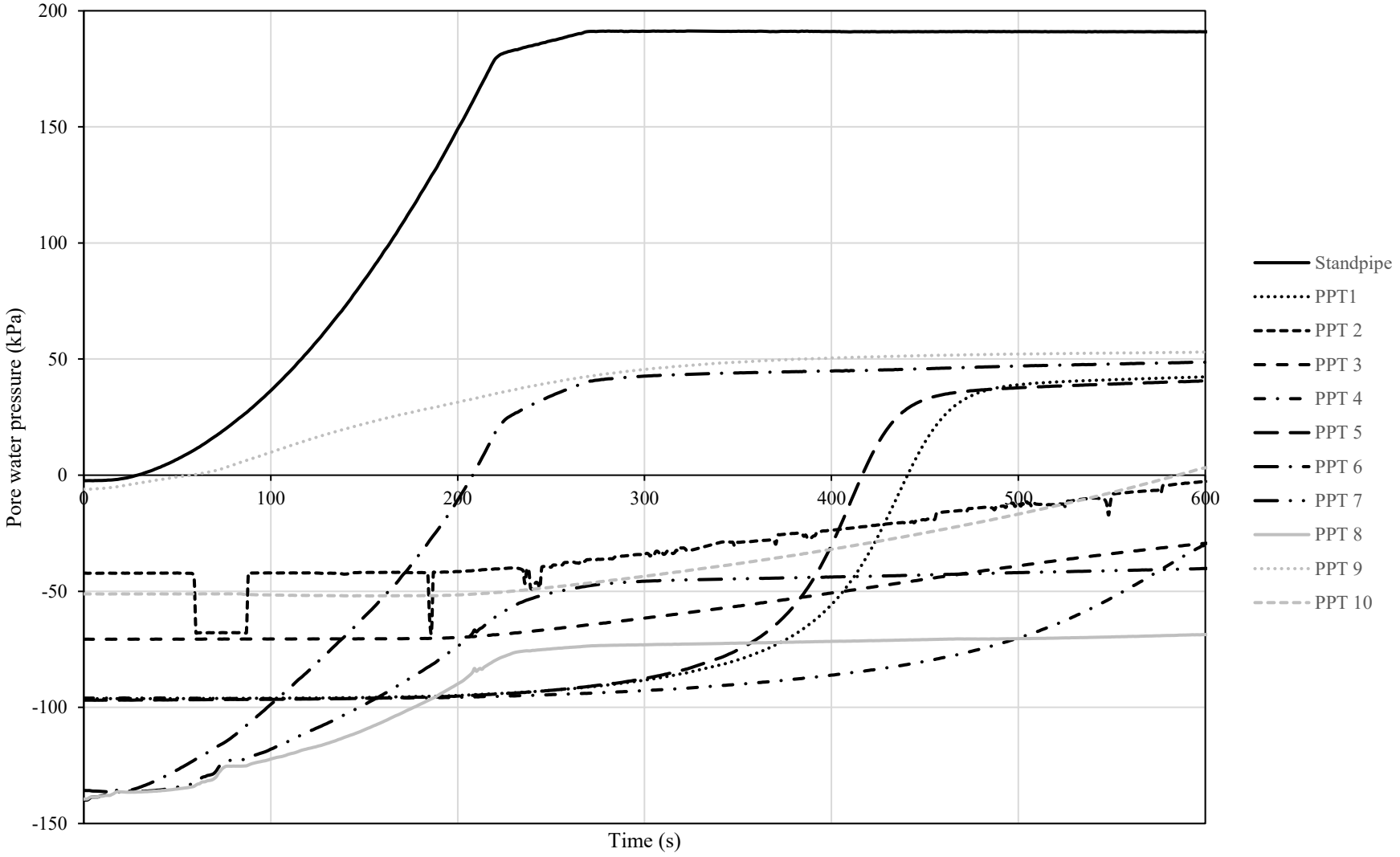

Figure 11.7- Initial response of the PPT within the sedimented centrifuge soil bed

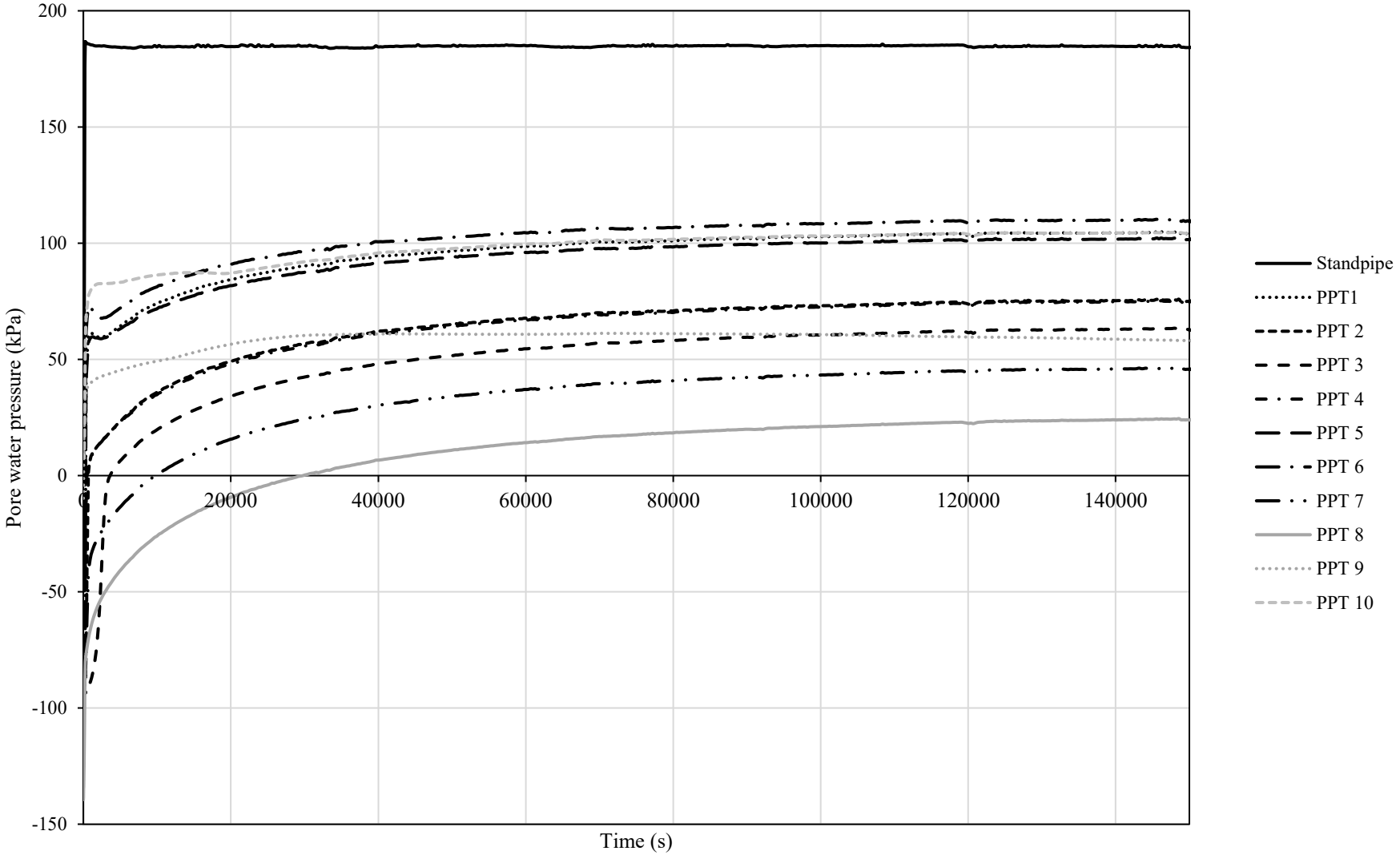

Figure 11.8- Response of the PPT to inflight consolidation within the Speswhite kaolin clay centrifuge soil bed

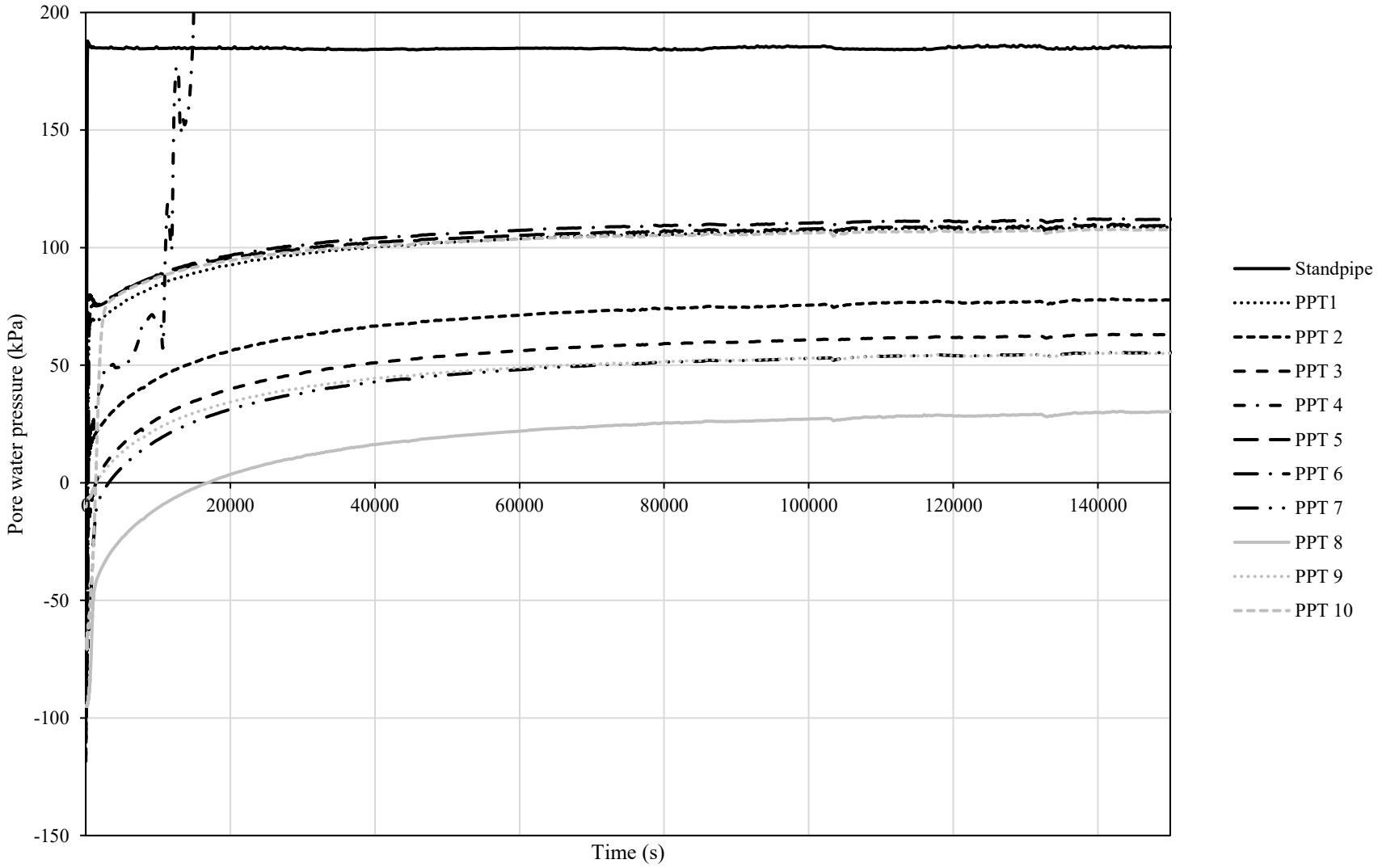

Figure 11.9- Response of the PPT to inflight consolidation within the Speswhite: Polwhite E kaolin clay centrifuge soil bed

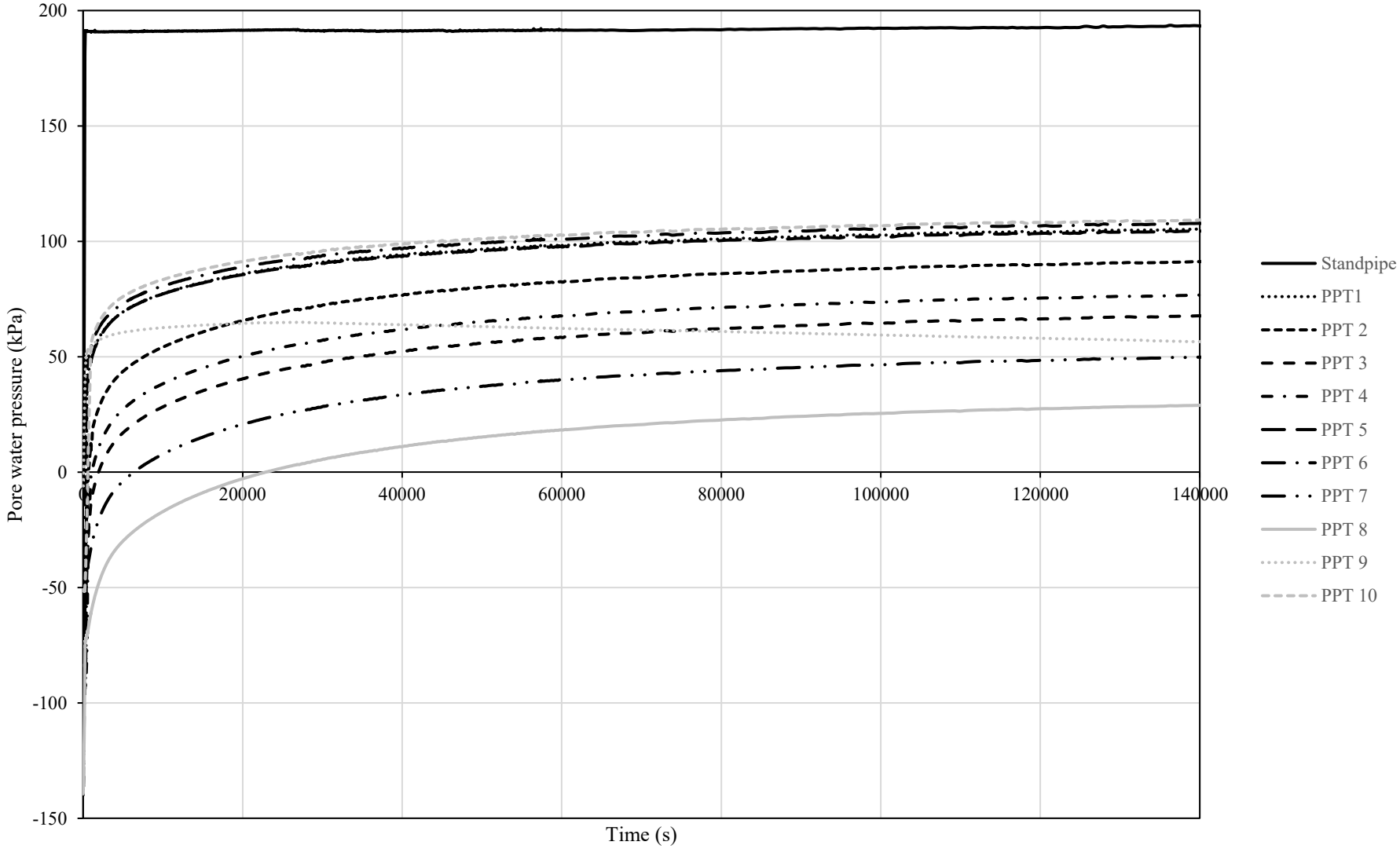

Figure 11.10- Response of the PPT to inflight consolidation within the sedimented centrifuge soil bed

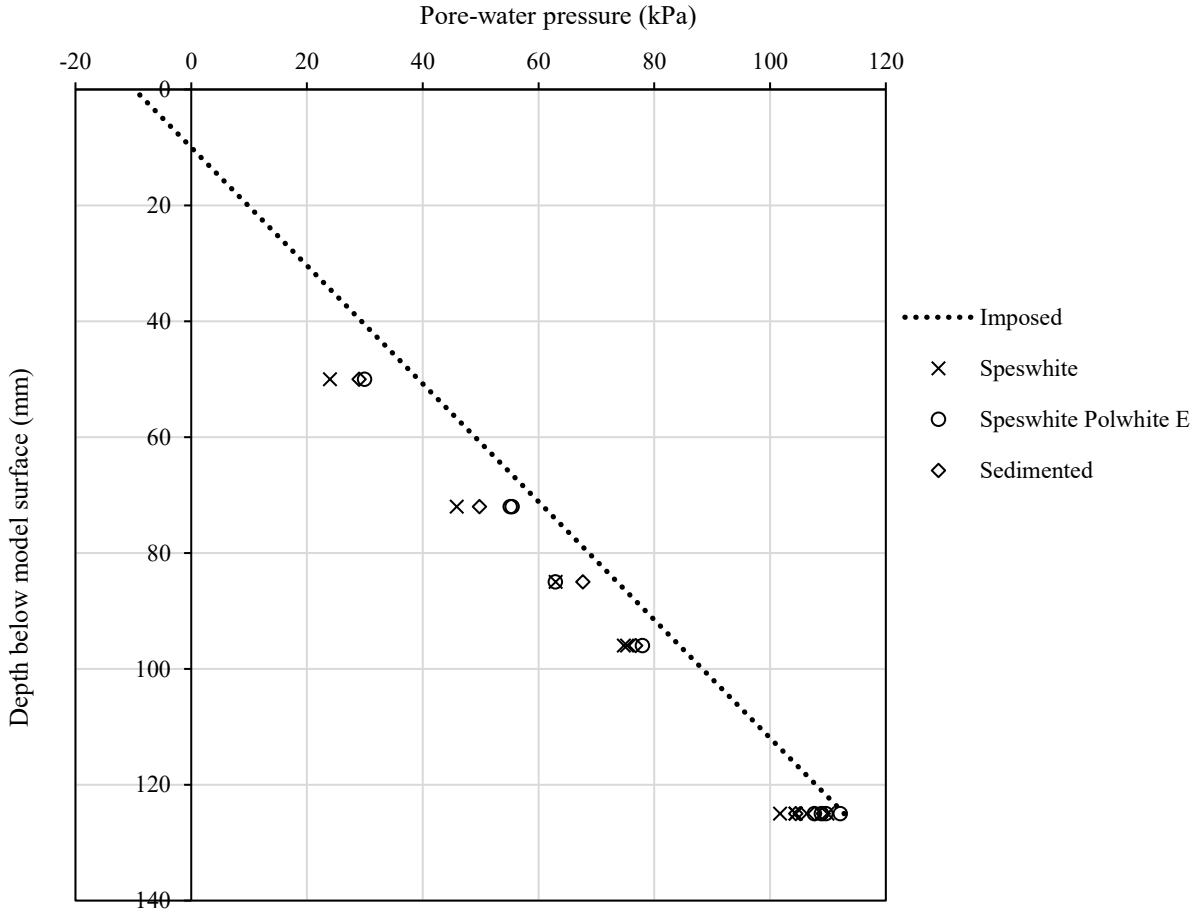

Figure 11.11-Measured against imposed ground water profile at the end of the inflight consolidation for the three centrifuge soil beds

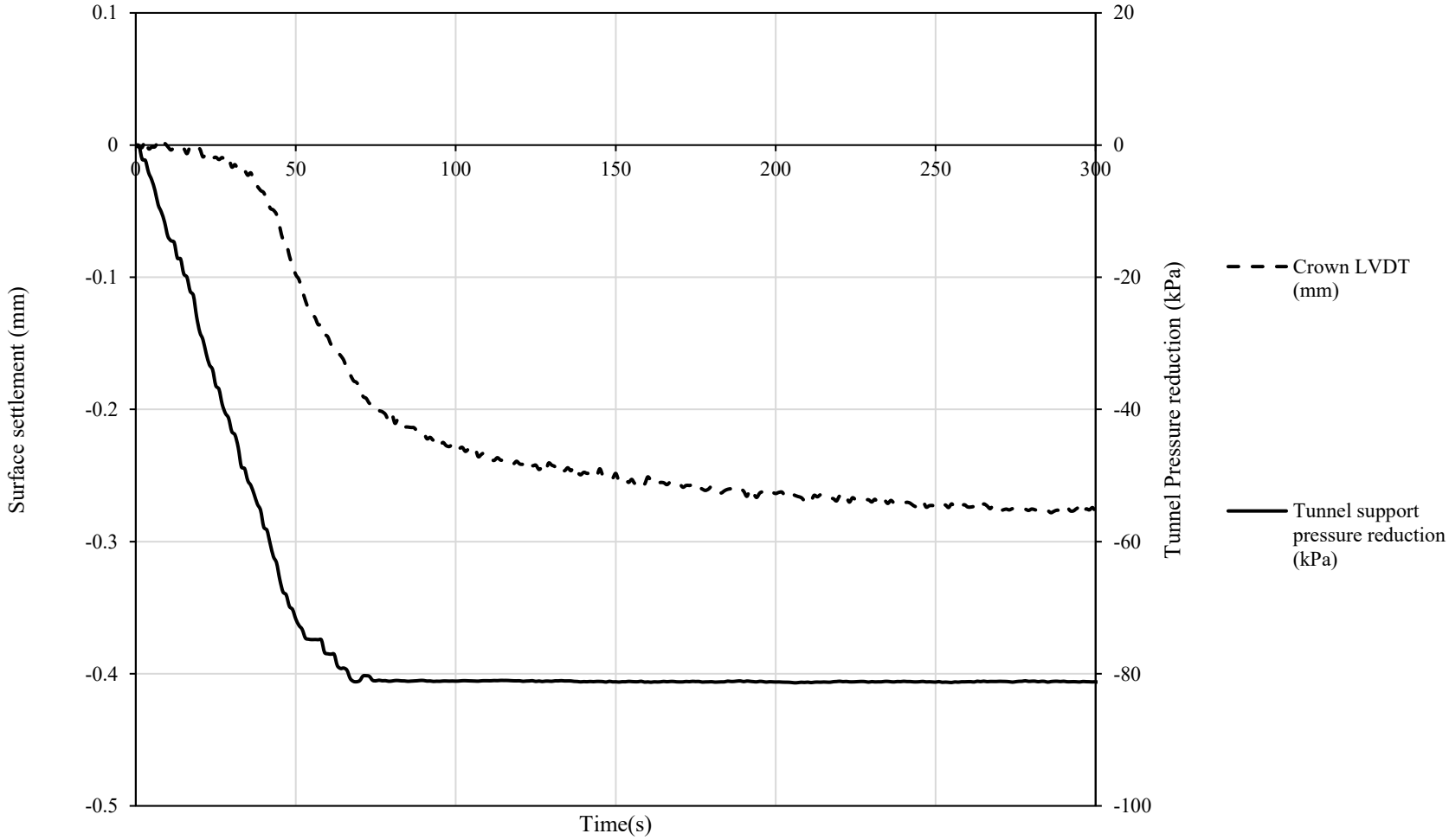

Figure 11.12- Surface displacement against tunnel support pressure above crown on the Speswhite kaolin clay centrifuge soil bed

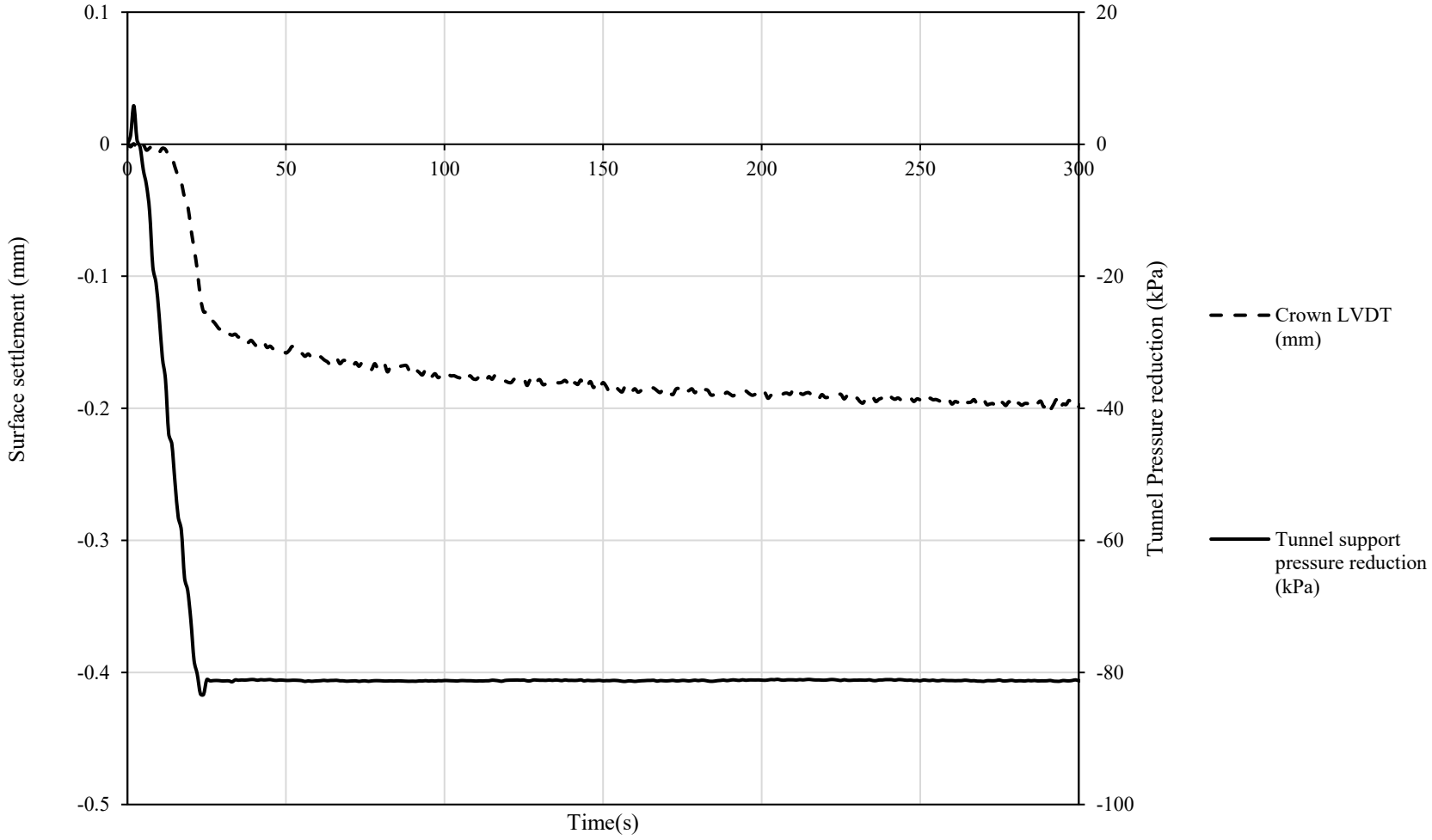

Figure 11.13- Surface displacement against tunnel support pressure above crown on the Speswhite: Polwhite E kaolin clay centrifuge soil bed

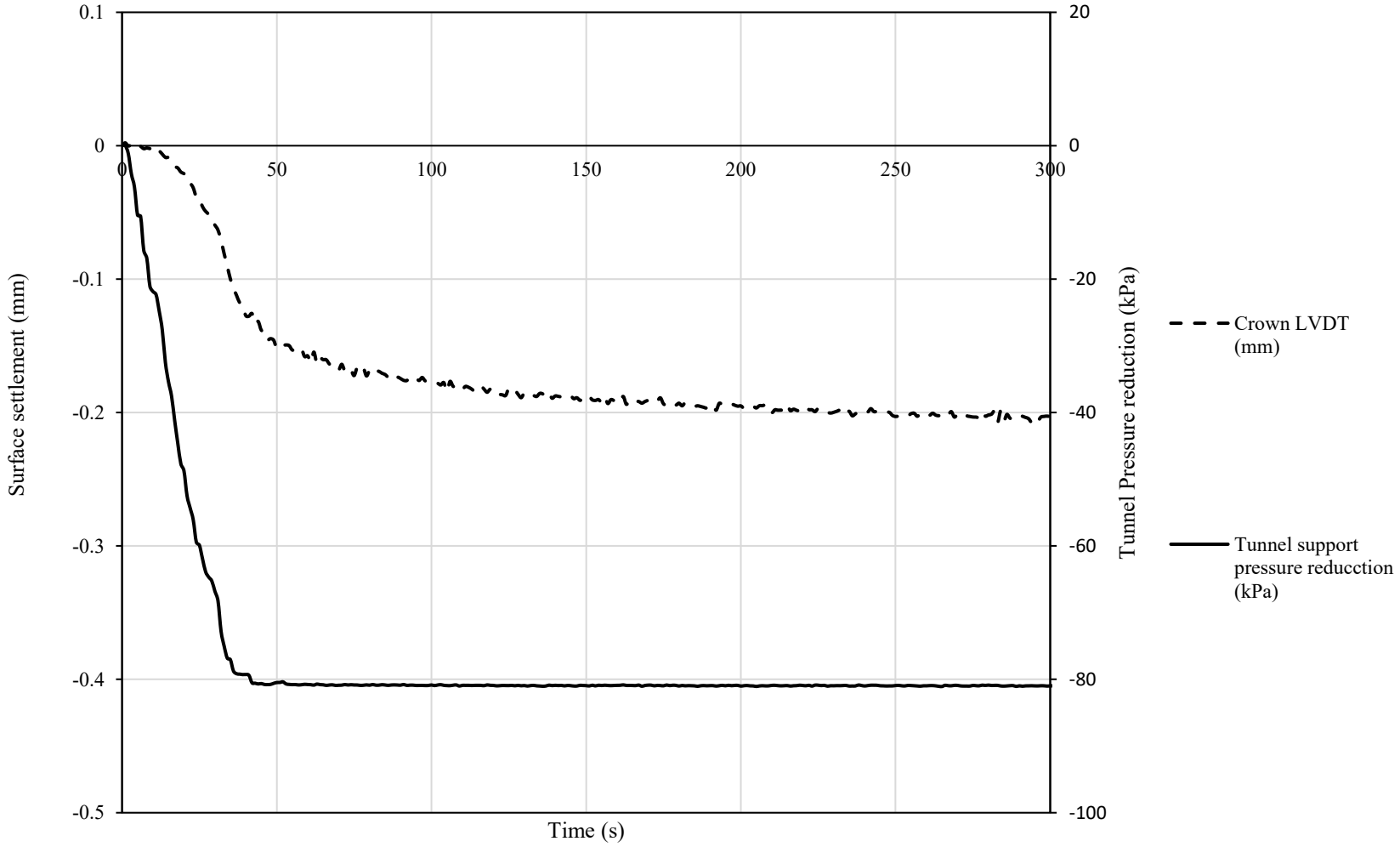

Figure 11.14- Surface displacement against tunnel support pressure above crown on the sedimented centrifuge soil bed

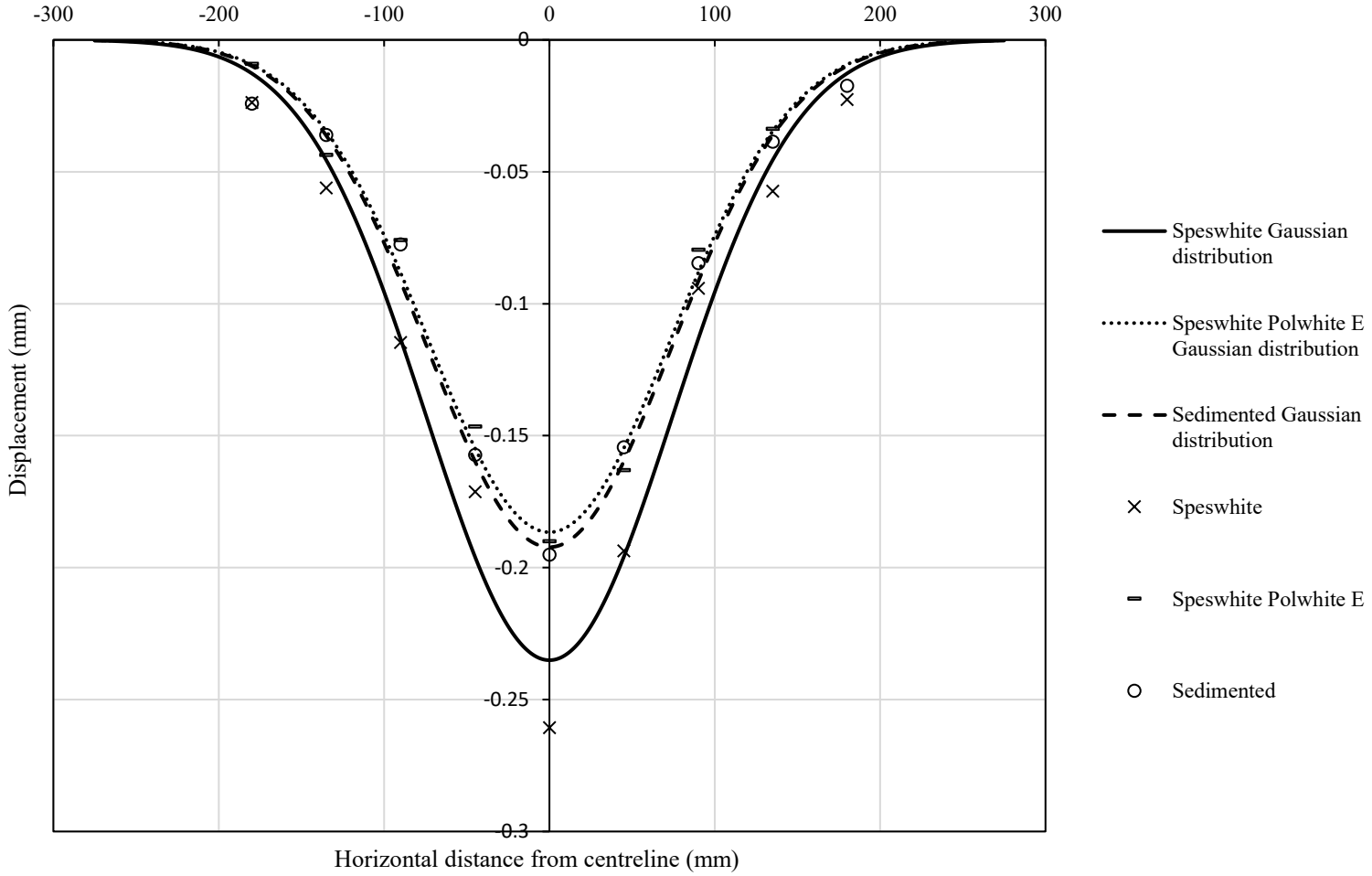

Figure 11.15- Surface settlement troughs developed 200 seconds after the reduction of tunnel support pressure

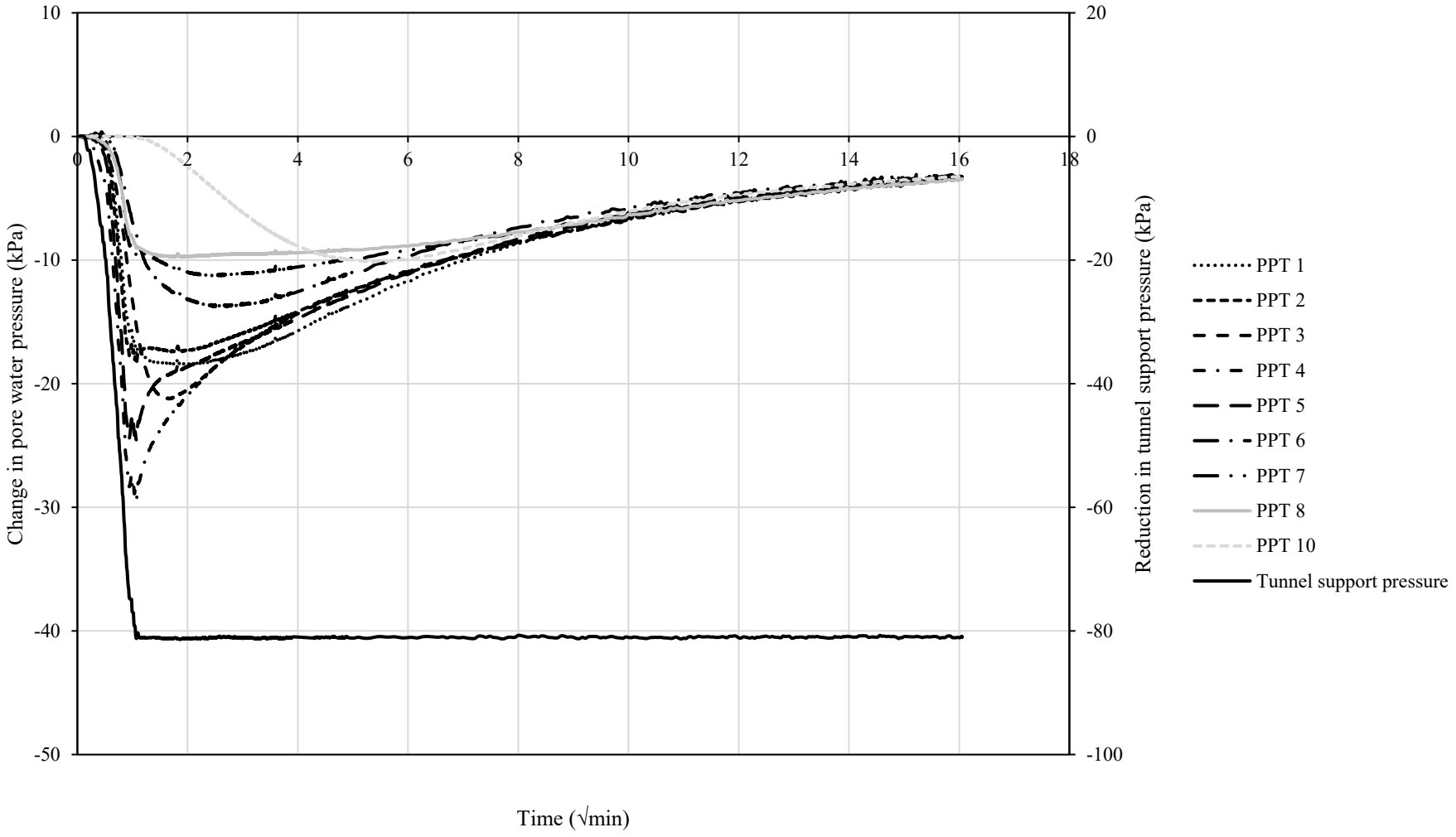

Figure 11.16- Change in pore pressure and tunnel support pressure against time (√min) for the Speswhite kaolin clay centrifuge test

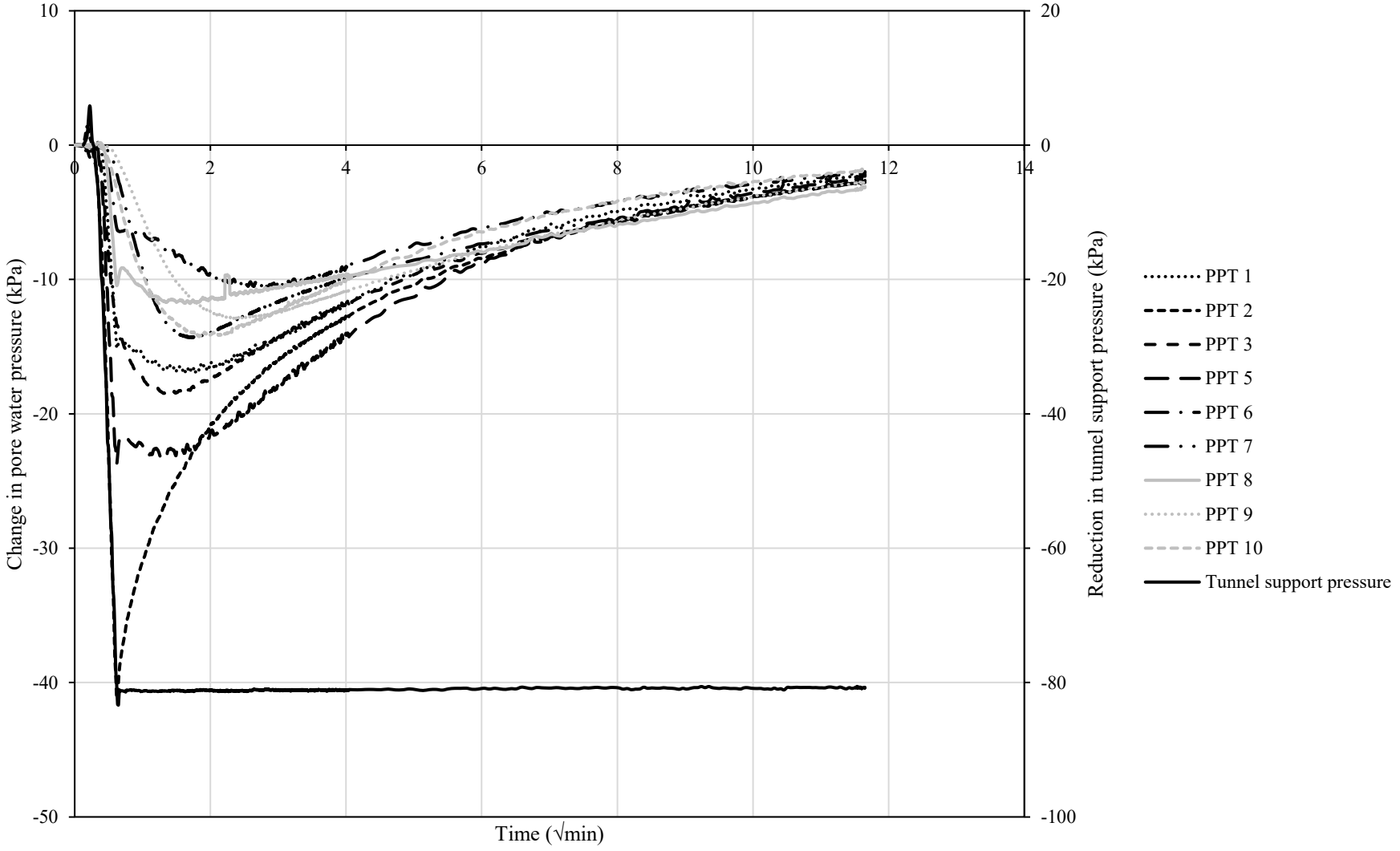

Figure 11.17- Change in pore pressure and tunnel support pressure against time (√min) for the Speswhite: Polwhite E kaolin clay centrifuge test

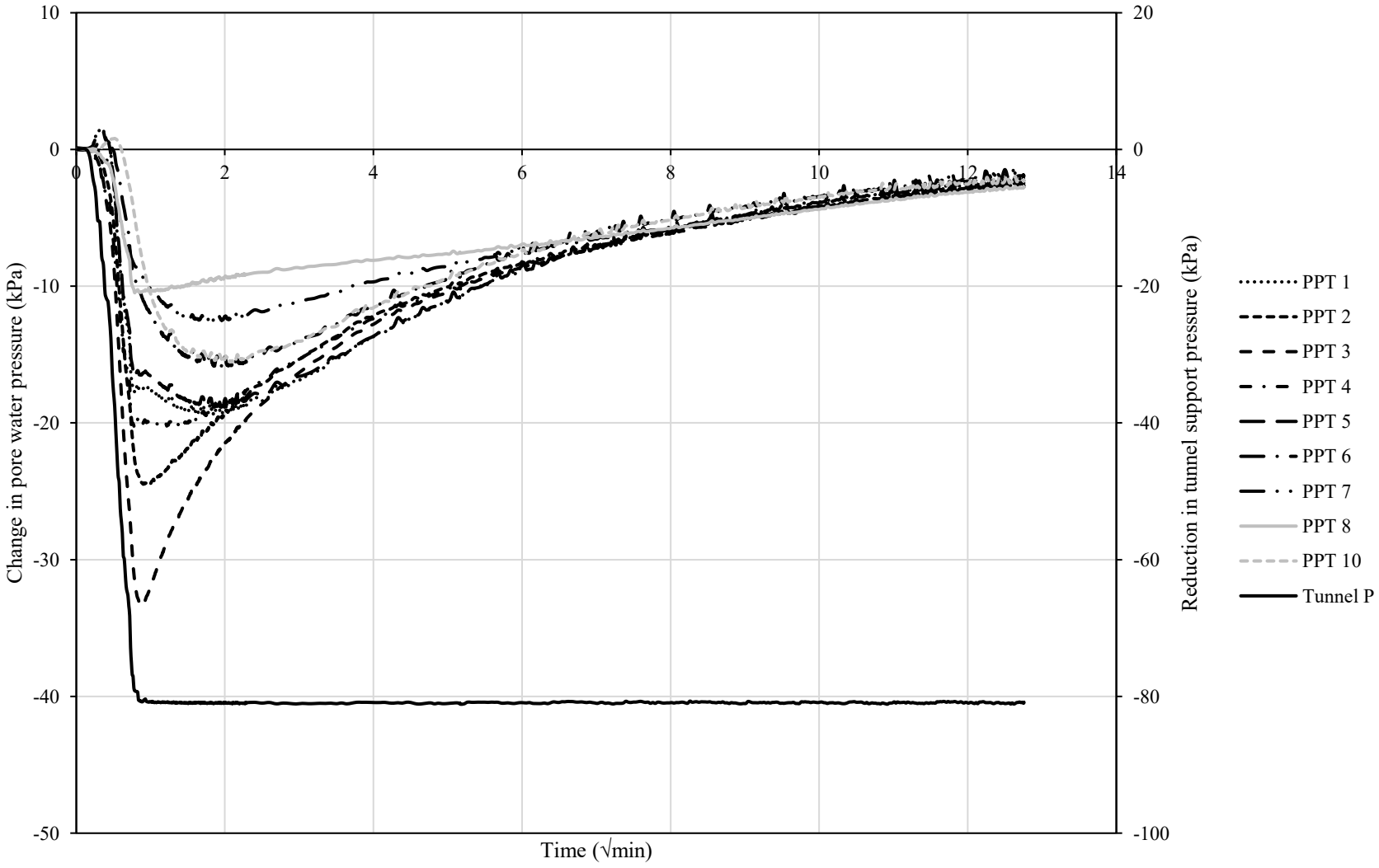

Figure 11.18- Change in pore pressure and tunnel support pressure against time (√min) for the sedimented centrifuge test

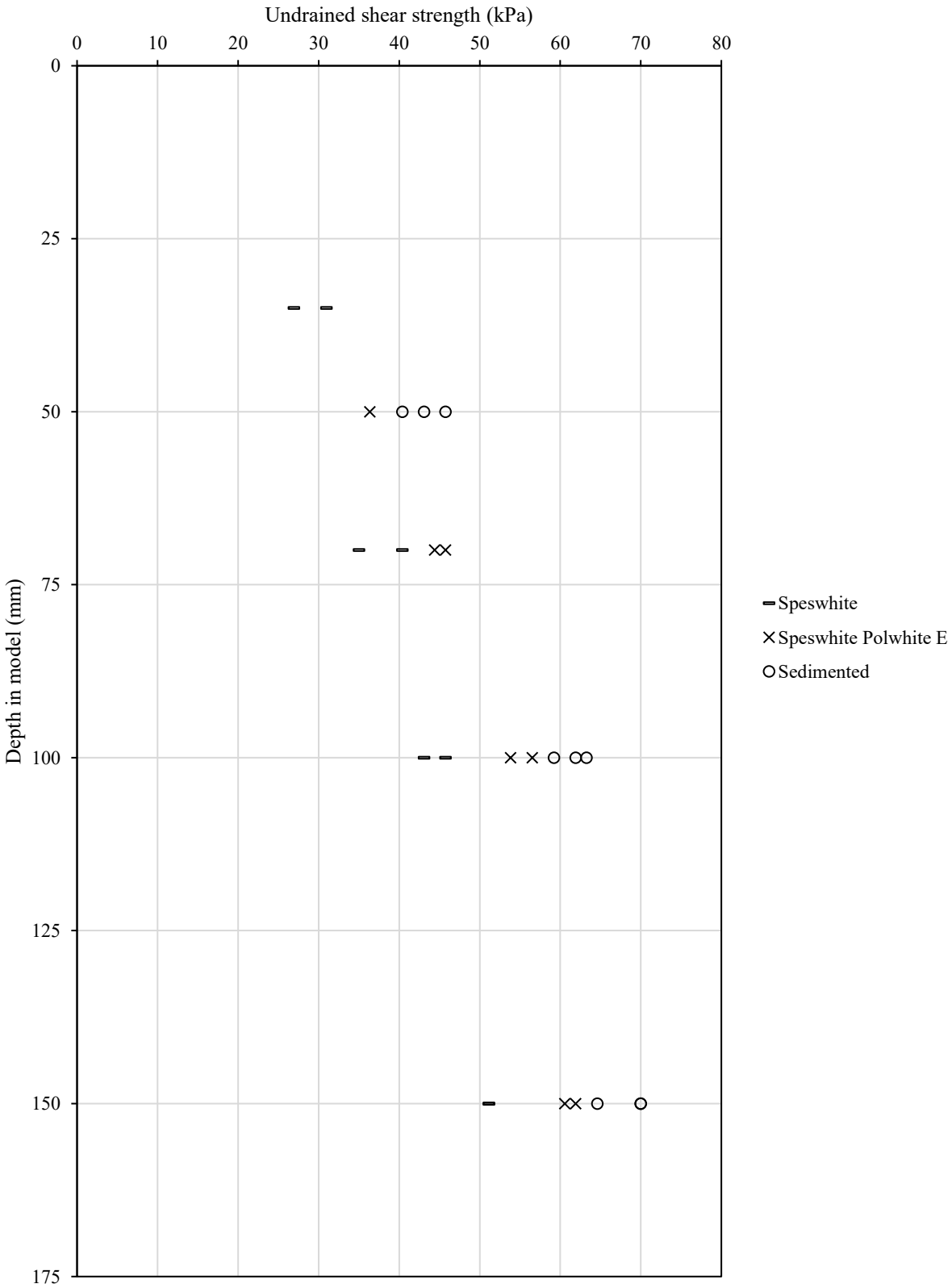

Figure 11.19-Undrained shear strength with depth profiles for the three different centrifuge soil beds

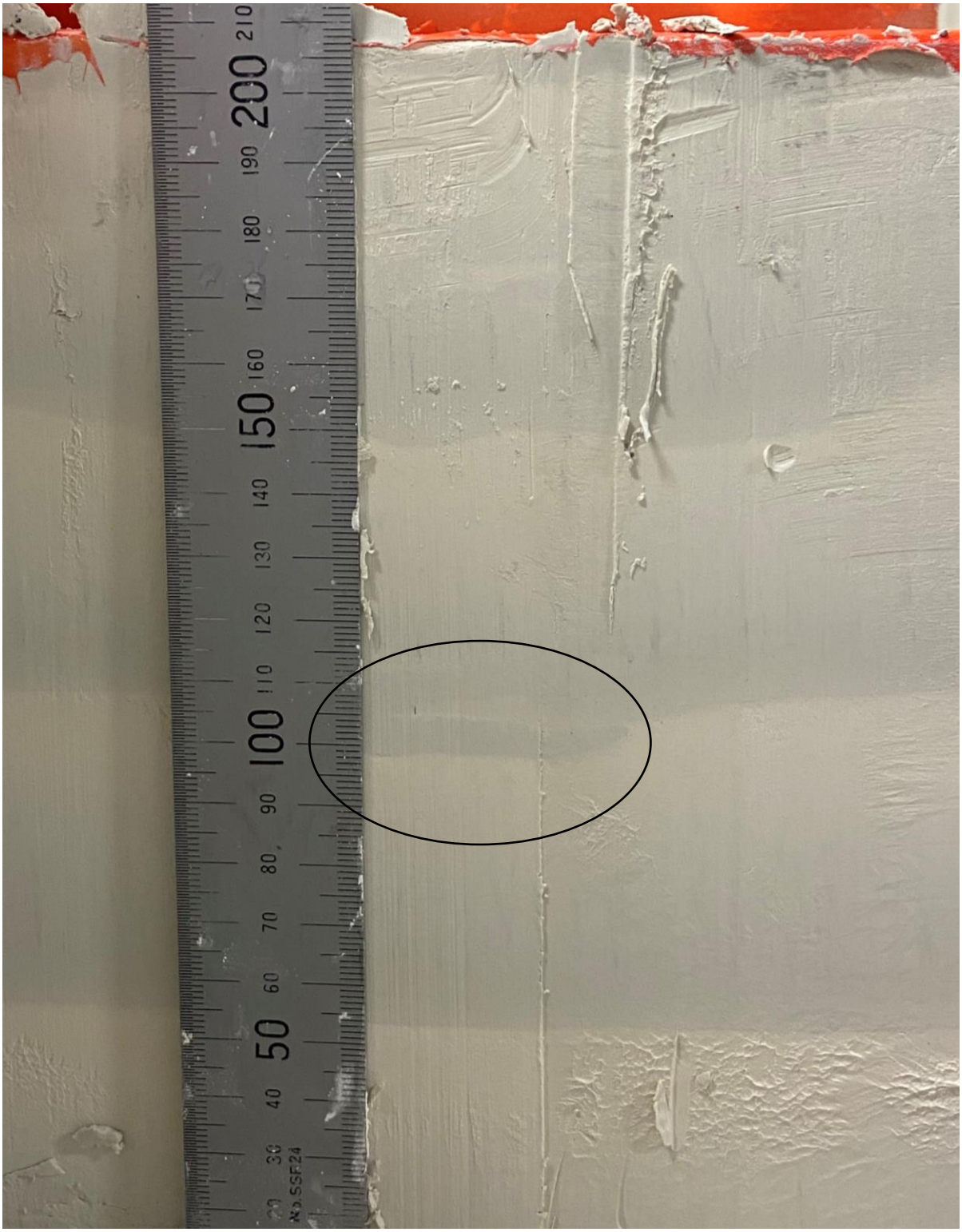

Figure 12.1- Layering disturbance when cutting the sedimented soil bed

More prominent hanging of soil bed against the sidewall indicating higher layers there was more sidewall friction.

Layer interface mostly horizontal with minor signs of friction between the sidewall and soil bed.

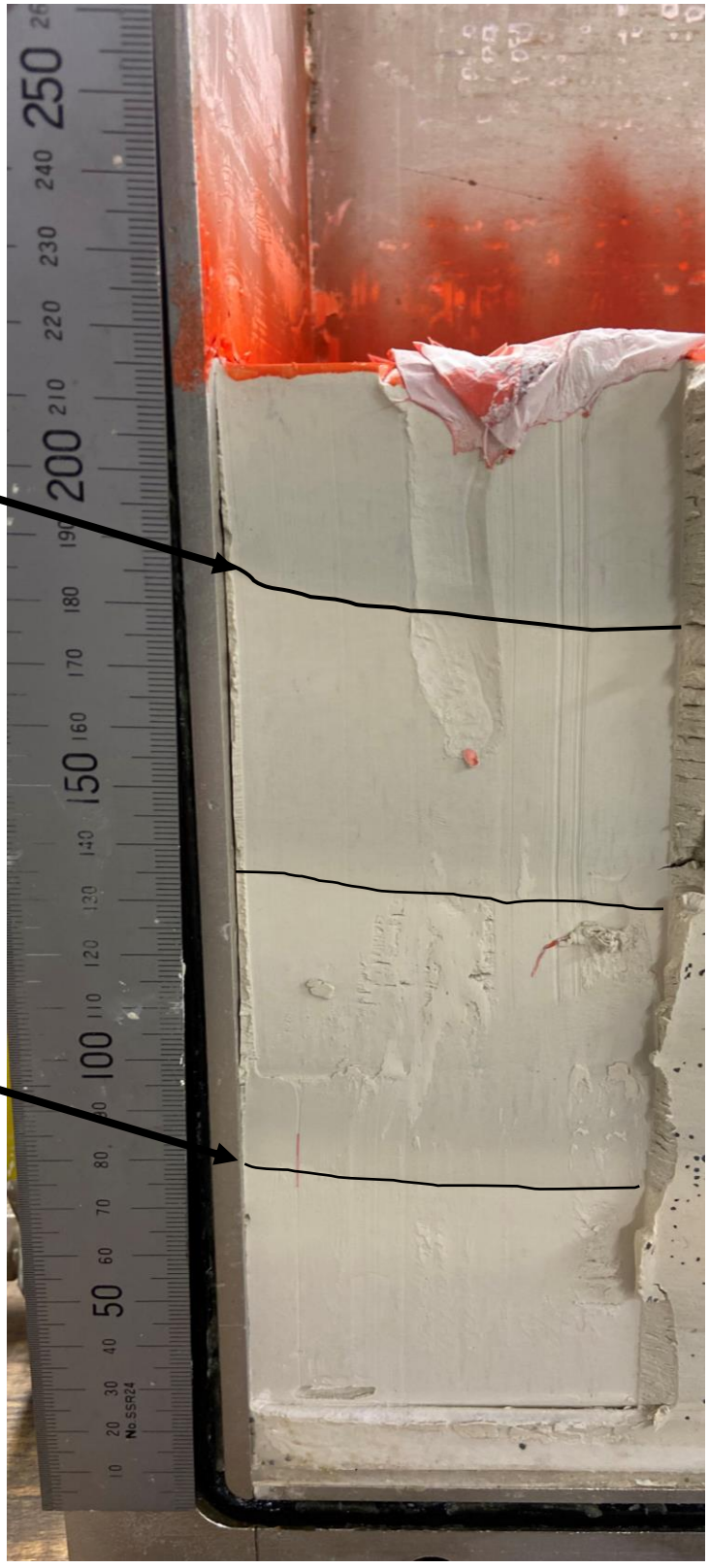

Figure 12.2- Annotated image indicating different zones of side wall friction

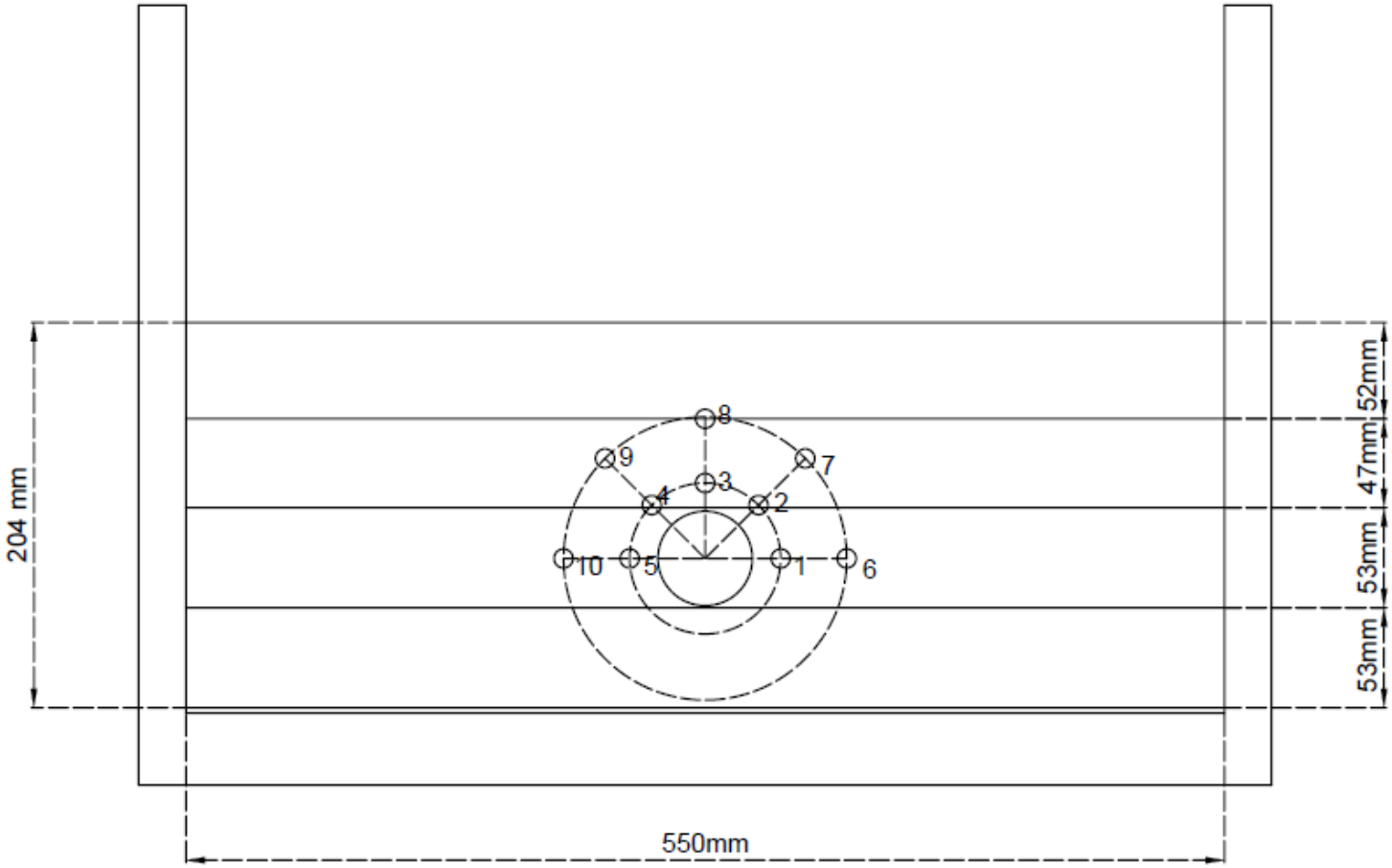

Figure 12.3- Measured sedimented soil bed layer thicknesses and PPT locations

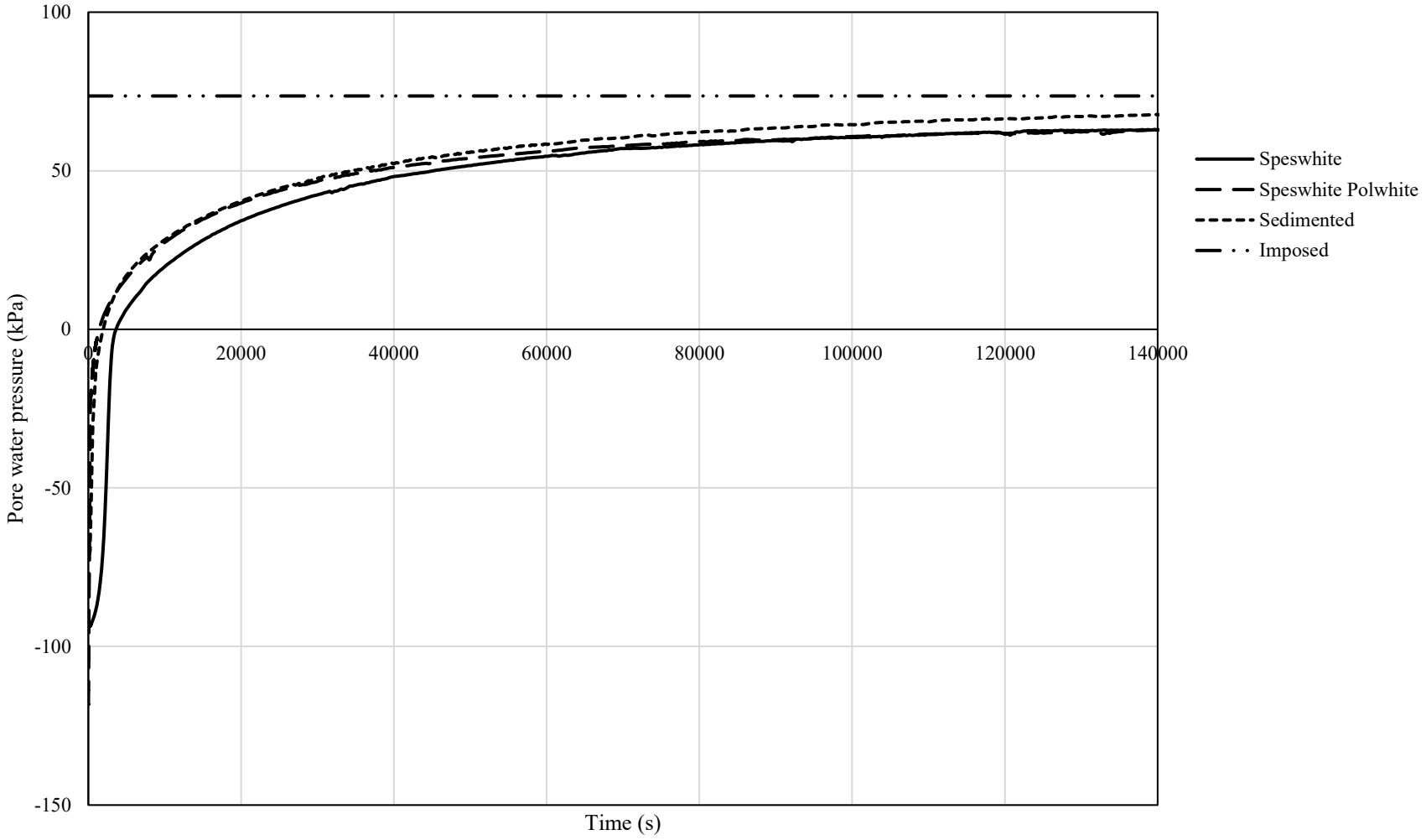

Figure 12.4- Response of PPT 3 during inflight consolidation during the three centrifuge tests

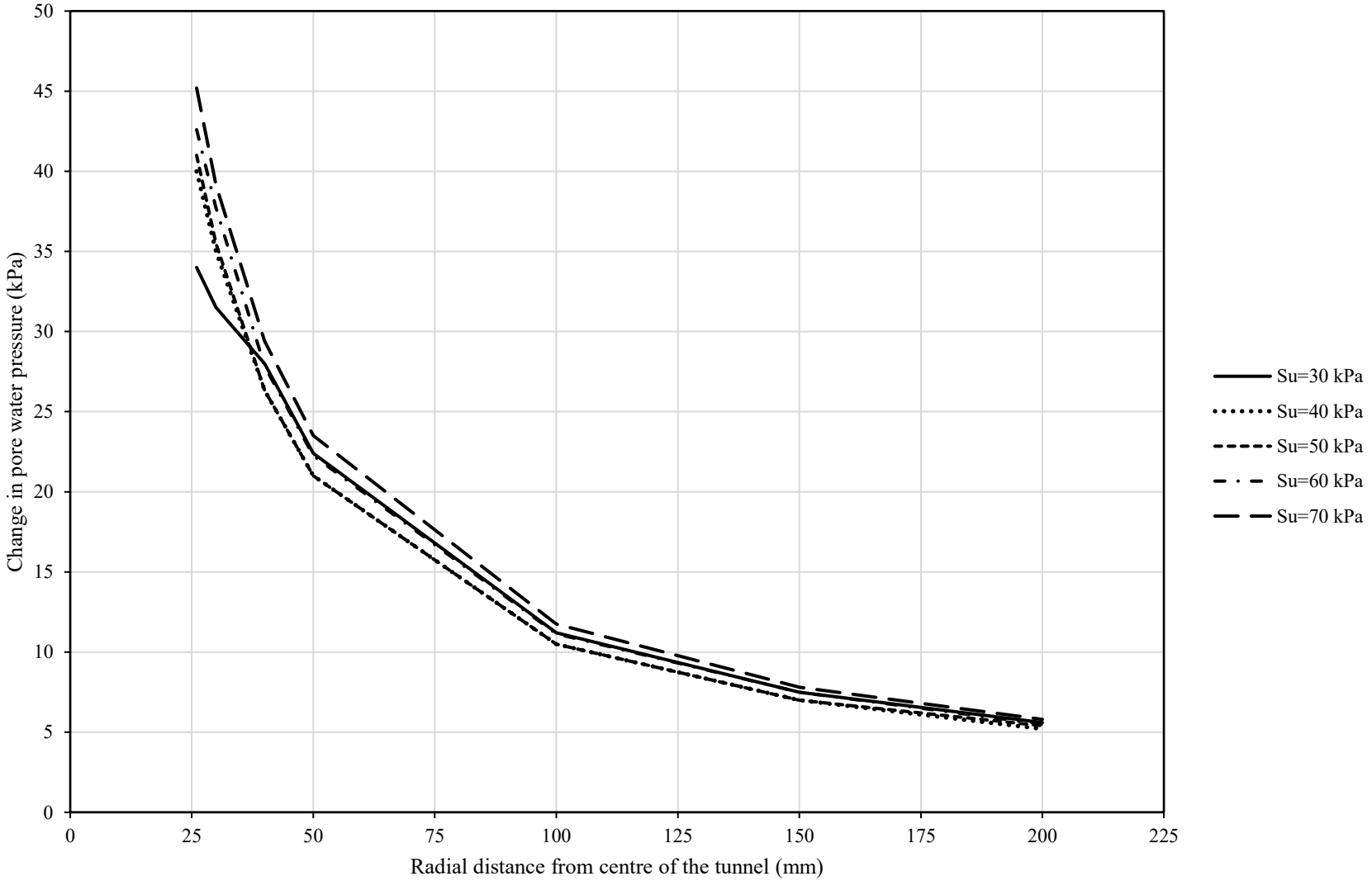

Figure 12.5- Predicted changes in pore pressure in idealised centrifuge soil bed with different undrained shear strengths

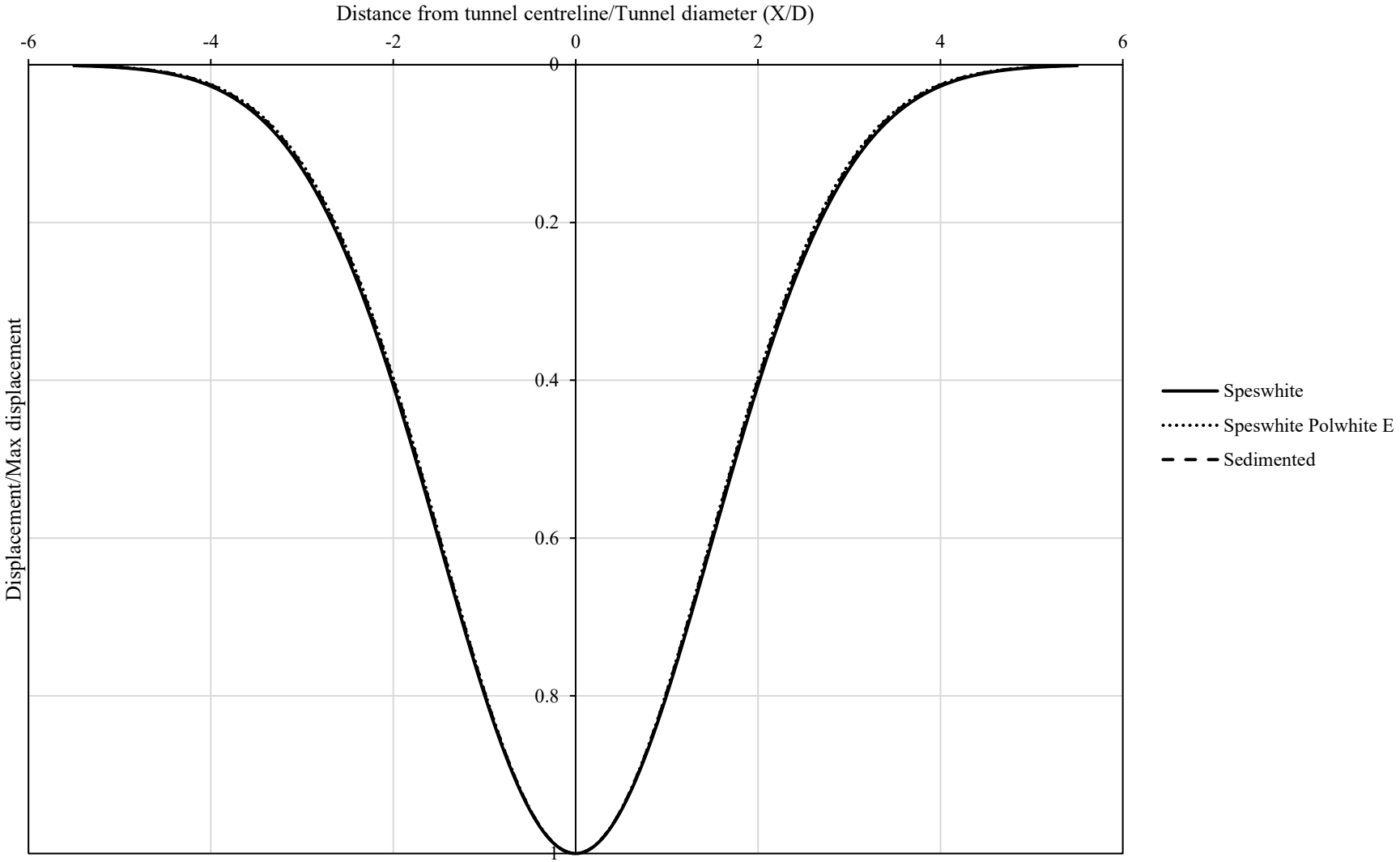

Figure 12.6- Normalised surface settlement troughs for the three centrifuge tests

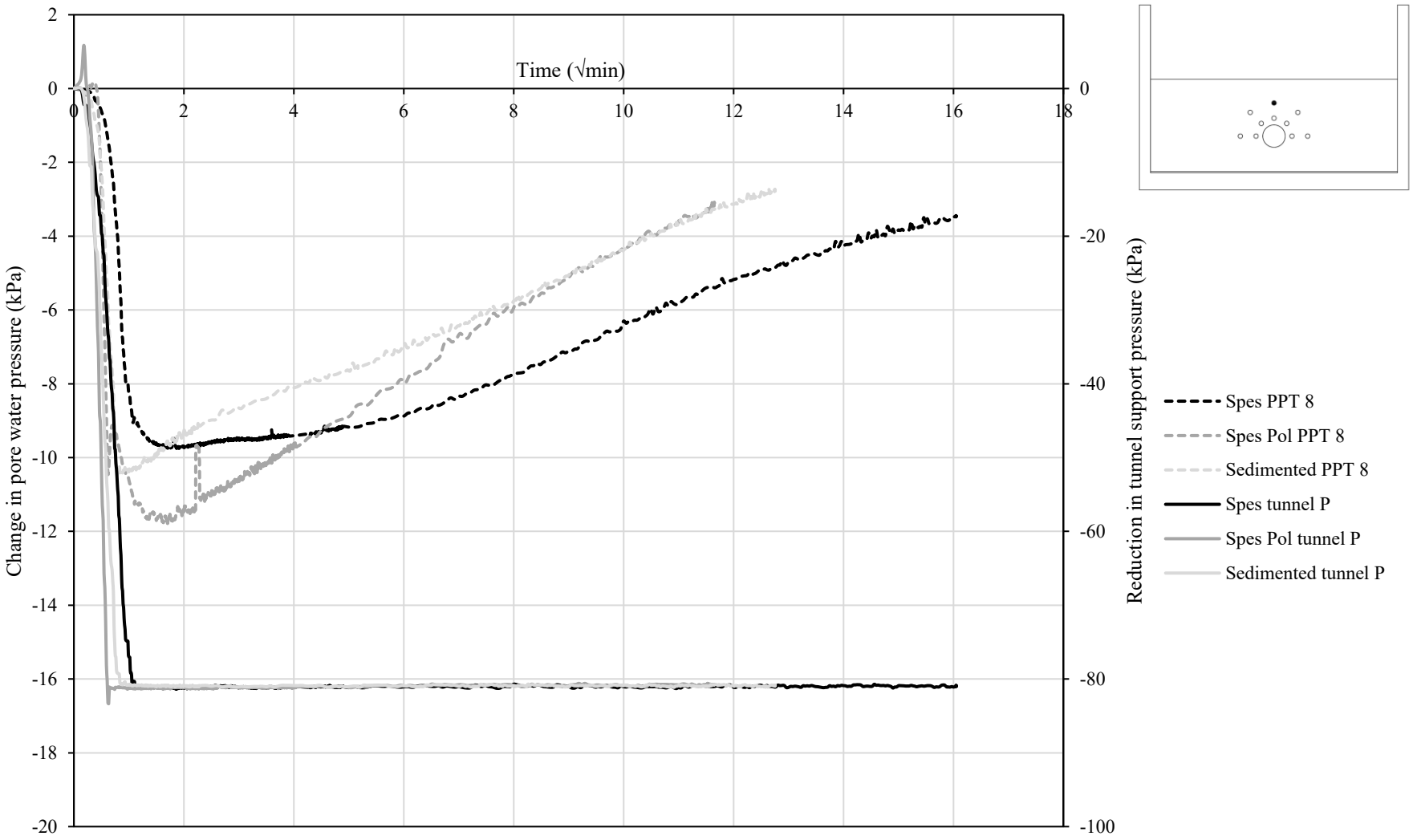

c

Figure 12.7- Response of PPT 8 with reduction in tunnel support pressure for the three different centrifuge tests

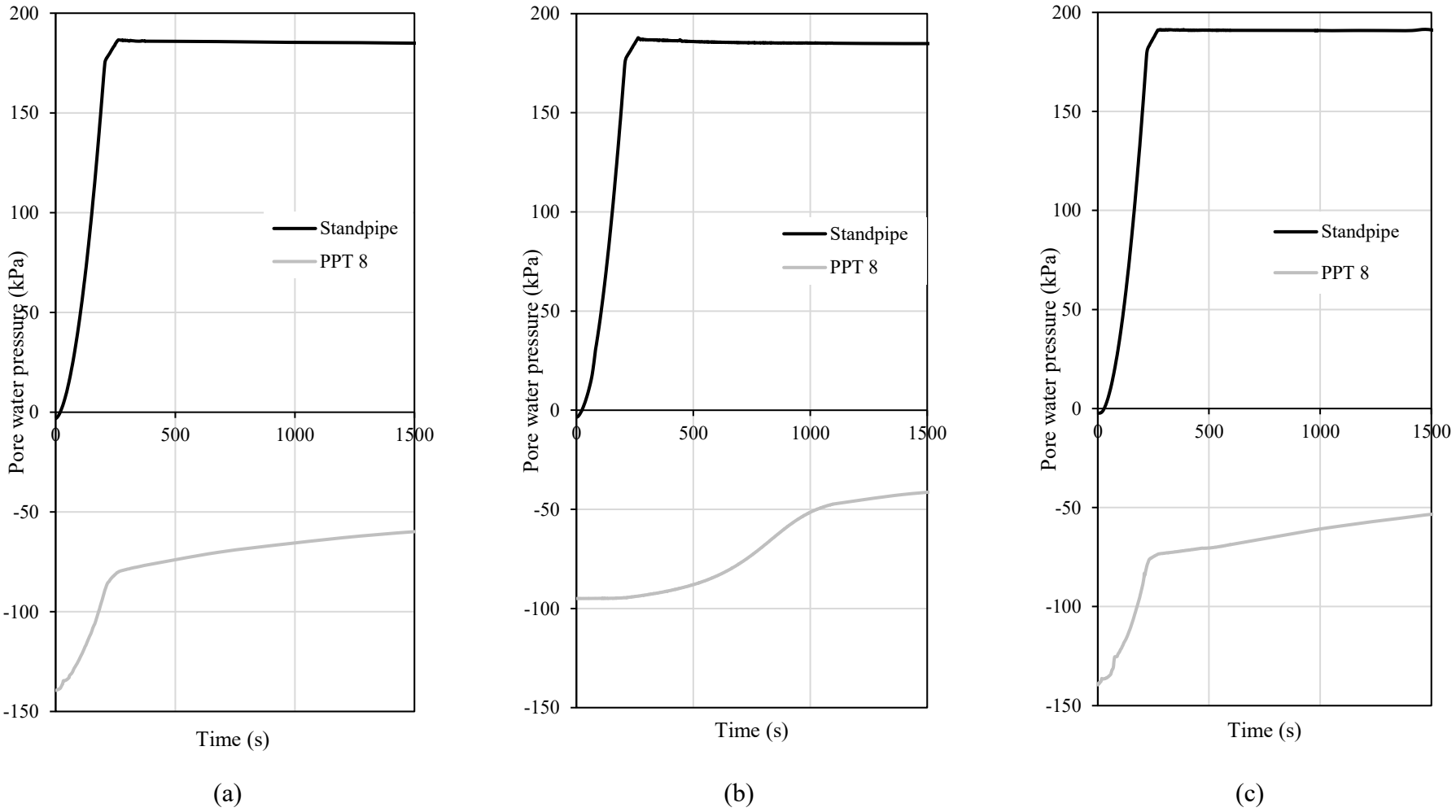

Figure 12.8- Initial response of PPT 8 to an increased acceleration field for the three centrifuge tests (a). Speswhite kaolin clay soil bed, (b). Speswhite: Polwhite E kaolin soil bed, (c) Sedimented soil bed.

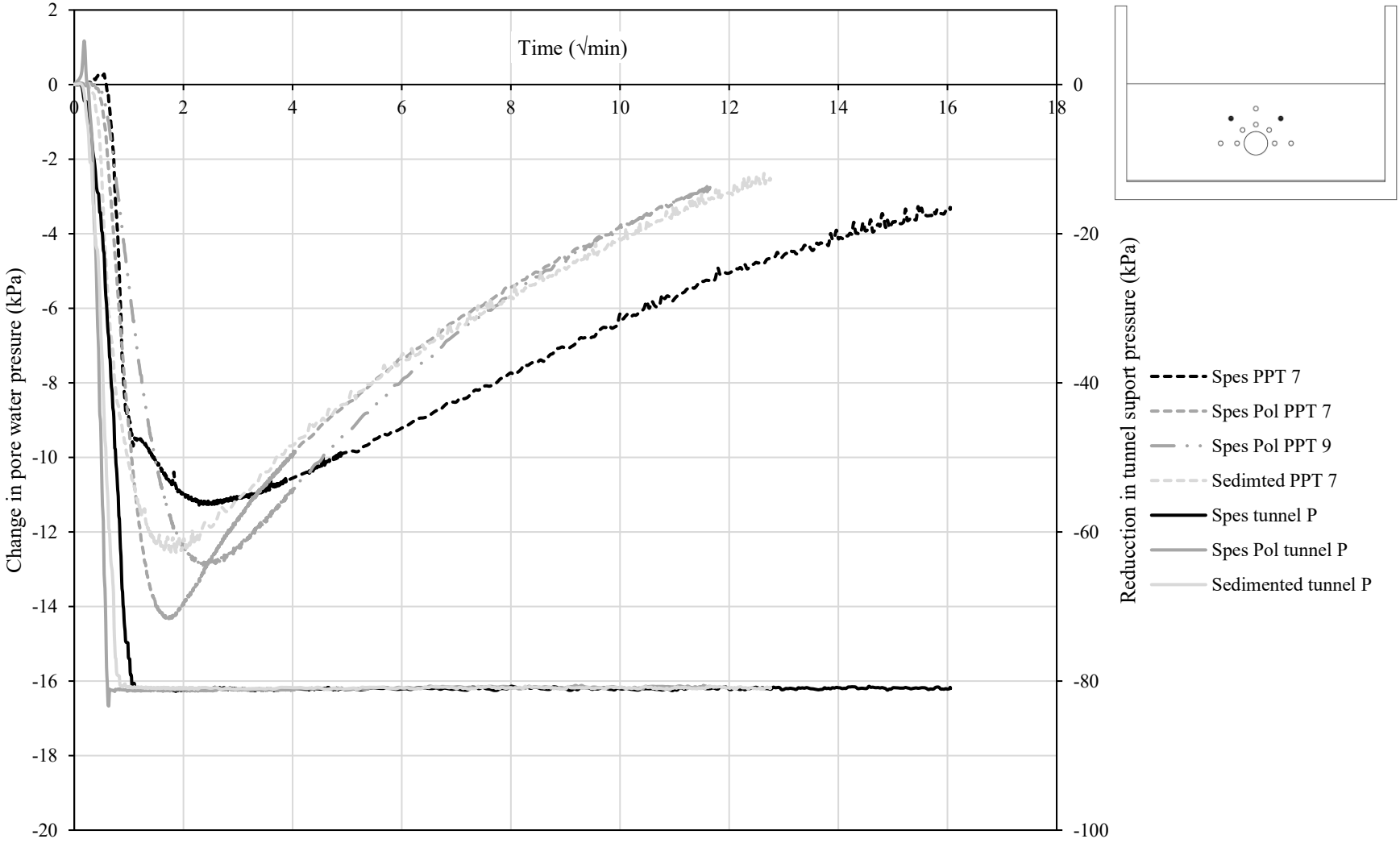

Figure 12.9- Response of PPT 7 and 9 with reduction in tunnel support pressure for the three different centrifuge tests

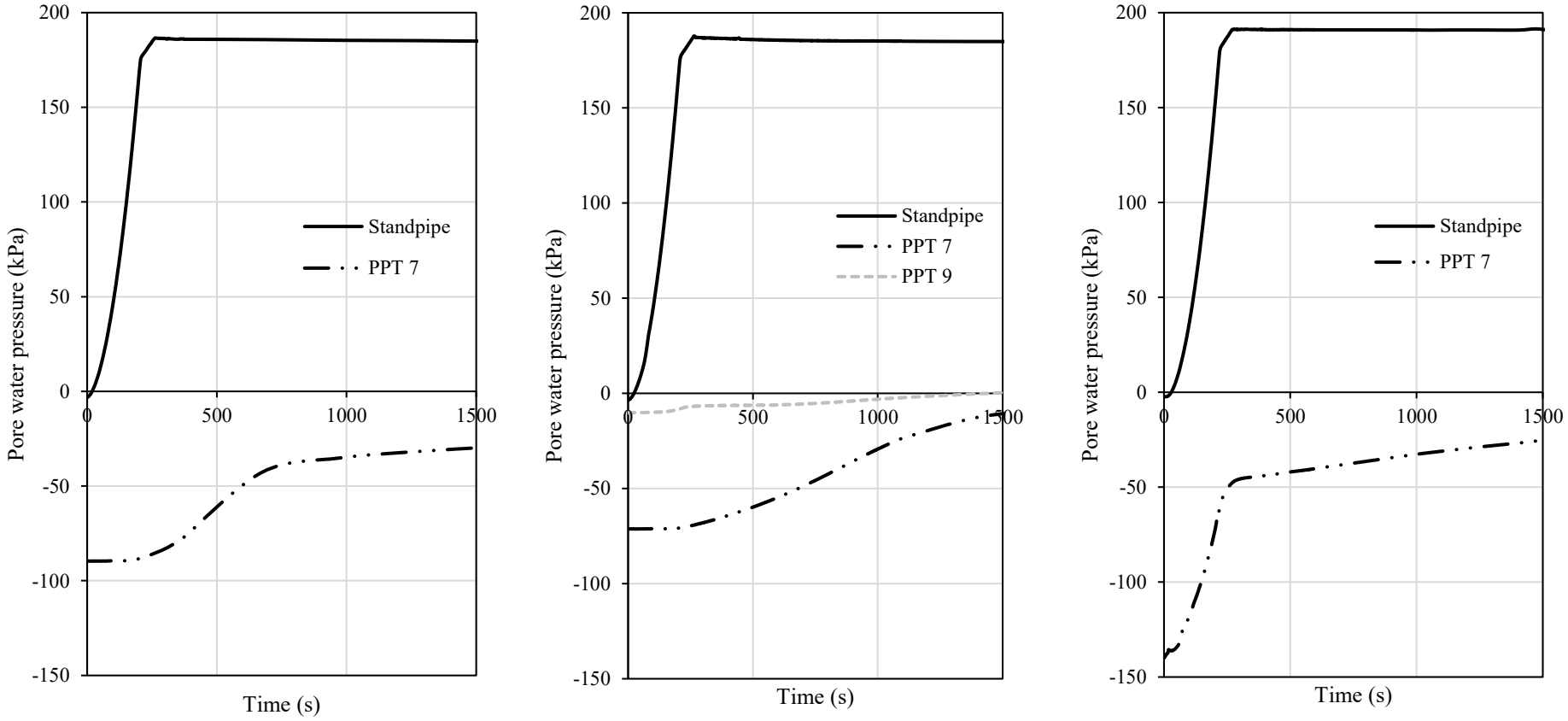

Figure 12.10- Initial response of PPT 7 and 9 to an increased acceleration field for the three centrifuge tests (a). Speswhite kaolin clay soil bed, (b). Speswhite: Polwhite E kaolin clay soil bed, (c) Sedimented soil bed

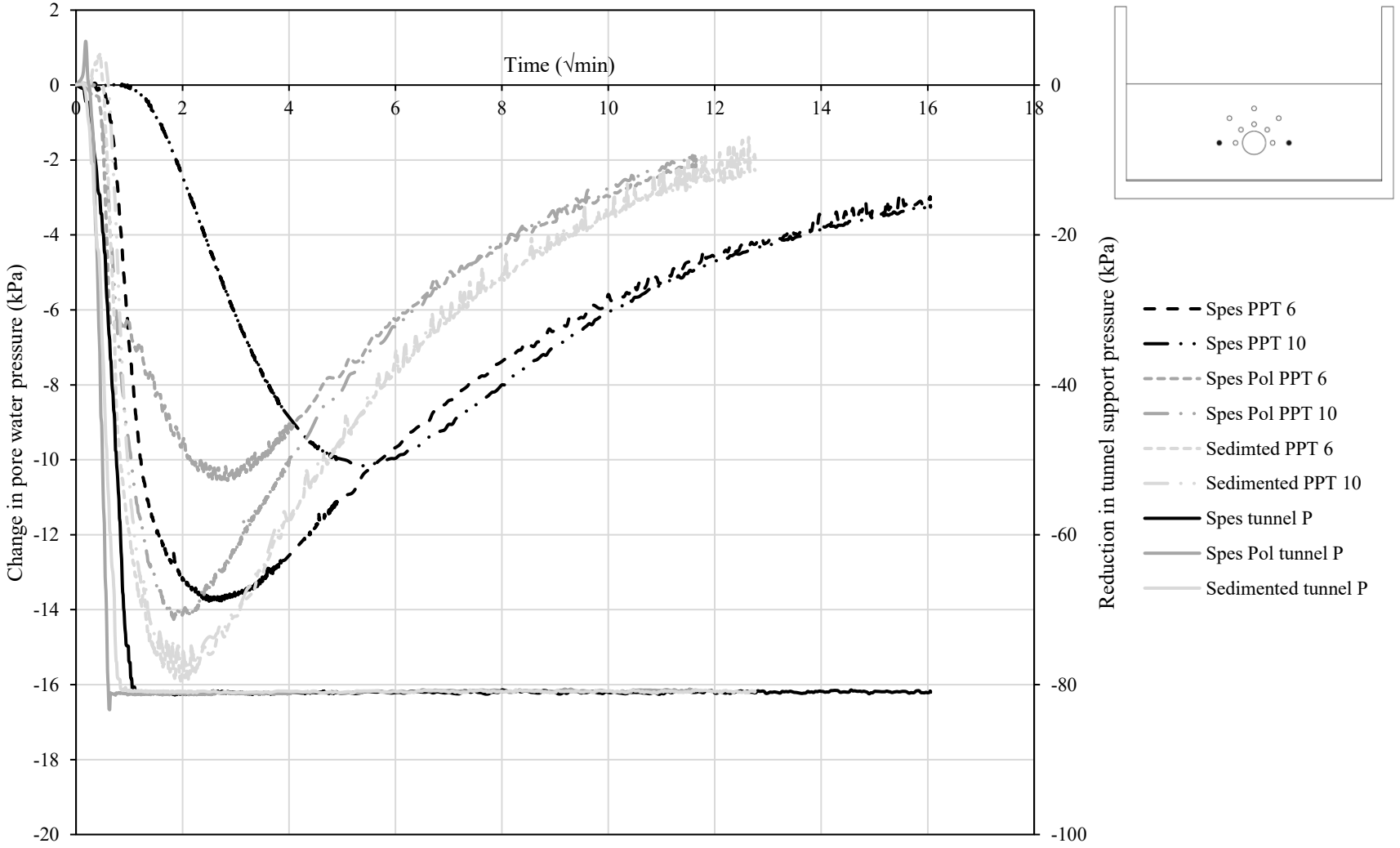

Figure 12.11- Response of PPT 6 and 10 with reduction in tunnel support pressure for the three different centrifuge tests

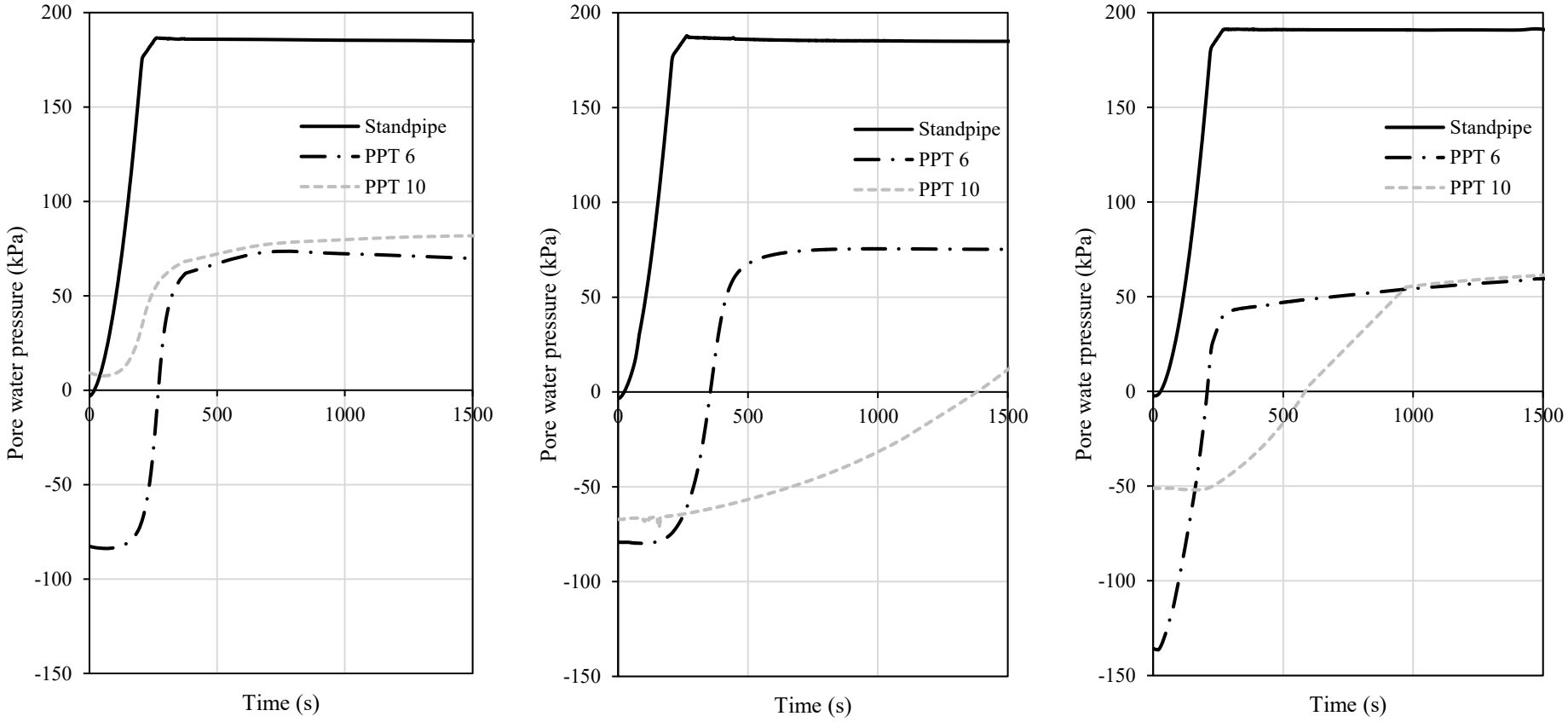

Figure 12.12- Initial response of PPT 6 and 10 to an increased acceleration field for the three centrifuge tests (a). Speswhite kaolin clay soil bed, (b). Speswhite: Polwhite E kaolin clay soil bed, (c) Sedimented soil bed

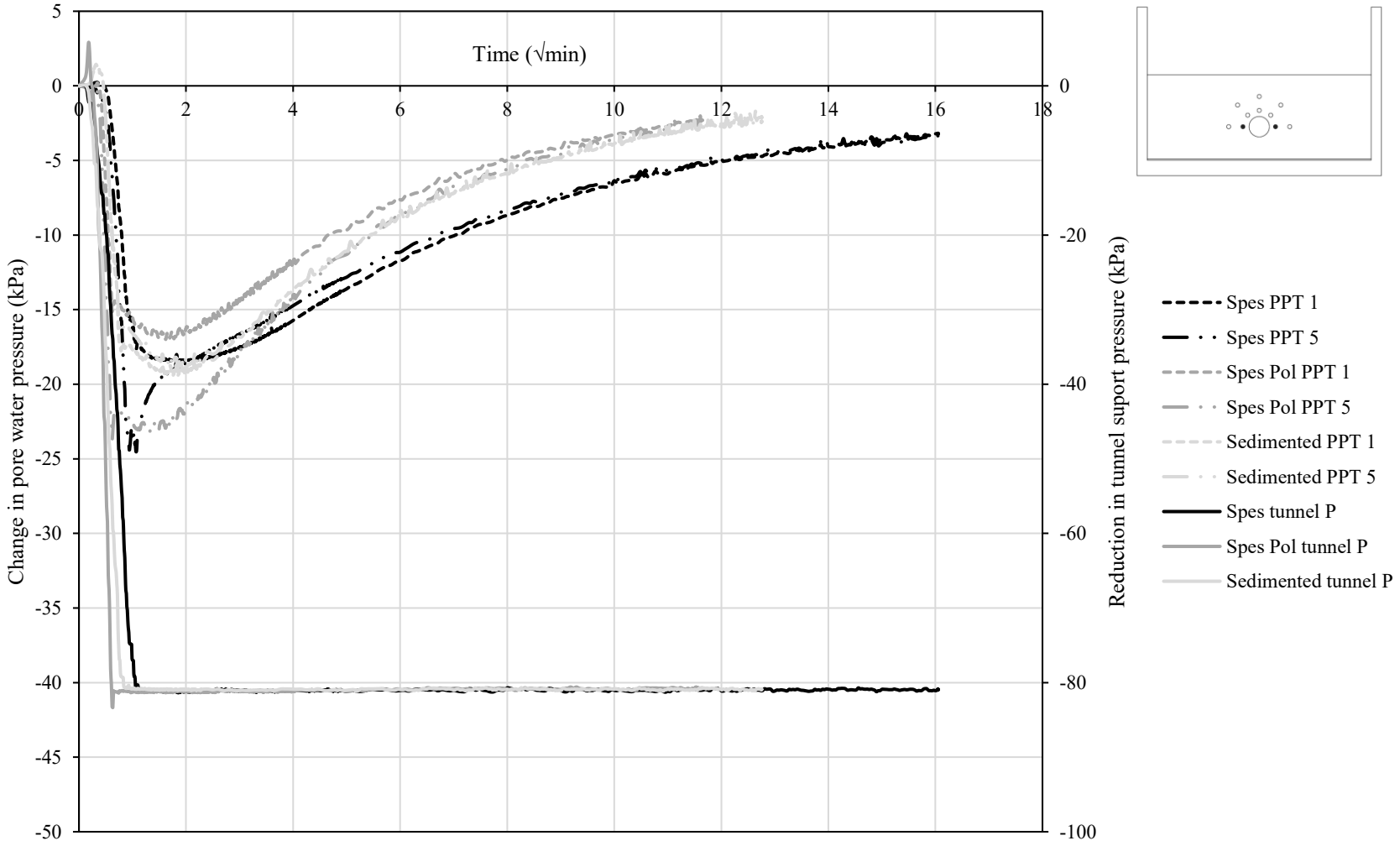

Figure 12.13- Response of PPT 1 and 5 with reduction in tunnel support pressure for the three different centrifuge tests

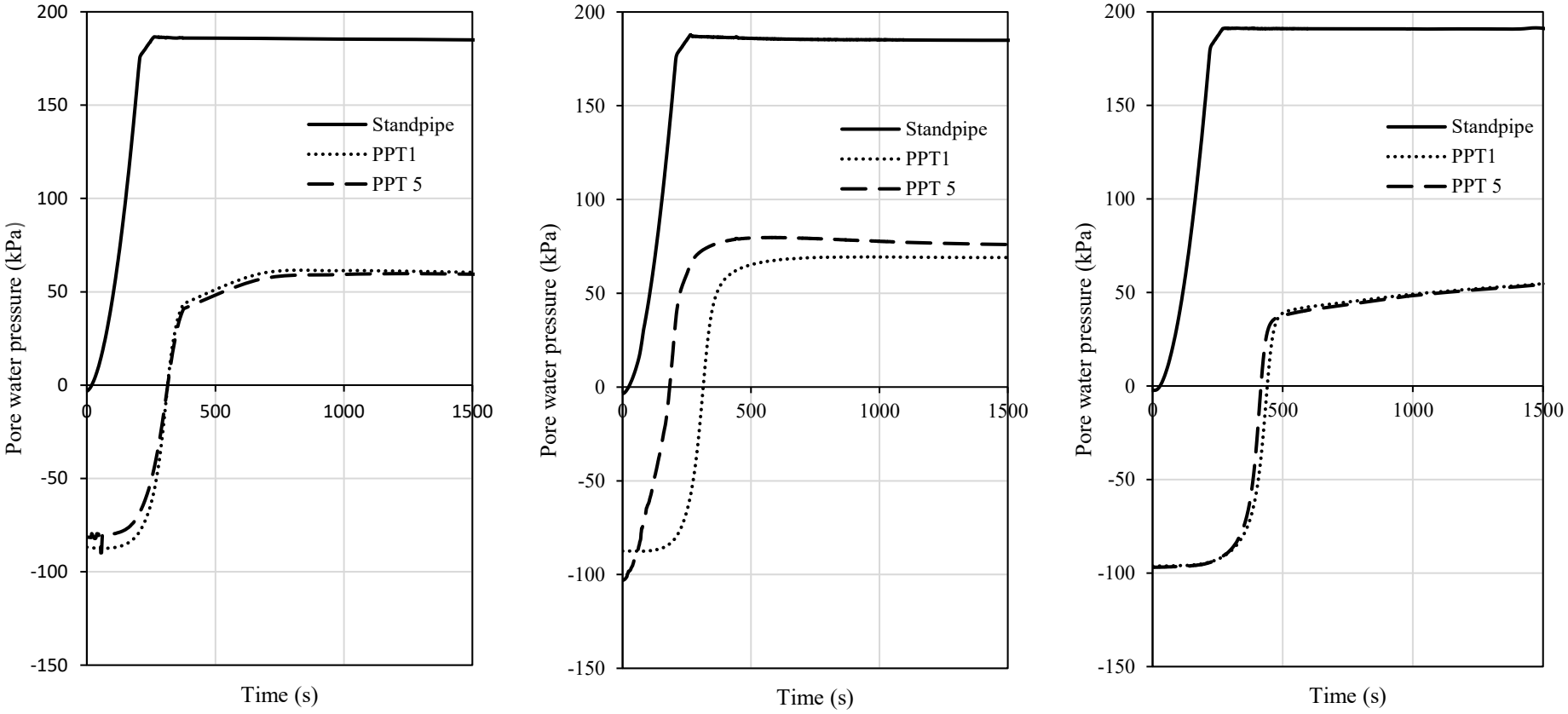

Figure 12.14- Initial response of PPT 1 and 5 to an increased acceleration field for the three centrifuge tests (a). Speswhite kaolin clay soil bed, (b). Speswhite: Polwhite E kaolin clay soil bed, (c) Sedimented soil bed

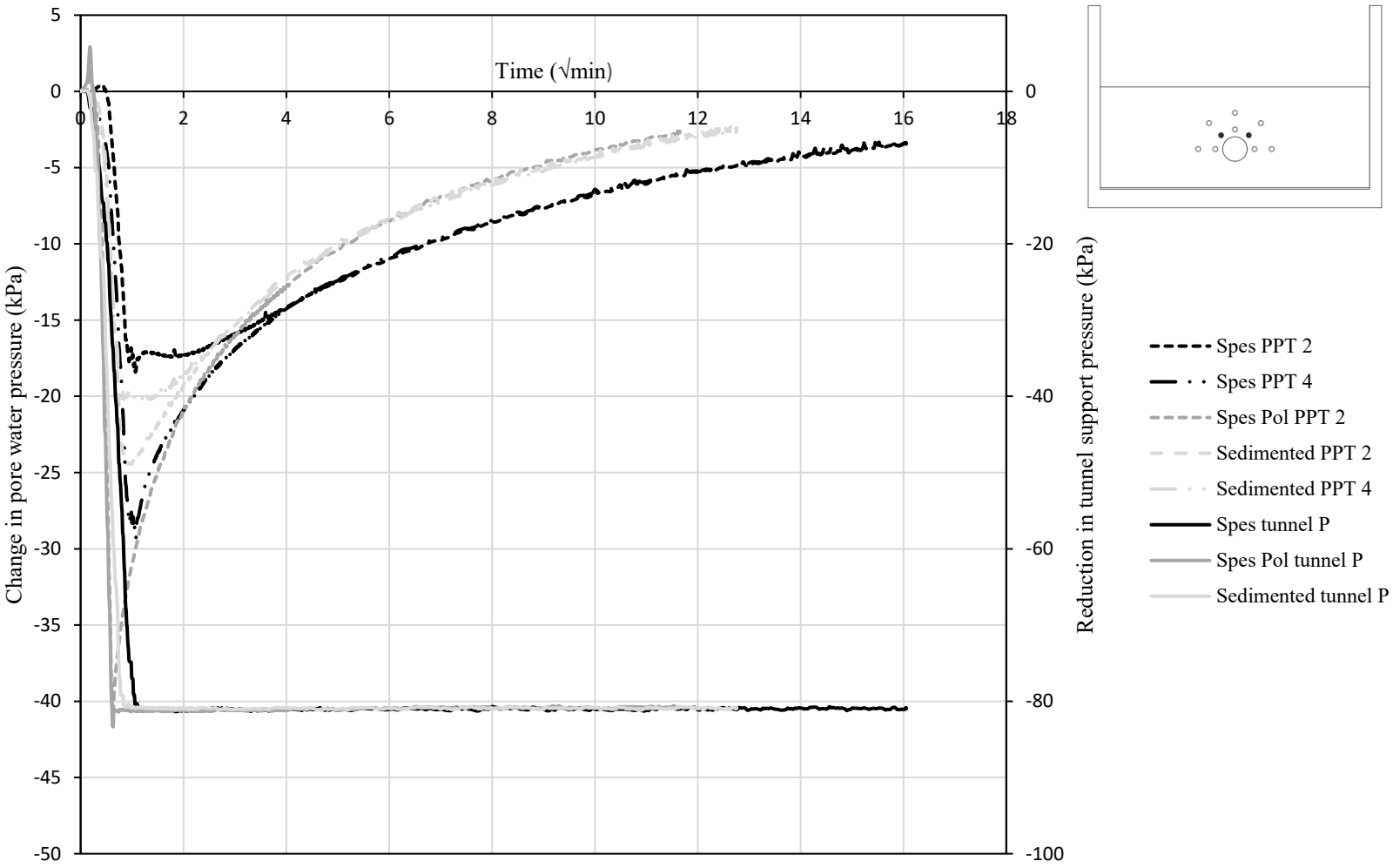

Figure 12.15- Response of PPT 2 and 4 with reduction in tunnel support pressure for the three different centrifuge tests

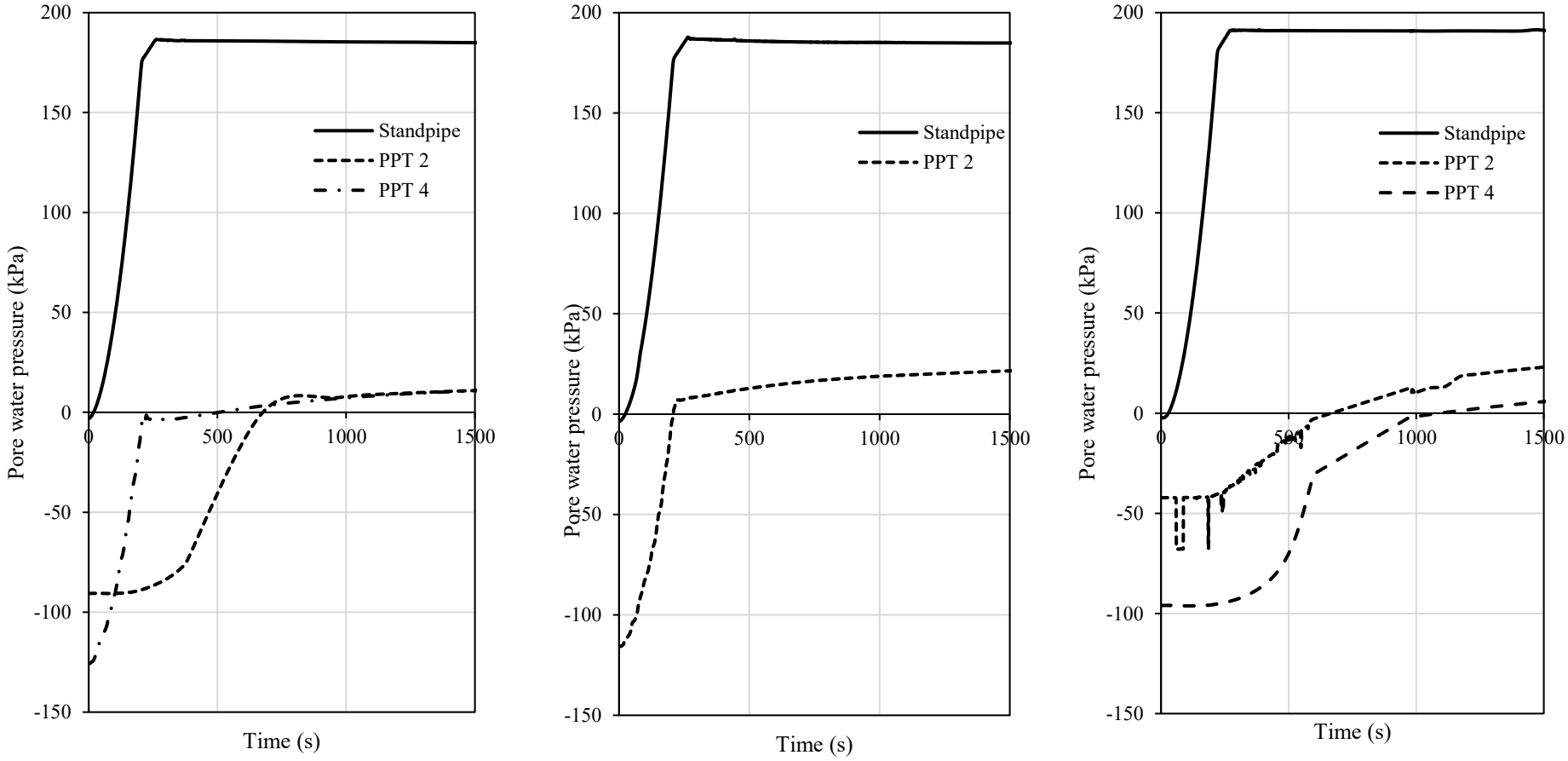

Figure 12.16- Initial response of PPT 2 and 4 to an increased acceleration field for the three centrifuge tests (a). Speswhite kaolin clay soil bed, (b). Speswhite Polwhite E kaolin clay soil bed, (c) Sedimented soil bed

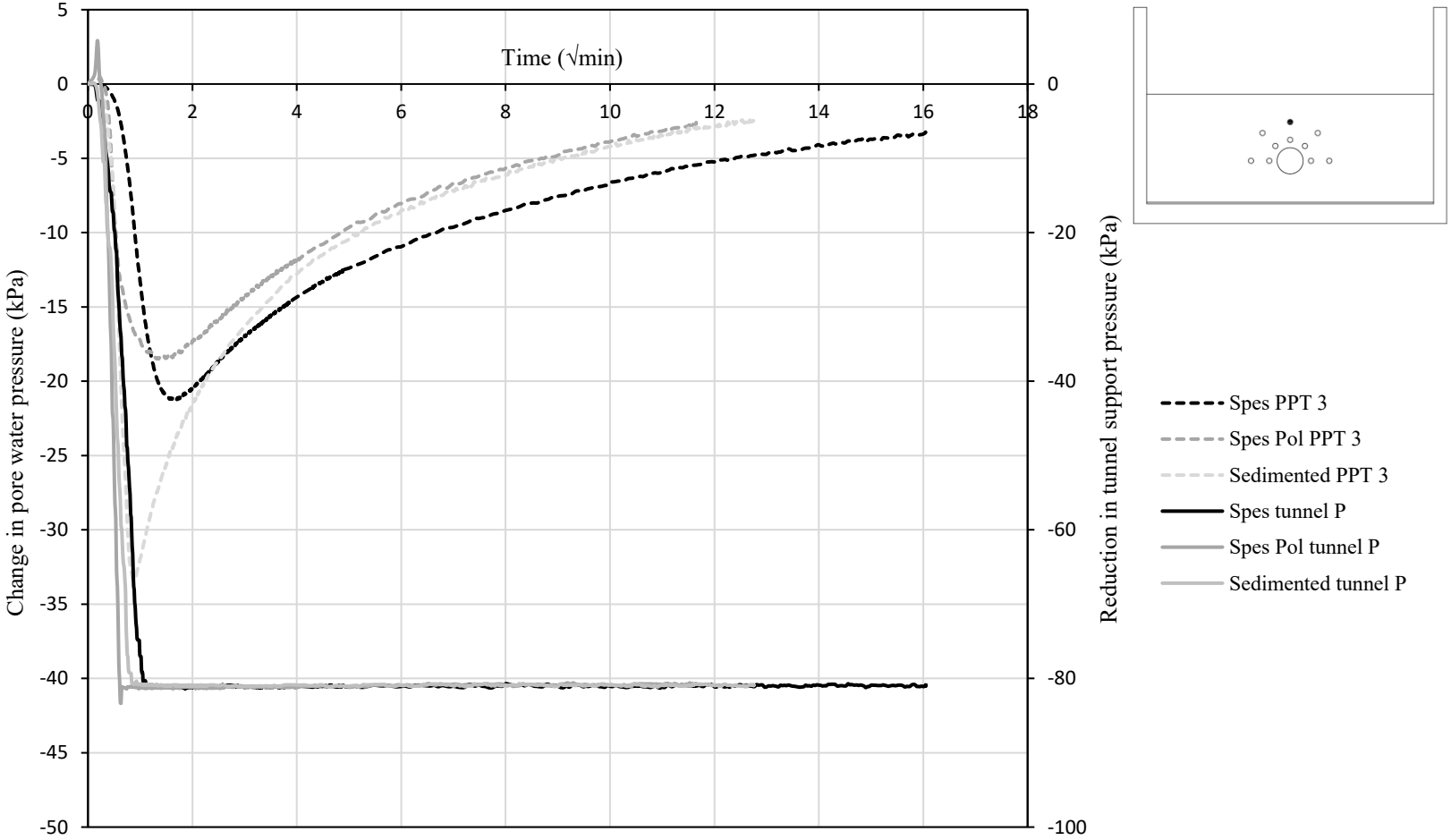

Figure 12.17- Response of PPT 2 and 4 with reduction in tunnel support pressure for the three different centrifuge tests

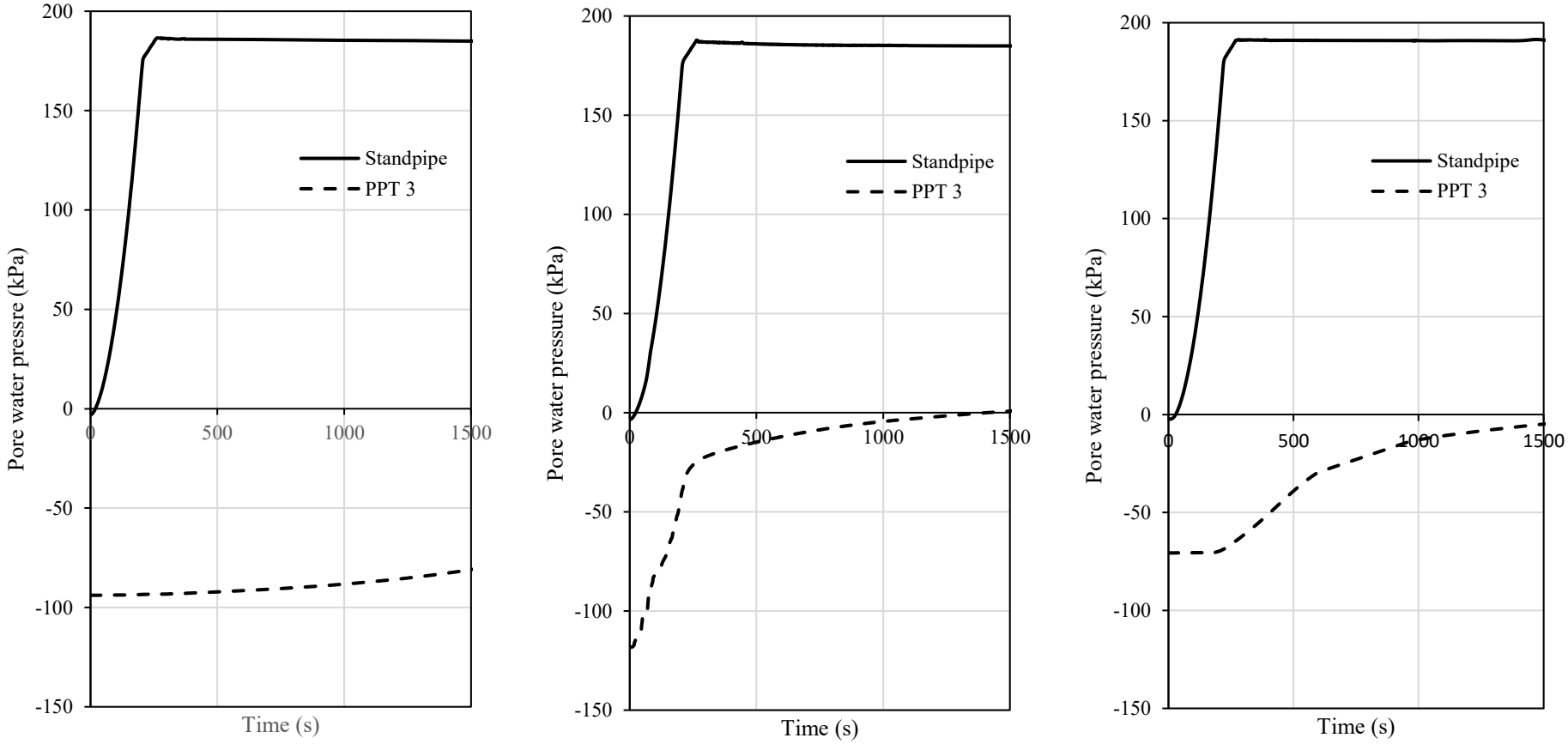

(a) (b) (c)

Figure 12.18- Initial response of PPT 1 and 5 to an increased acceleration field for the three centrifuge tests (a). Speswhite kaolin clay soil bed, (b). Speswhite Polwhite E kaolin clay soil bed, (c) Sedimented soil bed

Appendix

Publications

Ritchie, E.P., Divall, S. & Goodey, R.J. (2022). A method for creating larger clay samples with permeability anisotropy for geotechnical centrifuge modelling. 20th International Conference on Soil Mechanics and Geotechnical Engineering 1-6 May, Sydney, Australia.

Ritchie, E., McNamara, A.M., Davies, M.C.R., Taylor, N., Lalicata, L., Stallebrass, S.E. & Panchal, A.P. (2021). A low-cost miniature immersible pore water pressure transducer. Asian Conference on Physical Modelling in Geotechnics (Asiafuge-2021) 18-19 November, Singapore.

Ritchie, E., Lalicata, L., Divall, S. & Goodey, R. (2020). Tests of varied sample preparation methods for centrifuge modelling. 4th European Physical Modelling Conference in Geotechnics-ECPMG 2020 7-8 September, Luleå, Sweden.

Divall, S., Stallebrass, S.E., Goodey, R.J. & Ritchie, E.P. (2018). Development of layered models for geotechnical centrifuge tests. 9th International Conference on Physical Modelling in Geotechnics 17-20 July, London, UK.